0009

Document Information Form

Mine Number: C/015/019

File Name: INCOMING OK

To: Mr. Lowell Braxton

From:

Person

Company Bureau of Land Management

Date Received: 4-3-03

Explanation: Seismicity study of Joes Valley

cc:

FINAL REPORT

Cottonwood Coal TRACT

DEVELOPMENT OF GROUND MOTION ATTENUATION RELATIONSHIPS RELEVANT TO MINING-INDUCED SEISMICITY IN THE TRAIL MOUNTAIN AREA, EMERY COUNTY, UTAH

Prepared for: State of Utah, School and Institutional Trust Lands Administration, Salt Lake City, Utah

Prepared by: A. McGarr and J. B. Fletcher, USGS, Menlo Park, CA

With contributions from Russell Sell, Larry Baker, and Paul Spudich

March 28, 2002

1. INTRODUCTION

Future mining in the Cottonwood Coal Tract may pose a risk to the Joes Valley Dam, which is located less than 1 km from the southwest boundary of the tract. That is, ground motion caused by nearby mining-induced earthquakes might be high enough to impact the integrity of this earth-fill dam. Estimating the risk of damage to the dam involves knowing (1) the magnitude of the maximum credible earthquake that might be associated with nearby mining in the Cottonwood Tract, (2) attenuation relationships for this area that can be used to estimate various ground motion parameters as functions of magnitude, distance and site response, (3) the site response at the dam and (4) the ability of the dam to withstand seismic vibrations. In this report, we describe the development of ground motion attenuation relationships using seismic data from similar mining operations in 2000 and 2001. As explained by Arabasz et al. (2002), other institutions involved in this project were responsible for determining the remaining three factors associated with future seismic risk to the Joes Valley Dam.

Our analysis is based on data from a seismic network (Figure 1) installed and operated by the University of Utah Seismograph Stations in the environs of the Trail Mountain Mine during 2000 (Arabasz et al., 2001, 2002); the Trail Mountain Mine, situated immediately southeast of the Cottonwood Coal Tract, is the most appropriate source of earthquakes for this ground motion study because of its proximity to the Joes Valley Dam. This network was in operation at full strength from December 2000 until after late March 2001 when the mining operations at Trail Mountain were completed. After the earthquakes recorded by this network were processed at the University of Utah, ground motion records from a selected suite of earthquakes were transmitted to the USGS, in Menlo Park, CA, together with auxiliary information such as magnitudes and hypocentral coordinates. The ground motion analyses reported here are based mostly on this suite of Trail Mountain data.

During the December to March period, coal exploitation at the Trail Mountain Mine produced a rich set of earthquakes that, for the most part, was well suited to the purpose

of developing the ground motion attenuation relationships needed to assess the seismic hazard at the Joes Valley Dam due to future mining in this area. The main limitation of the Trail Mountain data set was the magnitude range, which is mostly from about 1 to 2 (Table 1). The largest event was assigned a magnitude of 2.17 (Arabasz et al., 2002) and the lower end of the range is dictated by the need for adequate signal to noise for the frequencies of interest, as will be seen. To extend our magnitude range upward, we also analyzed ground motion from a magnitude 4.2 earthquake that occurred during March, 2000, at the Willow Creek Coal Mine, about 50 km north of Trail Mountain (Ellenberger et al., 2001; Arabasz and Pechmann, 2001).

1.1 Need for New Ground Motion Attenuation Relationships

The development of new ground motion attenuation curves, specific to the circumstances of the Joes Valley Dam, was motivated by the realization that existing attenuation relationships for earthquakes, natural or induced, were inappropriate for assessing seismic hazard here. For natural earthquakes, the magnitude range of interest in terms of structural damage is generally 5 and higher (e.g., Boore et al., 1997) whereas the largest event induced by coal mining in Utah is 4.2 (Arabasz and Pechmann, 2001). Moreover, the distances used in developing attenuation relationships for natural earthquakes cover a range extending out to hundred km, or more, in contrast to the situation at Joes Valley where the earthquakes of most concern are likely to occur at distances of only a few km or less.

For mining-induced earthquakes, the few attenuation relationships that exist are inadequate or inappropriate for the present purpose. For example, McGarr et al. (1981) used ground motion data recorded at a depth of about 3 km in a deep gold mine in South Africa to develop the relationship

$$\log(Rv) = 3.95 + 0.57 M_L \qquad (1)$$

R is the hypocentral distance in cm, **v** is the peak velocity in cm/s, and M_L is the local magnitude. (1), which was developed from seismic data recorded underground, was intended mostly for use in estimating the potential for damage to nearby deep mine workings. In contrast to ground motion attenuation relationships for earthquakes, (1) is quite simple because both the mining-induced earthquakes and the mine workings are at comparable depths within a very solid and homogeneous rock mass so that complications associated with wave propagation and site effects are minimal and, thus, neglected. In the environs of the Cottonwood Coal Tract there are numerous factors that render (1) too simple to be appropriate for the purpose of estimating seismic hazard at Joes Valley Dam, including topography and geologic complexity.

1.2 General Description of New Ground Motion Attenuation Relationships

Using Joyner and Boore (1988) as a point of departure, the attenuation relationships developed here are assumed to have the form

$$\log(y) = a + bM + d\log(R) + kR + s \qquad (2)$$

where y is the ground motion parameter under consideration, M is intended to be moment magnitude (Hanks and Kanamori, 1979), s is the site factor at each seismograph station, and the logs are base 10. Essentially, a set of ground motion data is inverted, using linear programming and least squares techniques, to determine the constants a, b, d, k, and s, with some constraints to be described; in the first stage of the process, the data are inverted to determine d, k, and s and in the second stage the magnitude coefficients a and b are calculated.

(2) differs from its counterparts in Joyner and Boore (1988) in several ways. First, the magnitude dependence is assumed linear here whereas Joyner and Boore included a quadratic term. Second, our distance metric R is hypocentral distance because our seismic sources are small compared to the distances involved here; most of the corresponding relationships for earthquakes (e.g., Boore et al., 1997) use different distance metrics that take the finite size of the earthquake source into account.

The ground motion parameters investigated here are peak acceleration **a**, peak velocity **v**, and pseudovelocity response ps(T) at 5% damping at a set of periods T ranging from 0.1 s to 2 s. By fitting these parameters with relationships having the form of (2), we can account for the effects of magnitude, geometrical spreading (dlogR), anelastic attenuation and scattering (kR), and ground motion amplification due to the site specific near-surface structure (s).

1.3 The Ground Motion Network

At Trail Mountain, the seven stations (Figure 1) used to record ground motion data fall into three categories. Stations TMU, TS2, and TS3 are sited on the plateau approximately 600 m above the coal mining. Stations TB1, TB2 and TB3 are situated in the canyons around Trail Mountain and Station TU1 is located within the mine east of the active mining. For more details, see Arabasz et al. (2002).

2.0 Description of Data Set

Of the digital files for 50 events (49 from Trail Mountain plus the M4.2 Willow Creek event) transmitted from the University of Utah to Menlo Park, those for 12 earthquakes, listed in Table 1, were selected for the ground motion attenuation analysis. The event names are the seven digits indicating the julian day and approximate origin time. The depths are relative to a plateau base level 2600 m above sea level, except for the Willow Creek event, 0670215, for which the depth is relative to 2475 m above sea level (S. Nava, written communication, 2001). The magnitudes M_c in the last column of Table 1, are the coda magnitudes assigned by the University of Utah Seismograph Stations, except for the Willow Creek event, for which the magnitude listed is local magnitude M_L.

Table 1. Earthquake information

Event	Date	Time UTC	latitude	longitude	Depth, m	M_c
0670215	3/7/00	02:15	39°45.10′	110°51.08′	646	4.2 (M_L)
3580136	12/23/00	01:37	39°18.53′	111°13.31′	310	1.03
3580529	12/23/00	05:29	39°18.57′	111°13.66′	200	0.98
3580734	12/23/00	07:34	39°18.02′	111°13.73′	260	1.43
3602011	12/25/00	20:12	39°17.79′	111°11.65′	50	1.56
0050913	1/5/01	09:13	39°18.47′	111°13.36′	240	1.35
0090423	1/9/01	04:23	39°18.44′	111°13.21′	600	1.46
0091727	1/9/01	17:27	39°17.72′	111°12.63′	720	2.17
0182156	1/18/01	21:56	39°18.41′	111°13.22′	170	1.55
0322143	2/1/01	21:43	39°19.67′	111°13.26′	2070	1.24
0331032	2/2/01	10:33	39°18.63′	111°13.85′	0	1.4
0382053	2/7/01	20:54	39°18.56′	111°10.04′	570	1.61

(The locations listed for events 3580734, 0091727, 0182156, and 0331032 are slightly different from those reported by Arabasz et al. (2002) because of some revisions to the hypocentral coordinates after January 2002. These revisions are small and would have no material effect on our results.)

Among the criteria used to select these events were the following: (1) The event was recorded by at least six of the seven stations of the Trail Mountain ground motion network (Figure 1); (2) Events were selected for having high signal/noise; (3) We wished to include as broad a magnitude range as possible; (4) We tried to include a reasonably broad distribution of epicentral locations around the Trail Mountain Mine (Figure 1); (5) Event 0670215 (Table 1) at the Willow Creek Mine (See Arabasz and Pechmann, 2001, for the location of this event.), although recorded, by the University of Utah, at only two ground motion stations near that mine, was included in our analysis primarily to sample ground motion at a much higher magnitude of 4.2.

2.1 Examples of Ground Motion Parameters

Figure 2a shows processed ground acceleration, velocity, and displacement for the M4.2 Willow Creek event as recorded at Station WCS, located about 2 km south of the hypocenter near the mine entrance. The peak values automatically picked for the three components of acceleration and velocity are part of the data set used in the attenuation analysis of this report. The other data used in the analysis come from the pseudovelocity spectra (Figure 2b) from which spectral amplitudes are picked at periods of 0.1, 0.2, 0.5, 1.0, and 2.0 s. The pseudovelocity spectra show excellent signal/noise over this entire period range and beyond. Similar remarks apply to the ground motion data for this M4.2 event as recorded at Station EMU, about 7.5 km north of the epicenter.

Event 3580734 (Table 1) was located close to the active mining taking place beneath Station TS3 on Trail Mountain and, as seen in Figure 3a, the ground motion at this site shows very clear wave forms. On the horizontal components, the peak values of acceleration and velocity are associated with the S wave pulse; at more distant stations

surface waves sometimes account for the peak ground motion. Figure 3b shows the corresponding pseudovelocity spectra where we see high signal to noise for all periods. In contrast, pseudovelocity spectra from the same event at Station TB1 (Figure 3c), 3.6 km to the west of the epicenter (Figure 1), show that the signal is overwhelmed by the noise for periods greater than 0.5 s, or so.

The largest event, 0091727, of the Trail Mountain earthquakes (Table 1) analyzed here, with a magnitude of 2.17, was located near an area that had been mined in previous years below Station TMU (Figure 1). The ground motion records at this station (Figure 4a) are exceedingly clear and simple and, correspondingly, the pseudovelocity spectra have superb signal to noise. Even for this largest Trail Mountain event, however, signal/noise was quite poor for the longer periods at the more distant stations (Figure 4c).

2.2 Magnitudes

Except for the Willow Creek event, which was assigned a local magnitude, the magnitudes listed in Table 1 are coda magnitudes, M_c, assigned by the University of Utah. Although we had no reason to question these magnitude assignments, we decided to perform two independent assessments, partly to find out how the Utah coda magnitudes relate to moment magnitudes (Hanks and Kanamori, 1979). It has long been known (e.g., Wong et al., 1989; Wong and McGarr, 1990; Taylor, 1994; Arabasz and Pechmann, 2001) that many of the earthquakes induced by coal mining in Utah have implosive components in their source mechanisms, in contrast to natural earthquakes. We wished to find out if this was the case for the events at Trail Mountain and, if so, whether it might affect the magnitude assignments. As will be seen, we concluded finally that the coda magnitudes do not differ significantly from moment magnitudes despite source mechanisms with substantial implosive components.

2.2.1 Moment Tensors

To determine the moment tensors for a few of the mining-induced earthquakes at Trail Mountain, we modified a method developed by McGarr (1992a,b) to estimate moment tensors for tremors in some deep gold mines in South Africa. The method entails measuring the amplitudes at diagnostic points of the ground displacement waveforms (e.g., the P wave pulse amplitude) and then making corresponding measurements on the synthetic seismograms computed for each of the six components of the moment tensor; in calculating the synthetic seismograms, each component of the moment-rate tensor is assumed to have the same duration, t_s, which is determined for each event from the clearest P or S wave pulses. The amplitude measurements on the observed and synthetic seismograms define a set of over-determined (more than six) equations, which can be solved to determine the six components of the moment tensor (e.g., McGarr, 1992a). The main strength of this method is that three components of ground displacement recorded at several close-in stations can provide enough data to resolve the six components of the moment tensor, as long as the signal/noise is high.

Whereas in the gold mines of South Africa the velocity structure could be well approximated as homogeneous, this is not the case in the coal mining districts of Utah where considerable stratification in seismic velocity is encountered. To accommodate this, McGarr's (1992a,b) method was modified by using a program that computes synthetic seismograms for a layered, rather than homogeneous, earth (Olsen et al., 1984; Spudich and Xu, 2002). Thus, we now calculate synthetic seismograms for each component of a moment tensor buried in a layered medium.

Table 2. Moment tensor results for four Trail Mountain events

event	t_s, s	M11	M12	M13	M22	M23	M33	M_0	M_c	M
3580734	0.06	-5.77	1.40	2.52	-3.49	0.03	-19.49	15.0	1.43	2.08
0090423	0.04	-0.42	0.29	0.96	-0.68	-0.02	-2.52	2.12	1.46	1.52
0091727	0.10	-4.2	-1.5	0.00	-1.3	0.34	-6.8	6.82	2.17	1.86
0182156	0.04	-1.31	-0.12	-0.01	-2.38	0.78	-3.4	3.18	1.55	1.63

Table 2 summarizes the results of determining moment tensors for events 3580734, 0090423 and 0091727 and 0182156. The coordinate directions (1,2,3) are (north, east, vertical). The component M33, for example, represents two opposing vertically-oriented forces acting on a horizontal plane (normal to plane is vertical). In Table 2, all of the moment tensor components have units 10^{11} N-m. The scalar moment M_0 is estimated using the relation of Silver and Jordan (1982)

$$M_0 = \left(\frac{\sum m_i^2}{2}\right)^{1/2} \qquad (3)$$

where the m_i represent the three principal values found by diagonalizing the moment tensor. Using the generalized scalar moment from (3), the moment magnitude M (Hanks and Kanamori, 1979) is estimated from

$$M = (\log M_0 - 9.05)/1.5 \qquad (4)$$

where M_0 is in N-m.

The four moment tensors in Table 2 have some features in common. First, they all have negative traces, M11+M22+M33, indicating coseismic reductions in volume. Second, M33 is the dominant component. Indeed, after diagonalizing these tensors, we have found that they are all consistent with a normal faulting component plus an implosive component of comparable magnitude, similar to what was found in the South African gold mines McGarr, 1992a,b). In any case, the results summarized in Table 2 tend to confirm the findings of Wong et al. (1989) regarding the implosive character of at least some coal mine tremors in Utah.

With regard to how M_c, the coda magnitude used by the University of Utah, relates to M, the four sets of results listed in Table 2 suggest, tentatively, that there is no systematic difference.

2.2.2 Peak Velocity Parameter and Magnitude

Equation (1) is based on the observation that the peak velocity parameter R**v**, measured at close-in stations, is linearly dependent on the magnitude (McGarr et al., 1981). Here we apply this finding to test, in a different way, the hypothesis that M_c is essentially equivalent to M. Figure 5 shows log**Rv** , measured at the closest stations (e.g., Figure 3a), plotted as functions of M_c for the events of this study (Table 1, squares) and as functions of M for 11 events listed in Table 1 of McGarr (1993, diamonds); the 11 events from the 1993 study were selected because their moment tensors also showed significant implosive components, as was found for the limited sample of the Trail Mountain events (Table 2). As seen in figure 5, the two sets of peak velocity parameters show approximately the same relationship to magnitude, whether M_c or M. Thus, both the moment tensor results (Table 2) and the peak velocity observations (Figure 5) suggest that M_c is a reasonably good approximation to moment magnitude M.

3.0 Ground Motion Attenuation

Using the approach outlined in Section **1.2**, we fit Equation (2) to each set of ground motion parameters measured for the earthquakes listed in Table 1. Although the ground motion parameters themselves are listed in column 1 of Table 3, the attenuation relationships involve logs of these parameters. As analyzed here, the units for the parameters are cm/s/s for peak acceleration **a** and cm/s for peak velocity **v** and all of the pseudovelocities at 5% damping ps(T). R, the hypocentral distance, is in km. In all cases, y represents the maximum horizontal component of the ground motion parameter under consideration.

In fitting Equation (2), we found it necessary to apply several constraints. First, k was constrained to be in the range –2 to 0; without this constraint, two of the pseudovelocities, at the longest periods, yielded small positive values of k, a physically implausible outcome. Second, the site factors were constrained to be in the range 0 to 1.

Based on the variation in station settings mentioned before, we grouped the stations into three different site categories for each ground motion parameter. Stations TB1, TB2, and TB3, as well as stations WCS and EMU near the Willow Creek Mine, are all assigned site factor s_1, inasmuch as they are all situated near the bottoms of the canyons that dissect the plateaus. Stations TS2, TS3, and TMU, which are all on the plateau of Trail Mountain (Figure 1), are assumed to have site factor s_2. Finally, the underground station TU1 was assigned site factor s_3.

σ, listed in Table 3, for each parameter fit is the standard deviation of the residuals res_i for all observations obs_i. That is, $res_I = \log(obs_I) - \log(y_I)$. For example, a residual of 0.2 would correspond to a ratio obs_{ii}/y_i of 1.58. The standard deviations listed in Table 3 indicate that for all of the ground motion parameter fits using Equation (2), about 67% of the observations differ from the corresponding the predicted values by factors less than 1.8, or so.

Table 3. Ground motion attenuation relationships (Equation 2)

y	No.	a	b	d	k	s_1	s_2	s_3	σ
a	72	-1.421	0.8553	-1.601	-0.1245	1.0	0.645	0.844	0.255
v	72	-3.758	0.9539	-1.524	-0.0484	1.0	0.887	0.578	0.242
ps(0.1)	72	-3.044	0.8473	-1.228	-0.1204	0.7619	0.6082	0.0	0.228
ps(0.2)	72	-3.762	1.006	-1.152	-0.0651	0.738	0.884	0.0	0.234
ps(0.5)	54	-4.355	1.115	-1.241	-0.0278	0.687	0.7613	0.0	0.206
ps(1.0)	39	-4.492	1.127	-1.128	0.0	0.494	0.4781	0.0	0.207
ps(2.0)	31	-3.923	0.8486	-1.362	0.0	0.7819	0.0	0.1108	0.205

To illustrate how the ground motion attenuation relationships summarized in Table 3 might be applied, consider peak velocity. For this ground motion parameter the attenuation relationship (Table 3) is

$$\log v = -3.758 + 0.9539M - 1.524 \log R - 0.048R + 1.0 \qquad (5)$$

for a site in a canyon setting (e.g., TB1). If, for instance, a magnitude 4.2 earthquake occurred at a hypocentral distance of 1 km, then the predicted peak horizontal velocity is 15.9 cm/s, from evaluating Equation (5). If the distance were 0.5 km, then for the same magnitude earthquake, the peak horizontal velocity is predicted to be 48.2 cm/s.

Figures 6 and 7 illustrate the distance and magnitude dependence for peak acceleration and peak velocity and compare our results to a few corresponding relationships for earthquakes. As seen in Figure 6, which assumes a site factor of 0.7, the peak accelerations predicted for the mining-induced events are similar to those for SEA99 (Spudich et al., 1999) or the attenuation relationship of Joyner and Boore (1993), especially for distances under 1 km. For peak velocity (Figure 7), we see that for distances less than 1 km, the result from the study of Joyner and Boore (1993) also agrees surprisingly well with its M4 counterpart from this study, with an assumed site factor of 0.8. For both peak velocity and peak acceleration, the attenuation relationships developed here diminish more rapidly with distance than their counterparts for earthquakes, presumably because of the higher-frequency data used here and perhaps also due to the shallow source depths.

Although the information listed in Table 3 can be used to estimate the predicted ground motion for a given magnitude and hypocentral distance to the Joes Valley Dam, more information is required to estimate the ground motion at the dam itself. In particular, the actual response of the dam site must be determined before the information of this study (Table 3) can be applied to estimate the seismic hazard particular to the Joes Valley Dam. This could be done by comparing ground motion, for a given earthquake, at the Joes Valley Dam to that recorded at nearby stations TB1 and TB2 (Figure 1).

Acknowledgments

This study was funded by the State of Utah Schools and Institutional Trust Lands Administration (SITLA). We thank John Blake of SITLA for supporting and encouraging this study. Our analysis was based on ground motion data and auxilliary information provided by Walter Arabasz, Susan Nava, Kristine Pankow, James Pechmann and other members of the University of Utah Seismograph Stations. Peter Swanson of NIOSH provided useful information about the large magnitude earthquake at the Willow Creek Mine, including accurate hypocentral coordinates (Table 1). Paul Spudich played a key role in the development of an effective program for calculating synthetic seismograms for our moment tensor analysis. Russell Sell solved some difficult problems involved in transferring the digital seismic data from the Unversity of Utah to the USGS in Menlo Park.

References

Arabasz, W. J., S. J. Nava, and W. T. Phelps, Mining seismicity in the Wasatch Plateau and Book Cliffs coal mining districts, Utah, USA, in Rockbursts and Seismicity in Mines, S. J. Gibowicz and S. Lasocki (eds.), Balkema, pp. 111-116, 1997.

Arabasz, W. J. and J. C. Pechmann, with contributions from M. K. McCarter and J. D. McKenzie, Seismic characterization of coal-mining seismicity in Utah for CTBT monitoring, Final Report, Lawrence-Livermore National Laboratory Agreement No, B344836, 125 pp., 2001.

Arabasz, W. J., S. J. Nava, M. K. McCarter, and K. L. Pankow, Ground-motion recording and analysis of mining-induced seismicity in the Trail Mountain area, Emery County, Utah, Final Report prepared for State of Utah, SITLA, 2002.

Boore, D. M., W. B. Joyner and T. E. Fumal, Equations for estimating horizontal response spectra and peak acceleration from western North American earthquakes: A summary of recent work, Seismol. Res. Letters, **68**, No. 1, 128-153, 1997.

Ellenberger, J. L., K. A. Heasley, P. L. Swanson, and J. Mercier, Three dimensional ,microseismic monitoring of a Utah longwall, Proceedings of the 38th U.S. Symposium of Rock Mechanics, Washington, DC, pp. 1321-1326, 2001.

Hanks, T. C. and H. Kanamori, A moment magnitude scale, J. Geophys. Res., 84, 2348-2350, 1979.

Joyner, W. B. and D. M. Boore, Measurement, characterization, and prediction of strong ground motion, Proceedings of Earthquake Engineering & Soil Dynamics II, GT Div/ASCE, Park City, UT, pp. 43-102, 1988.

Joyner, W. B. and D. M. Boore, Methods for regression analysis of strong-motion data, Bull. Seismol. Soc. Am., **83**, 469-487, 1993.

McGarr, A. An implosive component in the seismic moment tensor of a mining-induced tremor, Geophys. Res. Lett., **19,** 1579-1582, 1992.

McGarr, A., Moment tensors of ten Witwatersrand mine tremors, Pure and Applied Geophys., **139**, 781-800, 1992.

McGarr, A., Keynote address: Factors influencing the strong ground motion from mining-induced tremors, Rockbursts and Seismicity in Mines, R. P. Young (ed.), Balkema, Rotterdam, pp. 3-12, 1993.

McGarr, A., R. W. E. Green, and S. M. Spottiswoode, Strong ground motion of mine tremors: some implications for near-source ground motion parameters, Bull. Seismol. Soc. Am., **71**, 295-319, 1981.

Olsen, A. H., J. A. Orcutt, and G. A. Frazier, The discrete wavenumber/finite element method for synthetic seismograms, Geophys. J. R. Astr. Soc., **77,** 421-460, 1984.

Silver, P. G. and T. H. Jordan, Optimal estimation of scalar seismic moment, Geophys. J. R. Astr. Soc., **70**, 755-787, 1982.

Spudich, P. and L. Xu, Documentation of software package Compsyn v3.0: Programs for earthquake ground motion calculation using complete 1-D Green's functions, International Handbook of Earthquake and Engineering Seismology, Elsevier, in press, 2002.

Spudich, P., W. B. Joyner, A. G. Lindh, D. M. Boore, B. M. Margeris and J. B. Fletcher, SEA99: A revised ground motion prediction relation for use in extensional tectonic regimes, Bull. Seismol. Soc. Am., **89**, 1156-1170, 1999.

Taylor, S. T., False alarms and mine seismicity: An example from the Gentry Mountain mining region, Utah, Bull. Seismol. Soc. Am., **84**, 350-358, 1994.

Wong, I. G. and A. McGarr, Implosional failure in mining-induced seismicity: A critical review, Rockbursts and Seismicity in Mines, C. Fairhurst (Ed.), Balkema, 45-51, 1990.

Wong, I. G., J. R. Humphrey, J. A. Adams, and W. J. Silva, Observations of mine seismicity in the eastern Wasatch Plateau, Utah, U.S.A.: A possible case of implosional failure, Pure and Applied Geophys., **129,** 369-405, 1989.

Figure Captions

Fig. 1. Shaded relief map of Joes Valley area showing ground motion network and the mining-induced earthquakes analyzed here. The three yellow symbols are epicenters of the events for which moment tensors (Table 2) were determined. Ten of the epicenters are associated with mining beneath Trail Mountain whereas the easternmost epicenter is presumably due to past mining beneath East Mountain. JVD indicates the Joes Valley Dam and the ground motion station there.

Fig. 2. a) Ground acceleration, velocity, and displacement recorded at station WCS at the Willow Creek Mine about 2 km south of the epicenter of the M4.2 event in March ,2000 Table 1).

b)Pseudovelocity spectra at 5% damping for the three components of ground motion recorded at station WCS.

Fig. 3. a) Ground acceleration, velocity and displacement for event 3580734 (Table 1) recorded at station TS3.

b) Pseudovelocity spectra for ground motion from event 3580734 recorded at TS3.

c) Pseudovelocity spectra for event 3580734 recorded at TB1.

Fig. 4. a) Ground acceleration, velocity and displacement for event 0091727 (Table 1) recorded at station TMU. On the displacement traces, note the near-field ramp between the P and S wave arrivals.
b) Pseudovelocity spectra for event 0091727 at station TMU.
c) Pseudovelocity spectra for event 0091727 at station TB1.

Fig. 5. Peak velocity parameter logRv, measured at small hypocentral distances, as a function of magnitude. The diamonds represent events with implosive components from McGarr (1993) with moment magnitudes and the squares are from this study (Table 1) with coda magnitudes or local magnitude in the case of the large Willow Creek event..

Fig. 6. Predicted peak horizontal acceleration (Table 3) as a function of distance. Upper plot shows predicted peak acceleration for M4 compared to corresponding predictions from SEA99 (Spudich et al., 1999) and Joyner and Boore (1993). Lower plot shows predicted **a** for various magnitudes of interest.

Fig. 7. Predicted peak horizontal velocity as a function of distance. Upper plot compares results of this study (Table 3) for magnitude 4 with those from Joyner and Boore (1993). Lower plot shows predictions for various magnitudes.

Joes Valley Stations and Epicenters

-4 0 4 8 kilometers

Fig. 1

Fig. 2a

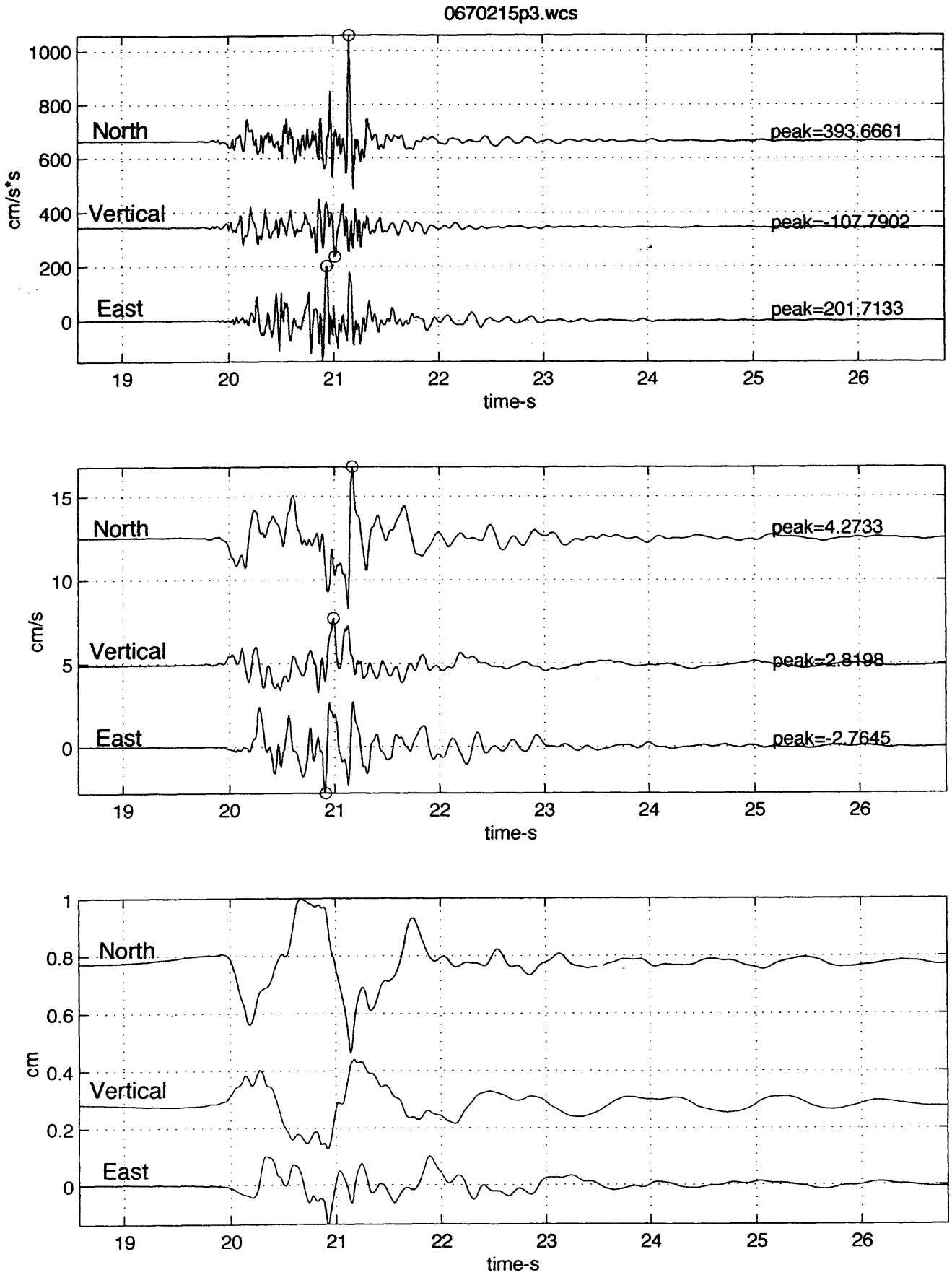
0670215p3.wcs
North
Vertical
East
peak=393.6661
peak=-107.7902
peak=201.7133
cm/s*s
time-s
North
Vertical
East
peak=4.2733
peak=2.8198
peak=-2.7645
cm/s
time-s
North
Vertical
East
cm
time-s

Fig. 2b

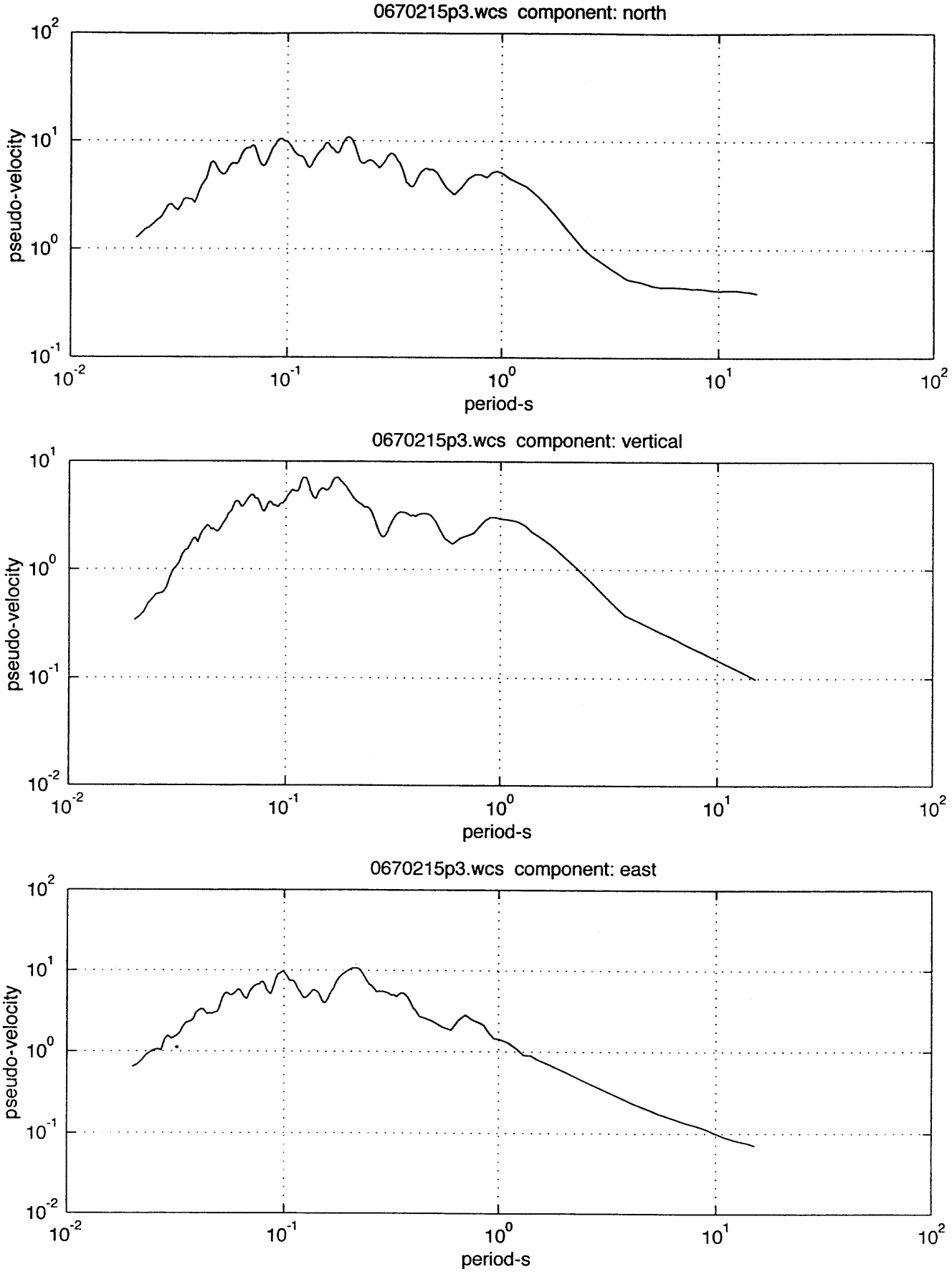
0670215p3.wcs component: north
pseudo-velocity
period-s
0670215p3.wcs component: vertical
pseudo-velocity
period-s
0670215p3.wcs component: east
pseudo-velocity
period-s

Fig. 3a

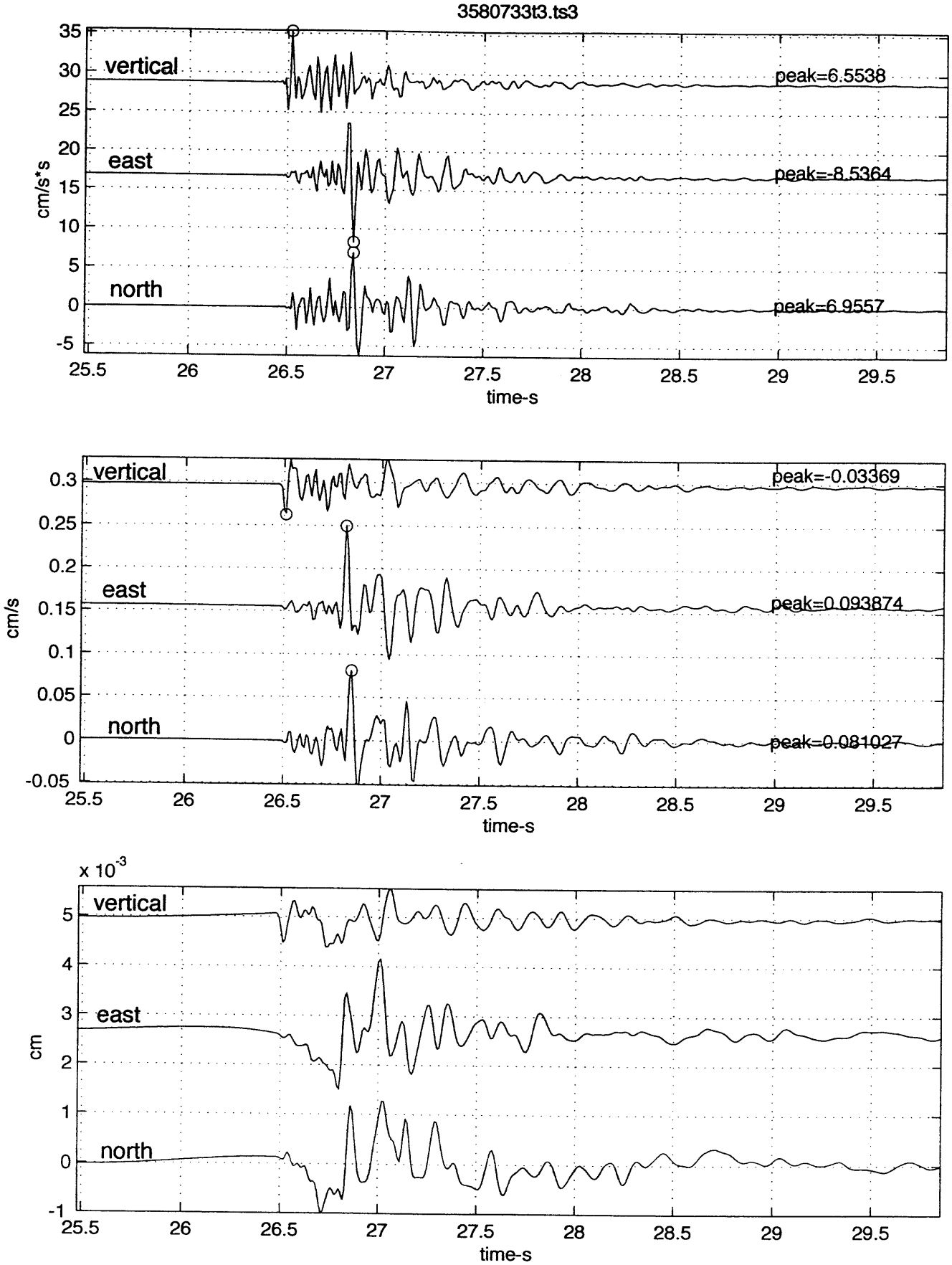
3580733t3.ts3
vertical
east
north
peak=6.5538
peak=-8.5364
peak=6.9557
cm/s*s
time-s
vertical
east
north
peak=-0.03369
peak=0.093874
peak=0.081027
cm/s
time-s
x 10^-3
vertical
east
north
cm
time-s

Fig. 3b.

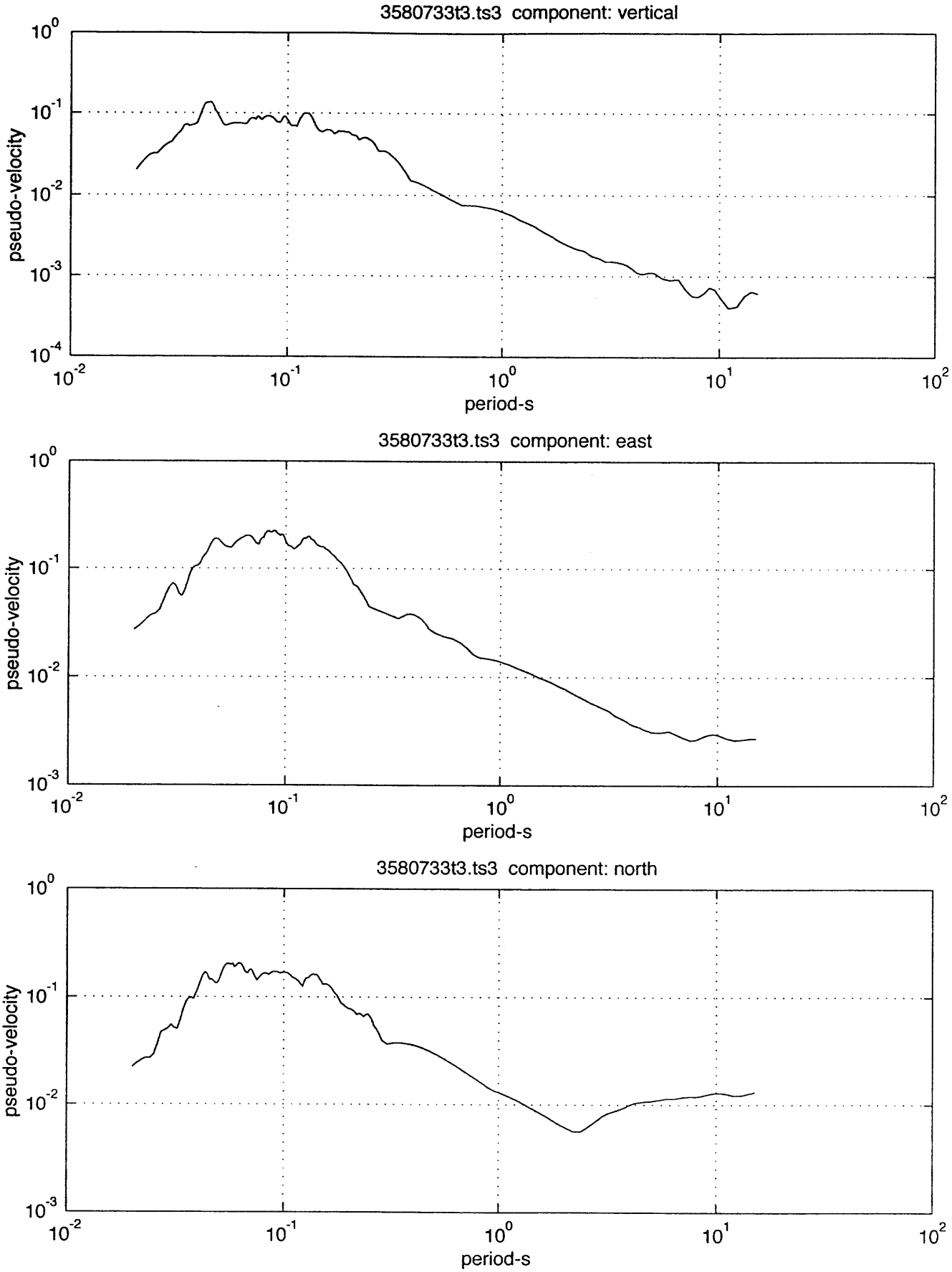
3580733t3.ts3 component: vertical
pseudo-velocity
period-s
3580733t3.ts3 component: east
pseudo-velocity
period-s
3580733t3.ts3 component: north
pseudo-velocity
period-s

Fig. 3c

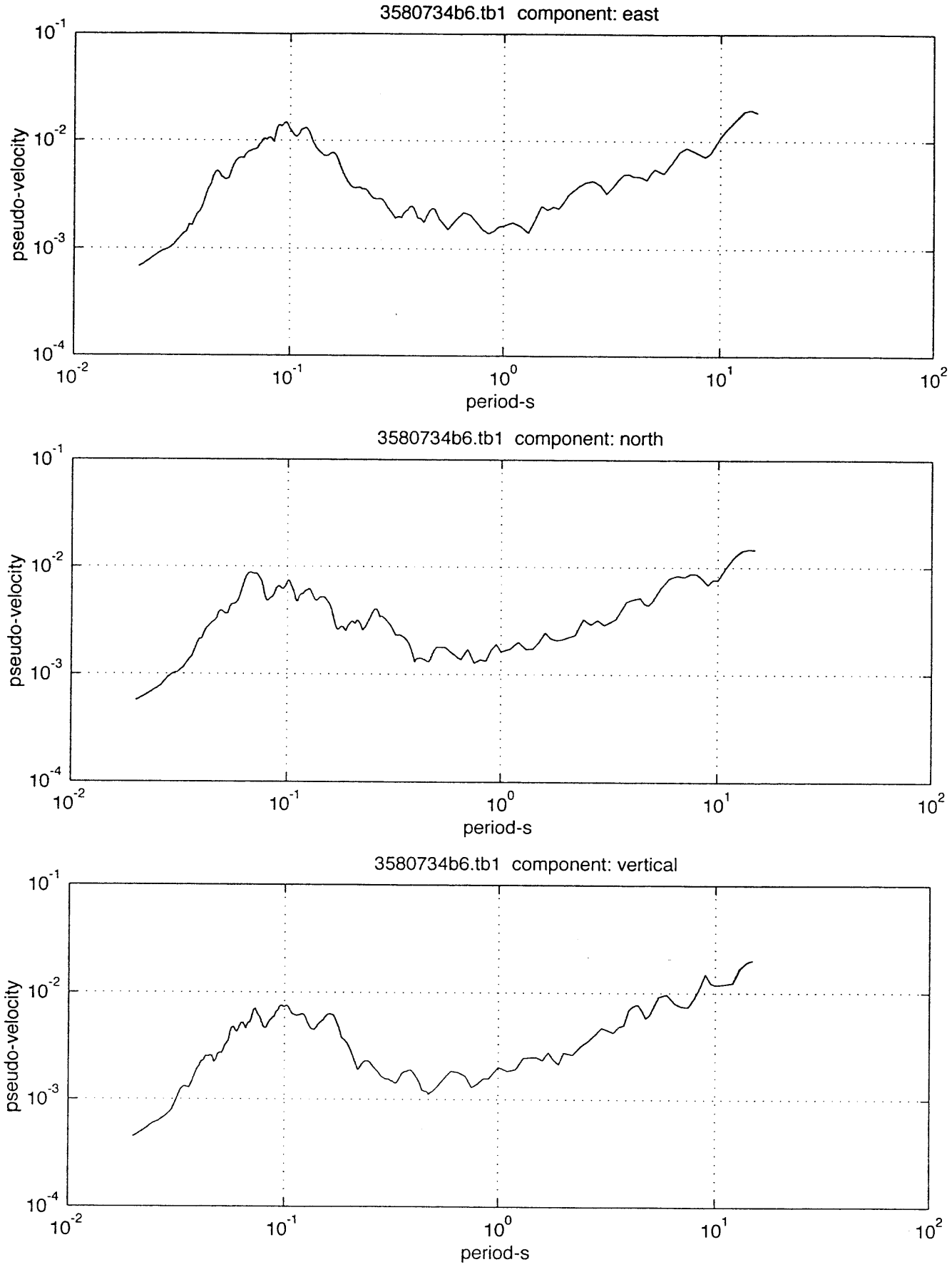
3580734b6.tb1 component: east
pseudo-velocity
period-s
3580734b6.tb1 component: north
pseudo-velocity
period-s
3580734b6.tb1 component: vertical
pseudo-velocity
period-s

Fig, 4a

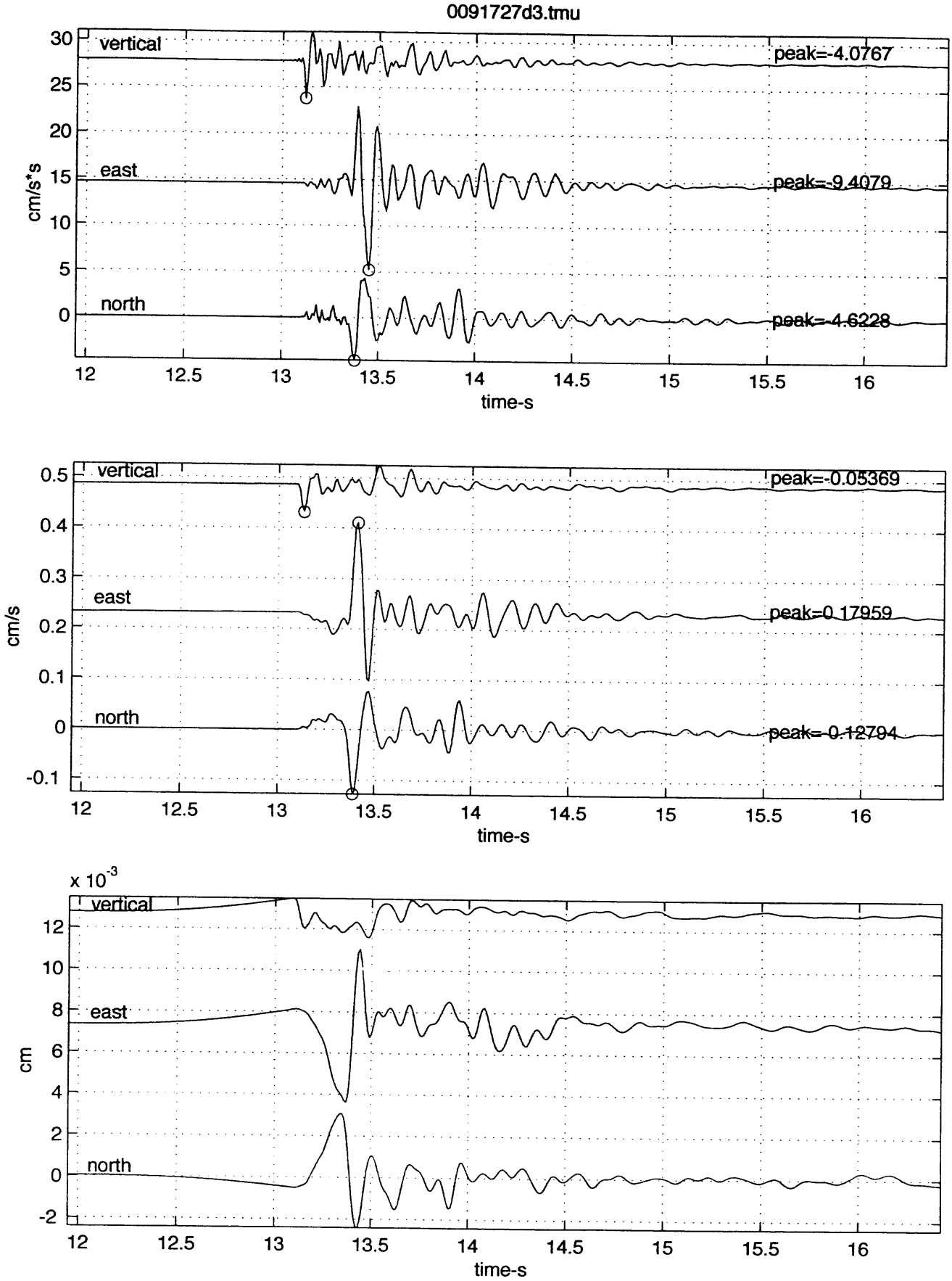
0091727d3.tmu
vertical
peak=-4.0767
east
peak=-9.4079
north
peak=-4.6228
cm/s*s
time-s
vertical
peak=-0.05369
east
peak=0.17959
north
peak=-0.12794
cm/s
time-s
x 10^-3
vertical
east
north
cm
time-s

Fig. 46

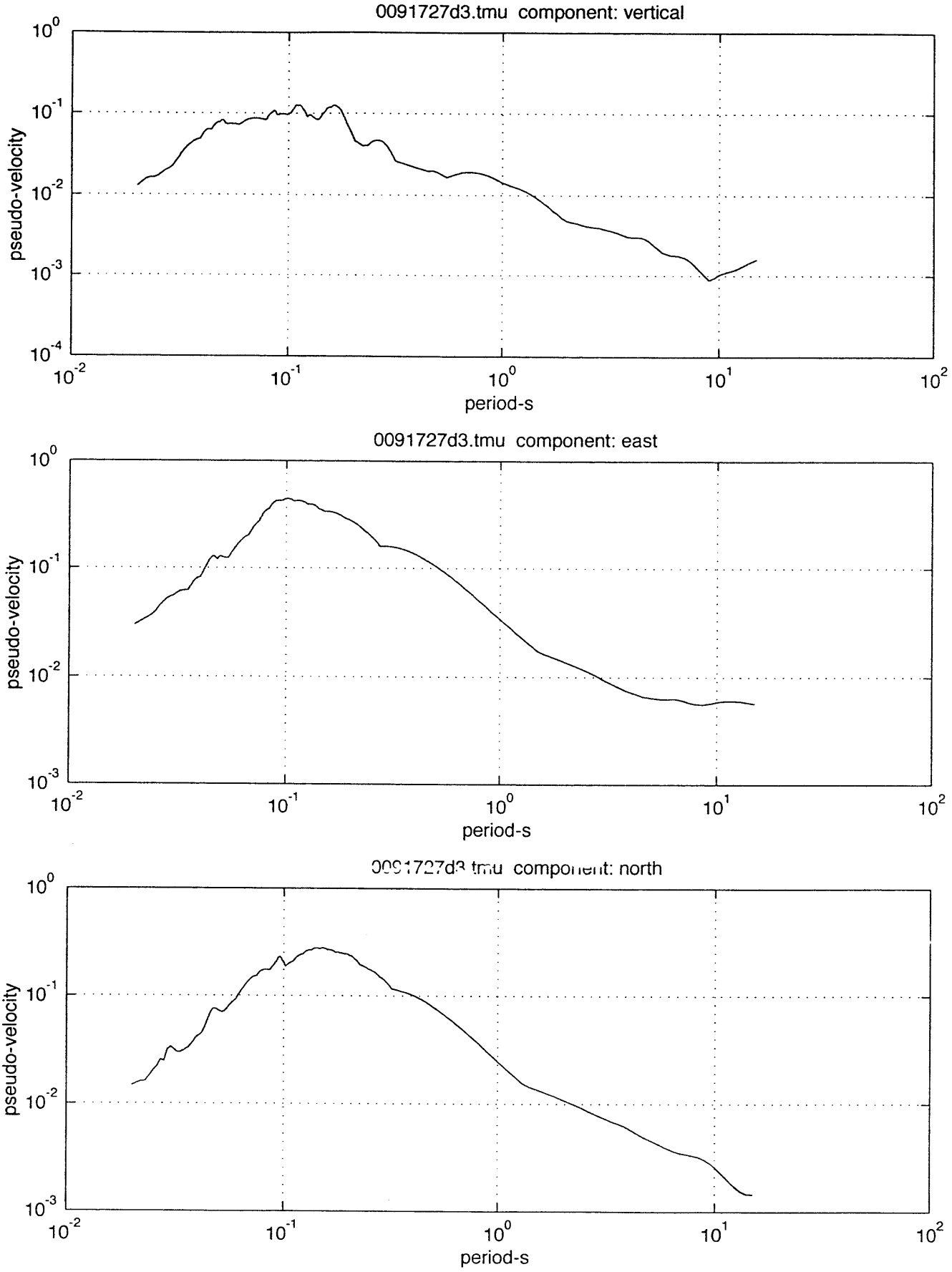
0091727d3.tmu component: vertical
pseudo-velocity
period-s
0091727d3.tmu component: east
pseudo-velocity
period-s
0091727d3.tmu component: north
pseudo-velocity
period-s

Fig. 4c

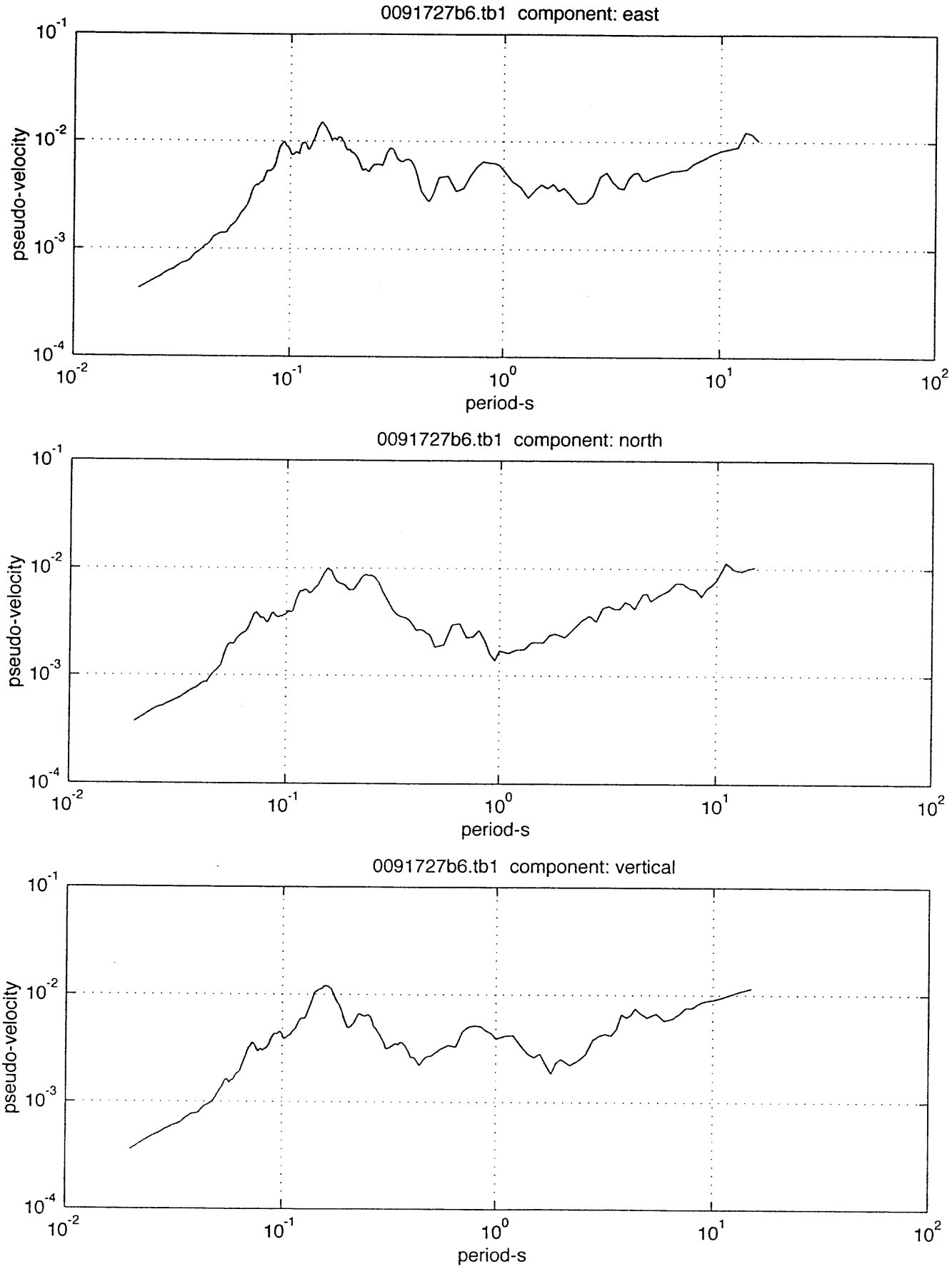
0091727b6.tb1 component: east
pseudo-velocity
period-s
0091727b6.tb1 component: north
pseudo-velocity
period-s
0091727b6.tb1 component: vertical
pseudo-velocity
period-s

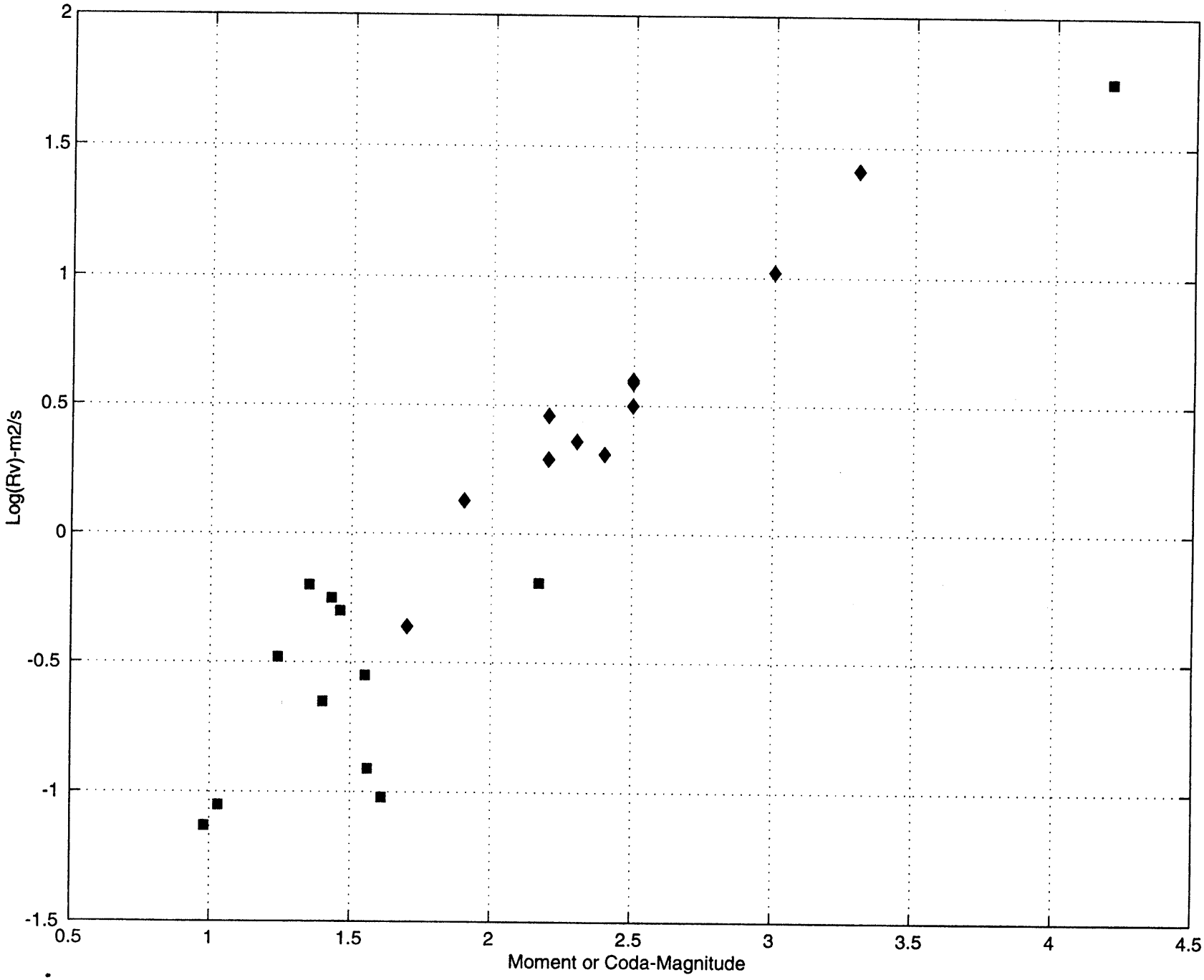
Log(Rv)-m2/s
Moment or Coda-Magnitude
2
1.5
1
0.5
0
-0.5
-1
-1.5
0.5
1
1.5
2
2.5
3
3.5
4
4.5

Fig. 5

Fig. 6

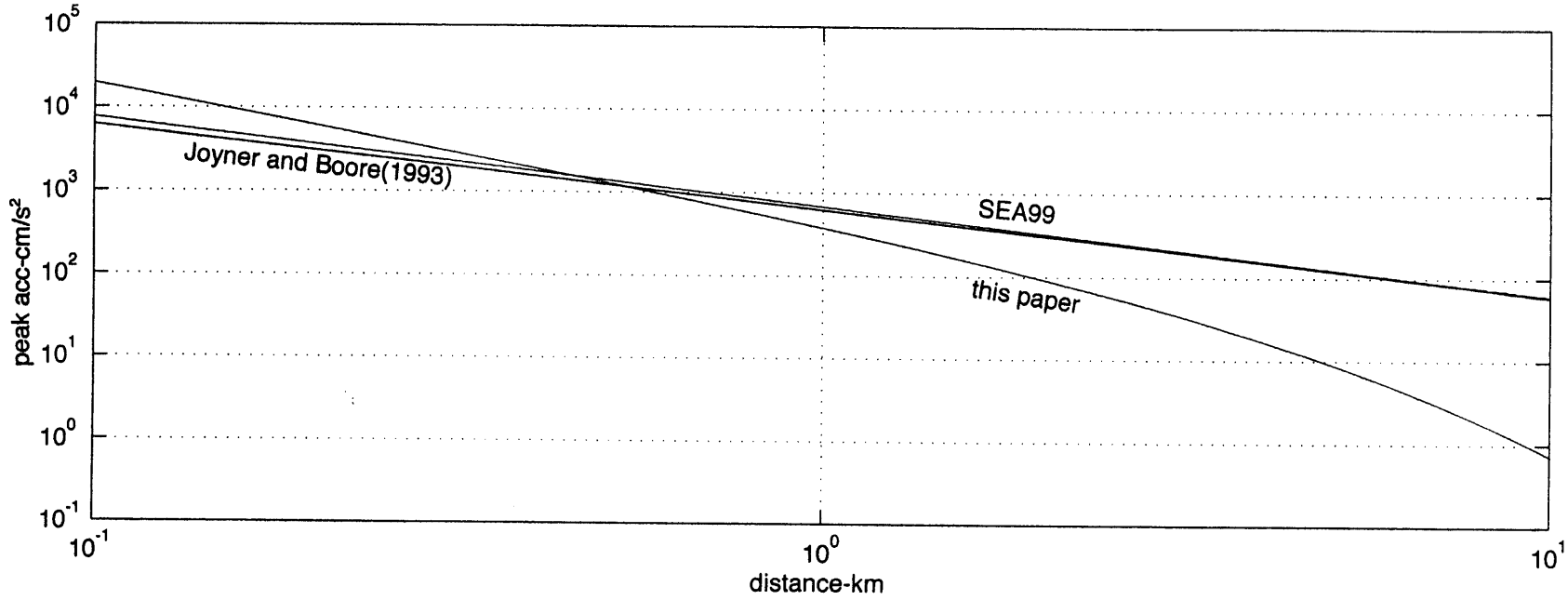
peak acc-cm/s²
distance-km
Joyner and Boore(1993)
SEA99
this paper

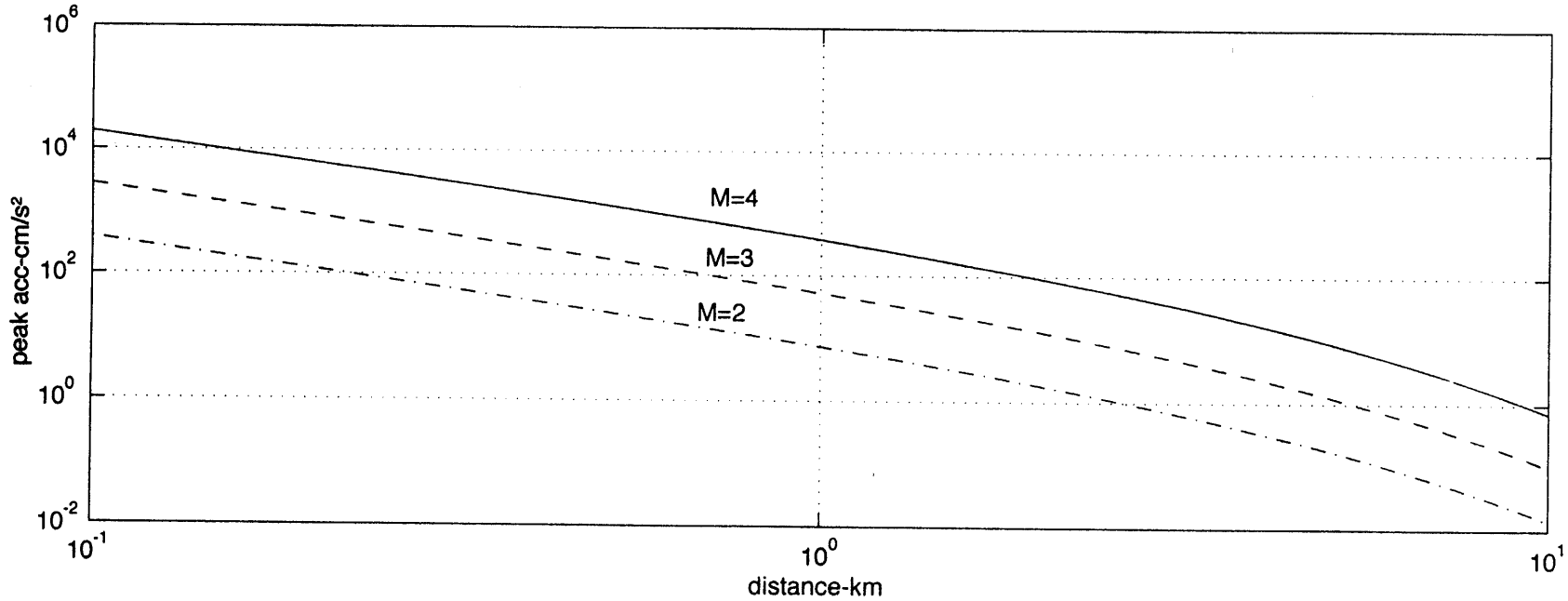
peak acc-cm/s²
distance-km
M=4
M=3
M=2

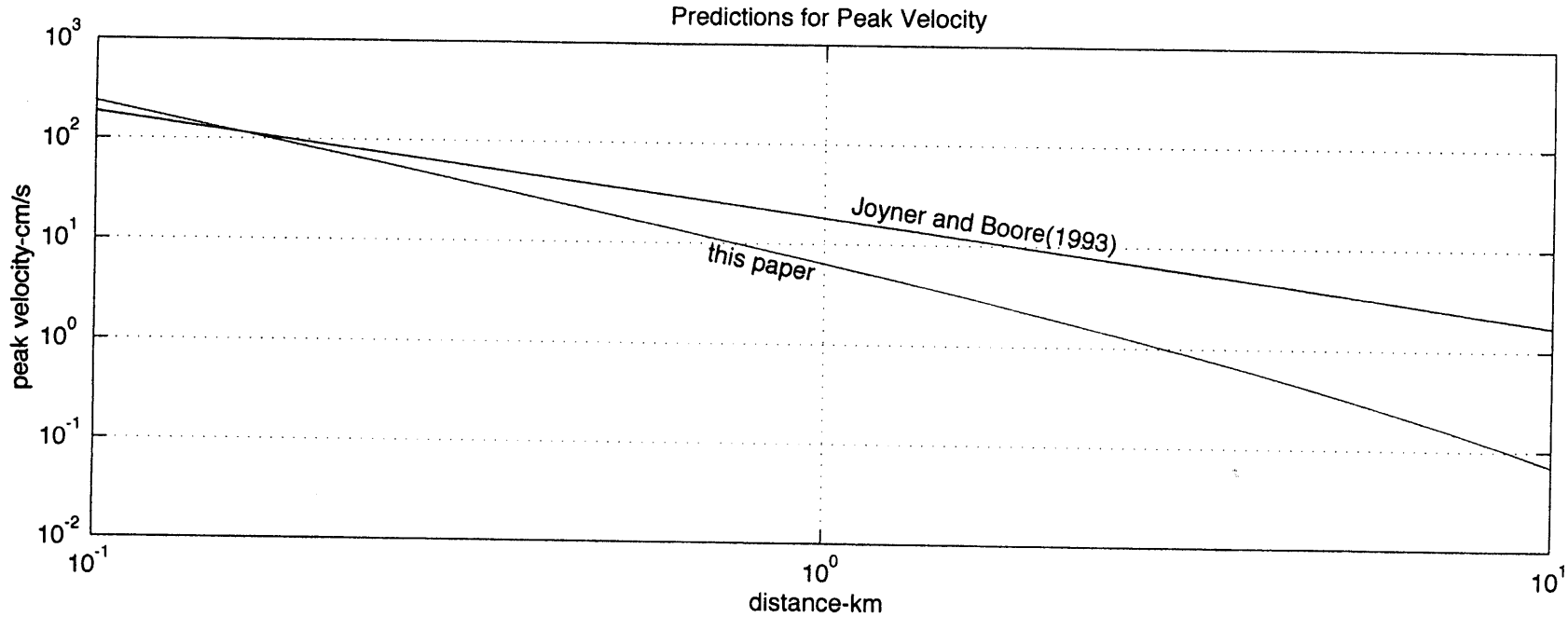
Predictions for Peak Velocity
peak velocity-cm/s
distance-km
Joyner and Boore(1993)
this paper
10^3
10^2
10^1
10^0
10^{-1}
10^{-2}
10^{-1}
10^0
10^1

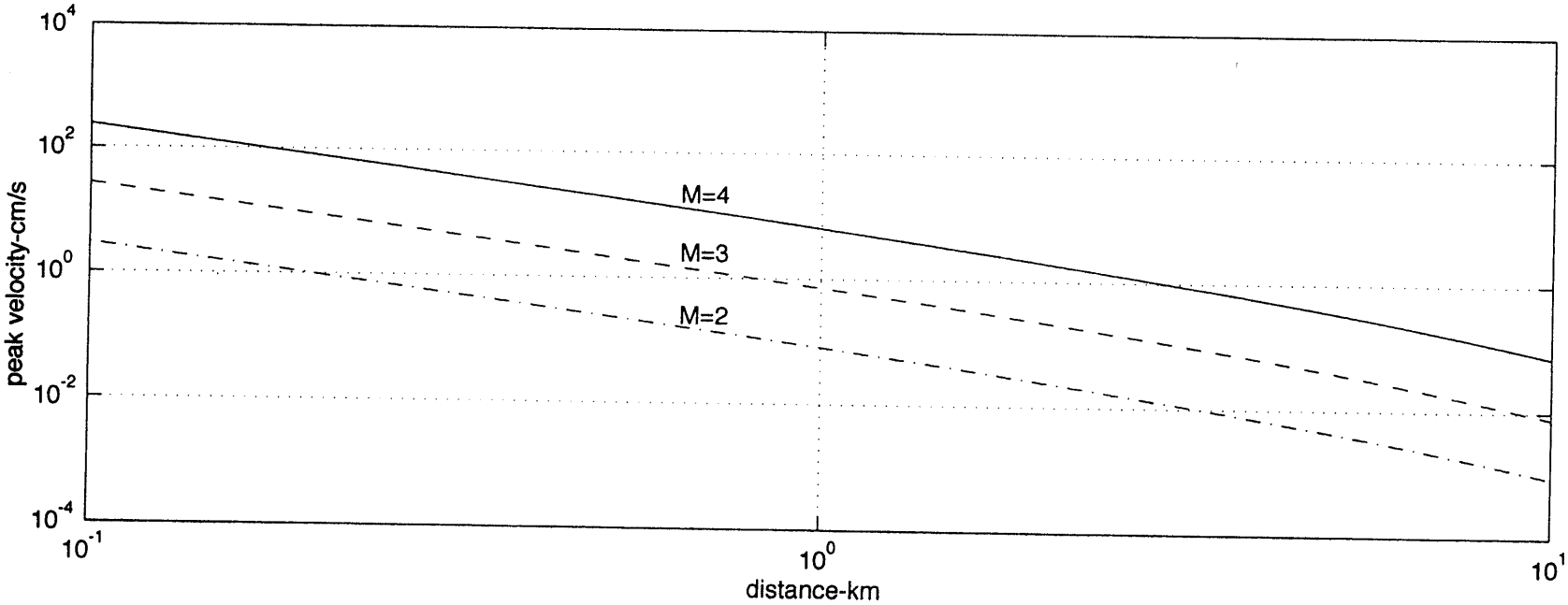
peak velocity-cm/s
distance-km
M=4
M=3
M=2
10^4
10^2
10^0
10^{-2}
10^{-4}
10^{-1}
10^0
10^1

FINAL REPORT

DRAFT

Ground-Motion Recording and Analysis of Mining-Induced Seismicity in the Trail Mountain Area, Emery County, Utah

Prepared for
State of Utah
School and Institutional Trust Lands Administration
Salt Lake City, Utah

Prepared by
Walter J. Arabasz [1], Susan J. Nava [1], Michael K. McCarter [2], and Kristine L. Pankow [1]

with contributions from James C. Pechmann [1], Matthew E. Jensen [2] and Jefferson D. McKenzie [2]

March 29, 2002

1 University of Utah Seismograph Stations
Department of Geology and Geophysics
University of Utah
135 South 1460 East, Rm 705 WBB
Salt Lake City, Utah 84112

2 Department of Mining Engineering
University of Utah
135 South 1460 East, Rm 313 WBB
Salt Lake City, Utah 84112

TABLE OF CONTENTS

		Page
EXECUTIVE SUMMARY		i
ACKNOWLEDGMENTS		iii
1.0	INTRODUCTION	1-1
1.1	General Setting and Geology	1-1
1.1.1	Mining Seismicity—Regional Context	1-2
1.2	Objectives and Scope of Work	1-2
1.2.1	The Problem	1-2
1.2.2	Key Elements of Planned UUSS-USGS-USBR Coordination	1-3
1.2.3	Objectives and Scope of This Report	1-4
2.0	SEISMIC ARRAY DESIGN	2-1
2.1	Requirements	2-1
2.1.1	Precise Measurements of Ground Motions	2-1
2.1.2	Location and Characterization of Seismic Sources	2-2
2.2	Array Configuration	2-3
2.2.1	Accelerographs	2-3
2.2.2	Seismic Monitoring	2-4
2.3	Installation and Duration of Array	2-5
2.3.1	Change in Mine Plan and Schedule	2-5
2.3.2	Duration of Monitoring	2-6
3.0	DATA ACQUISITION, PROCESSING, AND ANALYSIS	3-1
3.1	Data Acquisition and Recording	3-1
3.1.1	Analog-Telemetry Recording System	3-1
3.1.2	Digital -Telemetry Recording System	3-2
3.1.3	On-Site Recording Systems	3-2
3.2	Data Processing	3-3
3.2.1	Instrument Calibration	3-3
3.2.2	Trail Mountain Velocity Model	3-3
3.2.3	Preliminary Data Processing	3-4
	Data from Analog- and Digital-Telemetry Systems	3-4
	Data from On-Site Recording Systems	3-4
	Data Reporting on Project Web Site	3-5
3.3	Data Analysis	3-5
3.3.1	Selection of Seismic Events for Detailed Analysis	3-5
	USGS Data Set	3-5
	UUSS Refined Data Set	3-6
3.3.2	Refinement of Hypocenters	3-6
3.3.3	Magnitude Calculations	3-7
3.3.4	Focal-Mechanism Analysis	3-8

TABLE OF CONTENTS (continued)

4.0 OBSERVED MICROSEISMICITY 4-1
- 4.1 Time-Varying Rates of Seismic Activity 4-1
- 4.2 Magnitude Distribution 4-2
- 4.3 Earthquake Locations 4-3
  - 4.3.1 Epicentral Quality 4-3
  - 4.3.2 Overview of Epicentral Distributions 4-4
  - 4.3.3 Space-Time Seismicity in the Trail Mountain Mine Area 4-4
  - 4.3.4 Focal Depths 4-5
    - *Deeper Tectonic Earthquakes?* 4-5
    - *Depth of Shallow Shocks Relative to Mine Level?* 4-5
- 4.4 Source-Mechanism Information 4-6

5.0 REFERENCES 5-1

LIST OF TABLES

Table 2-1 Field Project Timeline

Table 3-1 Data-Acquisition Scheme for Trail Mountain Seismic Array

Table 3-2 Seismic Events Recorded on Independently Triggered Stations — October 3, 2000 – April 30, 2001

Table 3-3 Statistics for Hypocentral Location Error

Table 4-1 List of all Located Events in the TM Extended Study Area with Focal Depths ≥ 2.5 km

LIST OF FIGURES

Figure 1-1 Location map of the Trail Mountain study area.

Figure 1-2 Oblique aerial view to ENE looking across Joes Valley Reservoir and graben toward the steep western flank of Trail Mountain.

Figure 1-3 Oblique aerial view to NW looking toward the steep southern and eastern flanks of Trail Mountain.

Figure 1-4 Seismicity map of the Utah region, 1978-2000, showing the location and setting of the Wasatch Plateau-Book Cliffs coal mining region.

Figure 1-5 Epicenter map of all seismic events located by the University of Utah regional seismic network in the Wasatch Plateau-Book Cliffs coal mining region from January 1, 1978, through June 30, 2000.

TABLE OF CONTENTS (continued)

Figure 2-1 Map showing the distribution of eight triaxial accelerographs installed above, within, and surrounding the Trail Mountain Mine for ground-motion measurements.

Figure 2-2 Map of Trail Mountain seismic array.

Figure 2-3 Map showing stations of the University of Utah regional seismic network in the vicinity of the Trail Mountain study area.

Figure 2-4 Map of Trail Mountain showing details of the 1st and 2nd Right longwall panels—including timing of active mining, depth of cover, and areas of the two panels ultimately mined or left unmined.

Figure 3-1 Example webicorder images from stations TS2 and TS3 for a 24-hour period.

Figure 3-2 Scatter plots showing the distribution of 1,202 ground-motion measurements made at stations TB1, TB2, and TB3 in peak ground acceleration-distance space and corresponding magnitude-distance space.

Figure 3-3 Epicenter map of 49 seismic events selected as candidates for the USGS to consider for special analysis.

Figure 3-4 Epicenter map of 246 seismic events belonging to the UUSS refined data set and located within the local study area.

Figure 4-1 Histogram of the number of located earthquakes per day in the Trail Mountain earthquake catalog (October 3, 2000–April 30, 2001).

Figure 4-2 Histogram of 1,913 earthquakes in the Trail Mountain earthquake catalog (October 3, 2000–April, 30, 2001) showing distribution by time of day.

Figure 4-3 Histogram of magnitude distribution for 1,913 events in the Trail Mountain earthquake catalog (October 3, 2000–April 30, 2001).

Figure 4-4 Plots of magnitude versus time from continuous monitoring of seismicity in the Trail Mountain local study area during October 2000 through April 2001 and January 1999 through December 2001.

Figure 4-5 Epicenter map of entire Trail Mountain earthquake catalog (extended study area).

Figure 4-6 Epicenter map of better-located seismic events (Quality A, B, C) within the local study area.

TABLE OF CONTENTS (continued)

Figure 4-7 Epicenter maps of better-located earthquakes (Quality A, B, C) in the Trail Mountain Mine area for six consecutive time periods between October 2000 and April 2001 corresponding to periods of non-mining and active longwall mining.

Figure 4-8 Focal-depth histograms for the Trail Mountain earthquake catalog (October 3, 2000-April 30, 2001) and for earthquakes in the local study area with well-constrained depths < 2.5 km.

Figure 4-9 Epicenter map of extended study area showing locations of 24 earthquakes located with focal depth ≥ 2.5 km and 43 earthquakes recorded with at least one compressional first motion.

APPENDICES

Appendix A Specifications and Calibration Data for Instrumentation Used in the Trail Mountain Study

Appendix B Seismic Velocity Model for the Trail Mountain Study Area — By James C. Pechmann, Walter J. Arabasz, Kristine L. Pankow and Matthew E. Jensen

Appendix C Tabulation of Ground-Motion Data Delivered to USGS for Detailed Analysis

Appendix D List of All Located Seismic Events in the Trail Mountain Local Study Area, October 3, 2000–April 30, 2001

Appendix E Constraints on Locations of Mining Seismicity in the Trail Mountain Area — by Kristine L. Pankow, Matthew E. Jensen and James C. Pechmann

Appendix F Trail Mountain Project—Mining Engineering Considerations for Assessing Maximum Magnitude for Seismic Events — by Michael K. McCarter, with contributions from Jefferson D. McKenzie

EXECUTIVE SUMMARY

The issue addressed in this report is the hazard of surface ground shaking caused by mining seismicity. Of specific concern is whether Joes Valley Dam, a zoned earthfill dam 58 m (190 ft) high that impounds Joes Valley Reservoir, may be vulnerable to adverse impact by future underground coal mining in the nearby Cottonwood Coal Tract, a planned lease tract in the Trail Mountain area of northwestern Emery County, Utah.

The problem posed at the outset of this study was: *How close to the Joes Valley Dam should future underground mining be allowed in the Cottonwood Coal Tract in order to avoid adverse impact on the dam by mining-induced seismic events?*

The objectives for this project were (1) the collection of relevant seismological data and an assessment of the maximum credible earthquake (MCE) that might be induced by future underground mining in the Cottonwood Coal Tract and (2) determination of the expected attenuation of ground motion as a function of distance and magnitude. Evaluating the response of Joes Valley Dam to potential ground shaking induced by the MCE is the separate responsibility of the U.S. Bureau of Reclamation.

To address the objectives, an instrumentation and work plan was formulated jointly in May to July 2000 by Dr. Walter Arabasz of the University of Utah Seismograph Stations (UUSS), Dr. Art McGarr of the U.S. Geological Survey (USGS), and Dr. Jon Ake of the U.S. Bureau of Reclamation (USBR)—together with the involvement of colleagues from their respective institutions. Herein, we refer to these joint participants as the "Joint Working Group." The chief focus of the work plan was to use mining seismicity at the (then) active Trail Mountain Mine, owned and operated by PacifiCorp and its subsidiaries, as an opportune active source for investigating ground motion as a function of event size and distance. UUSS and the USGS were assigned primary responsibility for objectives (1) and (2), respectively.

In late 2001, with concurrence from SITLA, the Joint Working Group decided on the following approach to reporting results from the Trail Mountain Project. UUSS and USGS would initially prepare separate reports summarizing parts of the project for which they were responsible. Following completion of these informational reports, the Joes Valley Working Group would then write an overarching report to integrate findings, interpretations, and conclusions—including a probabilistic assessment of the MCE.

Consistent with the above framework, this UUSS report focuses on (1) the design of a multi-element seismic array that was installed in the Trail Mountain study area in late 2000 to acquire necessary data, (2) a description of details relating to the recording, processing, and routine analysis of the seismic data acquired by the special-study array, and (3) a description of the mining seismicity that was observed as a result of continuous seismic monitoring during the period October 3, 2000–April 30, 2001. We address the maximum-magnitude issue in a preliminary way in the form of an appended contribution by M. K. McCarter entitled, "Trail Mountain Project—Mining Engineering Considerations for Assessing Maximum Magnitude for Seismic Events."

The seismic array installed by the University of Utah in the Trail Mountain area was an artful combination of instruments aimed at meeting the dual objectives of (1) high-fidelity

accelerographic recordings of ground motions for selected seismic events and (2) continuous monitoring of seismic activity in the study area with the capability of locating events large enough to be sufficiently recorded by multiple instruments. Eight accelerograph stations (including a USBR station on Joes Valley Dam) were installed above, within, and surrounding the Trail Mountain Mine. Short-period sensors were added in a strategic way, including collocation, resulting in a 12-station local seismic array. Three types of data-recording systems, each independent, were used to record data, including a digital-telemetry recording system, an analog-telemetry recording system, and on-site digital recording systems. More than 17,000 event triggers were processed.

When this project was planned in mid-2000, mining of the last two longwall panels in the Trail Mountain Mine was projected to last from September 2000 through August 2001. But a change in mine plan and schedule in October 2000, due to unmanageable bumps and unsafe conditions, reduced the total duration of expected mining by four to five months, and the creation of a barrier pillar for mining the last panel significantly reduced both the frequency and magnitudes of mining seismicity. Nevertheless, sufficient data were successfully captured to meet the project objectives, thanks to the use of highly sensitive digital accelerographs.

High-quality digital accelerographic data for 50 earthquakes were given to the USGS as part of this project under the work plan. The earthquakes included 49 shocks recorded by multiple triaxial accelerographs in the Trail Mountain seismic array and selected as candidates for the USGS to consider for special analysis, plus three-component accelerograms captured by two digital accelerographs installed by the University of Utah that were about 2 km and 7.5 from the magnitude 4.2 earthquake near the Willow Creek Mine on March 7, 2000.

The primary database we present and discuss in this report relates to a set of 1,931 earthquakes located in the Trail Mountain study area during the period October 3, 2000–April 30, 2001, with magnitudes ranging from 0.0 up to 2.2. Using this database, we describe (1) temporal variations in seismic activity, (2) the magnitude distribution of the recorded seismicity, (3) the earthquake locations both in space and time, and (4) information regarding source mechanisms.

The observed seismicity is highly correlated with mining activity in both time and space. Time-varying rates of seismicity correlate with variations in mining operations on scales of weeks to days to hours. In map view the preponderance of seismicity can be associated spatially with identified areas of contemporaneous or past mining. On a fine scale, densely clustered epicenters coincident with the 1st Right longwall panel in the Trail Mountain Mine are laterally bounded by envelopes approximately 250 m to either side of the longwall panel. Space-time sampling allowed a clear tracking of seismicity with the eastward advance of the longwall on a time scale of days and weeks.

Given various tradeoffs that had to be made in the original design of the seismic array, precise resolution of the depth of mine tremors relative to mine level was not achievable. Nevertheless, the overwhelming majority of computed focal depths—including special subsets of data selected for refined processing—are very shallow (< 1 km). Constraints on focal-depth resolution allow us to conservatively state that most of the better-located seismic events occurred within ± 0.6 km of mine level of the Trail Mountain Mine.

ACKNOWLEDGMENTS

We thank John Blake and Tom Faddies of the State of Utah Schools and Institutional Trust Lands Administration (SITLA) for facilitating this project in many supportive ways. We also offer our hearty thanks to the co-participants in the Joint Working Group for this project—Art McGarr and Joe Fletcher of the U.S. Geological Survey (USGS) and Jon Ake of the U.S. Bureau of Reclamation (USBR). Thanks too to Chris Wood of the USBR for enabling instrumentation on the Joes Valley Dam and Russ Sell of the USGS for computing help.

The detailed monitoring of mining seismicity associated with the Trail Mountain Mine would have been impossible without the gracious cooperation and help of the mine's owners and operators. In particular, we thank Scott Child and Rodger Fry of Interwest Mining Company, a subsidiary of PacifiCorp, and Carl Pollastro, Chuck Semborski, Earl Snow, Bevan Branson, Larry LaFrentz, Kerry Larsen, Rick Cullum, and Vernon Childs, all of Energy West Mining Company, another subsidiary of PacifiCorp. We thank Dawn Soper of SITLA and Cindy Kiel of the University of Utah for making necessary legal arrangements with PacifiCorp.

Jim Kohler of the U.S. Bureau of Land Management (BLM) kindly guided the Joint Working Group in a geological field reconnaissance of the study area as part of the project planning and later served as a useful resource for non-proprietary geological information. Dale Harber and Leland Matheson of the U.S. Forest Service gave us timely help with the permitting and siting of eight of the surface stations—and we thank Dale Harber for welcome help with part of their field construction. Jay Mark Humphrey of the Emery County Water Conservancy kindly provided a field crew to help with site construction for one day. We also thank Joan Hubert of BLM for expediting a site permit for station TS6.

We owe special thanks to our colleague Jim Pechmann of the University of Utah Seismograph Stations (UUSS) for invaluable suggestions and critical evaluations relating to seismological aspects of the study, for his help with magnitude calibration, and for his contribution of Section 3.3.3 and Appendix B to this report. We are also indebted to many staff members of UUSS who were involved in completing a host of project tasks. In particular, we thank Ken Whipp and Dave Drobeck for engineering and field installation of the seismic array; Gordon Johansen and Marty Mason for field assistance; Greg Steiner for help in engineering and installing the underground station TU1; and Natalie Arseneau, Jeff Fotheringham, Matt Jensen, Ali Moeinvaziri, Lorraine Nelms, Elizabeth Siebeneck and Fabia Terra for extensive technical help with data analysis, computing, and graphics. Sid Hellman and Paul Friberg of Software Technologies, Inc., helped with programming support.

Many individuals provided key information and insights relating to mining-engineering aspects of this study. Several who are employees of Interwest Mining Company or Energy West Mining Company have been acknowledged above. Jeff McKenzie of the University of Utah's Department of Mining Engineering provided many useful insights from his mining engineering experience, and his contributions to Appendix F of this report are gratefully recognized. We thank Dave Tabet of the Utah Geological Survey, for information used in constructing a coal-bed model for the Cottonwood Lease Tract, and Tom Hurst and John Mercier of RAG American Holding, Inc., for information relating to the Willow Creek Mine.

Funding for this project was provided by the State of Utah Schools and Institutional Trust Lands Administration. Ongoing operational support for UUSS, which furnished important infrastructure, facilities, and some personnel effort for completing this project, is provided by the State of Utah under a line-item appropriation to UUSS and by the U.S. Geological Survey .

1.0 INTRODUCTION

The generation and triggering of seismic events by underground mining in the Wasatch Plateau and Book Cliffs coal fields in east-central Utah both are well-recognized phenomena (e.g., Wong, 1993; Arabasz et al., 1997; Arabasz and Pechmann, 2001; Ellenberger et al., 2001). While mining seismicity is usually viewed in terms of its threat to mining safety, the issue addressed in this report is the hazard of surface ground shaking caused by such seismicity and its potential impact on an offsite structure. Of specific concern is whether Joes Valley Dam, a zoned earthfill dam 58 m (190 ft) high that impounds Joes Valley Reservoir, may be vulnerable to adverse impact by future mining in the nearby Cottonwood Coal Tract—a planned lease tract in the Trail Mountain area (Figure1-1).

In this report, we use the terms mining seismicity and mine tremors as general terms encompassing all seismic events induced by mining. By convention, microseismic events (microseismicity) refer to seismic events smaller than magnitude 3. We follow Gibowicz (1990b), among others, in restricting the term rockburst (or "coal bump") to those seismic events associated with damage to accessible areas of a mine due to violent failure of rock. In an underground mine setting, seismic energy can radiate either from the sudden failure of material in the direct vicinity of mining openings or from seismic slip on a geologic structure hundreds to thousands of meters away in the surrounding rock mass (e.g., Gibowicz, 1990a; Knoll and Kuhnt, 1990).

1.1 GENERAL SETTING AND GEOLOGY

The Trail Mountain area (Figure 1-1) is located in the northwestern part of Emery County in east-central Utah about 45 km (28 mi) southwest of Price; the eastern boundary of the study area shown in Figure 1-1 is 9 km (5 mi) west of the town of Castle Dale on state highway 29. Oblique aerial photographs in Figures 1-2 and 1-3 give a visual overview of some of the major topographic features identified in Figure 1-1. Hereafter, we refer to the area outlined by the bounds of Figure 1-1 as the *extended study area* or simply the *study are*a; the smaller area outlined by the inset rectangle in Figure 1-1 will be referred to as the *local study area*.

The study area lies within the Wasatch Plateau coal field, a major coal field from which underground mines produce more than 60 percent of Utah's current annual coal production of about 25 million short tons (Jahanbani, 2001). The Wasatch Plateau itself is one of a series of NNE-trending, high-standing plateaus along the northwestern rim of the Colorado Plateau that coincide with a geologic transition zone between the Basin and Range and Colorado Plateau provinces (Figure 1-4; see also Arabasz and Julander, 1986).

The Wasatch Plateau is cut by a series of narrow, *en echelon* north-south-trending graben (down-dropped fault blocks), formed by relatively young geologic uplift and east-west extension. One of these, the Joes Valley graben—within which Joes Valley Reservoir is impounded—lies along the western edge of Trail Mountain (see Figure 1-2). The graben is structurally controlled by the Joes Valley fault zone, which shows evidence of young surface

faulting during Holocene to latest Pleistocene (0–30,000 yrs) time (Foley et al., 1986; Hecker, 1993).

Trail Mountain, a feature of central importance in the study area, is underlain by sedimentary strata of upper Cretaceous to Tertiary age that dip gently (< 5°) westward (e.g., Doelling, 1972). As an element of the Wasatch Plateau, the mountain's upper surface has flat-topped mesas standing at elevations ranging from about 2,600 m (8,500 ft) to more than 3,000 m (9,800 ft). The mountain's western side is structurally controlled by the Joes Valley fault zone (Figure 1-2); steep canyon walls forming its southern and eastern sides (Figure 1-3) are the result of erosional incision of the Wasatch Plateau from the east.

Figure 1-3 provides a good overview of the stratigraphy of the Trail Mountain study area (see Doelling, 1972; additional details are provided in Appendix F). Rock formations exposed in the canyon walls in the left foreground of the figure are (from bottom to top): (1) the light-colored, slope-forming Masuk Shale member of the Mancos Shale (sandy shales); (2) the cliff-forming Starpoint Sandstone (thick sandstones and interbedded shales); (3) the slope-forming, vegetated Blackhawk formation (interbedded sandstones, siltstones, shales, and coal—in the lowest part of the formation); (4) the light-colored Castlegate Sandstone (massive cliff-forming sandstone); and, immediately overlying the Castlegate Sandstone, (5) the slope-forming, vegetated Price River Formation (interbedded sandstones, shales, and conglomerates). The uppermost strata exposed on Trail Mountain, above the Price River Formation, belong to (6) the Cretaceous/Tertiary North Horn Formation (varicolored shales, bentonitic mudstones, and lacustrine limestones) and (7) the Tertiary Flagstaff Limestone (lacustrine limestone).

1.1.1 Mining Seismicity—Regional Context

Mining seismicity in the Wasatch Plateau (WP)-Book Cliffs (BC) coal-mining region is sizable enough to be routinely recorded by the University of Utah's regional seismic network (Arabasz et al., 1997; Arabasz and Pechmann, 2001). Clustered epicenters spatially coincident with sites of active underground mining in the WP-BC area form a prominent arcuate crescent on regional seismicity maps, such as shown in Figure 1-4. Abundant mining seismicity has occurred in the vicinity of mines within and near the Trail Mountain study area. This is shown by Figure 1-5, an epicenter map of 6,851 seismic events (magnitude ≤ 4.2) located by the regional seismic network for the period January 1978 through June 2000; large stars indicate what coincidentally are the three largest mining-related seismic events in the WP-BC region since instrumental monitoring began in July 1962.

1.2 OBJECTIVES AND SCOPE OF WORK

1.2.1 The Problem

The specific problem posed at the outset of this study was: *How close to the Joes Valley Dam should future underground mining be allowed in the Cottonwood Coal Tract (Figure 1-1) in order to avoid adverse impact on the dam by mining-induced seismic events?*

The answer to the problem, as stated, ultimately requires both an engineering analysis of the response of Joes Valley Dam to induced vibratory ground motions and regulatory decision-making. In May 2000, SITLA clarified the objectives for this project to be, first, the collection of relevant seismological data and an assessment of the maximum credible earthquake (MCE) that might be induced by future underground mining in the Cottonwood Coal Tract and (2) determination of the expected attenuation of ground motion as a function of distance and magnitude. Evaluating the response of Joes Valley Dam to potential ground shaking induced by the MCE was confirmed to be the separate responsibility of the USBR; an engineering analysis would have to be undertaken using results provided by this project.

To address the objectives posed by SITLA variously relating to seismological information, the MCE, and ground-motion attenuation, an instrumentation and work plan was formulated jointly in May to July 2000 by Dr. Walter Arabasz of the University of Utah Seismograph Stations (UUSS), Dr. Art McGarr of the U.S. Geological Survey (USGS), and Dr. Jon Ake of the U.S. Bureau of Reclamation (USBR)—together with the involvement of colleagues from their respective institutions. Herein, we refer to these joint participants as the "Joint Working Group."

The chief focus of the work plan was to use mining seismicity at the then active Trail Mountain Mine (Figure 1-1), owned and operated by PacifiCorp and its subsidiaries, as an opportune active source for investigating ground motion as a function of event size and distance. Results of the study could then serve as a basis for characterizing the effects on Joes Valley Dam of future mining seismicity in the Cottonwood Coal Tract.

1.2.2 Key Elements of Planned UUSS-USGS-USBR Coordination

1. The overall "Trail Mountain project" would be undertaken as a joint enterprise by the UUSS, USGS, and USBR participants in the Joint Working Group, who would write a joint final report summarizing results and conclusions.

2. UUSS would install and operate a multi-element seismic array designed for detailed seismic monitoring of the Trail Mountain source region and for the precise digital recording of ground motions from the larger events. UUSS would also take the lead in assessing the maximum credible earthquake (MCE) for mining-induced seismicity in the Cottonwood Coal Tract, including collapse-type seismic events.

3. USGS would specially process and analyze digital ground-motion data acquired by UUSS for the relatively larger events in the Trail Mountain study area in order to quantify ground motion as function of distance and magnitude and to assess the peak ground motion at Joes Valley Dam due to nearby mining-induced earthquakes.

4. Relevant data earlier collected by UUSS from the Willow Creek Mine in the nearby Book Cliffs coal field—notably accelerograms from a magnitude 4.2 seismic event on March 6, 2000—would be jointly studied by the Joint Working Group for applicability to the current project.

5. USBR, at its own expense, would upgrade seismic instrumentation on Joes Valley Dam to digitally measure ground motions from the Trail Mountain source region as part of the project. Using the results of Elements 2, 3, and 4, USBR would take the lead in formulating a probabilistic approach to quantifying the ground-shaking hazard, including corresponding uncertainties, at the Joes Valley dam site due to mining-induced earthquakes in the Cottonwood Coal Tract.

1.2.3 Objectives and Scope of <u>This</u> Report

In late 2001, with concurrence from SITLA, the Joint Working Group decided on the following approach to reporting results from the Trail Mountain Project. UUSS and USGS would initially prepare separate reports summarizing parts of the project for which they were responsible—that is, the UUSS report would summarize information dealing with Element 2 and the USGS report would summarize information dealing with Element 3 and the part of Element 4 relating to the analysis of ground-motion recordings of the magnitude 4.2 earthquake near Willow Creek Mine in March 2000. Following completion of these informational reports, the Joes Valley Working Group would then write an overarching report to integrate findings, interpretations, and conclusions.

Consistent with the above framework, this UUSS report focuses on Element 2 of section 1.2.2. We proceed to describe relevant information and results in the following order. First, in section 2, we describe the design of a multi-element seismic array that was installed in the Trail Mountain study area to acquire necessary data. Next, in section 3, we describe details relating to the recording, processing, and routine analysis of the seismic data acquired by the special-study array. Then, in section 4 we describe the mining seismicity that was observed as a result of continuous seismic monitoring during the project period. Because a formal probabilistic assessment of maximum magnitude in the Cottonwood Coal Tract will be reported in the Joint Working Group's integrated report, in this report we address the maximum-magnitude issue only in a preliminary way. This is done in a separate contribution by M. K. McCarter included here as Appendix F.

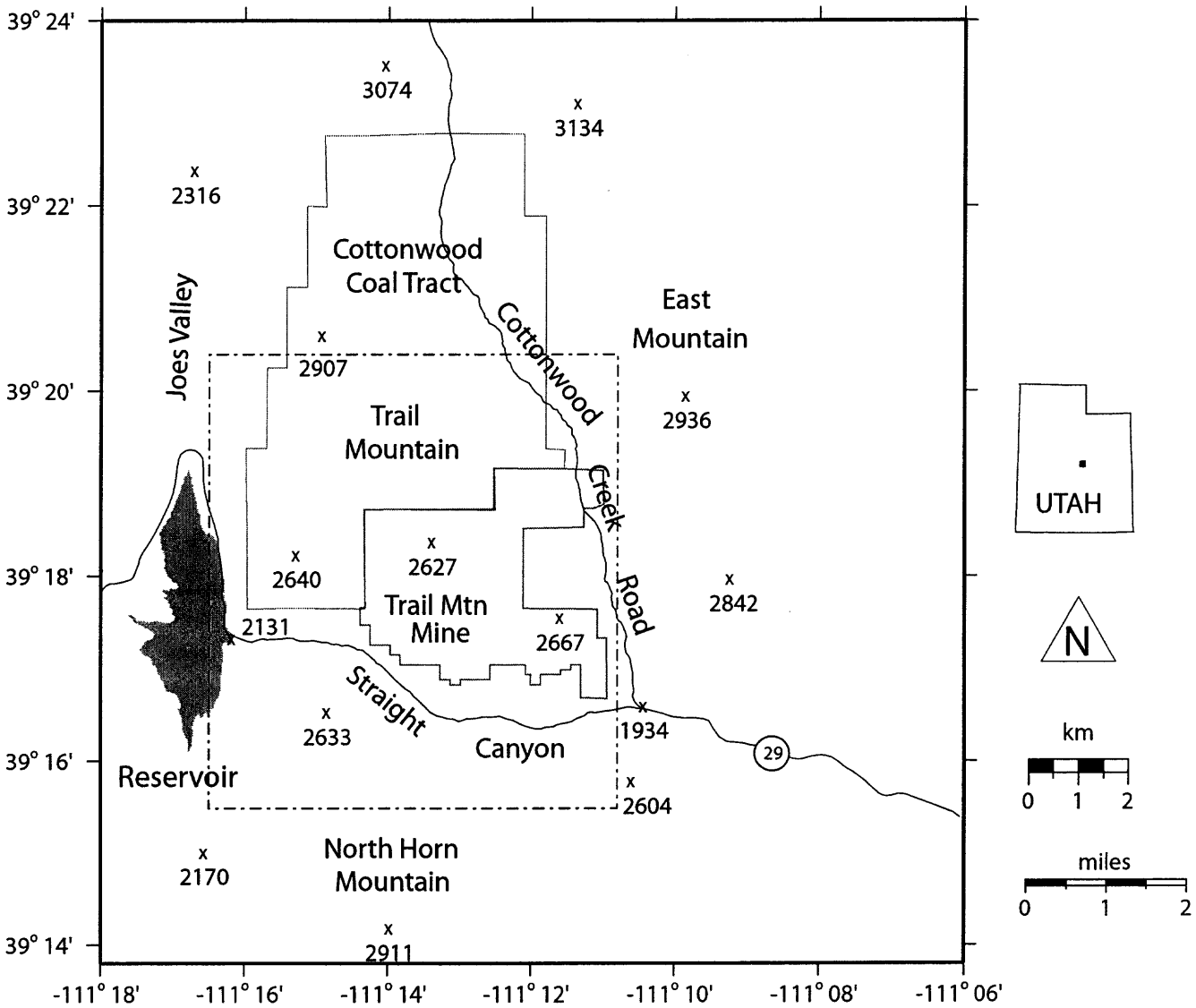

Figure 1-1. Location map of the Trail Mountain study area. For reference, the bounds of the map define the "extended study area"; dashed rectangular inset, the "local study area"; x's, selected elevations (in meters).

Figure 1-2. Oblique aerial view to ENE looking across Joes Valley Reservoir and graben toward the steep western flank of Trail Mountain. Topographic relief between the reservoir and Trail Mountain's summit height of 3,074 m (10,084 ft) is approximately 940 m (3,080 ft). Joes Valley Dam (spilling eastward into Straight Canyon) is in the middle right. (Photo by M. K. McCarter, November 3, 2001)

Figure 1-3. Oblique aerial view to NW looking toward the steep southern and eastern flanks of Trail Mountain; view is across Straight Canyon (lower left) and across the Cottonwood Creek drainage (rising from lower left to upper right). Topographic relief in left foreground is approximately 850 m (2,800 ft). (Photo by M. K. McCarter, November 3, 2001)

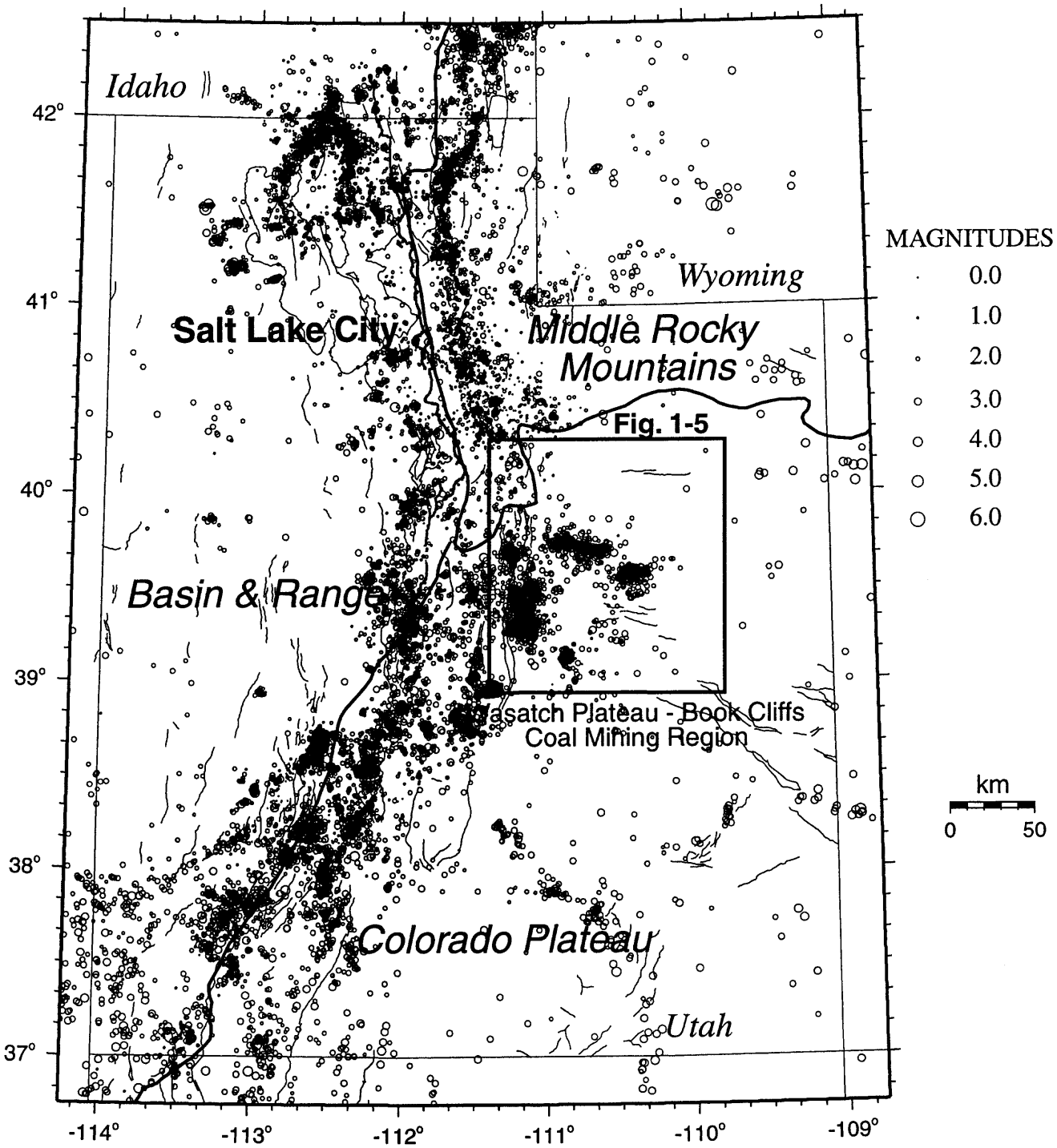

Figure 1-4. Seismicity map of the Utah region, 1978–2000, showing the location and setting of the Wasatch Plateau-Book Cliffs coal mining region (Figure1-5). Heavy lines indicate boundaries of major physiographic provinces; light lines, geologically young faults. Earthquake data from the University of Utah Seismograph Stations.

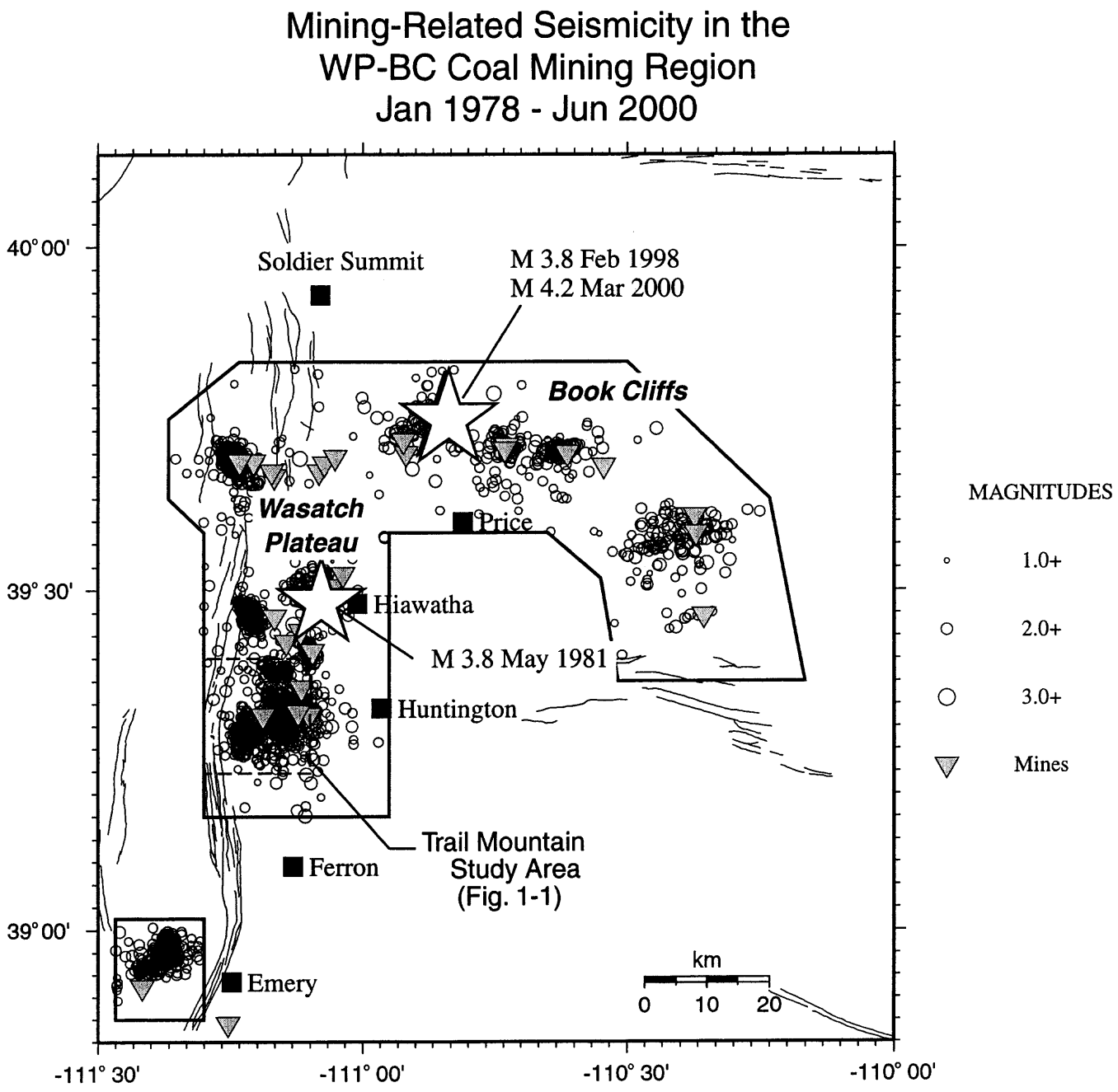

Figure 1-5. Epicenter map of all seismic events located by the University of Utah regional seismic network in the Wasatch Plateau (WP)-Book Cliffs (BC) coal mining region from January 1, 1978, through June 30, 2000. Polygons (after Arabasz et al., 1977) circumscribe areas within which nearly all seismicity is inferred to be mining-related. Stars (labeled) indicate the three largest mining-related seismic events in this area instrumentally recorded since 1962. Geologically young faults are shown by light lines. From Arabasz and Pechmann (2001).

2.0 SEISMIC ARRAY DESIGN

In this section we describe the makeup and geometry of the seismic array installed in the Trail Mountain area for this project together with factors and constraints that significantly influenced its design and operation. The starting point for planning the array was a reconnaissance of the Joes Valley Dam-Trail Mountain area by members of the Joint Working Group on June 1, 2000. The purpose of the field reconnaissance was, first, to become familiar with the local geology as it related to seismic wave propagation and surface site characteristics that might affect ground-shaking; second, to evaluate the physical aspects of the study area as they affected instrument siting, logistics, and telemetry; and, third, to develop a workable and effective design for a seismic array that would meet the project objectives. A preliminary design made at that time was later refined and proposed to SITLA on July 7, 2000.

The combined experience of the Joint Working Group was central in arriving at the final array design. Recognizing that instrumentation costs would be unavoidably high to meet the project requirements, the working group considered various alternatives but decided against choices that would compromise "doing it right" or jeopardize successful data acquisition. A robust final design was facilitated by UUSS providing equipment to meet about 30 percent of the required field instrumentation as well as facilities for data recording, processing, and analysis.

2.1 REQUIREMENTS

The basic design requirements for the field project were to ensure both (1) precise measurements of ground motions over a range of distances appropriate to the problem (i.e., quantifying ground shaking as a function of distance on a scale of kilometers (see Figure 2-1) and (2) accurate location (< 1 km) and characterization of the seismic sources giving rise to those motions. In order to determine an attenuation relation for ground motion as a function of distance, the independent variable of distance (and hence source location) must be known. The primary seismic sources were mining-induced earthquakes known to be occurring within and very close to the (then) active Trail Mountain Mine. When the project was planned in mid-2000, mining in the Trail Mountain Mine was projected to last through August 2001. A secondary target was the opportune recording of any naturally occurring tectonic earthquakes within the study area, given that the array would be operating for several months.

2.1.1 Precise Measurement of Ground Motions

The state of practice for precisely measuring earthquake ground motion for earthquake-engineering applications is to use triaxial digital accelerographs (which record one vertical and two horizontal components of acceleration and allow the accurate recovery of corresponding velocity and displacement by integration) with at least 18-bit resolution, more than 100 dB dynamic range, a response flat to acceleration in the band 0.02 to 50 Hz, timing accuracy to better than ± 0.5 millisecond (typically using a GPS timing system), and a selectable trigger threshold to enable recording weak as well as strong ground motions (accelerations << 0.1 g

and 0.1 g to 2 g or more, respectively). A relevant cost constraint was the fact that instrumentation of this type exceeds $10,000 per station without telemetry equipment.

2.1.2 Location and Characterization of Seismic Sources

The ability to resolve the *focus* or *hypocenter* of a seismic source (its origin point in three-dimensional space) basically requires (1) precise timing of seismic-wave arrivals, (2) an accurate velocity model, (3) a good azimuthal distribution of instruments surrounding the source to constrain its *epicenter* (map location), and (4) a nearest-station distance equal to or smaller than the depth of the source to constrain its *focal depth*. A seismic source is actually specified by four dimensions—x, y, and z coordinates together with origin time. If epicentral control is good but focal-depth control is poor, there is a trade-off between depth and origin time when a location algorithm inverts the arrival times of seismic waves to solve for the source's hypocenter, and large standard errors result in the focal-depth determination.

Scale considerations are important in designing an array for seismic monitoring. Given a limited number of instruments, there are invariable trade-offs between hypocentral resolution, which scales with instrument spacing, and geographic coverage. Fine-scale spatial resolution of mine tremors on a scale of tens of meters would ideally be achieved by an in-mine microseismic system (e.g., Ellenberger et al., 2001), but this was not considered an option because of cost (exceeding $100,000 for instrumentation) and logistics. An in-mine array would have required a degree of cooperation from the owners and operators of the Trail Mountain Mine—and engagement of expertise for the underground operations—that was unrealistic to arrange successfully without a lead time of many months.

Given that mine tremors were expected to occur in a depth range within a few hundred meters of mine level, it was judged that corresponding epicentral accuracy of the order of hundreds of meters to 1.0 km would suffice for the project objectives, and this was readily achievable with a surface array having a station spacing of a few kilometers. (The required epicentral resolution was not achievable with the University of Utah's existing regional seismic network; see Figure 2-3 below.) It was recognized that precise resolution of the depth of mine tremors, say to ±100 m, would have required a surface station spacing on the order of a few hundred meters (or expensive borehole seismographs), but the Joint Working Group was prepared to sacrifice this goal.

In contrast to the accelerographs required for high-fidelity recording of ground motions for digital signal processing, velocity sensors are better suited for high-magnification recording of small earthquakes, particularly for the precise measurement of P-wave arrival times used for hypocentral locations and for discerning the direction of P-wave first motions used for interpreting source mechanisms. Traditional systems with velocity sensors that are used in regional-scale seismic networks have a short-period response that peaks at about 10 Hz. Broadband velocity sensors (approximately flat to velocity in the band of about 0.03 Hz or lower to 35 Hz) are desirable for more informative signal analysis but are much more costly (several thousand dollars or more for a triaxial sensor).

2.2 ARRAY CONFIGURATION

The final array was an artful combination of instruments aimed at meeting the dual objectives of (1) high-fidelity accelerographic recordings of ground motions for selected seismic events and (2) continuous monitoring of seismic activity in the study area with the capability of locating events large enough to be sufficiently recorded by multiple instruments. The basic elements of the composite array are described next. Detailed specifications for instrumentation at each field site or "station" are provided in Appendix A.

For guidance in following the descriptions of the seismic array, each project station is identified by a unique three- or four-character station code beginning with the letter "T"—except for station JVD, independently installed by the U.S. Bureau of Reclamation on Joes Valley Dam. The prefix "TB" was used for accelerographic stations around the base of Trail Mountain; "TU" for a solitary underground station; and "TS" for six short-period seismograph stations forming part of an analog telemetry network (as explained presently, stations TS2 and TS3 have the added complexity of being collocated with digitally-telemetered accelerographs). For a field station with a digital signal processor, we refer to the field computer as a *data acquisition system* (DAS) if data are stored on-site and as a *data logger* if data are digitally telemetered for recording elsewhere.

2.2.1 Accelerographs

Figure 2-1 shows the distribution of eight accelerograph stations installed above, within, and surrounding the Trail Mountain Mine for ground-motion measurements. These include seven stations labeled with the prefix "T," each with one triaxial accelerometer, together with station JVD on Joes Valley Dam, where a 12-channel DAS was connected to two triaxial accelerometers respectively located on the right abutment and crest of the dam. The figure also shows the surface projection of two longwall mining panels where mining operations were expected during the project period.

Steep topography precluded a simple linear profile of stations between the Trail Mountain Mine and Joes Valley Dam to determine ground-motion attenuation. Instead, accelerographs were placed at accessible sites at different azimuths from the mine so that recordings would be made at varied distances over a range from near-source to about 6 km; because seismicity was expected to migrate along the east-west longwall panels, prospects were enhanced for good sampling throughout this distance range. The station configuration had added advantages. First, it provided sampling of ground-motion measurements with distance at varying azimuths to minimize bias from directional radiation-pattern effects and, second, the spread of stations contributed to areal coverage for source locations.

Accelerograph stations were sited around the base of Trail Mountain on its western side (TB1), in Straight Canyon (TB2), and near the Trail Mountain Mine portal in the Cottonwood Creek drainage (TB3). Another three stations were sited on top of Trail Mountain (TS2, TS3, and TMU). With special efforts, one accelerograph was sited underground within the Trail Mountain Mine itself (TU1).

Logistical constraints on top of Trail Mountain, notably the difficulty of winter-time access, and telemetry constraints within the steep canyon topography around the base of Trail Mountain loomed large in the operational design of the accelerograph array. Continuous data telemetry to the University of Utah's earthquake recording center in Salt Lake City via analog radio links, the state microwave system, and/or leased telephone lines is standardly used for data collection from remote stations in the University of Utah's regional seismic network. Special equipment and communication links are required for digital telemetry of accelerographic (and similar broadband, high-dynamic-range) data. Because of their inaccessibility in winter, the mountain-top accelerographs were designed to provide continuous digital telemetry to the University of Utah via radio links through station TMU to a state microwave node at Cedar Mountain, 53 km (33 mi) to the east.

Telemetry from the accelerograph stations around the base of Trail Mountain was precluded (without extraordinary effort and expense) by the steep canyon topography. Consequently, these stations, along with station JVD, were designed for on-site digital recording, with data to be retrieved weekly by a local field assistant. Similar planning was made for the underground station TU1—with the added complications of special legal arrangements with PacifiCorp for the underground installation and the need to engineer a mile-long cable with signal boosters in order to deliver GPS timing signals from outside the mine portal to the accelerograph.

2.2.2 Seismic Monitoring

To achieve a spatial distribution of stations suitable for continuous seismic monitoring and source locations (as described in section 2.1.2), short-period sensors were added to the designed array in the following strategic way. Six short-period stations (TS1–TS6) with continuous analog radio telemetry (linked to the University of Utah via the state microwave node at Cedar Mountain) were configured to surround the Trail Mountain Mine. Stations TS1–TS5 were within the extended study area and their locations are shown in Figure 2-2. To ensure detection and location capabilities independent of the accelerograph array, stations TS2 and TS3 were collocated with two of the digitally-telemetered triaxial accelerographs on top of Trail Mountain. Station TS6 was sited 12 km (7.4 mi) southeast of station TS5 to add instrumental coverage in the SE quadrant of the array on the scale of the University of Utah's regional seismic network, as shown in Figure 2-3. The regional seismic network has enabled long-term monitoring of the Trail Mountain area, albeit with poor focal-depth control, above a threshold slightly below magnitude 2.0 since 1978 (see Figure 1-5).

Short-period sensors were also installed on top of Trail Mountain at station TMU (Figure 2-2), where they were collocated with a triaxial accelerometer. In this case, three short-period sensors were arranged in a 3-component configuration (two horizontal and one vertical) for improved discrimination of S-waves, and a 6-channel data logger was used to digitally telemeter data simultaneously from the three short-period sensors and the triaxial accelerometer. (For reasons explained in Appendix A, the velocity channels are assigned the code TM2.) Station TS1 was the only other 3-component short-period station in the Trail Mountain array; all others had a single vertical-component sensor.

Finally, to maximize the recording and high-precision timing of P-waves throughout nearly the entire array shown in Figure 2-2, a vertical-component short-period sensor was collocated with the triaxial accelerometer at the accelerograph stations TB1, TB2, TB3, and TU1. At each of these stations, on-site recording was done using a 4-channel DAS. Station JVD (Figure 2-2) was the only station in the Trail Mountain array without a short-period sensor.

2.3 INSTALLATION AND DURATION OF ARRAY

Table 2-1 outlines a timeline for the field project, including the installation and duration of the seismic array. The timeline notes some prerequisite steps for the array deployment, notably site permitting, equipment acquisition, and the completion of a licensing agreement with PacifiCorp for installing the underground station TU1. Beginning in late summer 2000, major efforts were made to expedite all necessary steps for installing the array, mindful of the difficulties that snowfall at high elevations on top of Trail Mountain would pose. An unexpected change in PacifiCorp's mining plan in October 2000, reducing the remaining time of active mining in the Trail Mountain Mine, also brought added time pressures and affected the project timeline.

2.3.1 Change in Mine Plan and Schedule

When this project was planned in mid-2000, longwall operations (and associated seismicity) were anticipated in two east-west panels identified as "1st Right" and "2nd Right" in Figure 2-4. Mine operators originally estimated that mining in 2nd Right would occur from September 2000 to March 2001, after which the longwall would be moved to 1st Right, where mining would continue from March 2001 through August 2001.

Mining began in the 2nd Right panel on September 11, 2000, but was interrupted less than one month later on October 5 due to unmanageable bumps and unsafe conditions. As illustrated in Figure 2-4, the longwall at this point had advanced only about one-fifth the length of the panel. Based on a joint decision by the mine operators and officials of the Mine Safety and Health Administration (MSHA), mining in 2nd Right was suspended on October 23 and the longwall was moved to 1st Right. The set-up point in 1st Right was more than one-fifth the distance into the panel (Figure 2-4) so that the unmined coal in 2nd Right to the south would create a continuous barrier pillar. Mining commenced at the new set-up in 1st Right on November 7, 2000, and ended on March 7, 2001, thus reducing the total duration of expected mining by four to five months.

The unexpected longwall move had two consequences for the installation of the underground station TU1. The accelerograph was to be originally sited in the headgate entry on the north side of 1st Right, roughly near cross-cut 40, while the longwall advanced past it in 2nd Right; it was then to be moved to the eastern end of 1st Right (its ultimate site) when mining began in that panel. Because of the change in mining plan, only the latter site was occupied. The second consequence of the unexpected longwall move was that mine personnel could not assist in installing TU1 and its GPS cable until late November 2000.

2.3.2 Duration of Monitoring

As indicated in the field project timeline in Table 2-1, data from eight of the 13 stations of the UUSS array were being recorded by early to mid-October 2000. By December 12, the complete UUSS array was operational. Recording at the USBR station JVD on Joes Valley Dam began eight days later on December 20.

All eight stations of the accelerograph array (Figure 2-1) operated continuously (except for a minor interruption at station TB3) from December 2000 through March 7, 2001, when mining in the 1st Right longwall panel was completed and mine personnel removed the underground station TU1. Station TB3 near the mine portal was removed three months later on June 14. We tried to leave as many accelerographs in place as long as possible, simply to extend the opportunity to record any significant seismic events that might occur—whether mine tremors beneath Trail Mountain in the aftermath of mining or local tectonic earthquakes. Stations TS2 and TS3 were removed on October 17, 2001. Stations TB1, TB2, TMU, and JVD were still operating as of February 28, 2002, the end date of the contract for this project.

Together with leaving as many accelerographs in place as long as possible, we continued to operate the short-period array into late summer 2001 so that any sizable events recorded by the remaining accelerographs could be located. Short-period stations TS1 and TS6 were finally removed in August, and stations TS2, TS3, TS4, and TS5 were removed in October. Station TMU was still operating as a composite short-period/accelerographic station as of February 28, 2002, and will tentatively remain a permanent station of the UUSS regional seismic network.

Table 2-1

Field Project Timeline

Date	Action
— 2000 —	
Jul 7	UUSS project proposal submitted to SITLA
Jul 13	Site-permit applications submitted to U.S. Forest Service
Jul 21-31	Field equipment ordered under pre-contract agreement
Aug 1	Contract awarded to UUSS by SITLA
Sep 11	**Mining begins in "2nd Right" longwall panel**
Sep 14	U.S. Forest Service permits granted
Oct 3	Seismic stations TS2, TS3, TS4, and TS5 begin recording
Oct 5	**Mining interrupted in "2nd Right" longwall panel (longwall moved after Oct. 23)**
Oct 10-13	Stations TS1, TS6, TB1, and TB2 begin recording
Nov 7	**Mining begins in "1st Right" longwall panel**
Nov 9	PacifiCorp/SITLA/UUSS license agreement signed for underground station TU1
Dec 1	Station TMU (digital telemetry) begins recording
Dec 5	Station TU1 (underground station) begins recording
Dec 6-7	Stations TS2 and TS3 (digital telemetry) begin recording
Dec 12	**Installation of UUSS seismic array completed**; Station TB3 begins recording; Website for Trail Mountain Project online
Dec 20	Station JVD (USBR instrumentation on Joes Valley Dam) begins recording
Dec 22	Mining in "1st Right" longwall panel interrupted for Holidays
— 2001 —	
Jan 2	Mining in "1st Right" longwall panel resumes
Mar 7	**Mining completed in "1st Right" longwall panel**; Station TU1 removed
Jun 14	Station TB3 removed
Aug–Oct	Stations TS1, TS2, TS3, TS4, TS5, TS6 removed

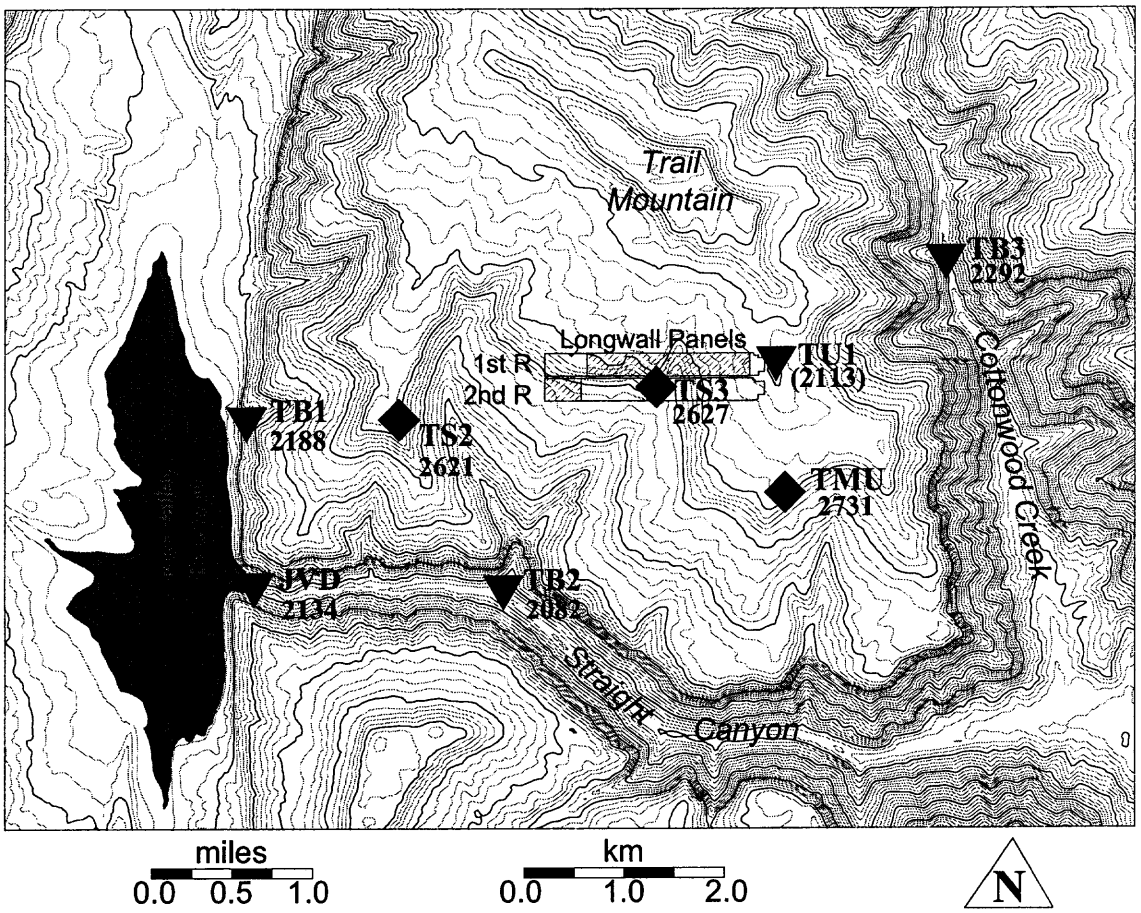

Figure 2-1. Map showing the distribution of eight triaxial accelerographs installed above, within, and surrounding the Trail Mountain Mine for ground-motion measurements (diamonds = digitally telemetered; inverted triangles = on-site recording). Identification code and elevation (m) shown for each station (TU1 is the sole underground station). Also shown are the map projections of the 1st and 2nd Right longwall panels mined during the monitoring period (see Figure 2-4 for explanation of patterns). Contour interval of topographic base is 20 meters.

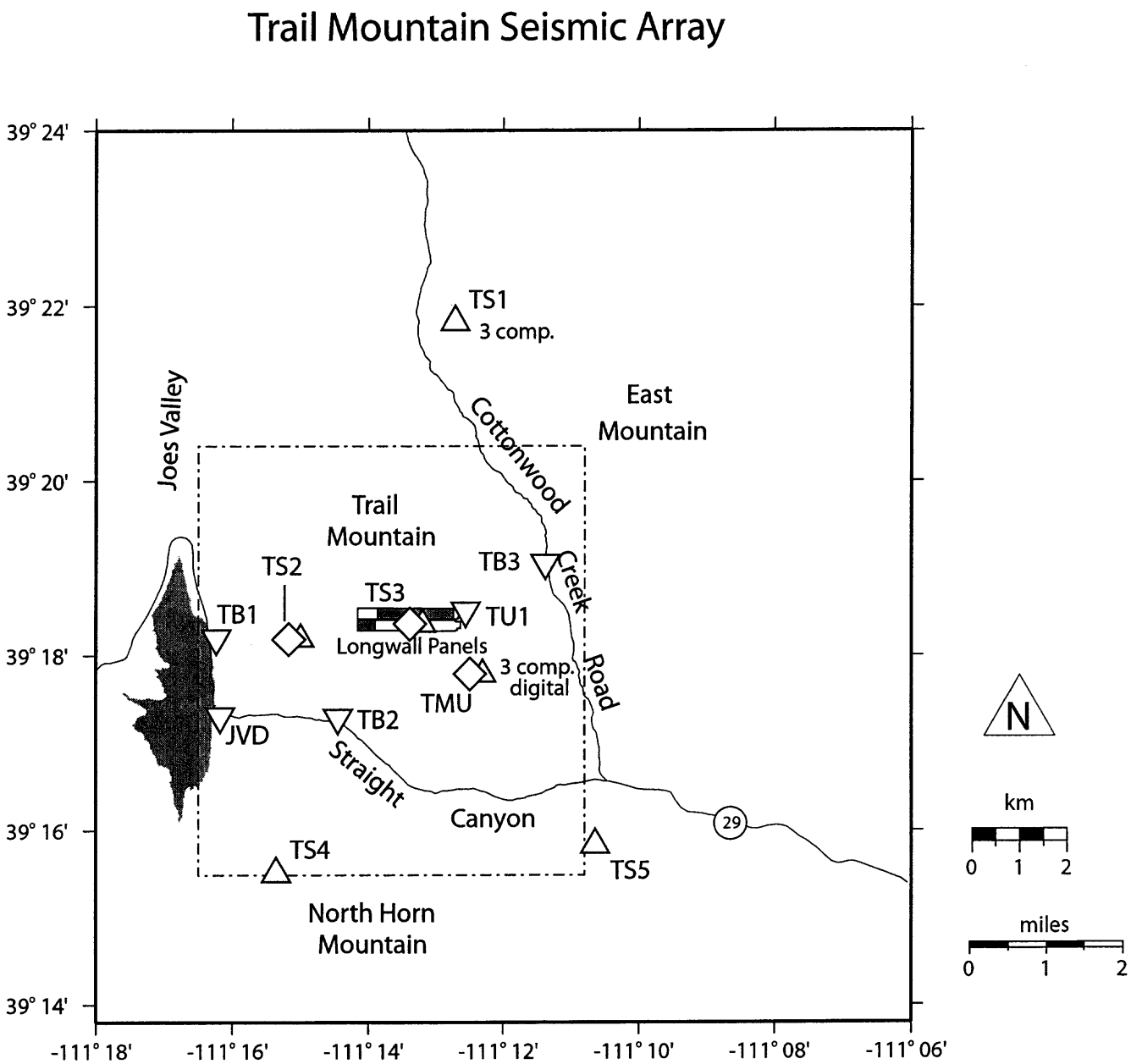

Figure 2-2. Map of Trail Mountain seismic array (station TS6 shown in Figure 2-3). Diamonds = digitally-telemetered accelerographs, inverted triangles = on-site-recording accelerographs, upright triangles = short-period stations. Double-symbols = collocated instruments, as described in text. Short-period stations have a single vertical component and analog telemetry-except for TS1 (3-component) and TMU (3-component, digital telemetry). Longwall panels as in Figure 2-4. Local study area (dashed rectangular inset) shown for reference.

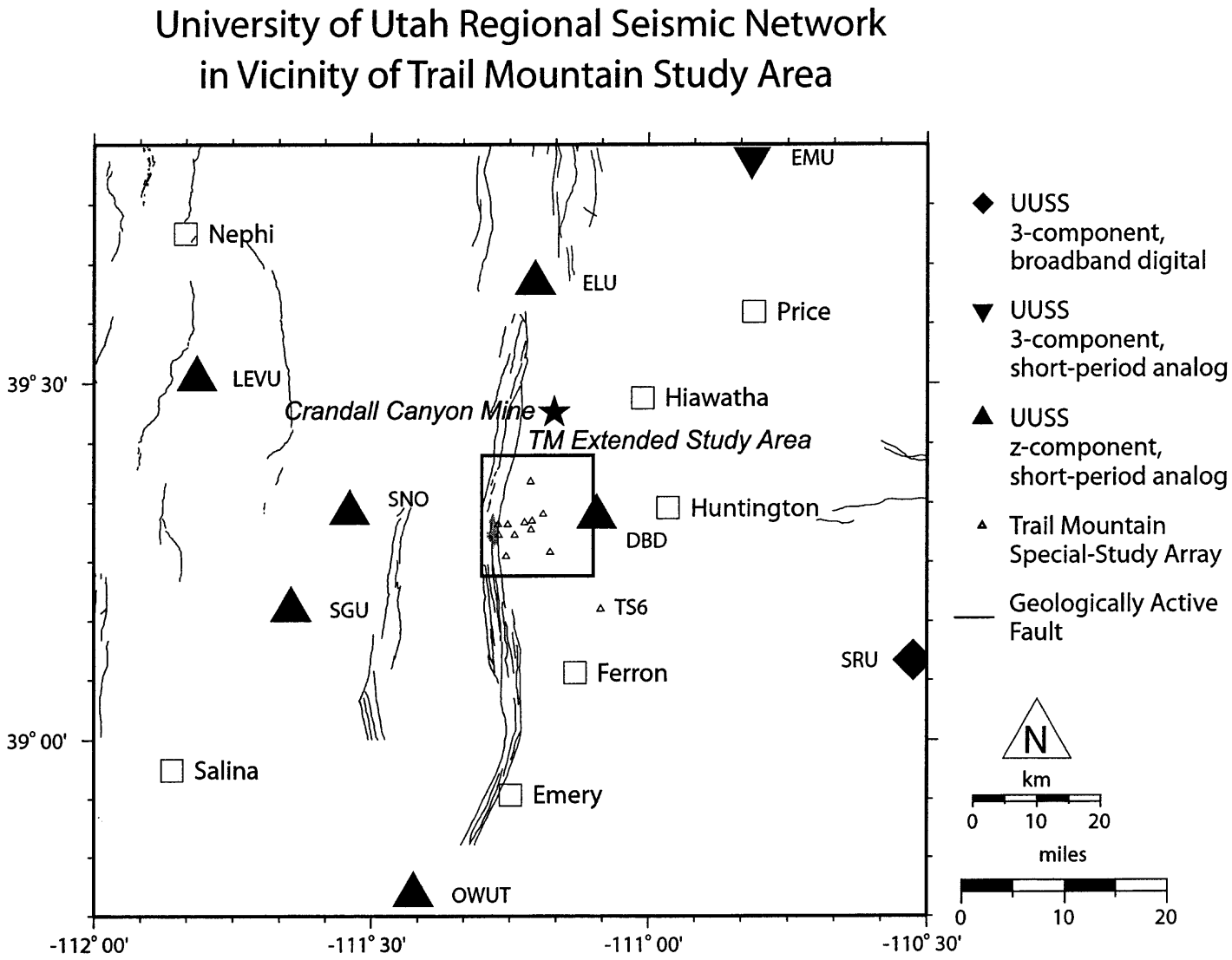

Figure 2-3. Map showing stations of the University of Utah regional seismic network in the vicinity of the Trail Mountain study area (inset rectangle). Star = location of Crandall Canyon Mine; TS6 = a temporary short-period analog station of the Trail Mountain seismic array.

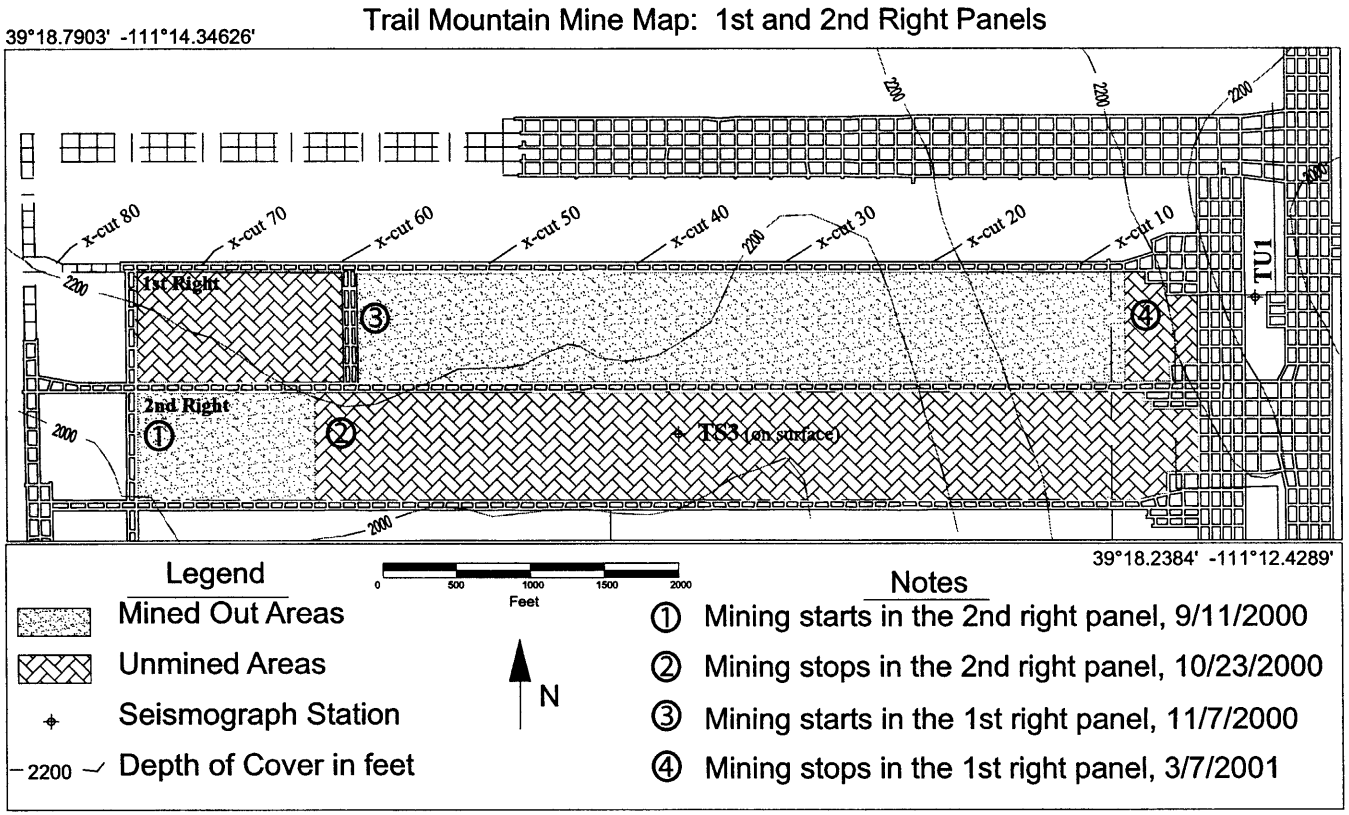

Figure 2-4. Map of Trail Mountain showing details of the 1st and 2nd Right longwall panels-including timing of active mining, depth of cover, and areas of the two panels ultimately mined or left unmined. Also shown are the locations of seismic stations TU1 (within the mine) and TS3 (on surface). Information courtesy of PacifiCorp.

3.0 DATA ACQUISITION, PROCESSING, AND ANALYSIS

3.1 DATA ACQUISITION AND RECORDING

Three types of data-recording systems, each independent, were used to record data from the Trail Mountain seismic array described in section 2.0: (1) an analog-telemetry recording system, (2) a digital-telemetry recording system, and (3) on-site recording systems. Variable types of data (acceleration or velocity records) of differing resolution (12- to 24-bit) resulted from the different combinations of sensors and field electronics. Some data streams were recorded continuously, others in a triggered mode for only discrete time periods. The data collected by the three types of recording systems were processed and analyzed in different ways, sometimes in combination with each other, depending on the type of analysis being performed. Independence of the recording systems provided some redundancy in case of an individual system failure. Each type of recording system is described in detail below. Table 3-1 outlines the data-acquisition scheme for each station of the array, with more details provided in Appendix A.

3.1.1 Analog-Telemetry Recording System

The analog-telemetry recording system applies to data streams from the six short-period stations TS1-TS6 (section 2.2.2; upright triangles, Figure 2-2), which were telemetered via FM analog radio to a central receiving site located on Cedar Mountain, approximately 55 km (34 mi) east of Trail Mountain. At Cedar Mountain, data were multiplexed and transmitted on a single leased microwave channel to the UUSS network center on the University of Utah campus in Salt Lake City. There they were digitized and recorded with 12 bits of resolution. Because of the analog telemetry, this system has a much lower dynamic range than the fully digital systems, causing signal amplitude for some shocks to be clipped. Data from the analog-telemetry network were used to constrain hypocentral locations and to determine "coda" magnitudes based on the duration of the recorded earthquake signal.

Data from the analog-telemetry stations were digitized and recorded as an integrated part of the UUSS regional seismic network. Data-acquisition software at the network center records time slices (a trigger) when the ratio of the short-term to long-term average of the incoming data streams exceeds a designated threshold on a defined number of geographically close seismograph stations (a subnet). For the Trail Mountain project, a special subnet of the Trail Mountain analog telemetry stations was created to enable the recording of very small seismic events that otherwise would be below the detection threshold of the regional network. By varying the number of stations in the subnet required to declare a trigger, the relative number of seismic events recorded could be controlled. Typically the local subnet was set to require four local stations to trigger local event recording. Data from all regional seismic network triggers are routinely archived on magneto-optical disks and on 8-mm tapes for long-term storage.

Data from station TS3 were also recorded on a helicorder (a drum recorder that produces a continuous visible paper recording) in the UUSS network center to provide a daily backup

record of seismic activity near the Trail Mountain Mine. The helicorder records are permanently archived at the University of Utah Seismograph Stations. A Webicorder record (a digital version of a helicorder recording, see Figure 3-1) was created and archived for each 24-hour period for stations TS2 and TS3.

3.1.2 Digital-Telemetry Recording System

The Trail Mountain seismic array included three stations (TS2, TS3, TMU; diamonds, Figure 2-2) whose data were continuously transmitted by digital telemetry from the top of Trail Mountain to the UUSS network center. At sites TS2 and TS3, two independent recording systems operated adjacent to each other: (1) the analog-telemetry system for the short period sensor(s) and (2) a digital-telemetry system, described in this section, for the collocated triaxial accelerometer. At station TMU, the digital-telemetry system had a 6-channel data logger, which was used to process signals from the triaxial accelerometer as well as from three short-period velocity sensors.

At each station with digital telemetry, a 24-bit data logger (either 3-channel or 6-channel) processed the output from each sensor to on-site computer memory and transmitted the data (with full two-way error correction) via spread spectrum digital radios to a relay point at Cedar Mountain. From there the data were digitally transmitted via leased microwave circuits to the UUSS network center. Data were recorded to continuous data files. For seismic events that triggered the analog-telemetry network, matching time slices were extracted from the continuous digital-telemetry data files and were subsequently merged with the analog-telemetry data for use in the hypocentral location process. For station TMU, continuous data files were archived separately to magneto-optical disk and to 8-mm tape from December 2000 through March 2001. Data from the digital-telemetry stations that were merged with the regional seismic network data were archived with the regional network data.

3.1.3 On-Site Recording Systems

Five stations of the Trail Mountain array (TB1, TB2, TB3, TU1, and JVD; inverted triangles, Figure 2-2) had an independently-triggered DAS with data recorded locally to internal disk. Data from these stand-alone stations were recorded in a triggered mode with 19-bits of resolution. A trigger occurred when local ground motion exceeded 0.001% g (acceleration). Because the on-site data disks had limited capacity, a local field assistant routinely visited each station weekly, swapped out recording disks, and mailed disks to Salt Lake City for data extraction and return. After mining ended in the Trail Mountain Mine on March 7, 2001, data were retrieved every two weeks through February 2002. A major time-consuming task was the necessary correlation of data from each on-site recording station with data from the other two recording systems as well as with data from other stand-alone stations. Because of differences in trigger sensitivity, some seismic events recorded on the stand-alone stations were not recorded on the short-period, analog-telemetry network. All data recorded by the stand-alone stations were archived to magneto-optical disk and to 8-mm tape for long-term storage.

3.2 DATA PROCESSING

3.2.1 Instrument Calibration

In order to use the data collected by the digital instruments for signal processing and ground-motion analysis, the instrument response had to be determined for each station component. For the digital telemetry stations and the stand-alone digital stations, existing UUSS methods of calculating the instrument response were used. First, theoretical response files were created from calibration information supplied by the manufacturers for the sensors and digital signal processors. Second, an input step function was applied to each sensor while installed in the field. The recorded waveform was fit using the theoretical response. If the calibration pulse could not be fit within ± 2%, we concluded that there was something wrong with the instrument and took remedial steps. Appendix A includes a tabulation of the theoretical response parameters for each station component together with the final displacement response data (in pole-zero format). For the short-period analog-telemetry stations, documentation of the field electronics sufficed for analysis needs.

The polarity of each station component was carefully verified and documented upon installation and again before removal from the field. When the ground beneath a sensor moves upward, the recording of the seismic wave should indicate a positive or upward motion. On occasion, during the installation phase of the seismograph station, the electronic connection between the sensor and the recorder or telemetry system may result in a reversal of this record (e.g., upward motion is recorded in a downward or negative direction on the seismic record). This condition is called reversed polarity. When analyzing the source mechanism for a given seismic event, correct polarity information is critical to avoid misinterpretations.

Polarity information for each station is reported in Appendix A. Reversed polarities were identified on horizontal components of station TU1. At station TB3, the following problem was identified. Based on inconsistent data, it was concluded that for the time period from January 23 to June 14, 2001, the sensor channels were wired incorrectly. We determined what we believe was the correct channel identification from the observed data. However, before our interpretation could be verified, the cable between the triaxial sensor and the DAS was cut and the instrument was removed by the Trail Mountain Mine personnel, making it impossible to reconstruct with certainty the instrument's *in situ* wiring.

3.2.2 Trail Mountain Velocity Model

To appropriately calculate the three-dimensional source locations of seismic events in the Trail Mountain study area, a local seismic velocity model was determined using data compiled from local sonic logs, geologic maps, seismic refraction lines, and measured P- and S-wave arrival times (details are provided in Appendix B). The resulting model was used to determine all hypocentral locations presented in this report.

The velocity model has two variations to account for seismic wave propagation through deeper parts of the crust, depending on whether the receiver station falls into one of two groups: (1)

surface stations located within the Colorado Plateau province and (2) surface stations located along the eastern margin of the Basin and Range Province (see Figure 1-2). In practice, version (1) applied to stations of the Trail Mountain array and to stations of the University of Utah's regional seismic network at azimuths of approximately 0° to 210° from Trail Mountain; version (2), to regional network stations at azimuths between 210° and 360° (see, for example, Figure 2-3. The two variations of the model effectively account for significant differences in crustal structure between the eastern Basin and Range Province and the Colorado Plateau interior (see Arabasz and Pechmann, 2001).

3.2.3 Preliminary Data Processing

Data from Analog- and Digital-Telemetry Systems. Data from the analog- and digital-telemetry systems were processed integrally with data from the existing UUSS regional seismic network. A data analyst visually examined each network trigger, identified the seismic events of interest, picked arrival times, located the event, calculated a magnitude, removed poor waveform data, and archived the data. Routine data processing included picking of P-wave arrival times on the continuously telemetered stations and preliminary determination of coda magnitudes. S-waves from the vast majority of recorded events were not easy to identify and were not routinely picked at this stage of processing. All triggered data from the local Trail Mountain array were archived regardless of whether a successful event location resulted. The computer program *Hypoinverse* (Klein, 1978) was routinely used to locate all seismic events.

Adding the telemetered data from the Trail Mountain array roughly doubled the work load of our data analyst during the primary monitoring period between October 2000 and March 2001. This was due to the increased recording of mine tremors not only from the Trial Mountain Mine but also unintentionally from the Crandall Canyon Mine, about 18 km (11 mi) to the north of Trail Mountain (see Figure 2-3). We made some effort to reduce the triggered recording of small shocks originating in the Crandall Canyon area but could not do so without compromising the recording of small shocks in the Trail Mountain study area.

Routine processing of continuously telemetered data collected from October 3, 2000, when four stations of the local Trail Mountain array began recording (see Table 2-1), through April 30, 2001, resulted in the location of 1,913 seismic events in the extended study area (discussed in section 4.0). During the same period, a total of 1,624 events were located in the Crandall Canyon Mine area, but most of these locations were poorly constrained because the shocks were outside the Trail Mountain array and too small to be effectively recorded by surrounding stations of the UUSS regional seismic network (Figure 2-3). The Crandall Canyon seismic events were located in a preliminary manner to confirm their general location but were not analyzed further for this project.

Data from On-Site Recording Systems. Data from the on-site DAS at each of stations TB1, TB2, TB3, TU1, and JVD were processed individually for each station. Because each DAS was independently triggered (when a set threshold value of ground acceleration was locally exceeded), these stations were more prone to false triggers due to local noise. Table 3-2 summarizes the number of seismic events recorded by each of the stand-alone stations. Routine

processing of the data collected by these stations included conversion to a format commonly used in seismological research (SAC), calculation of peak ground acceleration on each station component, and cross-correlation of trigger times with other stand-alone stations and with the regional network data. Figure 3-2 shows the distribution of 1,202 measurements of peak ground acceleration made at stations TB1, TB2, and TB3 as a function of distance, together with a corresponding plot in magnitude-distance space. The large sample of data are from recordings of the best located events in this study.

For each event trigger from an on-site DAS, a waveform plot was made for rapid visual discrimination of the event type—whether noise, a seismic event within the study area, or an event outside the study area. With more than 17,000 event triggers to be processed, dealing with the accelerographic data was a major task (data for all triggers are archived at the UUSS). The false alarm rate at most of the UUSS accelerograph stations was very low—TB1 (7%), TB2 (2%), TB3 (31%), and TU1 (0.4%). The rate of false triggers at station JVD was much higher (80%), due to passing vehicles. A similarly high rate of false triggers at station TB3, which was located at the mine portal, was caused by the operation of heavy machinery and other local noise. At both JVD and TB3, trigger thresholds intentionally were kept very low in order to capture as many as possible of the mine tremors recorded by the other lower-noise stations.

Data Reporting on Project Web Site. In order to keep project participants informed during the course of the project, a password-protected Web site was created and managed by UUSS. Posted information included: weekly maps and listings of seismic events located in the local study area; Webicorder images (updated several times per hour) for stations TS2 and TS3, the two telemetered stations closest to the active mining (see Figure 3-1); key information and instrumental specifications for the seismic array; data processing notes; occasional progress reports; photographs of station installations and the project area; and a detailed map of the location and progress of longwall mining.

3.3 DATA ANALYSIS

3.3.1 Selection of Seismic Events for Detailed Analysis

USGS Data Set. Digital accelerographic data for 50 earthquakes were given to the USGS as part of this project under the plan described in section 1.2.2. The earthquakes included 49 shocks from the Trail Mountain local study area, selected as candidates for the USGS to consider for special analysis, plus the magnitude 4.2 earthquake near the Willow Creek Mine on March 7, 2000. The 49 Trail Mountain shocks were chosen to include: (1) the larger events recorded during the monitoring period from October 3, 2000, to March 7, 2001; (2) events recorded by the most number of stations, regardless of the event magnitude; and (3) a sampling of some very small shocks. The Trail Mountain accelerographic data set consisted of three-component recordings from the eight accelerographs described in section 2.2.1 and shown in Figure 2-1. Data for the Willow Creek earthquake consisted of three-component accelerograms

captured by two digital accelerographs installed by the University of Utah that were about 2 km and 7.5 km, respectively, from the source.

The process of delivering accelerographic data to the USGS involved a number of steps, some of which were completed iteratively. First, UUSS contracted to have software written to convert the recorded data to a specific format required by the USGS for their analysis. Second, numerous header data for parametric files were carefully reviewed and corrected where needed. Third, refined hypocentral solutions were provided. All P-wave arrival times were scrutinized, and S-wave picks were added where possible in order to constrain the location in three-dimensions. Map locations for the 49 Trail Mountain earthquakes in the USGS data set are shown in Figure 3-3. Corresponding hypocentral solutions together with an outline of accelerographic data for each event are presented in Appendix C.

UUSS Refined Data Set. A special sample of 271 seismic events, encompassing the 49 earthquakes in the USGS data set, was selected for refined hypocentral analysis and the results are herein referred to as the *UUSS refined data set*. This set was a subset of the 1,913 events located in the extended study area between October 3, 2000, and April 30, 2001, and was originally intended to include all events above a threshold of about magnitude 1.0, based on preliminary data processing. However, after subsequent refinement of magnitudes (described below), this set contains most—but not all—of the largest located earthquakes. Hypocenters for this data set were improved chiefly by adding arrival-time information from the stand-alone stations and by adding S-wave arrival times, as described in the next section. Final hypocentral solutions for 246 of these events within the local study area are included in Appendix D, and their epicenters are plotted in Figure 3-4.

3.3.2 Refinement of Hypocenters

The general problem of locating the hypocenter of a seismic source was introduced in section 2.1.2. In this section we discuss improvements in the hypocentral locations for a subset of earthquakes located in the study area achieved by adding data and by additional processing. We also remark on factors posing limitations for hypocentral resolution in the study area, including the configuration of the seismic array, whose dual-purpose design—including constraints and trade-offs—was described in section 2.2. An expanded discussion of the challenges that were encountered relating to hypocentral resolution is presented in Appendix E.

After preliminary processing of 1,913 earthquake locations in the extended study area (section 3.2.3), subsets of the earthquake locations corresponding to the USGS and UUSS refined data sets were re-analyzed. P-wave arrival times were added from the stand-alone stations and S-wave arrival times were added from various recording systems. Precise S-wave arrival times can usefully constrain a hypocenter, particularly its depth. However, accurately picking S-wave arrival times for mining-related events at local stations was a non-trivial exercise. First, to generate an S wave, the event must have sufficient shear energy, which is not always the case for mining-induced events. Second, given the short travel paths from source to station, the S-wave arrival often coincides either with P-arrivals from multiple reflections in the layered structure or with surface waves. Because of these complications, S-wave arrival times at

stations in the local array were picked exclusively from transversely polarized seismograms, constructed through a time-consuming procedure of rotating the horizontal data to the direction of the incoming ray (see Figure E-4).

For reasons discussed in Appendix E, arrival times at stations TB1, TB2, and TU1 were removed in the reprocessing of hypocenters. While these stations were critical for ground-motion measurements, their inclusion in the hypocentral solutions led to systematic biases in source location due to an unusual combination of station elevation, topography, and velocity model.

Table 3-3 summarizes the mean and standard deviation of hypocentral location errors for earthquake locations in this study. For the USGS and UUSS refined data sets, results are compared between initial and final processing. The hypocentral location errors include: RMS, the root mean square of the travel-time residual in seconds; ERH, the standard horizontal error in kilometers; and ERZ, the standard vertical error in kilometers. ERH and ERZ are simplified errors from a three-dimensional error ellipsoid (Klein, 1978). To a first approximation, the 95-percent confidence intervals in horizontal location and depth are ± 202 ERH and ± 2.0 ERZ, respectively.

The statistical information presented in Table 3-3 shows some of the value added from the refined data processing. In general, for both the UUSS-refined and the USGS-data sets, the standard horizontal and vertical errors were reduced, indicating that the hypocenter's 3-dimensional location was better constrained than it was prior to additional processing. The addition of more arrival time data during the refinement stage had the added benefit of improving our ability to eliminate the ill-conditioned hypocentral locations.

3.3.3 Magnitude Determinations

The earthquake size measurement used in the Trail Mountain catalog is coda magnitude (M_C), an empirical estimate of Richter local magnitude (M_L) typically made for events smaller than about magnitude 3. The values of M_C in this report were calculated from measurements of seismic signal durations on records from short-period, vertical-component, velocity sensors using the following equation from Pechmann et al. (2001):

$$M_C = -1.83 + 2.11 \log\tau + .0025\Delta \qquad (1)$$

where Δ = epicentral distance in km
τ = signal duration in sec, measured from the P-wave onset to the time that the average absolute value of the ground velocity (approximated from the record amplitudes and the 5 Hz instrument gain) drops below 0.01724 microns/sec.

The threshold of 0.01724 microns/sec is the estimated median noise level for short-period analog-telemetry stations in the University of Utah network (as of August 1, 2000). All of the signal duration measurements for this study were made with the aid of UUSS-developed software which automatically determines signal duration by fitting an equation to the latter part

of the seismic record where the amplitude is decaying with time. Equation (1) was calibrated against Richter local magnitudes (M_L) for 439 Utah region earthquakes of M_L 1 to 4. Therefore, our coda magnitudes should be comparable to standard Richter local magnitudes, which are based on peak amplitude measurements on a specific type of instrument (or records processed to look like they were recorded on that type of instrument).

We were able to determine coda magnitudes for 1,816 of the 1,913 earthquakes in the Trail Mountain catalog. Most of these magnitudes are mean values from several stations, with an average of 4.5 stations per event. The average M_C standard deviation is 0.18. For some of the 97 events without M_C determinations, signal duration measurements could not be made because of interference from other seismic events. For the rest, all of the available duration measurements gave M_C values less than or equal to zero, which are discarded by the program *Hypoinverse* that we currently use for computing M_C. We cannot reliably calculate M_C values less than zero with equation (1), because this equation is not calibrated for earthquakes smaller than magnitude 1. An M_C value of zero in Appendix D indicates that the M_C could not be determined.

We also attempted to determine M_L for events in the Trail Mountain catalog. However, all but one of these events were too small for direct M_L determinations from at least two stations (the standard UUSS criterion). For this event (on Oct. 4, 2000, at 03:28 UTC), $M_C = 2.16$ and $M_L = 1.8$. We did not use data from the local Trail Mountain stations for M_L computations because these computations are problematic for events both at small epicentral distances and with such extremely shallow focal depths.

The preliminary magnitudes reported earlier on the project Web site were coda magnitudes computed using a prior empirical equation from Griscom and Arabasz (1979):

$$M_C = -3.13 + 2.74 \log\tau + .0012\Delta \qquad (2)$$

where Δ = epicentral distance in km
τ = signal duration in sec, measured from the P-wave onset to the point that the signal drops down below the noise level preceding the P wave.

The preliminary M_C's are not as reliable as the ones included in this report because equation (2) was calibrated using much fewer data (from 45 earthquakes) and does not account for differences in instrument gain. For the smallest earthquakes in the Trail Mountain catalog, the new M_C's are systematically larger than the old ones by approximately 0.4 magnitude unit. However, the average difference decreases with increasing size and is negligible for the largest Trail Mountain events.

3.3.4 Focal Mechanism Analysis

In addition to determining the hypocentral location and magnitude for each event, another objective of the UUSS data analysis was to constrain possible source mechanisms using the conventional approach of analyzing P-wave first motions. The two most likely types of

mechanisms expected to be encountered were shear-slip mechanisms, involving rupture on a fault or fracture, and implosional or collapse-type mechanisms, which involve sudden roof-floor closure (e.g., Arabasz and Pechmann, 2001). Shear-slip mechanisms produce both compressional and dilatational P-wave first motions in which the initial vertical ground motion is up or down, respectively. The mapping of a sufficient distribution of compressions and dilatations on a stereographic plot allows the determination of a *focal mechanism* (or *fault-plane solution*) which describes the possible fault planes (strike, dip and rake) and the relative motion on those planes (e.g., Bolt, 1993; Bjarnasson and Pechmann, 1989).

To be reliable, the observed P-wave first motions must be unambiguous with a good signal-to-noise ratio and be recorded with known polarity. If the station distribution is such that observed first motions cover wide azimuthal and distance ranges, a fault-plane solution can be reliably determined for a shear-slip source. An implosional source generates only dilatational first motions; an explosional source, only compressional first motions. If first motions are recoverable only at a few stations, one can deduce that the source involved shear slip if both compressions and dilatations are observed, but a fault-plane solution is usually indeterminate. In the case of an implosional or explosional source (absent independent information), single-type first motions alone do not suffice to infer the type of source mechanism. First-motion observations must cover wide azimuthal and distance ranges (as distributed on a stereographic plot) to rule out the possibility that the non-observation of mixed first motions was due to inadequate spatial sampling.

During the preliminary data processing, reliable P-wave first motions were routinely documented by the data analyst for all located seismic events. Additional P-wave first motion information was gathered for the UUSS refined data set (where possible) during the refinement phase of data processing. Recognizing the importance of discriminating shear-slip events from implosional-type ones, special care was taken to document compressional first motions.

Table 3-1

Data-Acquisition Scheme for Trail Mountain Seismic Array

Station Code	Sensor Type		Data Acquisition Type		
	No. of Short-Period Velocity Components	No. of Accelerometer Components	Continuous Telemetry		On-Site Recording *(Independently Triggered)*
			Analog	Digital	Digital
TS1	3	-	X	-	-
TS2	1	3	X	X	-
TS3	1	3	X	X	-
TS4	1	-	X	-	-
TS5	1	-	X	-	-
TS6	1	-	X	-	-
TB1	1	3	-	-	X
TB2	1	3	-	-	X
TB3	1	3	-	-	X
TU1	1	3	-	-	X
JVDA	-	3	-	-	X
JVDC	-	3	-	-	X
TMU	-	3	-	X	-
TM2	3	-	-	X	-

Table 3-2

Seismic Events Recorded* on Independently Triggered Stations
October 3, 2000 - April 30, 2001

	TB1	TB2	TB3	TU1	JVD
October 2000	2	5	0	0	0
November 2000	0	1	0	0	0
December 2000	335	720	286	235	12
January 2001	172	573	1094	1103	32
February 2001	1094	1576	1998	3328	17
March 2001	559	1071	2436	680	11
April 2001	86	92	224	0	20
Total	2248	4038	6038	5346	92

Grand Total Recorded: 17,762

*Includes seismic events located outside study area.
Number of events on at least 3 of 5 stations = 1,726
Number of events during Feb 16 - Mar 7, 2001 = 1,033

Table 3-3

Statistics for Hypocentral Location Errors

Data Set	N	RMS (sec)		ERH (km)		ERZ (km)	
		Median	Mean*	Median	Mean*	Median	Mean*
Entire Preliminary Set	1913	0.03	0.04 ± 0.03 (1790)	0.3	0.32 ± 0.15 (1790)	0.8	1.40 ± 1.32 (1790)
UUSS Refined (preliminary)	271	0.05	0.06 ± 0.04 (244)	0.3	0.32 ± 0.24 (244)	0.9	1.40 ± 1.10 (244)
UUSS Refined (final)	271	0.07	0.07 ± 0.04 (246)	0.3	0.31 ± 0.24 (246)	0.7	1.19 ± 1.25 (246)
USGS Subset (preliminary)	49	0.03	0.04 ± 0.03 (40)	0.3	0.26 ± 0.05 (40)	0.5	0.72 ± 0.61 (40)
USGS Subset (final)	49	0.06	0.06 ± 0.03 (41)	0.2	0.24 ± 0.06 (41)	0.7	0.72 ± 0.50 (41)

*Mean ± 1σ; recalculated after removing values beyond 2σ; number in parentheses indicates reduced sample size, relative to N, included in recalculated mean and standard deviation.

Data Collection – Sample Webicorder Records

Tuesday, February 13, 2001

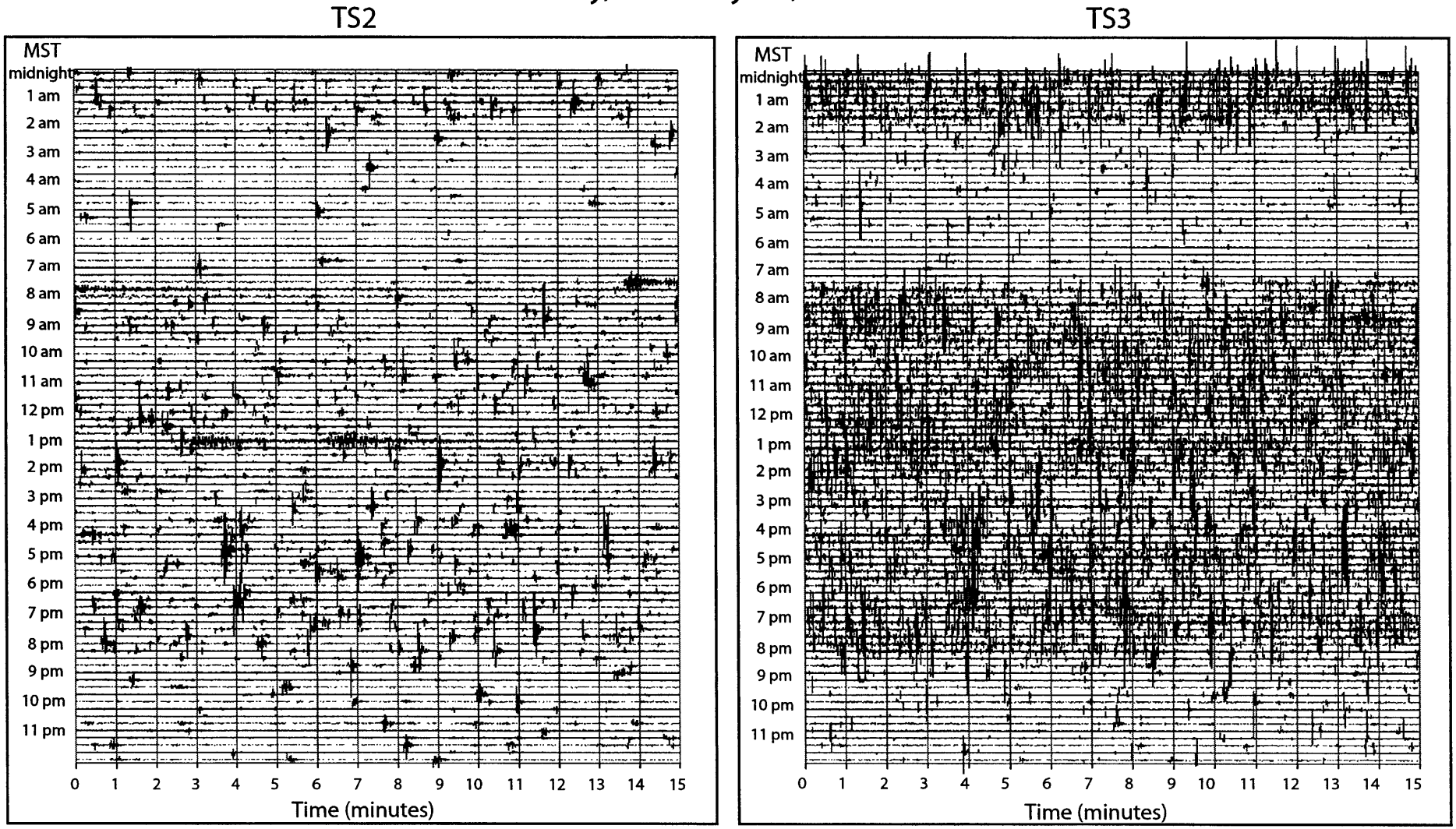

Figure 3-1. Example Webicorder images from stations TS2 and TS3 for a 24-hour period.

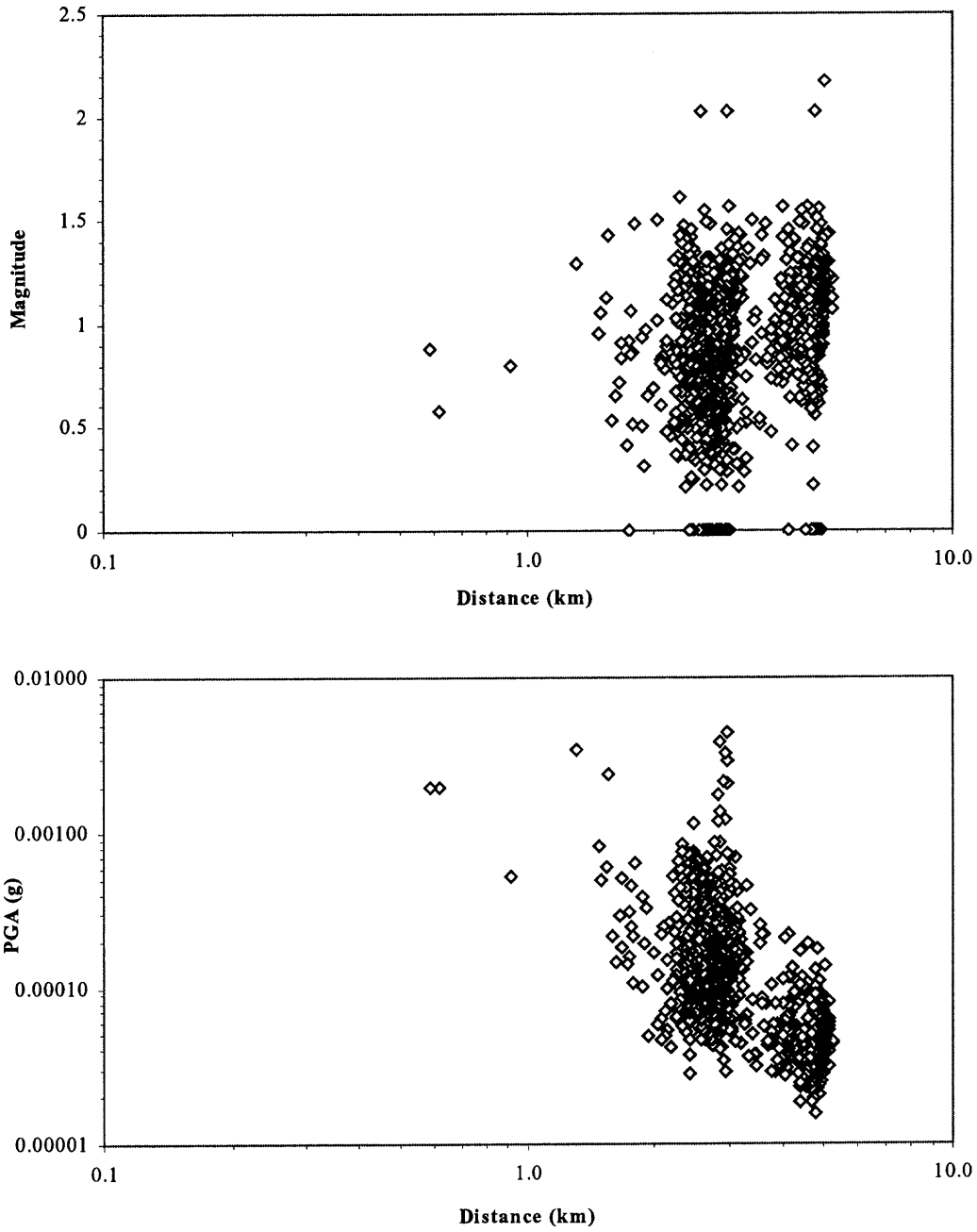

Figure 3-2. Scatter plot (below) showing the distribution in peak ground acceleration (PGA) and distance space of 1,202 measurements made at stations TB1, TB2, and TB3; a corresponding scatter plot (above) in magnitude and distance space includes a value of magnitude for each PGA measurement. The PGA measurements were made using data from 702 well-located (Quality A and B) earthquakes in the extended study area.

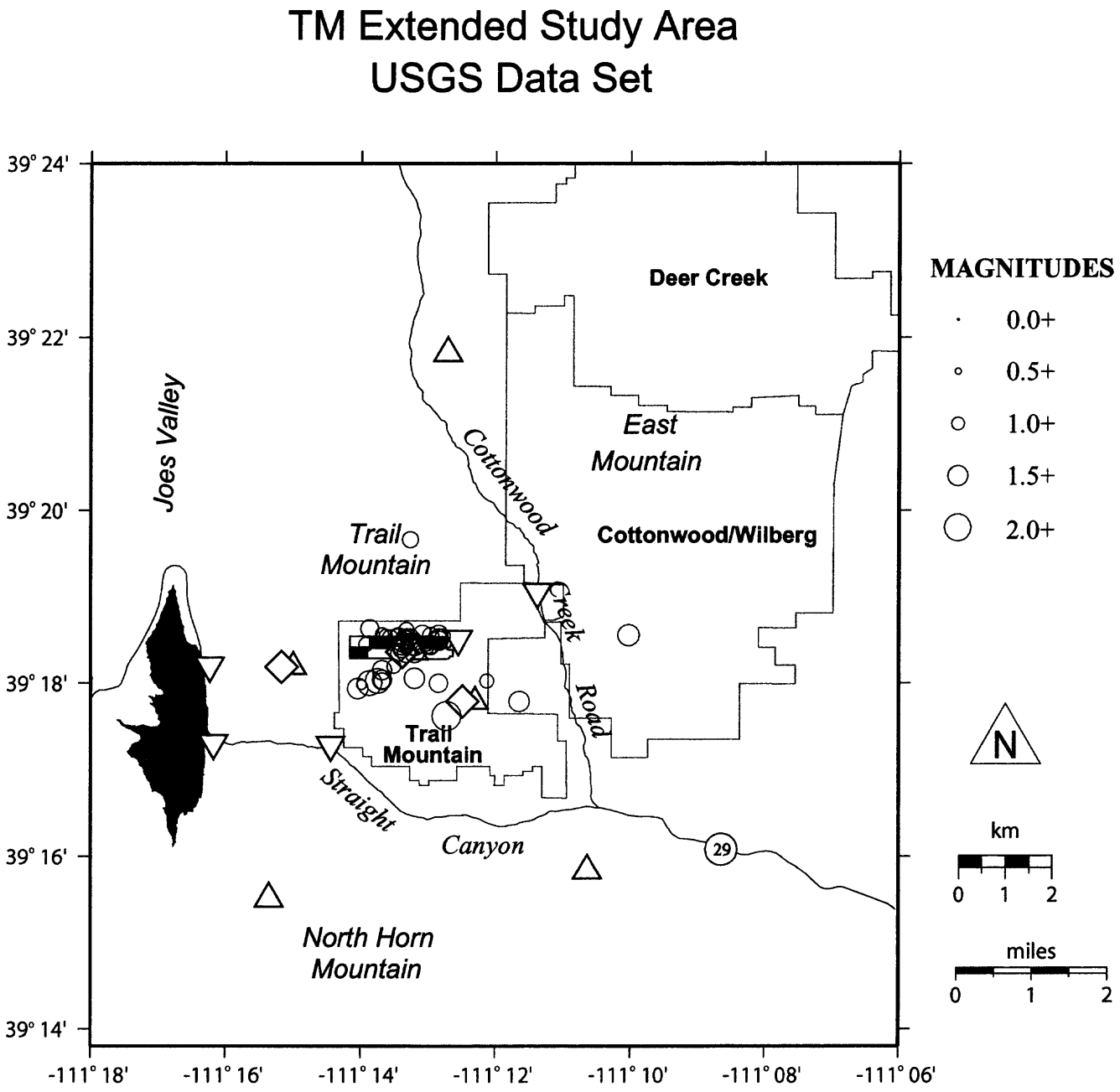

Figure 3-3. Epicenter map of 49 seismic events (scaled by magnitude) selected as candidates for the USGS to consider for special analysis (detailed list in Appendix C). Base map as in Figure 2-2, including longwall panels (green) mined during the monitoring period of this study (see Figure 2-4). The outline of the Trail Mountain Mine and lease boundaries of the Deer Creek and Cottonwood/Wilberg mines are shown for reference.

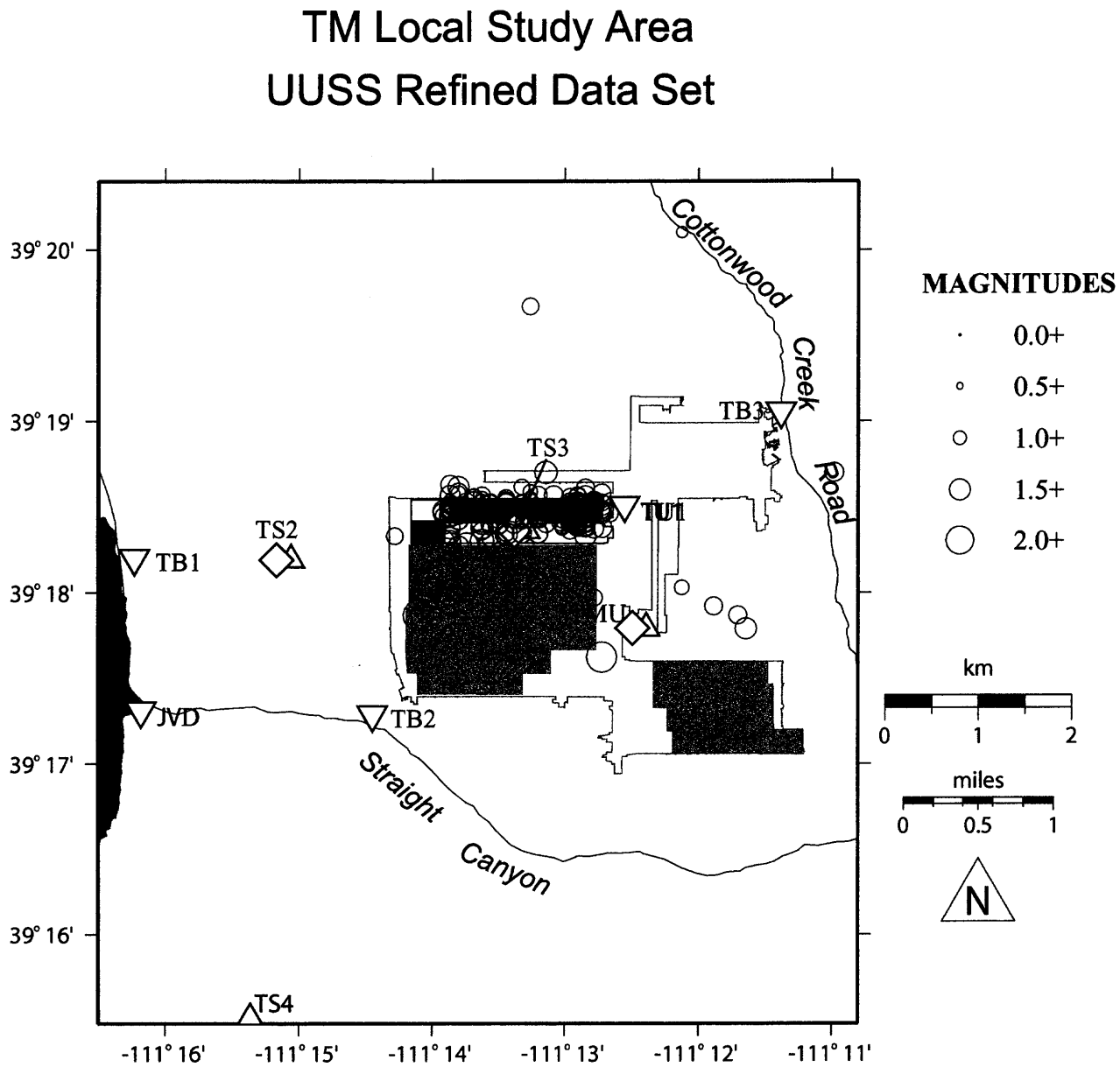

Figure 3-4. Epicenter map of 246 seismic events (scaled by magnitude) belonging to the UUSS refined data set and located within the local study area. Base map includes: seismic stations, as in Figure 2-2; outline of the Trail Mountain Mine (blue); longwall panels (green) mined during the monitoring period of this study (see Figure 2-4); and areas mined out by longwall operations prior to this study (shown in pink). The latter include an area in the southeastern part of the mine, mined during October 1995-March 1997, and an area in the western part of the mine where east-west panels were mined, with one exception, from south to north during March 1997–August 2000 (see Figure F-6).

4.0 OBSERVED MICROSEISMICITY

In this section we describe the microseismicity that was observed as a result of continuous seismic monitoring in the Trail Mountain extended and local study areas from October 3, 2000, through April 30, 2001. The main objective of the seismic monitoring, as outlined in section 2.1, was the accurate location (< 1 km) and characterization of those seismic sources for which accelerographic ground-motion measurements were made. We provide this information within the expanded context of the temporal and spatial association of the observed seismicity with the mining of the final two longwall panels in the Trail Mountain Mine.

The primary database we present and discuss relates to a set of 1,931 earthquakes recorded by five or more stations of the Trail Mountain seismic array and successfully located within the bounds of the extended study area, hereafter referred to as the *TM earthquake catalog*. Using this database, we proceed to describe (1) temporal variations in seismic activity, (2) the magnitude distribution of the recorded seismicity, (3) the earthquake locations both in space and time, and (4) information regarding source mechanisms.

4.1 TIME-VARYING RATES OF SEISMIC ACTIVITY

In rock deformation, the rate of occurrence of seismic (or acoustic) events as a function of size is well known to follow a power-law scaling, and the number of events recorded depends on instrumental sensitivity. During the October 2000–April 2001 recording period, at one extreme, more than 200,000 seismic events were cumulatively recorded by the high-magnification, short period station TS3, the closest surface station above the active longwall workings. The vast majority of these events, however, had magnitudes smaller than zero and were too small to be recorded by enough short-period stations in the Trail Mountain seismic array to enable source locations. In Figure 3-1 one can compare a 24-hr seismic record from station TS3 with one for the same period from station TS2, located 2.6 km (1.6 mi) away. The 1,931 located seismic events in the TM earthquake catalog, over a 7-month recording period, thus represent a size range energetic enough to be recorded by multiple stations of the local surface array—compared, say, to the 13,000 seismic events detected and located by Ellenberger et al. (2001) during their five-month monitoring of a longwall coal panel using an in-mine microseismic array.

A histogram in Figure 4-1 shows a breakdown of the TM earthquake catalog by day (local time). The time series gives a good overview of time-varying rates of occurrence during this period, but we caution that the total histogram does not reflect rigorously uniform sampling. For reasons explained below, the part of the histogram labeled "M ≥ 1" more accurately represents the relative temporal variation of seismic activity during the project period.

Asterisks in Figure 4-1 mark a 30-hr period beginning on 12/12/2000 and a 7-day period beginning 12/15/2000 when the network sensitivity was temporarily increased (trigger threshold lowered); the latter sample period aimed to capture more seismic events when the longwall in 1st Right passed closest to station TS3 (see Figure 2-4). On a longer time scale, the network sensitivity was relatively higher during the 55-day period from 12/22/2000 to 2/15/2001 compared to the preceding 80-day and following 74-day periods, when it was lower

and at roughly equal levels. Late on 2/15/2001, following a sharp sustained increase in seismic activity, the network sensitivity was reduced to mitigate impact on data recording and analysis.

Accounting for changes in network sensitivity, Figure 4-1 shows a positive temporal correlation between numbers of recorded earthquakes and longwall mining in the Trail Mountain Mine. The shaded and white backgrounds in Figure 4-1, keyed to dates described in Table 2-1, represent extended periods of active longwall operations and periods of no mining, respectively. On a weekly scale during periods of longwall operations, Figure 4-1 shows fewer recorded earthquakes on weekend days (non-mining) compared to regular weekdays (mining). An evident correlation in the histogram is the abrupt decrease in seismicity coinciding with the completion of mining on 3/7/2001.

On a daily scale, rates of microseismicity correlate with mining shifts. In Figure 3-1, for example, markedly fewer seismic events occurred on 2/13/2001 after a shift stop at 1:40 a.m. compared to the preceding hours and to the hours after 7:30 a.m. when mining resumed and continued until another shift stop at 8:15 p.m. The typical shift times for longwall mining at the Trail Mountain Mine were from 7:30 a.m. to 4:30 p.m. and from 4:30 p.m. to 1:30 a.m. This is well reflected in Figure 4-2, a histogram for the TM earthquake catalog showing the number of located events versus time of day. The histogram shows relatively high rates of seismicity during the hours of regular mining shifts, decaying rates after roughly 1:00 a.m. when mining usually stopped, and a minimum just before 8:00 a.m. when the morning shift began.

4.2 MAGNITUDE DISTRIBUTION

Figure 4-3 shows a magnitude histogram for the TM earthquake catalog, with coda magnitude (M_C) ranging from 0.0 to 2.21. The median magnitude is 0.8, and the 15th and 85th percentile values are approximately 0.4 and 1.2, respectively. A relative peak in the smallest magnitude bin is an artifact, due to the circumstance that 0.0 was an artificial lower limit for calculating values of M_C (see section 3.3.3). On the right-hand side of the histogram, there is the expected exponential increase (assuming a power-law scaling of number versus size) with decreasing size, down to the threshold for complete detection. From separate analyses, this threshold of completeness was determined to be $M_C = 1.2$, consistent with the observed fall-off in numbers of events to the left of this value in the histogram. Thus, while many earthquakes smaller than magnitude 1.2 were detected and located, the capturing of these smaller-size events was incomplete.

For a different perspective, Figure 4-4 (a) shows a time-series plot of the magnitudes of 1,829 earthquakes in the TM catalog located in the local study area. Of particular interest in this plot is the distribution of the larger size events—in terms both of their number and magnitude. The plot includes eight earthquakes of $M_C \geq 2.0$ (± 0.5) and 13 of $M_C \geq 1.8$ (± 0.5). Most of the largest events occurred in earliest October, just prior to the interruption of mining in the 2nd Right longwall panel and before the mining of 1st Right. The sparsity of seismicity after the completion of mining on March 7, 2001, is evident in the time series.

For comparison to Figure 4-4 (a), we sorted the University of Utah's regional earthquake catalog for the Trail Mountain local study area for the three-year period January 1, 1999–December 31, 2001. Prior to the monitoring period of this project, nearly continuous longwall mining in the Trail Mountain Mine during 1999 and the first three calendar quarters of 2000 was known to have produced abundant mining seismicity, and the mine was the only source of mining seismicity within the local study area. To ensure uniformity of magnitudes for the comparison, M_C values from the regional network catalog were recomputed using the same procedures as those for the TM catalog (section 3.3.3). Data from the Trail Mountain catalog of Figure 4-4 (a) for October 2000–April 2001 were spliced into the longer-term catalog. A time-series plot for 2,835 magnitudes in the resulting catalog is shown in Figure 4-4 (b). Apparent gaps in the seismicity during 1999 and 2000 are not due to gaps in monitoring but are inferred to be associated with interruptions in mining, such as during longwall moves. Sparse seismicity after the first calendar quarter of 2001, following the end of mining, continued through the rest of 2001.

A key point of Figure 4-4 (b) is the reduction in the upper size of earthquakes recorded during the project period , i.e., the last calendar quarter of 2000 and the first calendar quarter of 2001, compared to the seven preceding calendar quarters. During the latter 21 months, there were 111 earthquakes of $M_C \geq 2.0$ (5.3/mo average) and 470 of $M_C \geq 1.8$ (22/mo average). Based on these rates, and given the 4–5 months of active mining during the project period, we would have expected to record roughly 24 earthquakes of $M_C \geq 2.0$, compared to the eight actually recorded, and roughly 100 earthquakes of $M_C \geq 1.8$, compared to the 13 recorded. Figure 4-4 (b) shows that there was a reduction of 0.5 magnitude unit or more in the upper envelope of earthquake sizes during the project monitoring period compared to prior periods of mining. We attribute the reduction to the change in mining plan, involving mining 2nd Right between barrier pillars, as described in section 2.3.1.

4.3 EARTHQUAKE LOCATIONS

In presenting our observations of earthquake locations, we will emphasize epicentral (map) distributions—separately addressing the issue of focal depth, for which fine-scale resolution at or close to mine level was knowingly constrained in advance by the design of our seismic array (section 2.1.2). Despite limitations in the resolution of shallow focal depths, the TM earthquake catalog provides much useful information for the space-time association of observed seismicity with map locations of contemporaneous and past mining activity.

4.3.1 Epicentral Quality

To guide our interpretations of the map distribution of earthquakes, a quality parameter Q was assigned to each epicentral solution. A conventional scheme for evaluating epicentral quality is to consider both the distribution of stations that recorded the earthquake and the statistical measures of the solution. Our measures for Q are outlined at the bottom of Table 4-1 as well as in Appendices C and D. Assigned values of Q include A (excellent), B (good), C (fair), and D (poor). Recalling that the 95-percent confidence interval in horizontal location, to a first approximation, is ±2.2 ERH, where ERH is the standard horizontal error in kilometers (section

3.3.2), we estimate that this conservatively corresponds to ±0.5 km for quality A, ±1.0 km for quality B, ±1.5 km for quality C, and > ±1.5 km for quality D.

4.3.2 Overview of Epicentral Distributions

Figure 4-5 shows a map of all the earthquakes in the TM earthquake catalog, specially identifying Quality D (poor) locations in red. The latter are scattered in areas outside or marginal to the seismic array, chiefly in the northeast quadrant of the map where one might plausibly associate the seismicity with areas of past mining within the lease tracts of the Deer Creek and Cottonwood/Wilberg mines. We simply admit that these earthquakes are poorly located and avoid further interpretation. Focusing attention on the Quality A, B, and C solutions plotted as black open circles, the first-order features of Figure 4-5 are (1) extremely intense clustering in the northwest sector of the Trail Mountain Mine, (2) less dense but notable clustering elsewhere within and along the eastern boundary of the Trail Mountain mine property, and (3) loose clustering of relatively larger (magnitude 1.5–2.0) shocks in the southern part of the Cottonwood/Wilberg mine tract.

Figure 4-6 sharpens the focus on the local study area and includes only the better-located seismic events (Quality A, B, and C). In this view, the most intensely clustered epicenters align east-west along the 1st Right longwall panel, and fairly abundant seismicity appears within the mined-out area in the western zone of the Trail Mountain Mine, predominating in its northwestern part. We believe the latter epicenters are reasonably accurate and not simply mislocated to the south of the 1st and 2nd Right panels. Nearly all the epicenters in Figure 4-6 can be associated spatially with identified areas of contemporaneous or past mining. One apparent exception is the cluster of events outside the mine boundary and east of station TMU. As shown in Appendix F (Figure F-6), however, these earthquakes coincide with an area of old room-and-pillar mining in pre-Energy West workings. A magnitude 3.3 shock occurred in these workings in December 1987 (Appendix F).

4.3.3 Space-Time Seismicity in the Trail Mountain Mine Area

During the project period it was evident to us that our earthquake locations were following the eastward advance of the longwall in the 1st Right panel. To illustrate this, Figure 4-7 shows epicenter maps of better-located earthquakes (Quality A, B, C) in the Trail Mountain Mine area for six consecutive time frames during our monitoring, including time intervals of both active mining and no mining. The figure caption provides explanatory detail for each time frame.

In time frames (a), (d), and (e) of Figure 4-7, our earthquake locations clearly coincide with the part of the longwall panel that was mined during the corresponding period. Based on particle-motion data from the underground station (TU1) presented in Appendix E, the majority (> 90 percent) of the earthquakes in the USGS data set had inferred map locations within or immediately adjacent to (within a few hundred meters of) the coal panel being actively mined (see Figure E-10). This pattern is typical of microseismicity accompanying longwall coal mining (e.g., Ellenberger et al., 2001). On a fine scale, our densely clustered epicenters along 1st Right are laterally bounded by envelopes approximately 250 m to either side of the longwall panel. Among the time frames in Figure 4-7 of no mining, time frame (f), one of the longest

time intervals, emphasizes the paucity of seismic activity after the end of mining—including seismicity within mined-out areas.

4.3.4 Focal Depths

Figure 4-8 (a) shows a histogram of the focal depths for all 1,913 earthquakes in the TM earthquake catalog, with depths ranging from 0.0 to 7.3 km. Only 75 (3.9 percent) have a computed focal depth ≥ 1.0 km, and 34 (1.8 percent) have a depth ≥ 2.5 km. Thus, the overwhelming majority of the hypocenters are very shallow and, as we have seen, have epicenters spatially associated with map locations of contemporaneous and past mining. Two questions arise. First, how many deeper tectonic earthquakes, if any, are included in the TM catalog? Second, for the shallow earthquakes spatially associated with mine workings, how precisely can we constrain their focal depths relative to mine level?

Deeper tectonic earthquakes? We approached the first question by scrutinizing all hypocentral solutions in the TM catalog having a focal depth ≥ 2.5 km. Solutions for the 34 earthquakes are listed in Table 4.1 and their epicenters are plotted in Figure 4-9 as filled gray circles. Inspection of Table 4-1 shows that all but one of these events have a Quality D epicentral solution, all have a magnitude less than 1.5, and most of the hypocentral solutions have a standard vertical error, ERZ, of several kilometers or more; their epicenters (Figure 4-9) virtually all lie outside or at the margin of our local seismic array, thus tending to be poorly located because their small size precluded recordings at surrounding regional stations.

It is well known that in order to obtain good focal-depth accuracy for a local earthquake, it is necessary to have a P-wave arrival-time pick from at least one station at an epicentral distance of less than one focal depth. Gomberg et al. (1990) showed that good focal-depth control can also be achieved by having both P-wave and S-wave arrival-time picks of good quality from a station at an epicentral distance of 1.4 focal depths or less. The criteria we adopted for reliability of focal depth for these deeper events were to require ERZ to be less than or equal to 2.0 km and the closest epicentral distance, DMIN, to be less than or equal to the computed depth. Of the 34 events only three met these criteria and are labeled 1, 2, and 3 on Table 4-1 and Figure 4-9. All three are less than magnitude 1.0, and only Event 3 has a substantial depth (7.1 km).

Depth of shallow shocks relative to mine level? Our approach to the second question regarding constraining the depths of shallow shocks relative to mine level, notably in the Trail Mountain Mine area, was as follows. Using the same criteria for focal-depth reliability (DMIN ≤ depth; ERZ ≤ 2.0 km), we examined all earthquakes within the local study area having a computed focal depth less than 2.5 km (already knowing from the tectonic-earthquake analysis that there were no reliably deeper events in this area). Of the 1,829 earthquakes in our sample, 321 met the reliability criteria, and all of these have epicenters within 1.2 km of station TS3. Regarding the availability of S-wave arrival times mentioned earlier, for most of these events it was rarely possible to obtain S-wave arrival-time picks from stations at distances less than 1.4 focal depths because of the short S-P times at such close distances for these extremely shallow events.

Of these 321 events, all but three have Quality A, B, or C locations. The 95-percent confidence limits on the focal depths for these events (twice the standard vertical error) range from 0.4 to 2.0 km, with a median value of 0.8 km. Thus, all of these 321 events have reasonably well-constrained focal depths. A total of 302 (94 percent) have a depth of 0.4 km or less and the deepest is 2.12 km, as shown in Figure 4-8 (b). There is a sharp decrease in the frequency-depth distribution of this sample at 0.4 km depth. The median 95-percent confidence limit on the focal depths between 0.3 and 0.4 km depth is 0.8 km, the same as for the complete set of 321. Given the large uncertainties in the computed focal depths compared to the depths themselves, we cannot conclude that most of the events are shallower than 0.4 km. We do, however, expect that the great majority (> 90 percent) of the actual focal depths are less than the sum of the 94th-percentile *focal depth* of 0.4 km and the median 95-percent *focal-depth confidence limit* of 0.8 km, i.e., 1.2 km. The mine is at a depth of 0.5 to 0.6 km in the Trail Mountain model. Thus, based on this sample of well-constrained focal depths from the immediate vicinity of station TS3, we can conservatively state that most of the better-located seismic events occurred within ± 0.6 km of the mine level.

This conclusion regarding the focal-depth distribution near the mine is consistent with analyses of plots of RMS versus depth carried out for the USGS data set and summarized in Appendix E. It is also consistent with the observation that the first-arriving P-waves at station TUI, located underground in the mine, were usually much stronger on the east component than on the vertical component (see Appendix E). This observation suggests that the P waves arriving at TU1 had nearly horizontal ray paths and were therefore from seismic events located near the mine level. Unfortunately, we have been unable to determine from any of our focal depth analyses whether the events were occurring predominantly at, above, or below the mine level.

4.4 SOURCE-MECHANISM INFORMATION

From the entire TM earthquake catalog, only 43 earthquakes (2 percent) were recorded with at least one compressional P-wave first motion. The epicenters of these events are plotted in Figure 4-9 as open circles—except for events labeled 1 and 2 which had at least one recorded compressional first motion and were also at depths ≥ 2.5 km (hence, plotted as filled gray circles). Unsuccessful efforts were made to construct both single-event and composite focal mechanisms from the sparse first-motion data containing mixed compressions and dilatations (see section 3.3.4). The small size of the recorded earthquakes clearly was a factor limiting the recording of sufficient data.

The important result remains that 98 percent of the earthquakes in the TM catalog produced only dilatational first-motion observations. From this one can argue (a) that the non-observation of compressional first-motions was due to consistent under-sampling, (b) that an implosional-type source mechanism is operative, or (c) some combination of the above. For the 43 shocks with at least one compressional first motion, one can conclude that the source had at least a component of shear-slip. The fact that many of these 43 events were located near the Trail Mountain Mine (Figure 4-9) indicates that not all of the events near the mine had pure implosional mechanisms.

McGarr and Fletcher (2002) inverted waveform data from three Trail Mountain seismic events to determine their moment tensors. All three of their moment-tensor solutions indicate a combination of normal faulting and implosion, with each of these two components of the mechanism contributing comparable amounts to the overall seismic moment. Our first-motion observations, although inconclusive by themselves, are consistent with hybrid focal mechanisms of the type found by McGarr and Fletcher (2002).

TABLE 4-1

LIST OF ALL LOCATED EVENTS IN THE TM EXTENDED STUDY AREA WITH FOCAL DEPTHS ≥ 2.5 KM

ID	DATE	ORIGIN TIME	LATITUDE	LONGITUDE	DEPTH	MAG	NO	GAP	DMIN	RMS	ERH	ERZ	Q
	001016	1723 12.04	39° 20.67'	111° 7.63'	7.01	0.94	6	213	4.5	0.12	4.3	9.8	D
	001020	1015 25.73	39° 23.94'	111° 8.70'	5.03	0.80	6	279	7.0	0.12	8.4	11.3	D
	001025	1658 26.42	39° 20.10'	111° 12.12'	3.18	0.79	5	119	3.3	0.02	0.8	0.6	D
	001101	1121 07.13	39° 20.05'	111° 7.99'	7.11	0.00	5	187	4.2	0.08	3.2	10.3	D
	001205	1123 49.03	39° 18.55'	111° 11.48'	3.03	0.35	8	102	2.0	0.41	1.3	3.0	C
	001207	1237 11.95	39° 23.97'	111° 6.43'	4.36	1.42	9	226	9.6	0.15	1.9	19.4	D
	001207	1721 42.70	39° 22.47'	111° 12.17'	4.71	0.41	5	321	7.8	0.19	30.4	14.5	D
	001211	2342 53.48	39° 18.41'	111° 6.17'	7.26	0.91	6	185	1.2	0.16	6.6	11.2	D
	001212	1844 44.36	39° 22.68'	111° 12.75'	4.72	0.00	5	324	8.1	0.22	37.9	16.7	D
	001219	1430 42.77	39° 21.77'	111° 7.15'	6.65	0.48	6	246	5.9	0.12	7.9	13.5	D
	001220	2024 59.66	39° 22.60'	111° 13.17'	4.90	1.26	5	325	7.8	0.23	44.3	13.6	D
	001221	0918 28.81	39° 21.85'	111° 15.86'	4.21	0.00	5	329	6.8	0.09	231.1	134.1	D
	001223	0917 18.14	39° 24.00'	111° 6.31'	4.29	1.40	9	226	9.6	0.17	2.0	31.4	D
	001223	2302 15.59	39° 21.46'	111° 8.28'	6.06	0.50	7	225	6.2	0.32	7.2	16.6	D
	001224	1150 20.00	39° 18.10'	111° 8.23'	4.16	0.64	7	150	4.1	0.19	4.2	20.5	D
	001227	0725 57.39	39° 21.39'	111° 7.35'	6.81	0.57	6	236	5.4	0.07	7.3	14.2	D
	001229	1748 48.07	39° 17.67'	111° 17.81'	4.27	0.80	5	264	5.3	0.34	7.1	33.1	D
	010103	1138 21.85	39° 23.92'	111° 6.34'	4.25	1.46	9	226	9.5	0.17	2.1	40.2	D
	010103	1325 49.25	39° 23.34'	111° 6.51'	4.43	1.48	9	224	8.4	0.15	2.1	16.9	D
	010103	1723 38.11	39° 20.05'	111° 7.55'	4.21	0.58	7	194	3.7	0.20	6.8	21.4	D
	010104	0500 19.30	39° 22.45'	111° 11.77'	4.71	0.30	5	320	7.9	0.22	31.0	16.3	D
1	010110	0418 33.72	39° 14.59'	111° 10.23'	2.58*	0.41	9	243	2.4	0.09	0.8	0.5	D
	010110	2202 04.99	39° 22.61'	111° 12.22'	4.72	0.47	5	323	8.1	0.23	36.5	17.6	D
3	010111	0732 09.13	39° 23.05'	111° 14.02'	7.10*	0.93	9	293	3.0	0.18	2.0	1.1	D
	010116	0424 17.80	39° 20.70'	111° 9.31'	7.02	1.13	5	190	5.3	0.11	1.8	9.5	D
2	010125	0613 47.95	39° 14.69'	111° 10.29'	2.50*	0.63	7	241	2.2	0.07	1.1	0.6	D
	010125	1554 23.76	39° 22.51'	111° 12.53'	3.95	0.39	5	323	7.8	0.23	999.9	999.9	D
	010126	2324 31.41	39° 21.09'	111° 6.57'	6.87	0.70	7	242	4.4	0.14	6.0	10.3	D
	010131	1923 53.54	39° 20.21'	111° 10.22'	2.50	0.00	7	161	4.7	0.26	2.1	26.6	D
	010201	1159 40.55	39° 23.49'	111° 10.06'	6.02	0.36	7	272	4.9	0.13	5.7	5.9	D
	010201	1922 14.50	39° 22.49'	111° 12.96'	3.95	0.42	5	323	7.7	0.22	999.9	999.9	D
	010201	2318 38.30	39° 22.74'	111° 12.33'	4.71	0.00	5	323	8.2	0.24	37.3	19.8	D
	010207	0314 30.70	39° 20.03'	111° 8.32'	4.82	0.96	7	181	4.6	0.22	3.1	12.4	D
	010425	1330 26.72	39° 18.35'	111° 8.59'	4.35	1.31	7	134	4.5	0.24	2.2	12.6	C

EXPLANATION

ID	Identification number assigned to three seismic events for reference purposes.
DEPTH	Seismic event depth in kilometers. The asterisk indicates an "A" quality depth (DMIN ≤ DEPTH and ERZ ≤ 2.0 km).
MAG	Duration magnitude.
NO	The number of P and S arrival readings used in the event solution.
GAP	The largest azimuthal separation in degrees between the recording stations used in the solution.
DMIN	The epicentral distance in kilometers.
RMS	The root mean square of the travel time residuals in seconds.
ERH	Standard horizontal error in kilometers.
ERZ	Standard vertical error in kilometers.
Q	Assigned epicentral quality parameter based on an average of the following two schemes:

	Station Distribution Scheme			Statistical Measure Scheme	
	NO	GAP		RMS (sec)	ERH (km)
A	≥ 8	≤ 90°	A	≤ 0.05	< 0.2
B	≥ 6	≤ 135°	B	≤ 0.10	< 0.4
C	≥ 6	≤ 180°	C	≤ 0.20	< 0.6
D	others	others	D	others	

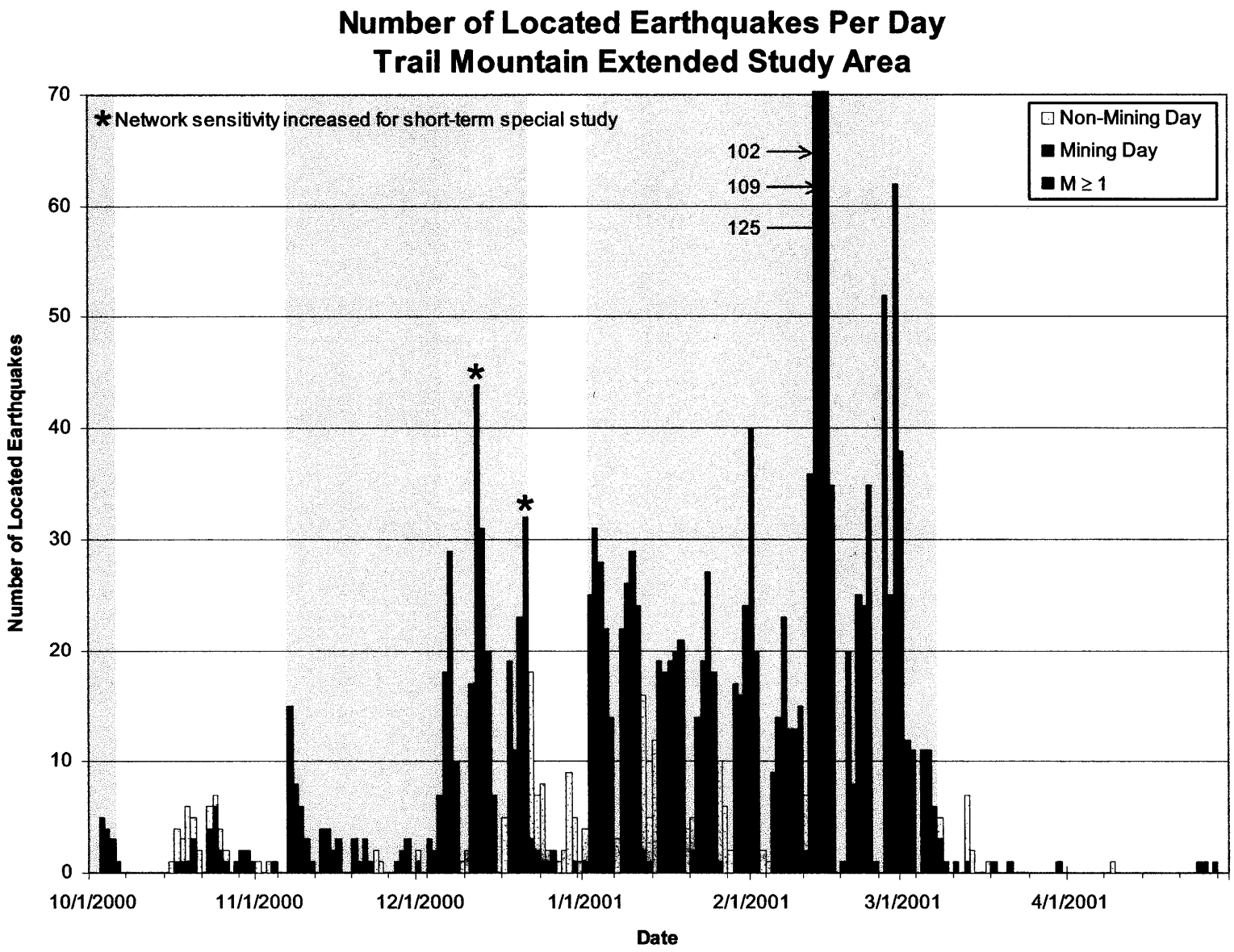
Number of Located Earthquakes Per Day
Trail Mountain Extended Study Area
* Network sensitivity increased for short-term special study
Non-Mining Day
Mining Day
M ≥ 1
102
109
125
*
*
Number of Located Earthquakes
70
60
50
40
30
20
10
0
10/1/2000
11/1/2000
12/1/2000
1/1/2001
2/1/2001
3/1/2001
4/1/2001
Date

Figure 4-1

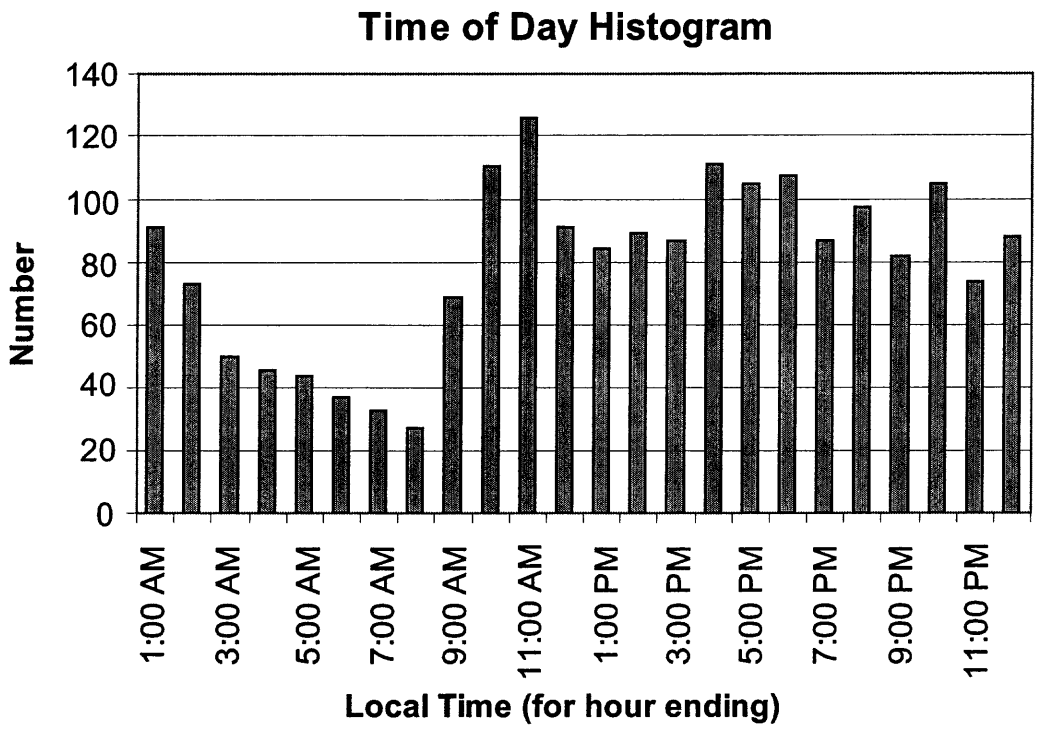

Figure 4-2. Histogram of 1,913 earthquakes in the Trail Mountain earthquake catalog (October 3, 2000–April, 30, 2001) showing distribution by time of day. Each bin is for one hour (for the hour ending with the labeled time).

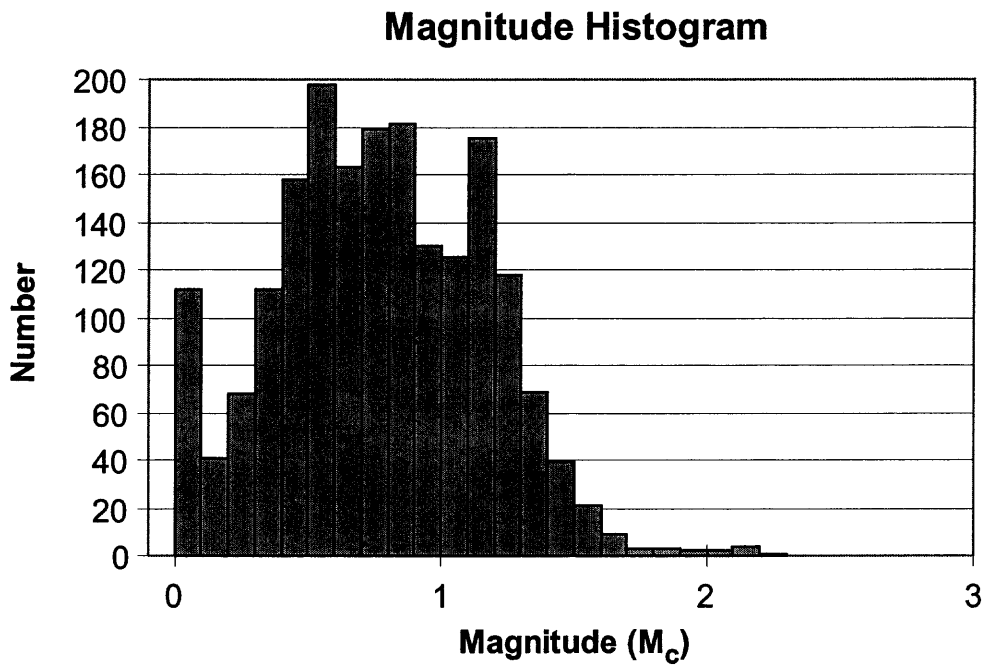

Figure 4-3. Histogram of magnitude (M_c) for 1,913 earthquakes in the Trail Mountain earthquake catalog (October 3, 2000-April 30, 2001).

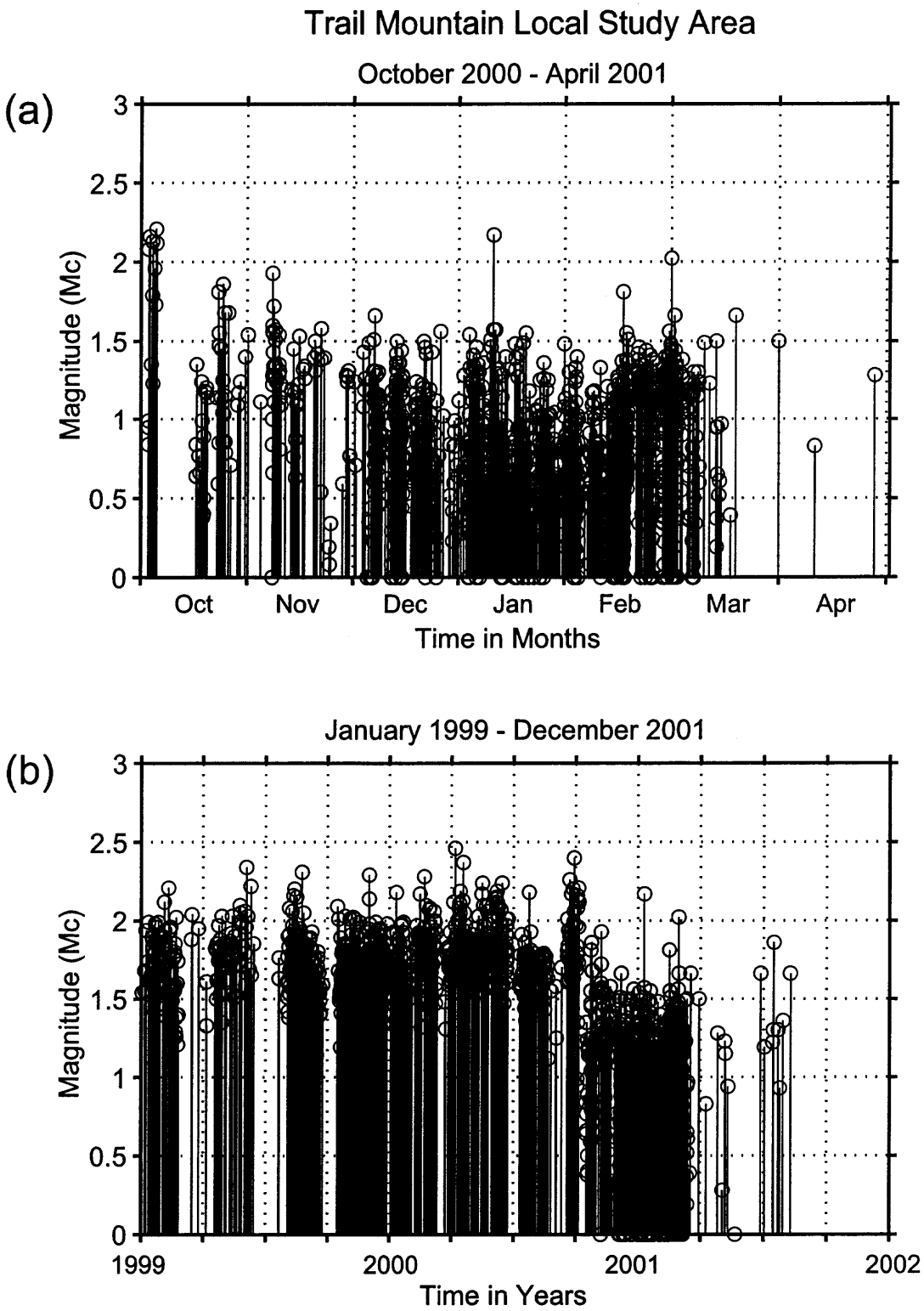

Figure 4-4. Plots of magnitude versus time from continuous monitoring of seismicity in the Trail Mountain local study area during (a) the seven-month period of this project (October 2000 through April 2001) and (b) a three-year period (January 1999 through December 2001), encompassing the sample from (a). Data for the extended period of sample (b) are from the University of Utah regional seismic network.

TM Extended Study Area
Oct 2000 - Apr 2001 (All Located Events)

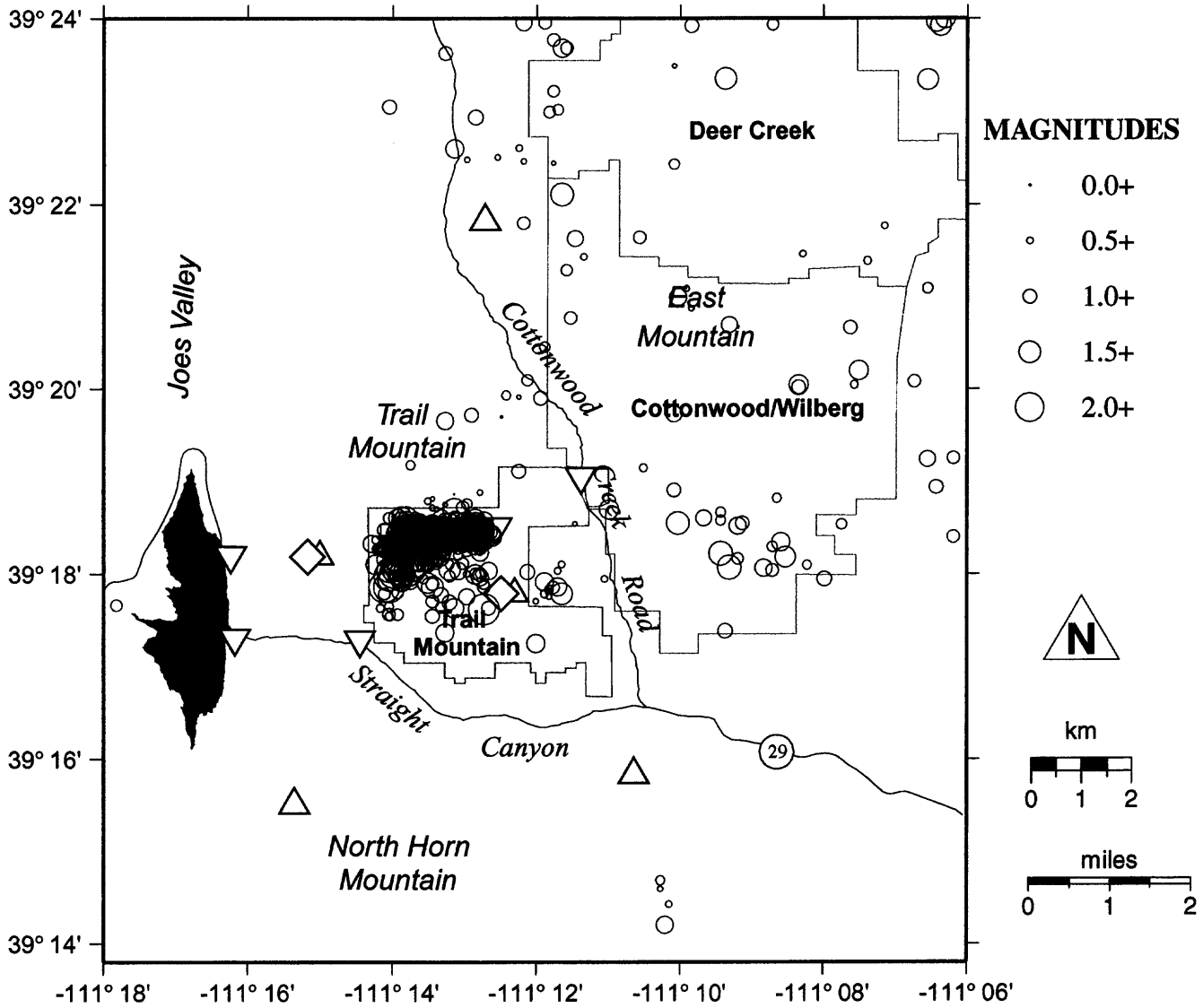

Figure 4-5. Epicenter map of entire Trail Mountain earthquake catalog. Epicenters (circles) are for 1,913 earthquakes (scaled by magnitude), October 3, 2000-April 30, 2001; red indicates Quality D (poor) solutions; black, Quality A, B, C. Base map as in Figure 2-2. The outline of the Trail Mountain Mine and lease boundaries of the Deer Creek and Cottonwood/Wilberg mines are shown for reference.

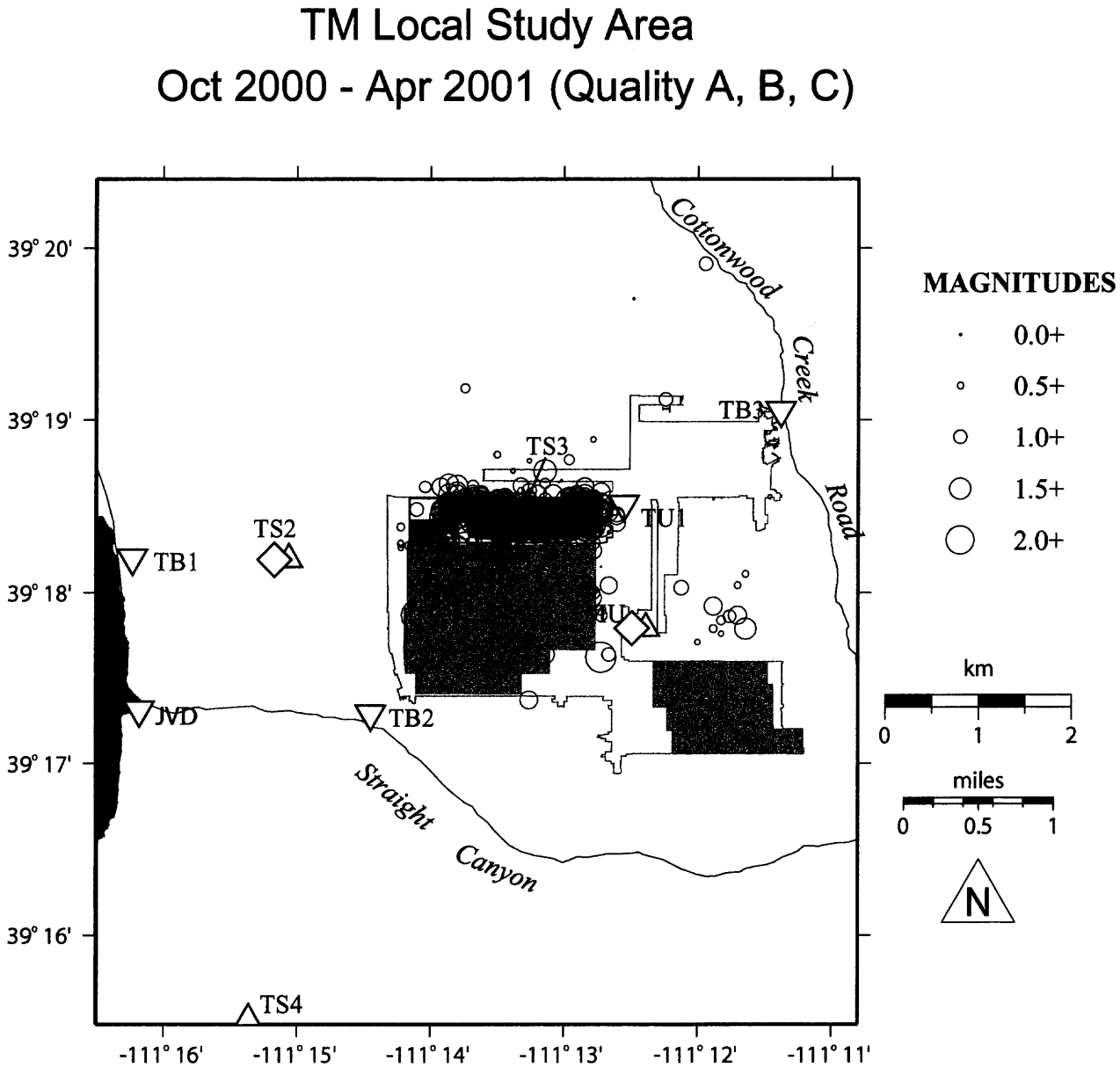

Figure 4-6. Epicenter map of better-located seismic events (scaled by magnitude) within the local study area. Epicenters include Quality A (20 events), B (1,449) and C (332). Base map includes: seismic stations, as in Figure 2-2; outline of the Trail Mountain Mine (blue); longwall panels (green) mined during the monitoring period of this study (see Figure 2-4); and areas mined out by longwall operations prior to this study (shown in pink). The latter include an area in the southeastern part of the mine, mined during October 1995–March 1997, and an area in the western part of the mine where east-west panels were mined, with one exception, from south to north during March 1997–August 2000 (see Figure F-6).

Figure 4-7. (following pages) Epicenter maps of better-located earthquakes (Quality A, B, C) in the Trail Mountain Mine area for six consecutive time periods between October 2000 and April 2001 (compare with field project timeline in Table 2-1 and temporal distribution of located earthquakes in Figure 4-1):

a) 32-day non-mining period (10/6/2000–11/6/2000) after interruption of mining in 2nd Right panel and before start of mining in 1st Right (N = 44 earthquakes, magnitude ≤ 2.1);

b) 46-day mining period (11/7/2000–12/22/2000) from start of mining in 1st Right panel to beginning of Christmas–New Year's holiday break (N = 340 earthquakes, magnitude ≤ 1.9);

c) 10-day non-mining period (12/23/2000–1/1/2001) during Christmas–New Year's holiday break (N = 38 earthquakes, magnitude ≤ 1.7);

d) 41-day mining period 1/2/2001–2/11/2001) beginning after holiday break and ending just prior to onset of markedly increased seismicity (N = 624 earthquakes, magnitude ≤ 2.2);

e) 32-day mining period (2/12/2001–3/15/2001) beginning with onset of increased seismicity and ending approximately one week after completion of mining in 1st Right (N = 760 earthquakes, magnitude ≤ 2.0);

f) 46-day non-mining period (3/16/2001–4/30/2001) after completion of mining in 1st Right through end of project monitoring (N = 7, magnitude ≤ 1.7).

Base map information as in Figure 4-6. Yellow rectangle in frames (b), (d), and (e) outlines the part of the longwall panel that was mined during the corresponding time period.

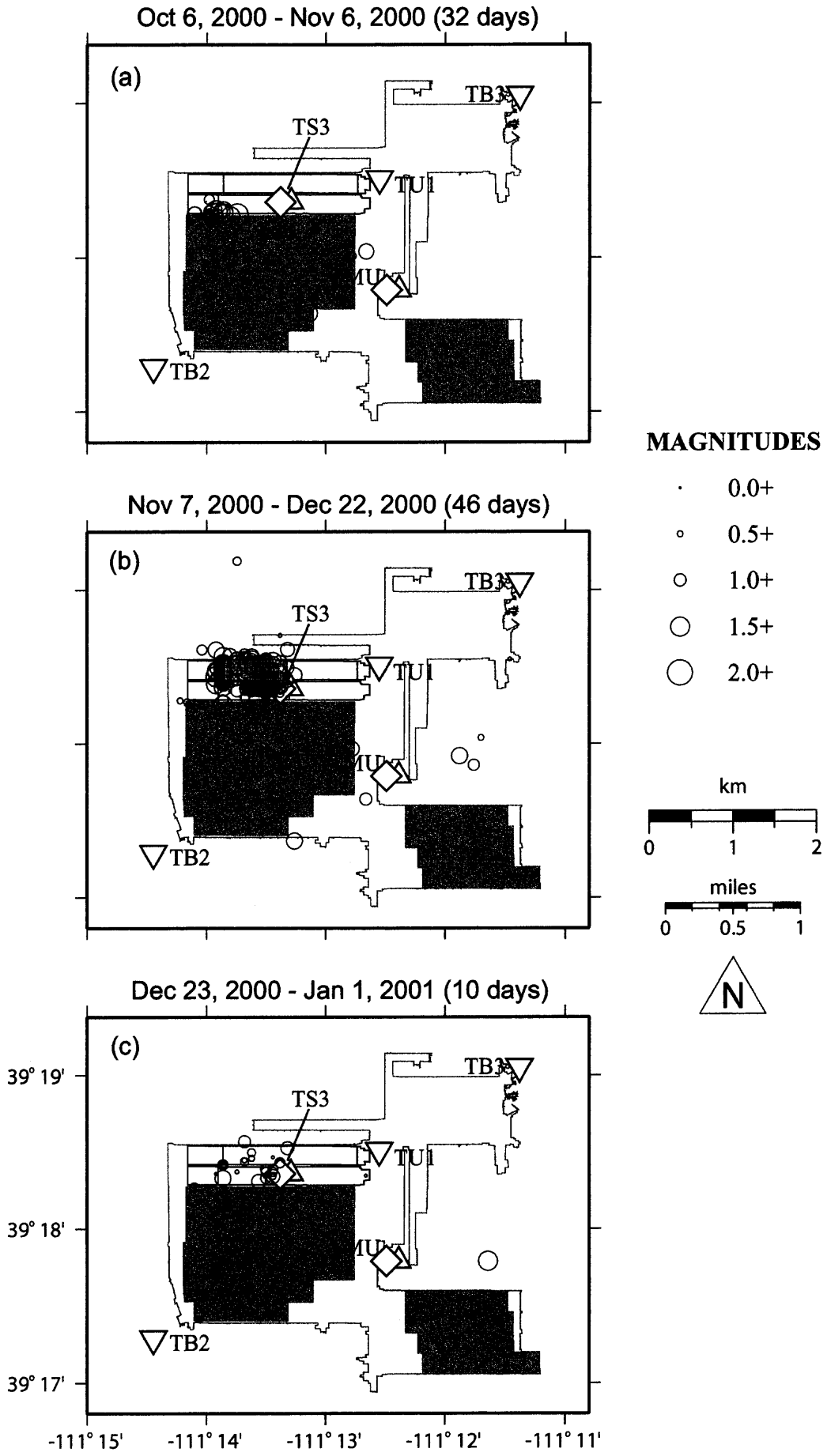
Oct 6, 2000 - Nov 6, 2000 (32 days)
(a)
TS3
TB3
TU1
TB2
Nov 7, 2000 - Dec 22, 2000 (46 days)
(b)
TS3
TB3
TU1
TB2
Dec 23, 2000 - Jan 1, 2001 (10 days)
(c)
TS3
TB3
TU1
TB2
39° 19'
39° 18'
39° 17'
-111° 15'
-111° 14'
-111° 13'
-111° 12'
-111° 11'
MAGNITUDES
0.0+
0.5+
1.0+
1.5+
2.0+
km
0
1
2
miles
0
0.5
1
N

Figure 4-7

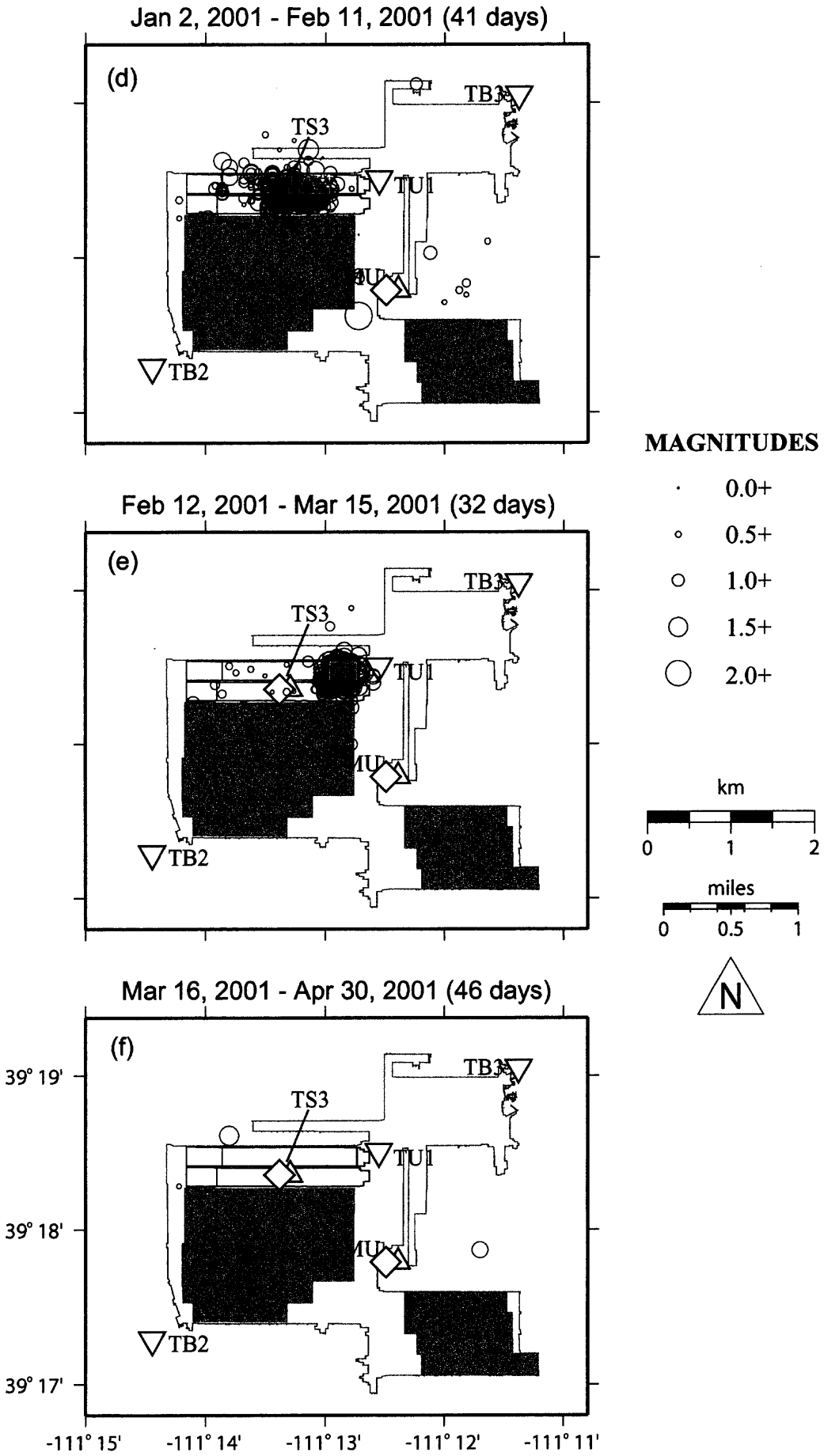

Figure 4-7 (cont'd)

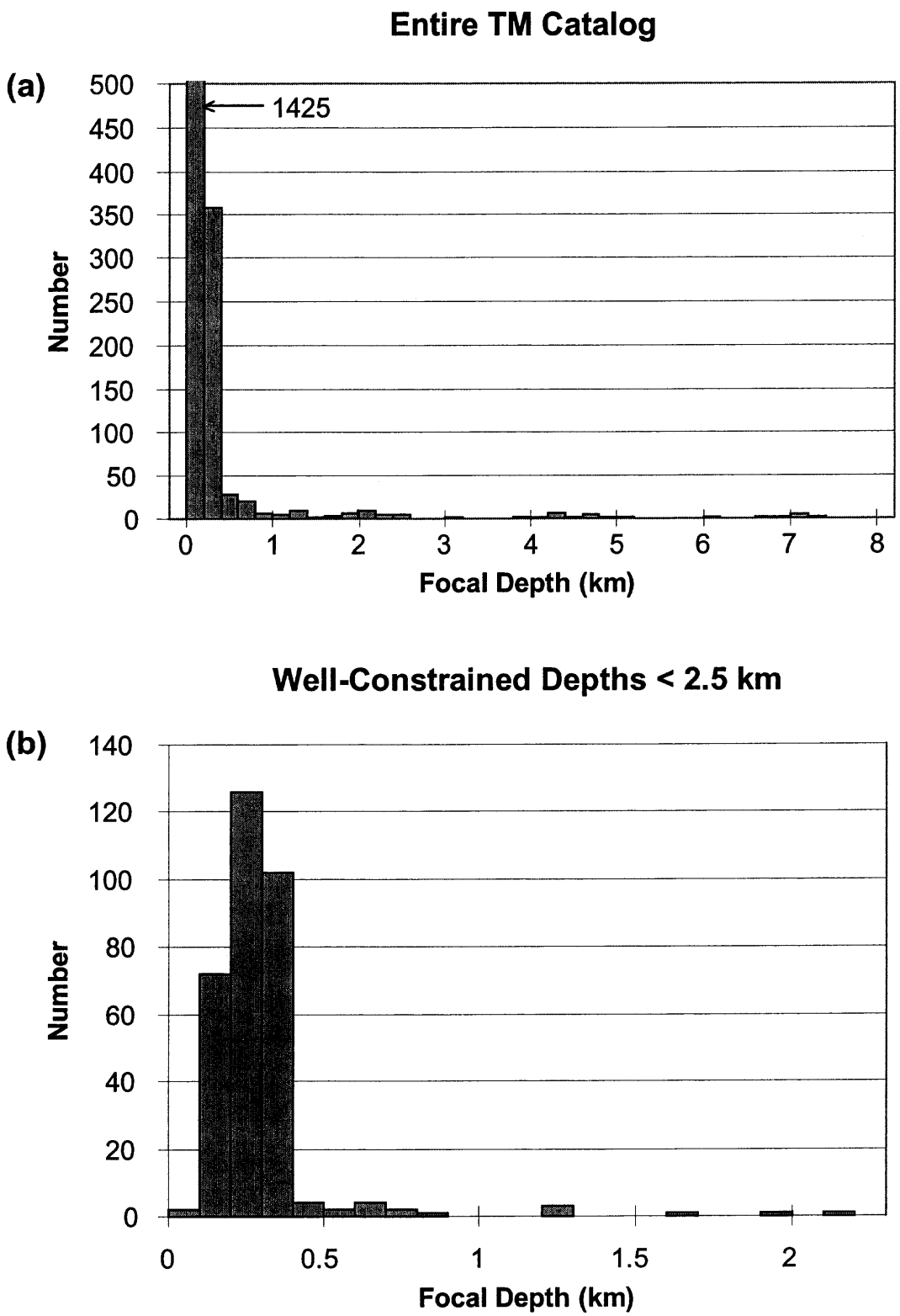

Figure 4-8. Focal-depth histograms (a) for all 1,913 events in the Trail Mountain earthquake catalog (October 3, 2000-April 30, 2001) and (b) for 321 earthquakes in the local study area with well-constrained depths < 2.5 km.

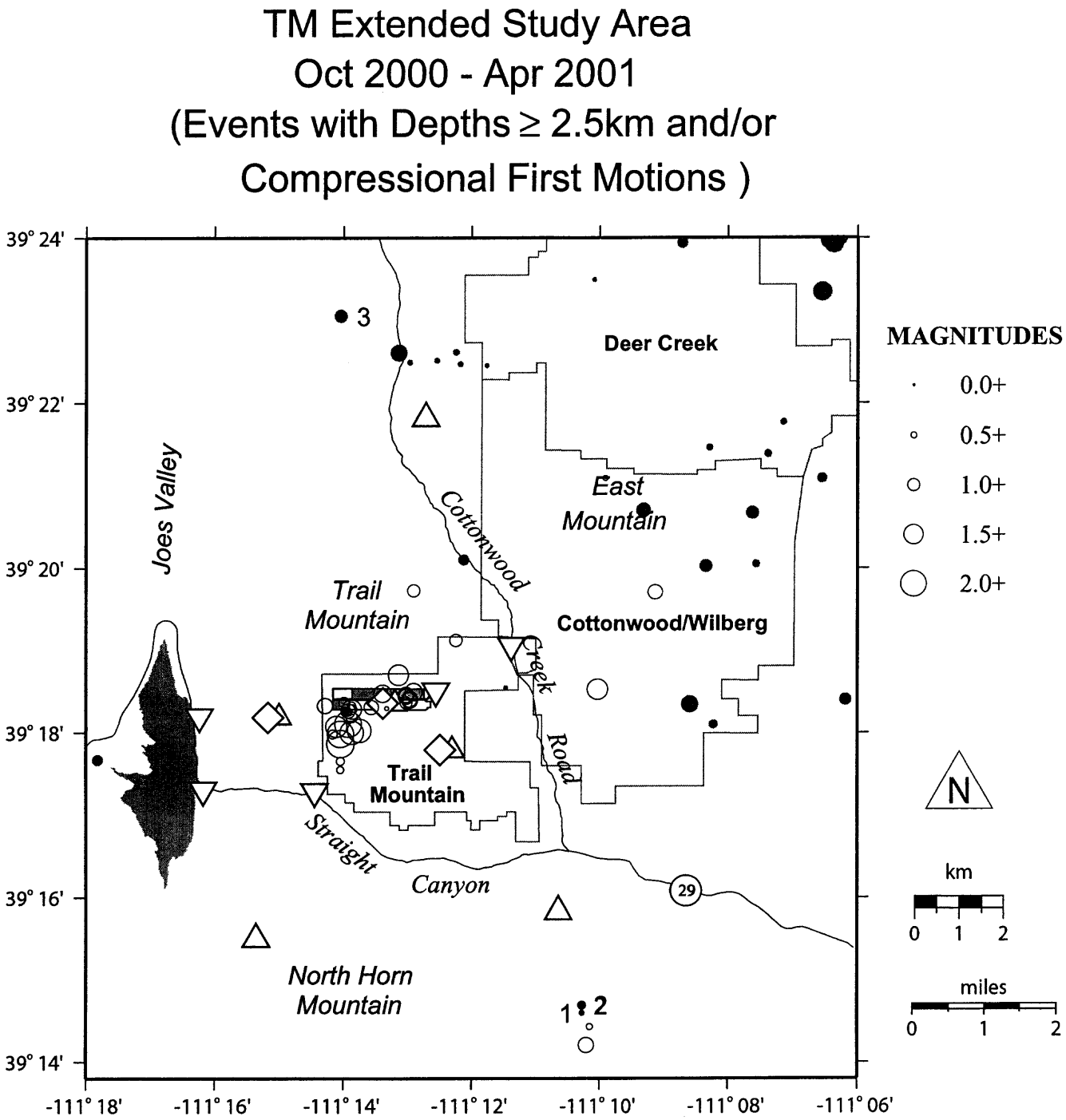

Figure 4-9. Epicenter map showing locations (scaled by magnitude) of 24 earthquakes located with focal depth ≥ 2.5 km (filled gray circles) and 43 earthquakes recorded with at least one compressional first motion (open circles, except as noted below). The epicentral locations for the deep events are poorly constrained, and only three of these events (labeled 1, 2, and 3–keyed to Table 4-1) had well-constrained focal depths. Events labeled 1 and 2 were both deep and had at least one recorded compressional first motion. Base map as in Figure 4-5.

5.0 REFERENCES

Arabasz, W. J. and D. R. Julander (1986). Geometry of seismically active faults and crustal deformation within the Basin and Range-Colorado Plateau transition, in *Cenozoic Tectonics of the Basin and Range Province: A Perspective on Processes and Kinematics of an Extensional Origin,* L. Mayer, Editor, *Geol. Soc. Am. Special Paper 208,* 43-74.

Arabasz, W. J., S. J. Nava, and W. T. Phelps (1997). Mining seismicity in the Wasatch Plateau and Book Cliffs coal mining districts, Utah, USA, in *Rockbursts and Seismicity in Mines*, S. J. Gibowicz and S. Lasocki (eds.), A. A. Balkema, Rotterdam, 111-116.

Arabasz, W. J., and J. C. Pechmann (2001). Seismic characterization of coal-mining seismicity in Utah for CTBT monitoring, *Technical Report UCRL-CR-143772*, Lawrence Livermore National Laboratory, Livermore, California, LLNL Research Agreement No. B344836, 120 pp.

Bjarnason, I. T. and J. C. Pechmann (1989). Contemporary tectonics of the Wasatch Front region, Utah, from earthquake focal mechanisms, *Bull. Seism. Soc. Am.* **79**, 731-755.

Bolt, Bruce A. (1993). *Earthquakes*, W. H. Freeman and Company, New York, 331 pp.

Doelling, H. H. (1972). Central Utah coal fields: Sevier-Sanpete, Wasatch Plateau, Book Cliffs, and Emery, *Utah and Geological and Mineral Survey Monograph 3*, Salt Lake City, Utah, 571 pp.

Ellenberger, J. L., K. A. Heasley, P. L. Swanson, and J. Mercier (2001). Three dimensional microseismic monitoring of a Utah longwall, in *Rock Mechanics in the National Interest,* D. Elsworth, J. P. Tinucci, and K. A. Heasley (eds.), A. A. Balkema, Rotterdam, 1321-1326.

Foley, L. L., R. A. Martin, and J. T. Sullivan (1986). Seismotectonic study for Joes Valley, Scofield, and Huntington North dams, Emery County and Scofield Projects, Utah, *Seismotectonic Report 86-7*, U.S. Bureau of Reclamation, Denver, Colorado, 132 pp.

Gibowicz, S. J. (1990a). Keynote lecture: The mechanism of seismic events induced by mining, in *Rockbursts and Seismicity in Mines*, C. Fairhurst (ed.), A. A. Balkema, Rotterdam, 3-27.

Gibowicz, S. J. (1990b). Seismicity induced by mining: *Advances in Geophysics* **32**, 1-74.

Gomberg, J.S., Shedlock, K.M., and S.W. Roecker (1990). The effect of S-wave arrival times on the accuracy of hypocenter estimation, *Bull. Seism. Soc.* **80**, 1605-1628.

Griscom, M., and W. J. Arabasz (1979). Local magnitude (M_L) in the Wasatch Front and Utah region: Wood-Anderson calibration, coda-duration estimates of M_L, and M_L versus m_b,

in *Earthquake Studies in Utah, 1850 to 1978*, Arabasz, W. J., R. B. Smith, and W. D. Richins (eds.), University of Utah Seismograph Stations, Salt Lake City, Utah, 433-443.

Hecker, S. (1993). Quaternary tectonics of Utah with emphasis on earthquake-hazard characterization, *Utah Geological Survey Bulletin 127*, Salt Lake City, Utah, 157 pp.

Jahanbani, F. R. (2001). *2000 Annual Review and Forecast of Utah Coal Production and Distribution*, State of Utah Department of Natural Resources, Salt Lake City, Utah, 39 pp.

Klein, F. W. (1978). Hypocenter location program HYPOINVERSE, *U.S. Geol. Surv., Open-File Rept. 78-694,* 113 pp.

Knoll, P. and W. Kuhnt (1990). Seismological and technical investigations of the mechanics of rockbursts, in *Rockbursts and Seismicity in Mines*, C. Fairhurst (ed.), A. A. Balkema, Rotterdam, 129-138.

McGarr, A. and Fletcher, J. B. (2002). Development of ground motion attenuation relationships relevant to mining-induced seismicity in the Trail Mountain area, Emery County, Utah, *Final Report*, State of Utah, School and Institutional Trust Lands Administration, Salt Lake City, Utah, 23 pp.

Pechmann, J. C., J. C. Bernier, S. J. Nava, F. M. Terra, and W. J. Arabasz (2001). Correction of systematic time-dependent coda-magnitude errors in the Utah and Yellowstone National Park Region earthquake catalogs, 1981-2001 (abstract), *Eos, Trans. Am. Geophys. Union* **81**, (49), Fall Meeting Suppl., S11B-0572, F809.

Wong, I. G. (1993). Tectonic stresses in mine seismicity: Are they significant?, in *Rockbursts and Seismicity in Mines 93*, R. P. Young (ed.), A. A. Balkema, Rotterdam, 273-278.

APPENDIX A

SPECIFICATIONS AND CALIBRATION DATA FOR INSTRUMENTATION USED IN THE TRAIL MOUNTAIN STUDY

Station TB1

Location Information

Latitude:	39° 18.20′ North	UTM North:	14273173.8
Longitude:	111° 16.23′ West	UTM East:	1563890.1
Elevation:	2188 meters		

Telemetry

On-site digital recording to local disk; independently triggered when local ground motion exceeds 0.001%g (acceleration).

Instrumentation

A.. Valid Date/Time Range: October 13, 2000 (installation date) – December 15, 2000 (21:34 UTC)
Digitizer: Kinemetrics Altus Series K2 (19-bit resolution); SN 1562

Component	Digitizer Channel No.	Sensor Serial No.	Sensor Model	Sensor Component Serial No.	Gain	Span (volts/g)	Cal-Coil Sensitivity (g/volts)	Instrument Sensitivity (volts/g)
E	1	755	Episensor	2717	0.25	1.2504	0.0595	1.2504
N	2	755	Episensor	2510	1	1.2517	0.0562	1.2517
Z	3	755	Episensor	2264	1	1.2519	0.0532	1.2519
Z	4	2913	L4C	2913	1	n/a	n/a	n/a

Comments:

A Kinemetrics gain board was installed in the K2s used for the Trail Mountain project. This board is used to damp the signal from an external short period sensor. The board was factory installed in channels 1-3. UUSS Technicians thought the gain board was installed in channels 4-6 since K2s with internal sensors came wired that way. As a result of this misunderstanding, channel 1 records of Episensor data have a gain of 0.25 during this time period. The problem was corrected by moving the Episensor to channels 4-6, beginning on December 15, 2000 for this station (TB1).

Polarity Convention

Episensor: positive output for positive acceleration
L4C: positive output for positive ground motion

Displacement Response Data

The Poles and Zeros listed below are those of a ratio of polynomials of the Laplace Transform variable "s".

	Z	E	N
Zeros 2 (radians/second)	0.0 ± 0.0i	0.0 ± 0.0i	0.0 ± 0.0i
	0.0 ± 0.0i	0.0 ± 0.0i	0.0 ± 0.0i
Poles 4 (radians/second)	-981.0 ± 1009.0i	-981.0 ± 1009.0i	-981.0 ± 1009.0i
	-3290.0 ± 1263.0i	-3290.0 ± 1263.0i	-3290.0 ± 1263.0i
Gain Constant (counts/micron)	0.1054×10^{14}	0.2630×10^{13}	0.1054×10^{14}

B. *Valid Date/Time Range: December 15, 2000 (installation date) – February 28, 2002 (end of project)*
Digitizer: Kinemetrics Altus Series K2 (19-bit resolution); SN 1562

Component	Digitizer Channel No.	Sensor Serial No.	Sensor Model	Sensor Component Serial No.	Gain	Span (volts/g)	Cal-Coil Sensitivity (g/volts)	Instrument Sensitivity (volts/g)
Z	1	2913	L4C	2913	0.25	n/a	n/a	n/a
E	4	755	Episensor	2717	1	1.2504	0.0595	1.2504
N	5	755	Episensor	2510	1	1.2517	0.0562	1.2517
Z	6	755	Episensor	2264	1	1.2519	0.0532	1.2519

Comments:

A Kinemetrics gain board was installed in the K2s used for the Trail Mountain project. This board is used to damp the signal from an external short period sensor. The board was factory installed in channels 1-3. UUSS Technicians thought the gain board was installed in channels 4-6 since K2s with internal sensors came wired that way. As a result of this misunderstanding, channel 1 records of Episensor data have a gain of 0.25 during this time period. The problem was corrected by moving the Episensor to channels 4-6, beginning on December 15, 2000 for this station (TB1).

For the time period December 15, 2000 to January 2, 2001 the K2 header values Alt, and Azi (deg) were entered improperly. The following contains the correct values.

Digitizer Channel No.	Component	Alt	Azi
1	Z-L4	-90	0
4	E	0	90
5	N	0	0
6	Z	-90	0

Polarity Convention

Episensor: positive output for positive acceleration
L4C: positive output for positive ground motion

Displacement Response Data

The Poles and Zeros listed below are those of a ratio of polynomials of the Laplace Transform variable "s".

	Z	E	N
Zeros 2 (radians/second)	0.0 ± 0.0i	0.0 ± 0.0i	0.0 ± 0.0i
	0.0 ± 0.0i	0.0 ± 0.0i	0.0 ± 0.0i
Poles 4 (radians/second)	-981.0 ± 1009.0i	-981.0 ± 1009.0i	-981.0 ± 1009.0i
	-3290.0 ± 1263.0i	-3290.0 ± 1263.0i	-3290.0 ± 1263.0i
Gain Constant (counts/micron)	0.1054×10^{14}	0.1052×10^{14}	0.1054×10^{14}

Station TB2

Location Information

Latitude:	39° 17.29′ North	UTM North:	14267630.3
Longitude:	111° 14.45′ West	UTM East:	1572296.7
Elevation:	2082 meters		

Telemetry

On-site digital recording to local disk; independently triggered when local ground motion exceeds 0.001%g (acceleration).

Instrumentation

A. *Valid Date/Time Range: October 13, 2000 (installation date) – December 18, 2000 (21:55 UTC)*
Digitizer: Kinemetrics Altus Series K2 (19-bit resolution); SN 1563

Component	Digitizer Channel No.	Sensor Serial No.	Sensor Model	Sensor Component Serial No.	Gain	Span (volts/g)	Cal-Coil Sensitivity (g/volts)	Instrument Sensitivity (volts/g)
E	1	757	Episensor	2810	1	1.2526	0.0595	1.2526
N	2	757	Episensor	2836	1	1.2495	0.0579	1.2495
Z	3	757	Episensor	4625	1	1.2517	0.0599	1.2517
Z	4	2914	L4C	2914	1	n/a	n/a	n/a

B. *Valid Date/Time Range: December 18, 2000 (22:57 UTC) – November 11, 2001*
Digitizer: Kinemetrics Altus Series K2 (19-bit resolution); SN 1563

Component	Digitizer Channel No.	Sensor Serial No.	Sensor Model	Sensor Component Serial No.	Gain	Span (volts/g)	Cal-Coil Sensitivity (g/volts)	Instrument Sensitivity (volts/g)
Z	1	2914	L4C	2914	1	n/a	n/a	n/a
E	4	757	Episensor	2810	1	1.2526	0.0595	1.2526
N	5	757	Episensor	2836	1	1.2495	0.0579	1.2495
Z	6	757	Episensor	4625	1	1.2517	0.0599	1.2517

Comments:

A Kinemetrics gain board was installed in the K2s used for the Trail Mountain project. This board is used to facilitate damping the signal from an external short period sensor. The board was factory installed in channels 1-3. UUSS Technicians thought the gain board was installed in channels 4-6 since K2s with internal sensors came wired that way. The gain at this station was set to 1, so there was no change to the data as result of the gain board. To be consistent with other K2 station wiring, we changed to channels 4-6 for Episensor recording and to channel 1 for L4C recording.

For the time period December 18, 2000 to January 2, 2001, the anti-aliasing filter was inadvertently set to causal.

Polarity Convention

Episensor: positive output for positive acceleration
L4C: positive output for positive ground motion

Displacement Response Data

The Poles and Zeros listed below are those of a ratio of polynomials of the Laplace Transform variable "s".

	Z	E	N
Zeros 2 (radians/second)	0.0 ± 0.0i	0.0 ± 0.0i	0.0 ± 0.0i
	0.0 ± 0.0i	0.0 ± 0.0i	0.0 ± 0.0i
Poles 4 (radians/second)	-981.0 ± 1009.0i	-981.0 ± 1009.0i	-981.0 ± 1009.0i
	-3290.0 ± 1263.0i	-3290.0 ± 1263.0i	-3290.0 ± 1263.0i
Gain Constant (counts/micron)	0.1054×10^{14}	0.1054×10^{14}	0.1052×10^{14}

C. *Valid Date/Time Range: November 11, 2001- February 28, 2002 (end of project)*
Digitizer: Kinemetrics Altus Series K2 (19-bit resolution); SN 1561

Component	Digitizer Channel No.	Sensor Serial No.	Sensor Model	Sensor Component Serial No.	Gain	Span (volts/g)	Cal-Coil Sensitivity (g/volts)	Instrument Sensitivity (volts/g)
Z	1	2914	L4C	2914	1	n/a	n/a	n/a
E	4	757	Episensor	2810	1	1.2526	0.0595	1.2526
N	5	757	Episensor	2836	1	1.2495	0.0579	1.2495
Z	6	757	Episensor	4625	1	1.2517	0.0599	1.2517

Comments:

The K2 digitizer was removed for repairs and replaced with a new unit (SN 1561) on November 11, 2001.

Polarity Convention

Episensor: positive output for positive acceleration
L4C: positive output for positive ground motion

Displacement Response Data

The Poles and Zeros listed below are those of a ratio of polynomials of the Laplace Transform variable "s".

	Z	E	N
Zeros 2 (radians/second)	0.0 ± 0.0i	0.0 ± 0.0i	0.0 ± 0.0i
	0.0 ± 0.0i	0.0 ± 0.0i	0.0 ± 0.0i
Poles 4 (radians/second)	-981.0 ± 1009.0i	-981.0 ± 1009.0i	-981.0 ± 1009.0i
	-3290.0 ± 1263.0i	-3290.0 ± 1263.0i	-3290.0 ± 1263.0i
Gain Constant (counts/micron)	0.1054×10^{14}	0.1054×10^{14}	0.1052×10^{14}

Station TB3

Location Information

Latitude:	39° 19.10′ North	UTM North:	14278606.9
Longitude:	111° 11.44′ West	UTM East:	1586483.7
Elevation:	2292 meters		

Telemetry

On-site digital recording to local disk; independently triggered when local ground motion exceeds 0.001%g (acceleration).

Instrumentation

A. Valid Date/Time Range: December 12, 2000 (installation date) – December 15, (19:29 UTC)
Digitizer: Kinemetrics Altus Series K2 (19-bit resolution); SN 1561

Component	Digitizer Channel No.	Sensor Serial No.	Sensor Model	Sensor Component Serial No.	Gain	Span (volts/g)	Cal-Coil Sensitivity (g/volts)	Instrument Sensitivity (volts/g)
E	1	756	Episensor	4025	0.125	1.2501	0.0548	1.2501
N	2	756	Episensor	4038	1	1.2509	0.0555	1.2509
Z	3	756	Episensor	4043	1	1.2490	0.0552	1.2490
Z	4	2915	L4C	2915	1	n/a	n/a	n/a

Comments:

A Kinemetrics gain board was installed in the K2s used for the Trail Mountain project. This board is used to damp the signal from an external short period sensor. The board was factory installed in channels 1-3. UUSS Technicians thought the gain board was installed in channels 4-6 since K2s with internal sensors came wired that way. As a result of this misunderstanding, channel 1 records of Episensor data have a gain of 0.125 during this time period. The problem was corrected by moving the Episensor to channels 4-6, beginning on December 15, 2000 for this station (TB3).

Polarity Convention

Episensor: positive output for positive acceleration
L4C: positive output for positive ground motion

Displacement Response Data

The Poles and Zeros listed below are those of a ratio of polynomials of the Laplace Transform variable "s".

	Z	E	N
Zeros 2 (radians/second)	0.0 ± 0.0i	0.0 ± 0.0i	0.0 ± 0.0i
	0.0 ± 0.0i	0.0 ± 0.0i	0.0 ± 0.0i
Poles 4 (radians/second)	-981.0 ± 1009.0i	-981.0 ± 1009.0i	-981.0 ± 1009.0i
	-3290.0 ± 1263.0i	-3290.0 ± 1263.0i	-3290.0 ± 1263.0i
Gain Constant (counts/micron)	0.1051×10^{14}	0.1315×10^{13}	0.1053×10^{14}

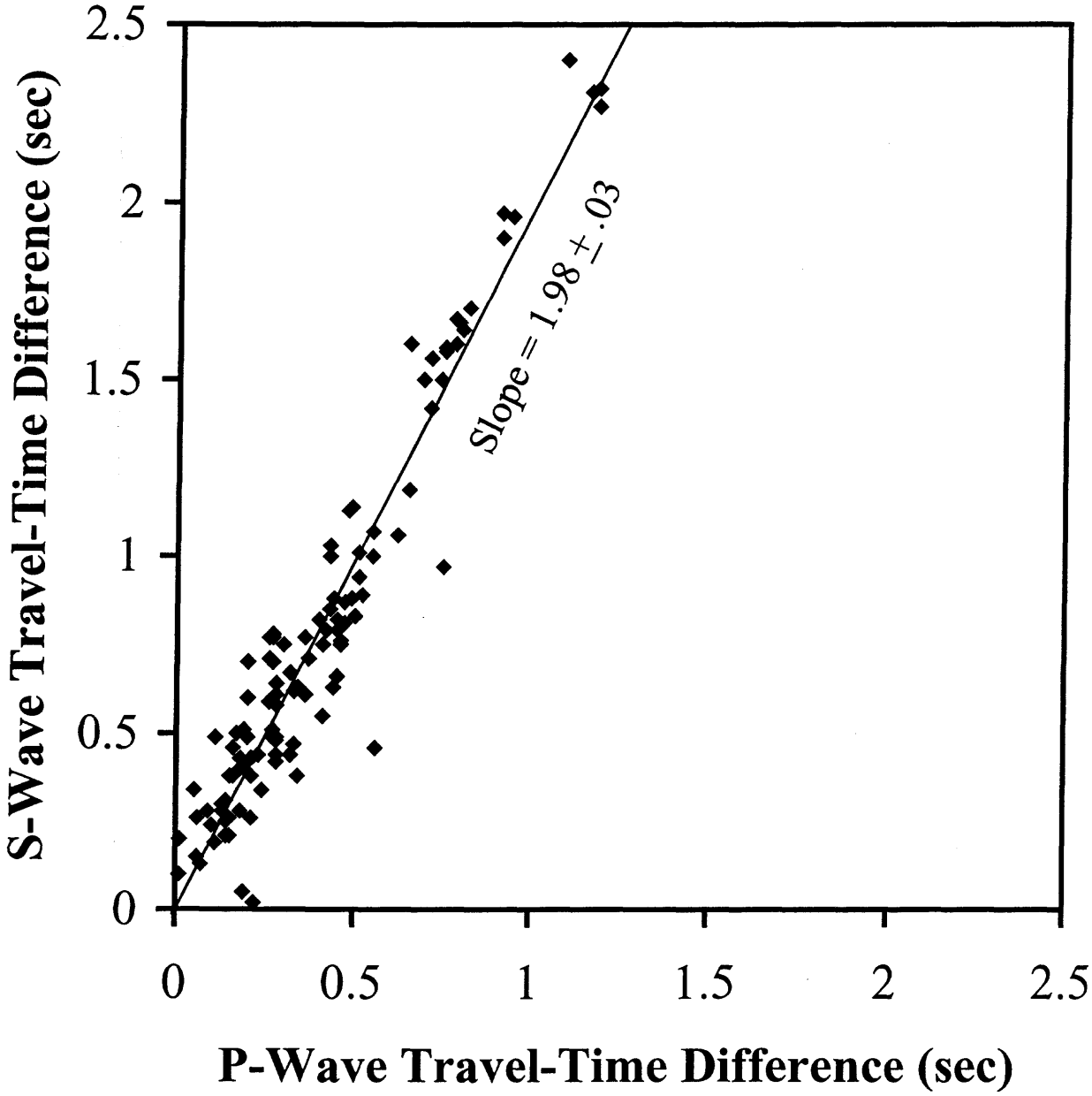

Figure B-3. Plot of S-wave travel-time difference versus P-wave travel-time difference for station pairs in the UUSS data set with P-wave pick weights of 0 and S-wave pick weights of 2. Linear regression of these 111 data points, with the line constrained to pass through the origin, yields an average V_P/V_S ratio of 1.98 ± .03 (95% confidence limits).

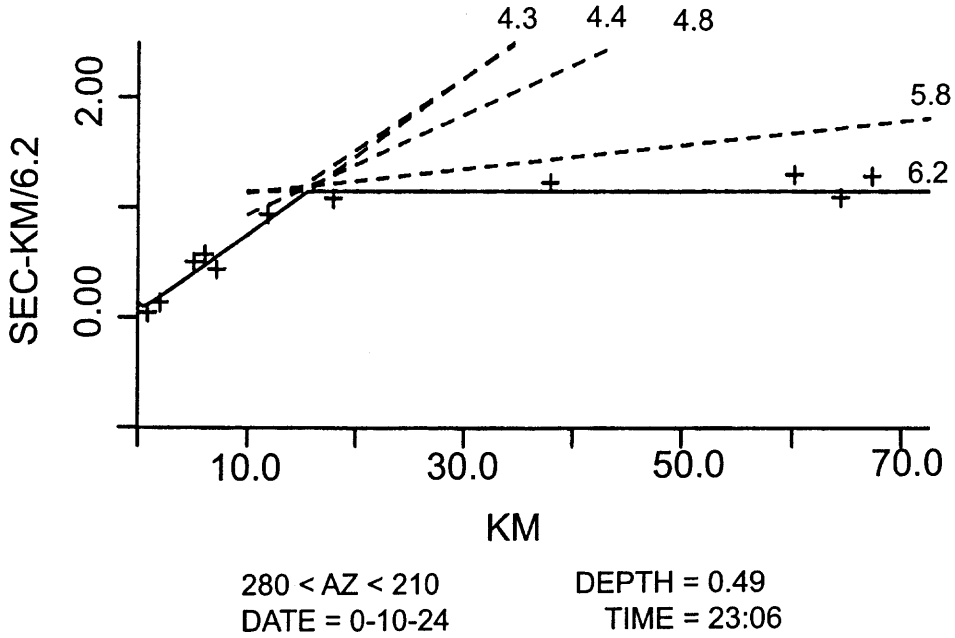

Figure B-4. Plot of reduced travel time, time (sec) – distance (km)/6.2 km/sec, versus distance in km for an M_C 1.9 earthquake in the Trail Mountain area on October 24, 2000. The crosses show observed, elevation-corrected travel times for first arrivals at stations in the Colorado Plateau Province (azimuth range 280° to 210°). The solid lines indicate first arrival times calculated from the Colorado Plateau version of the Trail Mountain velocity model (Table B-1). The numbers are P-wave velocities in km/sec.

APPENDIX C

TABULATION OF GROUND-MOTION DATA DELIVERED TO USGS FOR DETAILED ANALYSIS

TABLE C-1

TABULATION OF GROUND-MOTION DATA DELIVERED TO THE USGS FOR DETAILED ANALYSIS – HYPOCENTRAL DATA SUMMARY

ID	Date	Origin Time	Latitude	Longitude	Depth	Mag	No	Gap	Dmin	Rms	Erh	Erz	Q
1	001023	1529 56.45	39° 18.03'	111° 13.74'	0.37	1.81	16	57	0.8	0.19	0.4	0.6	B
2	001024	2306 02.40	39° 18.00'	111° 13.83'	0.49	1.86	18	48	0.9	0.19	0.4	0.5	B
3	001220	1404 07.95	39° 18.53'	111° 13.58'	0.04	1.11	7	116	0.4	0.02	0.3	0.7	B
4	001221	2222 45.67	39° 18.42'	111° 13.31'	0.19	0.91	9	107	0.2	0.04	0.2	0.3	B
5	001222	0251 05.19	39° 18.55'	111° 13.59'	0.11	0.95	10	118	0.5	0.08	0.3	0.9	B
6	001222	0624 51.90	39° 18.62'	111° 13.30'	0.69	1.15	12	90	0.5	0.19	0.4	0.8	B
7	001222	0859 00.84	39° 18.41'	111° 13.35'	0.24	0.99	8	106	0.1	0.03	0.3	0.4	B
8	001222	1758 00.02	39° 17.98'	111° 14.00'	0.40	0.71	9	129	1.1	0.10	0.4	5.7	B
9	001222	2022 15.47	39° 18.03'	111° 13.68'	0.01	1.19	9	93	0.8	0.09	0.3	0.8	B
10	001223	0137 05.92	39° 18.53'	111° 13.31'	0.31	1.03	10	111	0.3	0.06	0.2	0.4	B
11	001223	0529 41.34	39° 18.57'	111° 13.66'	0.20	0.98	10	120	0.6	0.05	0.2	0.6	B
12	001223	0734 24.54	39° 18.04'	111° 13.70'	0.34	1.43	17	93	0.8	0.08	0.2	0.4	B
13	001224	1753 09.64	39° 18.34'	111° 13.46'	0.20	1.12	10	105	0.1	0.05	0.2	0.3	B
14	001225	2012 00.10	39° 17.79'	111° 11.65'	0.05	1.56	10	81	1.2	0.12	0.3	1.5	B
15	001226	1608 41.77	39° 18.20'	111° 13.52'	0.36	1.02	11	100	0.3	0.04	0.2	0.3	B
16	010103	0049 03.19	39° 18.51'	111° 13.33'	0.31	1.54	12	95	0.3	0.04	0.2	0.3	B
17	010103	0850 13.21	39° 18.55'	111° 13.45'	0.13	1.18	7	115	0.3	0.01	0.2	0.8	B
18	010104	0330 27.30	39° 18.49'	111° 13.31'	0.19	1.41	12	109	0.2	0.05	0.2	0.4	B
19	010104	2028 51.89	39° 18.53'	111° 13.43'	0.34	1.31	9	113	0.3	0.05	0.3	0.4	B
20	010104	2239 46.24	39° 18.44'	111° 13.38'	0.33	1.46	9	96	0.2	0.03	0.2	0.3	B
21	010104	2347 08.67	39° 18.53'	111° 13.27'	0.24	1.28	10	110	0.3	0.04	0.2	0.5	B
22	010105	0846 27.07	39° 18.48'	111° 13.27'	0.26	1.25	11	108	0.2	0.04	0.2	0.3	B
23	010105	0913 24.95	39° 18.47'	111° 13.36'	0.24	1.35	12	109	0.2	0.04	0.2	0.3	B
24	010109	0423 26.89	39° 18.44'	111° 13.21'	0.60	1.46	14	93	0.3	0.12	0.2	0.3	C
25	010109	1727 23.44	39° 17.62'	111° 12.73'	0.13	2.17	17	86	0.5	0.19	0.3	0.8	B
26	010113	0242 15.17	39° 18.40'	111° 13.40'	0.21	1.40	9	107	0.1	0.02	0.2	0.3	B
27	010115	2008 34.00	39° 18.15'	111° 13.68'	0.01	1.48	8	99	0.6	0.02	0.2	0.7	B
28	010116	0036 58.72	39° 18.34'	111° 13.35'	0.21	1.39	10	77	0.1	0.04	0.2	0.3	A
29	010116	0320 58.11	39° 18.48'	111° 13.22'	0.09	1.32	14	94	0.3	0.05	0.1	0.3	B
30	010117	0411 12.01	39° 18.35'	111° 13.19'	0.08	1.42	9	92	0.2	0.04	0.2	0.5	B
31	010118	2156 26.59	39° 18.44'	111° 13.18'	0.08	1.55	12	105	0.3	0.07	0.2	0.5	B
32	010123	2318 44.18	39° 18.57'	111° 13.10'	0.17	1.36	10	108	0.6	0.05	0.3	0.7	B
33	010127	0257 56.28	39° 18.45'	111° 13.91'	0.00	1.04	11	119	0.8	0.11	0.4	1.8	C
34	010201	0014 10.45	39° 18.03'	111° 12.13'	0.09	1.08	10	73	0.7	0.05	0.2	1.2	A
35	010201	2143 50.01	39° 19.67'	111° 13.26'	2.07	1.24	7	146	2.5	0.15	0.7	1.6	D
36	010202	1033 08.92	39° 18.63'	111° 13.85'	0.01	1.40	13	128	0.9	0.09	0.3	1.0	B
37	010202	1822 39.40	39° 18.42'	111° 13.03'	0.10	1.02	9	102	0.5	0.06	0.3	2.3	B
38	010207	2054 01.55	39° 18.56'	111° 10.04'	0.57	1.61	13	117	2.2	0.07	0.3	0.5	B
39	010208	2333 12.20	39° 18.45'	111° 12.98'	0.05	1.33	8	101	0.6	0.10	0.3	3.8	B
40	010214	0226 21.32	39° 18.46'	111° 13.01'	0.08	1.15	9	103	0.6	0.03	0.2	1.0	B
41	010215	0456 50.45	39° 18.57'	111° 12.85'	0.08	1.37	11	90	0.9	0.07	0.3	1.1	B
42	010215	0613 39.30	39° 18.56'	111° 12.94'	0.04	1.24	12	105	0.8	0.05	0.2	0.8	B
43	010222	0613 34.60	39° 18.53'	111° 12.82'	0.14	1.27	10	101	0.9	0.07	0.3	0.7	B
44	010222	0718 35.72	39° 18.54'	111° 12.81'	0.08	1.14	11	88	0.9	0.07	0.2	1.4	B
45	010223	0617 31.04	39° 18.43'	111° 12.93'	0.02	1.31	8	184	0.7	0.09	0.5	0.8	D
46	010224	1305 33.45	39° 18.00'	111° 12.86'	0.45	1.36	9	80	0.7	0.04	0.3	0.6	B
47	010228	2202 04.38	39° 18.49'	111° 12.83'	0.09	1.45	9	101	0.8	0.08	0.3	2.1	B
48	010310	0405 02.19	39° 18.06'	111° 13.18'	0.43	1.49	10	75	0.6	0.06	0.2	0.8	B
49	010313	1223 06.65	39° 17.94'	111° 14.05'	0.10	1.50	13	89	1.2	0.06	0.2	0.9	B

EXPLANATION

ID	A sequential identification number assigned to each seismic event for reference purposes.
Date	Date in Universal Coordinated Time (UTC). Subtract seven hours to Mountain Standard Time.
Origin Time	Hour, minute, and seconds of the start time of the seismic event (UTC).
Latitude	Seismic event location coordinates in degrees and minutes, North.
Longitude	Seismic event location coordinates in degrees and minutes, West.
Depth	Seismic event depth in kilometers.

MAG	Duration magnitude.
NO	The number of P and S arrival readings used in the event solution.
GAP	The largest azimuthal separation in degrees between the recording stations used in the solution.
DMIN	The epicentral distance in kilometers.
RMS	The root mean square of the travel time residuals in seconds.
ERH	Standard horizontal error in kilometers.
ERZ	Standard vertical error in kilometers.
Q	Assigned epicentral quality parameter based on an average of the following two schemes:

	Station Distribution Scheme			Statistical Measure Scheme	
	NO	GAP		RMS (sec)	ERH (km)
A	≥ 8	≤ 90°	A	≤ 0.05	< 0.2
B	≥ 6	≤ 135°	B	≤ 0.10	< 0.4
C	≥ 6	≤ 180°	C	≤ 0.20	< 0.6
D	others	others	D	others	

TABLE C-2

TABULATION OF GROUND-MOTION DATA DELIVERED TO THE USGS FOR DETAILED ANALYSIS – DATA SOURCES

ID	Date	Origin Time		Mag	Station Accelograms Provided To USGS							
					TB1	TB2	TB3	TU1	JVD	TMU	TS2	TS3
1	001023	1529	56.45	1.81	Y	Y		-	-	-	-	-
2	001024	2306	02.40	1.86		Y		-	-	-	-	-
3	001220	1404	07.95	1.11	Y	Y		Y		Y	Y	Y
4	001221	2222	45.67	0.91	Y	Y	Y	Y		Y		Y
5	001222	0251	05.19	0.95	Y	Y	Y	Y		Y	Y	Y
6	001222	0624	51.90	1.15	Y	Y	Y	Y		Y	Y	Y
7	001222	0859	00.84	0.99	Y	Y	Y	Y		Y	Y	Y
8	001222	1758	00.02	0.71	Y	Y	Y			Y	Y	Y
9	001222	2022	15.47	1.19	Y	Y	Y	Y		Y	Y	Y
10	001223	0137	05.92	1.03	Y	Y	Y	Y		Y	Y	Y
11	001223	0529	41.34	0.98	Y	Y	Y	Y		Y	Y	Y
12	001223	0734	24.54	1.43	Y	Y	Y	Y	Y	Y	Y	Y
13	001224	1753	09.64	1.12	Y	Y	Y	Y		Y	Y	Y
14	001225	2012	00.10	1.56	Y	Y	Y	Y		Y	Y	Y
15	001226	1608	41.77	1.02	Y	Y	Y	Y		Y	Y	Y
16	010103	0049	03.19	1.54	Y	Y		Y		Y	Y	Y
17	010103	0850	13.21	1.18	Y	Y		Y		Y	Y	Y
18	010104	0330	27.30	1.41	Y	Y	Y	Y		Y	Y	Y
19	010104	2028	51.89	1.31	Y	Y	Y	Y		Y	Y	Y
20	010104	2239	46.24	1.46	Y	Y		Y		Y	Y	Y
21	010104	2347	08.67	1.28	Y	Y	Y	Y		Y	Y	Y
22	010105	0846	27.07	1.25	Y	Y		Y		Y	Y	Y
23	010105	0913	24.95	1.35	Y	Y	Y	Y		Y	Y	Y
24	010109	0423	26.89	1.46	Y	Y		Y		Y	Y	Y
25	010109	1727	23.44	2.17	Y	Y		Y		Y	Y	Y
26	010113	0242	15.17	1.40	Y	Y		Y		Y	Y	Y
27	010115	2008	34.00	1.48	Y	Y		Y		Y	Y	Y
28	010116	0036	58.72	1.39	Y	Y		Y		Y	Y	Y
29	010116	0320	58.11	1.32	Y	Y		Y		Y	Y	Y
30	010117	0411	12.01	1.42	Y	Y		Y		Y	Y	Y
31	010118	2156	26.59	1.55	Y	Y	Y	Y	Y	Y	Y	Y
32	010123	2318	44.18	1.36		Y	Y	Y	Y	Y		
33	010127	0257	56.28	1.04	Y	Y	Y	Y	Y	Y	Y	Y
34	010201	0014	10.45	1.08	Y	Y	Y	Y		Y	Y	Y
35	010201	2143	50.01	1.24		Y	Y	Y		Y	Y	Y
36	010202	1033	08.92	1.40	Y	Y	Y	Y	Y	Y	Y	Y
37	010202	1822	39.40	1.02	Y	Y	Y	Y		Y	Y	Y
38	010207	2054	01.55	1.61	Y	Y	Y	Y		Y	Y	Y
39	010208	2333	12.20	1.33	Y	Y	Y			Y	Y	Y
40	010214	0226	21.32	1.15	Y	Y		Y		Y	Y	Y
41	010215	0456	50.45	1.37	Y	Y	Y	Y		Y	Y	Y
42	010215	0613	39.30	1.24	Y	Y	Y	Y		Y	Y	Y
43	010222	0613	34.60	1.27	Y	Y	Y			Y	Y	Y
44	010222	0718	35.72	1.14	Y	Y	Y	Y		Y	Y	Y
45	010223	0617	31.04	1.31	Y	Y		Y		Y	Y	Y
46	010224	1305	33.45	1.36	Y	Y		Y		Y	Y	Y
47	010228	2202	04.38	1.45	Y	Y	Y			Y	Y	Y
48	010310	0405	02.19	1.49	Y	Y	Y			Y	Y	Y
49	010313	1223	06.65	1.50	Y	Y			Y	Y	Y	Y

EXPLANATION

Y	Data provided to the USGS from this station
-	Station not installed
BLANK	No data were available from this station

APPENDIX D

LIST OF ALL LOCATED SEISMIC EVENTS IN THE TRAIL MOUNTAIN LOCAL STUDY AREA, OCTOBER 3, 2000 - APRIL 30, 2001

TABLE D-1

LIST OF ALL LOCATED SEISMIC EVENTS IN THE TRAIL MOUNTAIN LOCAL STUDY AREA, OCTOBER 3, 2000 – APRIL 30, 2001

Date	Origin Time	Latitude	Longitude	Depth	Mag	No	Gap	Dmin	Rms	Erh	Erz	Q
001003	2018 38.25	39° 18.48'	111° 14.08'	0.88	0.99	6	112	1.1	0.10	0.6	1.0	C
001003	2104 51.44	39° 18.18'	111° 13.95'	0.06	0.95	5	157	0.9	0.04	0.8	7.3	D
001003	2144 16.37	39° 18.28'	111° 14.05'	0.00	0.84	5	176	0.9	0.01	0.9	7.4	D
001003	2232 2.36	39° 18.11'	111° 13.91'	0.71	2.08	17	77	0.9	0.16	0.4	0.4	B
001004	328 43.78	39° 17.87'	111° 14.09'	1.05	2.16	18	69	1.4	0.24	0.4	0.3	C
001004	1422 20.31	39° 18.11'	111° 14.22'	0.07	1.35	5	152	1.3	0.04	0.7	6.8	D
001004	2131 44.63	39° 18.00'	111° 13.89'	0.24	1.79	10	77	1.0	0.19	0.5	0.8	B
001005	59 27.16	39° 17.87'	111° 14.02'	1.08	2.13	18	54	1.3	0.27	0.4	0.4	C
001005	228 42.22	39° 18.33'	111° 14.27'	0.06	1.23	5	187	1.3	0.01	0.5	4.9	D
001005	1242 44.32	39° 18.00'	111° 13.95'	0.74	1.96	17	53	1.1	0.17	0.3	0.4	B
001005	2105 38.02	39° 18.22'	111° 13.85'	0.69	1.73	10	114	0.8	0.11	0.3	0.4	C
001005	2257 5.36	39° 18.07'	111° 13.94'	0.67	2.21	18	69	0.9	0.20	0.5	0.5	B
001006	616 29.28	39° 17.98'	111° 14.04'	1.24*	2.12	19	53	1.2	0.26	0.5	0.4	C
001017	1110 23.09	39° 18.01'	111° 12.81'	0.04	0.64	6	81	1.1	0.01	0.3	4.7	B
001017	1150 13.33	39° 18.01'	111° 12.85'	0.22	0.84	6	80	1.0	0.01	0.3	1.0	B
001017	1510 18.77	39° 17.64'	111° 13.17'	0.12	1.35	8	82	1.4	0.05	0.3	1.0	B
001018	553 8.67	39° 18.38'	111° 13.95'	0.00	0.77	6	117	0.8	0.08	0.4	4.1	B
001018	1219 27.97	39° 18.27'	111° 13.97'	0.04	0.66	6	109	0.9	0.02	0.3	3.3	B
001018	2257 27.46	39° 18.04'	111° 13.05'	0.03	1.24	7	78	0.8	0.12	0.4	3.6	C
001019	328 18.24	39° 18.16'	111° 13.43'	0.25	0.99	6	97	0.4	0.01	0.3	0.6	B
001019	907 19.24	39° 18.26'	111° 14.08'	0.00	0.38	6	111	1.1	0.08	0.4	4.2	B
001019	1457 15.69	39° 18.26'	111° 13.91'	0.02	0.40	6	107	0.8	0.03	0.3	4.0	B
001019	1515 4.91	39° 18.29'	111° 13.94'	0.12	0.50	6	110	0.8	0.02	0.3	0.9	B
001019	1546 36.96	39° 18.32'	111° 13.92'	0.00	0.89	6	112	0.8	0.03	0.3	3.4	B
001019	1548 43.36	39° 18.28'	111° 13.95'	0.00	0.89	6	110	0.9	0.05	0.3	3.6	B
001019	2227 41.99	39° 18.13'	111° 13.58'	0.00	1.18	6	97	0.5	0.03	0.3	0.8	B
001020	944 22.11	39° 17.99'	111° 13.81'	0.09	1.17	7	91	0.9	0.07	0.3	2.5	B
001020	1002 10.55	39° 18.03'	111° 13.83'	0.10	1.20	7	94	0.9	0.03	0.3	2.1	B
001020	1522 41.15	39° 18.27'	111° 13.91'	0.03	1.14	6	109	0.8	0.03	0.3	3.4	B
001023	753 57.16	39° 18.17'	111° 13.39'	0.31*	1.14	6	91	0.3	0.01	0.3	0.5	B
001023	1529 56.45	39° 18.03'	111° 13.74'	0.37	1.81	16	57	0.8	0.19	0.4	0.6	B
001023	1750 56.92	39° 18.27'	111° 13.98'	0.00	0.59	6	109	0.9	0.07	0.4	3.7	B
001023	1944 9.37	39° 18.12'	111° 13.91'	0.06	1.47	7	99	0.9	0.18	0.5	3.9	C
001023	2155 22.50	39° 18.30'	111° 13.86'	0.02	1.55	9	100	0.7	0.11	0.4	1.7	C
001023	2209 53.99	39° 18.27'	111° 13.98'	0.15	0.85	5	109	0.9	0.00	0.3	0.9	C
001024	1135 47.39	39° 18.21'	111° 13.46'	0.01	1.14	9	95	0.3	0.07	0.3	0.7	B
001024	1146 54.11	39° 18.27'	111° 13.78'	0.38	1.45	10	99	0.6	0.06	0.3	0.5	B
001024	2147 30.28	39° 18.30'	111° 13.89'	0.26	1.04	5	172	0.8	0.01	0.4	0.8	C
001024	2304 33.69	39° 18.30'	111° 13.95'	0.00	0.86	5	116	0.8	0.04	0.4	3.6	C
001024	2306 2.40	39° 18.00'	111° 13.83'	0.49	1.86	18	48	0.9	0.19	0.4	0.5	B
001024	2314 34.17	39° 17.25'	111° 12.00'	1.10	1.25	7	93	2.9	0.02	0.3	0.9	B
001025	518 13.30	39° 18.29'	111° 14.08'	0.24	1.03	5	115	1.0	0.01	0.4	0.7	C
001025	1111 13.58	39° 18.28'	111° 13.75'	0.52	1.68	11	99	0.6	0.08	0.3	0.4	B
001025	1522 14.69	39° 18.18'	111° 13.33'	0.06	1.15	10	77	0.3	0.08	0.2	0.5	B
001025	1608 51.25	39° 18.26'	111° 13.99'	0.02	0.86	6	108	0.9	0.03	0.3	3.4	B
001025	1658 26.42	39° 20.10'	111° 12.12'	3.18	0.79	5	119	3.3	0.02	0.8	0.6	D
001026	1323 27.00	39° 18.30'	111° 13.93'	0.89*	1.68	13	101	0.8	0.08	0.2	0.3	B
001027	433 23.15	39° 18.28'	111° 13.95'	0.06	0.71	5	117	0.9	0.02	0.4	3.3	C
001029	253 19.32	39° 18.01'	111° 13.78'	0.09	1.09	7	92	0.9	0.04	0.3	2.1	B
001029	1020 51.98	39° 18.04'	111° 12.67'	0.22	1.17	8	83	1.2	0.06	0.3	0.8	B
001029	2027 1.38	39° 18.28'	111° 14.09'	0.01	1.24	8	103	1.1	0.07	0.3	2.5	B
001031	550 16.38	39° 18.03'	111° 14.00'	0.01	1.40	9	95	1.1	0.02	0.2	1.3	B
001101	119 4.88	39° 18.29'	111° 13.83'	0.12	1.54	10	100	0.7	0.03	0.2	0.5	B
001104	1525 59.75	39° 18.15'	111° 13.80'	0.07	1.11	8	99	0.7	0.02	0.2	2.2	B
001107	2248 53.34	39° 18.45'	111° 13.85'	0.01	1.56	7	102	0.7	0.03	0.3	0.7	B
001107	2305 53.70	39° 18.47'	111° 13.82'	0.05	1.22	8	101	0.7	0.11	0.4	1.8	C
001107	2308 29.45	39° 18.47'	111° 13.86'	0.02	1.28	8	102	0.7	0.07	0.3	0.7	B
001107	2310 9.41	39° 18.44'	111° 13.85'	0.06	0.00	7	107	0.7	0.01	0.3	2.4	B
001107	2310 20.06	39° 18.39'	111° 13.88'	0.03	1.00	6	116	0.7	0.01	0.3	3.1	B
001107	2311 52.77	39° 18.44'	111° 13.90'	0.15	1.60	5	118	0.8	0.01	0.3	0.9	C

Date	Origin Time	Latitude	Longitude	Depth	Mag	No	Gap	Dmin	Rms	Erh	Erz	Q
001107	2324 47.41	39° 18.61'	111° 14.03'	1.62*	0.84	7	119	1.1	0.11	0.5	0.5	C
001107	2356 46.27	39° 18.12'	111° 13.70'	0.26	1.93	16	48	0.7	0.20	0.4	0.7	B
001108	258 51.86	39° 18.61'	111° 13.90'	0.76	1.27	9	92	0.9	0.18	0.5	0.9	C
001108	334 48.41	39° 18.43'	111° 13.78'	0.52	1.55	11	101	0.6	0.07	0.3	0.4	B
001108	346 54.92	39° 18.37'	111° 13.86'	0.12	1.43	8	101	0.7	0.03	0.2	0.7	B
001108	425 44.48	39° 18.40'	111° 13.88'	0.03	0.66	6	116	0.8	0.03	0.3	3.4	B
001108	456 58.04	39° 18.47'	111° 13.91'	0.10	1.33	6	121	0.8	0.01	0.3	3.3	B
001108	535 9.95	39° 18.44'	111° 13.86'	0.03	1.34	9	102	0.7	0.03	0.2	1.4	B
001108	620 56.66	39° 18.30'	111° 13.64'	0.74*	1.72	19	48	0.4	0.15	0.3	0.2	B
001108	856 40.96	39° 18.51'	111° 13.85'	0.09	1.11	10	102	0.8	0.05	0.2	1.2	B
001108	1727 42.02	39° 18.49'	111° 13.86'	0.03	1.28	8	102	0.8	0.09	0.3	2.2	B
001108	1806 52.20	39° 18.50'	111° 13.89'	0.36	1.51	7	122	0.8	0.02	0.3	0.7	B
001108	1819 16.37	39° 18.42'	111° 13.63'	0.66*	1.57	12	90	0.4	0.11	0.3	0.3	B
001108	1852 39.86	39° 18.53'	111° 13.89'	0.01	1.35	7	123	0.8	0.02	0.3	2.5	B
001108	1957 17.81	39° 18.44'	111° 13.88'	0.14	1.27	6	118	0.8	0.01	0.3	0.9	B
001108	2012 19.28	39° 18.49'	111° 13.89'	0.00	1.34	7	121	0.8	0.08	0.3	0.8	B
001109	307 21.34	39° 18.47'	111° 13.78'	0.61*	1.24	10	101	0.6	0.07	0.3	0.4	B
001109	1344 18.90	39° 18.58'	111° 13.79'	0.04	1.08	9	102	0.7	0.12	0.4	1.7	C
001109	1801 41.88	39° 18.45'	111° 13.80'	0.13	1.28	9	101	0.6	0.07	0.3	0.6	B
001109	2049 40.74	39° 18.25'	111° 13.86'	0.01	1.54	9	100	0.7	0.15	0.4	0.9	C
001109	2138 3.89	39° 18.48'	111° 13.90'	0.01	1.35	7	121	0.8	0.08	0.3	2.3	B
001110	26 42.22	39° 18.40'	111° 13.83'	0.12	1.31	6	115	0.7	0.01	0.3	0.9	B
001110	449 27.48	39° 18.44'	111° 13.91'	0.14	0.81	6	119	0.8	0.01	0.3	0.9	B
001110	724 0.53	39° 18.10'	111° 13.74'	0.12	1.14	10	97	0.7	0.24	0.5	1.3	C
001110	1122 40.22	39° 18.47'	111° 13.84'	0.21	1.22	9	102	0.7	0.03	0.3	0.5	B
001110	1135 58.65	39° 18.51'	111° 13.82'	0.05	1.09	8	101	0.7	0.12	0.4	1.9	C
001111	1434 45.25	39° 18.46'	111° 13.85'	0.02	1.19	8	102	0.7	0.09	0.3	2.5	B
001113	908 5.23	39° 17.97'	111° 12.81'	0.01	1.19	10	80	1.1	0.09	0.3	1.8	B
001114	9 9.79	39° 18.39'	111° 13.84'	0.16	0.76	6	114	0.7	0.01	0.3	0.8	B
001114	19 42.11	39° 18.57'	111° 13.83'	0.01	1.45	9	102	0.8	0.10	0.4	1.5	B
001114	547 24.54	39° 18.44'	111° 13.89'	0.23	1.17	6	118	0.8	0.02	0.3	0.7	B
001114	1210 39.26	39° 18.52'	111° 13.89'	0.01	0.87	6	123	0.8	0.02	0.3	3.3	B
001114	1537 53.80	39° 18.45'	111° 13.89'	0.10	0.63	6	119	0.8	0.03	0.3	1.0	B
001114	2051 42.63	39° 18.43'	111° 13.88'	0.19	1.10	6	118	0.8	0.01	0.3	0.7	B
001115	109 36.22	39° 18.41'	111° 13.88'	0.00	1.09	8	102	0.8	0.06	0.3	0.7	B
001115	749 45.82	39° 18.48'	111° 13.87'	0.33	1.22	7	120	0.8	0.02	0.3	0.6	B
001115	1719 19.27	39° 18.45'	111° 13.89'	0.00	1.53	7	119	0.8	0.05	0.3	0.7	B
001116	1855 24.69	39° 18.42'	111° 13.77'	0.01	1.32	8	100	0.6	0.07	0.3	0.7	B
001117	324 1.94	39° 18.54'	111° 13.74'	0.04	1.34	8	101	0.6	0.03	0.2	0.6	B
001117	447 28.33	39° 18.50'	111° 13.77'	0.03	1.26	9	101	0.6	0.05	0.2	0.6	B
001119	2044 56.45	39° 18.50'	111° 13.73'	0.10	1.39	8	100	0.6	0.03	0.2	0.7	B
001120	146 26.31	39° 18.51'	111° 13.83'	0.13	1.31	10	102	0.7	0.09	0.3	0.6	B
001120	352 49.44	39° 18.29'	111° 13.55'	0.33*	1.50	12	69	0.3	0.12	0.3	0.4	B
001120	1906 12.67	39° 18.52'	111° 13.72'	0.05	1.42	7	100	0.6	0.05	0.3	0.7	B
001121	1910 54.08	39° 18.38'	111° 13.61'	0.71*	1.58	10	98	0.3	0.06	0.3	0.3	B
001121	1934 5.93	39° 18.50'	111° 13.80'	0.17	1.38	7	101	0.7	0.01	0.3	0.7	B
001121	2003 38.93	39° 18.45'	111° 13.78'	0.01	0.54	5	189	0.6	0.01	0.6	0.7	D
001122	1647 23.60	39° 18.49'	111° 13.89'	0.00	1.39	8	102	0.8	0.11	0.4	0.9	C
001124	512 39.74	39° 18.48'	111° 13.94'	0.01	0.19	6	122	0.9	0.05	0.4	3.4	B
001124	647 10.13	39° 18.18'	111° 13.98'	0.08	0.08	6	104	0.9	0.05	0.5	5.2	C
001124	1528 25.04	39° 18.43'	111° 13.91'	0.01	0.34	6	118	0.8	0.07	0.3	0.9	B
001127	2250 9.36	39° 18.58'	111° 13.71'	0.03	0.59	6	122	0.6	0.02	0.3	0.7	B
001128	2156 3.55	39° 17.97'	111° 13.83'	0.09	1.28	6	91	0.9	0.04	0.3	4.2	B
001129	346 7.39	39° 18.55'	111° 13.72'	0.01	1.24	7	120	0.6	0.06	0.3	0.7	B
001129	734 7.52	39° 18.54'	111° 13.67'	0.04	1.27	8	119	0.6	0.05	0.3	0.6	B
001129	1129 33.58	39° 17.92'	111° 11.85'	0.65	1.31	8	89	2.4	0.02	0.3	0.8	B
001129	2204 34.89	39° 18.53'	111° 13.78'	0.14	0.77	6	121	0.7	0.01	0.3	0.8	B
001201	1004 1.70	39° 18.53'	111° 13.60'	0.28	1.24	7	99	0.5	0.01	0.2	0.5	B
001201	1726 3.34	39° 18.51'	111° 13.71'	0.17	0.71	6	118	0.6	0.01	0.3	0.7	B
001203	1835 37.51	39° 17.91'	111° 13.48'	0.42	1.43	10	87	0.9	0.04	0.2	0.5	A
001203	2003 2.52	39° 18.40'	111° 13.63'	0.09	1.08	7	111	0.3	0.03	0.3	2.0	B
001204	238 45.16	39° 18.57'	111° 13.63'	0.06	1.19	10	99	0.5	0.06	0.2	0.5	B
001204	813 48.35	39° 18.48'	111° 13.89'	0.01	1.26	8	102	0.8	0.07	0.3	0.7	B
001205	221 6.57	39° 18.44'	111° 13.74'	0.06	0.00	7	115	0.6	0.05	0.3	1.5	B
001205	933 0.12	39° 18.40'	111° 13.51'	0.38*	1.49	11	97	0.2	0.04	0.2	0.3	B
001205	1123 49.03	39° 18.55'	111° 11.48'	3.03	0.35	8	102	2.0	0.41	1.3	3.0	C
001206	45 46.96	39° 18.41'	111° 13.62'	0.06	0.00	7	186	0.3	0.05	0.5	0.4	D
001206	143 26.41	39° 18.48'	111° 13.64'	0.02	0.00	8	115	0.5	0.03	0.3	0.6	B

Date	Origin Time		Latitude		Longitude		Depth	Mag	No	Gap	Dmin	Rms	Erh	Erz	Q
001206	406	43.81	39°	18.72'	111°	13.45'	0.00	0.44	5	252	0.7	0.03	1.0	0.6	D
001206	419	27.96	39°	17.37'	111°	13.25'	1.40	1.25	7	94	1.4	0.30	0.8	2.8	C
001206	520	8.17	39°	18.82'	111°	13.42'	0.47	0.29	5	260	0.9	0.02	1.1	1.5	D
001206	1356	31.44	39°	18.41'	111°	13.61'	0.01	0.00	8	111	0.3	0.03	0.3	0.6	B
001206	1402	31.39	39°	18.77'	111°	13.60'	0.32	0.00	6	254	0.9	0.02	1.0	0.5	D
001206	1416	6.44	39°	18.53'	111°	13.55'	0.27	1.31	11	98	0.4	0.04	0.2	0.4	B
001206	1912	11.15	39°	18.52'	111°	13.68'	0.05	0.23	7	118	0.5	0.03	0.3	0.6	B
001206	1952	11.83	39°	18.40'	111°	13.59'	0.24	1.51	8	110	0.3	0.03	0.3	0.5	B
001206	1957	49.09	39°	18.50'	111°	13.60'	0.32	0.61	8	116	0.4	0.02	0.2	0.4	B
001206	2029	57.13	39°	18.39'	111°	13.88'	0.02	1.16	8	116	0.7	0.08	0.3	1.8	B
001206	2312	17.30	39°	18.47'	111°	13.73'	0.01	0.78	8	117	0.6	0.02	0.2	0.6	B
001206	2316	43.41	39°	18.38'	111°	13.60'	0.07	1.31	6	109	0.3	0.02	0.3	0.5	B
001206	2341	47.23	39°	18.53'	111°	13.87'	0.01	1.11	7	123	0.8	0.04	0.3	2.1	B
001207	113	30.41	39°	18.39'	111°	13.62'	0.29	0.71	9	110	0.3	0.02	0.2	0.4	B
001207	208	22.26	39°	18.38'	111°	13.54'	0.08	1.66	8	97	0.2	0.03	0.3	0.4	B
001207	247	27.95	39°	18.52'	111°	13.59'	0.32	0.54	8	117	0.4	0.03	0.2	0.4	B
001207	314	41.89	39°	17.64'	111°	12.65'	0.00	0.96	7	86	1.7	0.06	0.3	5.1	B
001207	404	7.83	39°	18.48'	111°	13.56'	0.27	1.15	12	98	0.3	0.03	0.2	0.3	B
001207	557	54.40	39°	18.35'	111°	13.67'	0.04	0.71	8	109	0.4	0.02	0.3	0.6	B
001207	623	33.22	39°	18.51'	111°	13.56'	0.12	0.94	8	115	0.3	0.03	0.2	0.7	B
001207	626	6.96	39°	18.44'	111°	13.45'	0.51*	1.31	13	97	0.2	0.06	0.2	0.3	B
001207	800	30.80	39°	18.48'	111°	13.52'	0.28	0.80	8	112	0.3	0.03	0.2	0.4	B
001207	821	28.47	39°	18.35'	111°	13.57'	0.12	0.70	8	108	0.3	0.04	0.3	0.7	B
001207	843	16.42	39°	18.36'	111°	13.62'	0.08	1.16	7	108	0.3	0.02	0.3	0.5	B
001207	921	1.59	39°	18.45'	111°	13.56'	0.27	0.61	7	112	0.3	0.02	0.3	0.5	B
001207	942	45.53	39°	19.19'	111°	13.73'	0.40	0.64	7	149	1.6	0.10	0.5	13.9	C
001207	1151	51.46	39°	18.35'	111°	13.71'	0.03	0.74	7	110	0.5	0.03	0.3	0.7	B
001207	1240	42.06	39°	18.53'	111°	13.61'	0.03	0.88	8	117	0.5	0.03	0.2	0.6	B
001207	1304	48.60	39°	18.38'	111°	13.38'	0.70*	1.28	7	105	0.1	0.07	0.4	0.6	B
001207	1603	46.54	39°	18.37'	111°	13.53'	0.32*	1.00	7	107	0.2	0.01	0.3	0.4	B
001207	1642	37.87	39°	18.49'	111°	13.65'	0.31	0.79	7	116	0.5	0.02	0.3	0.5	B
001207	1645	46.77	39°	18.36'	111°	13.57'	0.10	0.74	7	109	0.2	0.02	0.3	0.5	B
001207	1811	35.26	39°	18.48'	111°	13.53'	0.19	1.13	8	114	0.3	0.02	0.2	0.5	B
001207	2053	5.04	39°	18.36'	111°	13.56'	0.18	1.02	7	108	0.2	0.01	0.3	0.5	B
001207	2158	14.93	39°	18.50'	111°	13.76'	0.03	1.10	8	119	0.6	0.05	0.3	0.7	B
001207	2259	27.55	39°	18.52'	111°	13.67'	0.24	1.10	7	119	0.5	0.03	0.2	0.6	B
001207	2325	7.20	39°	18.48'	111°	13.69'	0.30	1.16	9	117	0.5	0.05	0.3	0.5	B
001207	2359	48.52	39°	18.48'	111°	13.52'	0.26	0.78	7	114	0.3	0.03	0.3	0.5	B
001208	12	5.01	39°	18.11'	111°	13.59'	0.01	1.00	7	96	0.6	0.02	0.2	0.8	B
001208	50	30.54	39°	18.38'	111°	13.56'	0.09	1.02	7	109	0.2	0.02	0.3	0.5	B
001208	239	38.08	39°	18.40'	111°	13.54'	0.05	1.30	8	110	0.2	0.03	0.2	0.5	B
001208	336	22.32	39°	18.49'	111°	13.59'	0.30	1.16	8	114	0.4	0.04	0.3	0.5	B
001208	336	36.87	39°	18.38'	111°	13.60'	0.16	0.75	7	109	0.3	0.02	0.3	0.6	B
001208	454	24.59	39°	18.58'	111°	13.68'	0.37	0.97	7	121	0.6	0.03	0.4	1.3	B
001208	504	56.17	39°	18.39'	111°	13.59'	0.34*	1.05	7	110	0.3	0.01	0.3	0.4	B
001208	646	18.43	39°	18.50'	111°	13.63'	0.35	0.86	7	116	0.5	0.01	0.3	0.5	B
001208	700	59.43	39°	18.38'	111°	13.59'	0.30*	0.87	7	109	0.3	0.01	0.3	0.4	B
001208	903	28.90	39°	18.38'	111°	13.65'	0.06	0.69	7	111	0.4	0.01	0.3	0.6	B
001208	925	16.97	39°	18.48'	111°	13.62'	0.08	0.47	7	115	0.4	0.02	0.3	2.8	B
001208	955	33.18	39°	18.50'	111°	13.74'	0.23	0.57	7	118	0.6	0.02	0.3	0.7	B
001208	1241	32.66	39°	18.54'	111°	13.83'	0.13	0.92	8	123	0.8	0.03	0.3	0.8	B
001208	1415	28.67	39°	18.38'	111°	13.50'	0.20*	0.90	7	108	0.2	0.01	0.3	0.4	B
001208	1615	54.15	39°	18.25'	111°	14.05'	0.00	0.46	7	109	1.0	0.08	0.4	3.6	B
001208	1748	13.89	39°	18.45'	111°	13.86'	0.18	1.11	7	119	0.7	0.01	0.3	0.7	B
001208	2047	30.96	39°	18.50'	111°	13.56'	0.13	0.91	7	114	0.3	0.02	0.3	0.8	B
001209	625	52.88	39°	18.24'	111°	13.55'	0.15	1.08	8	102	0.3	0.01	0.2	0.5	B
001210	427	56.00	39°	17.71'	111°	13.42'	0.05	0.89	7	83	1.2	0.08	0.3	3.9	B
001210	2145	46.31	39°	18.27'	111°	14.18'	0.07	0.53	7	113	1.1	0.01	0.3	2.8	B
001211	56	8.02	39°	18.51'	111°	13.55'	0.26	0.71	7	115	0.3	0.02	0.3	0.5	B
001211	1926	34.30	39°	18.36'	111°	13.53'	0.28*	0.97	7	107	0.2	0.01	0.3	0.4	B
001211	2131	1.32	39°	18.51'	111°	13.60'	0.13	1.07	7	116	0.4	0.01	0.3	0.8	B
001211	2140	38.95	39°	18.49'	111°	13.70'	0.22	0.84	7	117	0.5	0.02	0.3	0.6	B
001211	2337	51.72	39°	18.38'	111°	13.53'	0.29*	1.18	7	108	0.2	0.02	0.3	0.4	B
001212	24	20.07	39°	18.71'	111°	13.36'	0.19	0.29	6	135	0.7	0.01	0.3	1.0	B
001212	37	35.58	39°	18.54'	111°	13.76'	0.32	0.86	7	121	0.7	0.01	0.3	0.6	B
001212	51	17.85	39°	18.26'	111°	13.86'	0.03	0.00	6	168	0.7	0.10	0.6	5.2	C
001212	56	58.07	39°	18.29'	111°	13.54'	0.03	0.08	6	153	0.2	0.02	0.5	1.1	C
001212	204	44.43	39°	18.36'	111°	13.49'	0.33*	0.85	7	107	0.2	0.01	0.3	0.3	B

Date	Origin Time		Latitude		Longitude		Depth	Mag	No	Gap	Dmin	Rms	Erh	Erz	Q
001212	246	31.57	39°	18.48'	111°	13.54'	0.35*	0.83	7	113	0.3	0.02	0.3	0.4	B
001212	514	18.83	39°	18.41'	111°	13.54'	0.10	0.00	6	110	0.2	0.03	0.3	1.0	B
001212	515	57.50	39°	18.51'	111°	13.53'	0.31*	0.60	7	115	0.3	0.02	0.3	0.4	B
001212	541	33.26	39°	18.48'	111°	13.50'	0.31*	0.79	7	112	0.3	0.02	0.3	0.4	B
001212	542	36.59	39°	18.52'	111°	13.60'	0.31	1.13	7	117	0.5	0.02	0.3	0.5	B
001212	607	33.03	39°	18.46'	111°	13.60'	0.27	0.57	7	113	0.3	0.03	0.3	0.5	B
001212	1554	7.55	39°	18.50'	111°	13.52'	0.32*	1.02	7	114	0.3	0.02	0.3	0.4	B
001212	1623	11.21	39°	18.44'	111°	13.55'	0.05	0.81	7	112	0.3	0.04	0.3	0.6	B
001212	1739	23.71	39°	18.30'	111°	13.53'	0.06	0.20	6	158	0.2	0.02	0.5	0.8	C
001212	1752	59.77	39°	18.22'	111°	13.94'	0.00	0.74	7	106	0.9	0.04	0.3	3.1	B
001212	1758	47.22	39°	18.36'	111°	13.48'	0.35*	0.75	7	107	0.2	0.02	0.3	0.3	B
001212	1819	59.43	39°	18.36'	111°	13.51'	0.30*	0.63	7	107	0.2	0.02	0.3	0.4	B
001212	1925	58.29	39°	18.38'	111°	13.61'	0.09	0.61	7	109	0.3	0.01	0.3	0.5	B
001212	2009	48.14	39°	18.34'	111°	13.82'	0.02	0.28	7	112	0.7	0.03	0.3	0.7	B
001212	2059	43.18	39°	18.38'	111°	13.41'	0.30*	0.52	6	121	0.1	0.02	0.3	0.2	B
001212	2100	55.04	39°	18.46'	111°	13.52'	0.31*	0.63	7	111	0.3	0.02	0.3	0.4	B
001212	2110	53.92	39°	18.36'	111°	13.56'	0.10	0.73	7	108	0.2	0.02	0.3	0.5	B
001212	2112	33.76	39°	18.37'	111°	13.56'	0.18	0.53	7	109	0.2	0.02	0.3	0.5	B
001212	2142	3.85	39°	18.49'	111°	13.59'	0.33	0.79	7	114	0.4	0.02	0.3	0.5	B
001212	2157	8.27	39°	18.51'	111°	13.56'	0.13	0.78	7	115	0.4	0.02	0.3	0.8	B
001212	2209	5.77	39°	18.37'	111°	13.51'	0.28*	0.76	7	107	0.2	0.02	0.3	0.4	B
001212	2215	33.47	39°	18.46'	111°	13.51'	0.27*	0.45	7	112	0.2	0.04	0.3	0.4	B
001212	2246	40.23	39°	18.42'	111°	13.54'	0.20*	0.86	6	186	0.2	0.02	0.4	0.5	C
001212	2347	9.23	39°	18.36'	111°	13.59'	0.08	0.53	6	183	0.3	0.03	0.5	0.6	D
001213	1	26.96	39°	18.47'	111°	13.58'	0.07	0.49	7	113	0.3	0.03	0.3	0.6	B
001213	13	8.19	39°	18.36'	111°	13.59'	0.08	0.56	7	109	0.3	0.03	0.3	0.5	B
001213	26	22.90	39°	18.41'	111°	13.46'	0.32*	0.88	7	109	0.2	0.02	0.3	0.3	B
001213	29	32.47	39°	18.43'	111°	13.53'	0.02	0.13	7	111	0.2	0.03	0.3	0.7	B
001213	139	1.82	39°	18.37'	111°	13.51'	0.24*	0.88	7	107	0.2	0.02	0.3	0.4	B
001213	208	21.73	39°	18.48'	111°	13.52'	0.19	0.34	7	113	0.3	0.02	0.3	0.6	B
001213	209	14.67	39°	18.49'	111°	13.43'	0.15	0.73	7	111	0.2	0.07	0.3	0.8	B
001213	227	25.75	39°	18.48'	111°	13.47'	0.35*	1.20	8	112	0.2	0.02	0.2	0.3	B
001213	229	8.98	39°	18.45'	111°	13.59'	0.06	0.26	7	112	0.3	0.03	0.3	0.6	B
001213	234	4.34	39°	18.36'	111°	13.50'	0.31*	1.16	7	107	0.2	0.02	0.3	0.4	B
001213	239	12.30	39°	18.28'	111°	14.24'	0.26	0.49	7	114	1.2	0.02	0.3	0.7	B
001213	341	20.67	39°	18.45'	111°	13.55'	0.37*	0.41	7	112	0.3	0.03	0.3	0.6	B
001213	354	46.80	39°	18.49'	111°	13.65'	0.06	1.16	7	116	0.5	0.03	0.3	0.6	B
001213	403	9.08	39°	18.49'	111°	13.57'	0.30*	1.22	7	114	0.3	0.01	0.3	0.5	B
001213	404	28.16	39°	18.49'	111°	13.53'	0.37*	1.01	7	114	0.3	0.01	0.3	0.7	B
001213	408	25.68	39°	18.49'	111°	13.48'	0.25	1.32	8	113	0.3	0.02	0.2	0.4	B
001213	415	54.91	39°	18.43'	111°	13.47'	0.29*	1.36	8	110	0.2	0.04	0.3	0.4	B
001213	416	9.67	39°	18.24'	111°	13.42'	0.17	1.12	7	101	0.2	0.01	0.2	0.6	B
001213	458	0.49	39°	18.50'	111°	13.50'	0.08	0.41	7	113	0.3	0.02	0.3	0.5	B
001213	508	48.08	39°	18.41'	111°	13.52'	0.07	0.84	7	109	0.2	0.03	0.3	0.5	B
001213	516	15.40	39°	18.38'	111°	13.59'	0.22	1.42	7	109	0.3	0.01	0.3	0.5	B
001213	546	0.12	39°	18.37'	111°	13.46'	0.29*	0.71	7	106	0.1	0.02	0.3	0.3	B
001213	603	25.19	39°	18.36'	111°	13.53'	0.22*	0.00	7	107	0.2	0.03	0.3	0.5	B
001213	605	24.53	39°	18.38'	111°	13.48'	0.25*	1.25	8	108	0.2	0.02	0.3	0.3	B
001213	644	35.12	39°	18.55'	111°	13.48'	0.03	1.03	8	115	0.4	0.03	0.2	0.6	B
001213	706	36.39	39°	18.46'	111°	13.43'	0.35*	0.00	6	123	0.2	0.02	0.3	0.3	B
001213	736	5.99	39°	18.41'	111°	13.44'	0.31*	1.50	8	108	0.2	0.01	0.2	0.3	B
001213	751	4.11	39°	18.38'	111°	13.61'	0.21	0.97	7	110	0.3	0.01	0.3	0.6	B
001213	847	31.79	39°	18.23'	111°	13.71'	0.07	1.09	7	104	0.5	0.03	0.3	2.9	B
001213	906	58.44	39°	18.49'	111°	13.50'	0.26	0.57	7	113	0.3	0.03	0.3	0.5	B
001213	1121	39.84	39°	18.36'	111°	13.55'	0.09	0.45	7	108	0.2	0.02	0.3	0.5	B
001213	1345	39.18	39°	18.25'	111°	13.62'	0.06	0.39	7	103	0.4	0.01	0.3	0.6	B
001213	1511	11.99	39°	18.48'	111°	13.76'	0.01	0.65	7	118	0.6	0.01	0.3	0.7	B
001213	1603	31.24	39°	18.18'	111°	13.52'	0.01	0.40	6	120	0.4	0.08	0.7	1.9	C
001213	1639	41.25	39°	18.48'	111°	13.57'	0.30*	0.43	7	113	0.3	0.02	0.3	0.5	B
001213	1701	30.96	39°	18.30'	111°	13.35'	0.10*	0.31	7	77	0.1	0.06	0.4	0.4	B
001213	1758	7.64	39°	18.39'	111°	13.47'	0.33*	1.30	7	108	0.2	0.02	0.3	0.3	B
001213	1801	35.60	39°	18.36'	111°	13.85'	0.04	0.44	7	113	0.7	0.07	0.4	3.4	B
001213	1816	42.53	39°	18.50'	111°	13.66'	0.35	0.92	7	116	0.5	0.02	0.3	0.5	B
001213	1838	45.95	39°	18.40'	111°	13.57'	0.15	0.76	7	110	0.3	0.01	0.3	0.6	B
001213	1841	45.11	39°	18.30'	111°	13.67'	1.94*	0.75	7	107	0.5	0.10	0.4	0.6	B
001213	1846	37.79	39°	18.49'	111°	13.50'	0.33*	1.10	7	112	0.3	0.02	0.3	0.4	B
001213	2041	9.65	39°	18.52'	111°	13.83'	0.31	0.80	7	122	0.7	0.01	0.3	0.6	B
001213	2046	41.18	39°	18.46'	111°	13.57'	0.05	0.66	7	113	0.3	0.03	0.3	0.6	B

Date	Origin Time	Latitude	Longitude	Depth	Mag	No	Gap	Dmin	Rms	Erh	Erz	Q
001213	2104 54.23	39° 17.86'	111° 11.78'	0.02	0.90	7	89	1.1	0.07	0.4	4.4	B
001213	2205 48.26	39° 18.38'	111° 13.68'	0.04	0.43	7	111	0.5	0.02	0.3	0.7	B
001213	2213 42.39	39° 18.35'	111° 13.52'	0.08	0.78	7	107	0.2	0.03	0.3	0.5	B
001213	2215 6.36	39° 18.35'	111° 13.48'	0.26*	0.64	7	107	0.2	0.02	0.3	0.4	B
001213	2220 26.62	39° 18.49'	111° 13.45'	0.31*	0.91	7	112	0.2	0.02	0.3	0.4	B
001213	2243 29.26	39° 18.49'	111° 13.49'	0.30*	1.20	7	113	0.3	0.03	0.3	0.4	B
001213	2307 2.72	39° 18.34'	111° 13.51'	0.16	1.23	7	106	0.2	0.02	0.3	0.5	B
001213	2308 17.50	39° 18.49'	111° 13.59'	0.08	0.96	8	114	0.4	0.03	0.2	0.5	B
001213	2313 49.66	39° 18.49'	111° 13.46'	0.34*	1.07	7	112	0.2	0.02	0.3	0.4	B
001214	12 19.01	39° 18.37'	111° 13.48'	0.30*	1.21	6	183	0.2	0.02	0.5	0.3	D
001214	103 3.71	39° 18.55'	111° 13.62'	0.06	1.36	9	99	0.5	0.04	0.2	0.6	B
001214	420 56.76	39° 18.54'	111° 13.41'	0.02	1.36	9	96	0.3	0.08	0.3	0.7	B
001214	816 19.48	39° 18.38'	111° 13.45'	0.29*	1.26	7	107	0.1	0.02	0.3	0.3	B
001214	1051 18.36	39° 18.53'	111° 13.51'	0.07	1.16	8	115	0.3	0.03	0.2	0.5	B
001214	1107 4.92	39° 18.24'	111° 13.49'	0.08	0.94	7	101	0.3	0.01	0.2	0.6	B
001214	1117 43.83	39° 18.49'	111° 13.47'	0.32*	0.98	7	112	0.2	0.02	0.3	0.4	B
001214	1204 49.44	39° 18.53'	111° 13.38'	0.07	1.22	9	96	0.3	0.05	0.2	0.5	B
001214	1347 22.19	39° 18.24'	111° 13.59'	0.09	0.87	7	103	0.3	0.01	0.3	2.8	B
001214	1347 48.21	39° 18.50'	111° 13.59'	0.33	0.00	7	115	0.4	0.02	0.3	0.5	B
001214	1639 30.97	39° 18.40'	111° 13.48'	0.02	1.44	9	109	0.2	0.04	0.3	0.5	B
001214	1746 11.59	39° 18.50'	111° 13.52'	0.37*	0.92	7	113	0.3	0.02	0.3	0.7	B
001214	2113 58.71	39° 18.39'	111° 13.53'	0.11	0.76	7	109	0.2	0.03	0.3	0.7	B
001214	2120 15.41	39° 18.39'	111° 13.49'	0.19	0.44	7	108	0.2	0.02	0.3	0.4	B
001214	2147 24.08	39° 18.53'	111° 13.47'	0.03	0.64	7	114	0.3	0.02	0.3	0.7	B
001214	2206 22.81	39° 18.45'	111° 13.26'	2.12*	1.19	7	131	0.2	0.21	0.7	1.0	C
001214	2221 18.48	39° 18.38'	111° 13.43'	0.33*	1.02	7	107	0.1	0.02	0.3	0.3	B
001215	11 33.20	39° 18.36'	111° 13.59'	0.00	1.28	7	109	0.3	0.02	0.3	0.7	B
001215	31 40.95	39° 18.40'	111° 13.41'	0.27*	0.00	6	121	0.1	0.02	0.3	0.3	B
001215	33 19.22	39° 18.43'	111° 13.51'	0.14	0.70	7	110	0.2	0.03	0.3	0.6	B
001215	51 27.64	39° 18.51'	111° 13.54'	0.06	0.53	7	115	0.3	0.04	0.3	0.6	B
001215	56 14.33	39° 18.51'	111° 13.53'	0.08	1.13	8	115	0.3	0.05	0.3	0.5	B
001215	258 16.99	39° 18.55'	111° 13.65'	0.02	1.27	8	118	0.5	0.02	0.2	0.6	B
001215	809 37.76	39° 18.55'	111° 13.52'	0.33	0.77	7	116	0.4	0.02	0.3	0.5	B
001215	816 26.47	39° 18.36'	111° 13.50'	0.25*	0.97	7	107	0.2	0.02	0.3	0.4	B
001215	903 54.80	39° 18.48'	111° 13.45'	0.29*	0.98	7	112	0.2	0.02	0.3	0.4	B
001215	1018 4.36	39° 18.39'	111° 13.60'	0.21	0.75	7	110	0.3	0.01	0.3	0.5	B
001215	1152 48.26	39° 18.38'	111° 13.55'	0.28*	0.86	7	109	0.2	0.01	0.3	0.4	B
001215	1845 30.37	39° 18.48'	111° 13.88'	0.12	1.05	7	121	0.8	0.02	0.3	0.8	B
001216	35 22.41	39° 18.42'	111° 13.73'	0.18	0.99	5	122	0.5	0.01	0.3	0.8	C
001217	1212 26.38	39° 18.04'	111° 11.72'	0.21	0.45	6	92	2.5	0.03	684.1	999.9	C
001217	1605 21.67	39° 18.41'	111° 13.72'	0.14	0.61	6	113	0.5	0.01	0.3	0.8	B
001217	1701 54.84	39° 18.42'	111° 13.78'	0.16	0.63	5	122	0.6	0.02	0.4	0.8	C
001217	1706 38.20	39° 18.49'	111° 13.91'	0.23	0.96	5	122	0.8	0.00	0.3	0.8	C
001218	612 38.93	39° 18.41'	111° 13.64'	0.15	0.93	6	112	0.4	0.00	0.3	0.7	B
001218	836 20.85	39° 18.53'	111° 13.76'	0.09	0.58	6	121	0.7	0.03	0.3	3.4	B
001218	1242 6.63	39° 18.39'	111° 13.56'	0.27*	0.93	6	110	0.2	0.01	0.3	0.4	B
001218	1610 46.69	39° 18.37'	111° 13.49'	0.34*	1.08	6	107	0.2	0.01	0.3	0.3	B
001218	1726 13.09	39° 18.36'	111° 13.44'	0.22*	0.65	7	106	0.1	0.02	0.3	0.3	B
001218	1753 4.24	39° 18.40'	111° 13.60'	0.29	0.67	7	110	0.3	0.02	0.3	0.4	B
001218	1838 48.93	39° 18.51'	111° 13.47'	0.13	0.73	7	113	0.3	0.01	0.3	0.7	B
001218	1931 48.16	39° 18.45'	111° 13.40'	0.39*	0.64	7	109	0.2	0.01	0.3	0.5	B
001218	2012 25.44	39° 18.41'	111° 13.37'	0.20*	1.17	6	107	0.1	0.02	0.3	0.3	B
001218	2156 2.90	39° 18.50'	111° 13.50'	0.11	1.10	8	113	0.3	0.04	0.3	0.7	B
001218	2257 36.65	39° 18.44'	111° 13.44'	0.06	0.75	6	109	0.2	0.00	0.3	0.4	B
001218	2356 10.53	39° 18.52'	111° 13.46'	0.09	1.24	9	97	0.3	0.03	0.2	0.4	B
001218	2358 1.56	39° 18.48'	111° 13.44'	0.49*	0.73	8	111	0.2	0.03	0.3	0.5	B
001219	154 1.81	39° 18.48'	111° 13.41'	0.33*	0.85	7	111	0.2	0.02	0.3	0.4	B
001219	321 46.02	39° 18.52'	111° 13.48'	0.07	0.95	7	114	0.3	0.03	0.3	0.5	B
001219	322 57.08	39° 18.37'	111° 13.38'	0.32*	1.00	7	105	0.0	0.02	0.3	0.3	B
001219	323 59.68	39° 18.36'	111° 13.41'	0.34*	1.13	7	106	0.1	0.01	0.3	0.3	B
001219	453 41.08	39° 18.41'	111° 13.37'	0.32*	1.03	7	106	0.1	0.02	0.3	0.3	B
001219	703 45.91	39° 18.50'	111° 13.30'	0.10	1.08	8	95	0.3	0.07	0.3	2.4	B
001219	744 44.06	39° 18.52'	111° 13.66'	0.29	0.87	8	99	0.5	0.02	0.2	0.5	B
001219	924 10.19	39° 18.47'	111° 13.47'	0.18	0.45	7	112	0.2	0.02	0.3	0.5	B
001219	1154 34.84	39° 18.35'	111° 13.43'	0.22*	0.87	7	105	0.1	0.02	0.3	0.4	B
001219	1452 38.56	39° 18.36'	111° 13.41'	0.23*	0.78	7	106	0.1	0.01	0.3	0.3	B
001219	1509 49.30	39° 18.33'	111° 13.40'	0.21*	0.67	7	104	0.1	0.02	0.2	0.3	B
001219	1810 54.05	39° 18.34'	111° 13.48'	0.17	0.74	7	106	0.2	0.03	0.3	0.4	B

Date	Origin Time	Latitude	Longitude	Depth	Mag	No	Gap	Dmin	Rms	Erh	Erz	Q
001219	1932 34.09	39° 18.35'	111° 13.72'	0.09	0.99	8	173	0.5	0.05	0.4	1.8	C
001219	2126 10.50	39° 18.29'	111° 13.88'	0.06	0.78	7	109	0.8	0.01	0.3	2.7	B
001220	1044 1.20	39° 18.17'	111° 13.78'	0.02	0.99	7	101	0.7	0.03	0.3	0.8	B
001220	1325 33.12	39° 18.48'	111° 13.51'	0.30*	1.22	7	112	0.3	0.02	0.3	0.4	B
001220	1404 7.95	39° 18.53'	111° 13.58'	0.04	1.11	7	116	0.4	0.02	0.3	0.7	B
001220	1859 8.71	39° 18.50'	111° 13.91'	0.28	0.36	7	123	0.8	0.03	0.3	0.8	B
001220	2059 2.35	39° 18.30'	111° 13.41'	0.11*	0.54	7	103	0.1	0.02	0.2	0.5	B
001220	2332 31.30	39° 18.48'	111° 13.47'	0.30*	0.71	7	112	0.2	0.03	0.3	0.4	B
001221	3 36.77	39° 18.51'	111° 13.44'	0.19	0.34	7	113	0.3	0.02	0.3	0.6	B
001221	7 56.41	39° 18.50'	111° 13.38'	0.37*	1.20	7	111	0.2	0.02	0.3	0.6	B
001221	47 57.82	39° 18.37'	111° 13.43'	0.19*	0.74	7	106	0.1	0.03	0.3	0.3	B
001221	123 9.68	39° 18.55'	111° 13.47'	0.06	1.05	8	115	0.4	0.04	0.3	0.6	B
001221	248 13.55	39° 18.50'	111° 13.47'	0.13	0.45	7	113	0.3	0.02	0.3	0.8	B
001221	255 44.39	39° 18.40'	111° 13.39'	0.25*	0.66	6	122	0.1	0.03	0.3	0.4	B
001221	303 57.26	39° 18.39'	111° 13.90'	0.00	1.50	7	116	0.8	0.04	0.3	0.8	B
001221	341 28.50	39° 18.36'	111° 13.45'	0.18*	0.34	7	106	0.1	0.03	0.3	0.4	B
001221	357 23.68	39° 18.51'	111° 13.39'	0.31*	0.21	6	127	0.2	0.03	0.3	0.4	B
001221	417 43.99	39° 18.38'	111° 13.44'	0.18*	0.85	7	107	0.1	0.02	0.3	0.4	B
001221	436 56.91	39° 18.38'	111° 13.47'	0.23*	0.83	7	108	0.2	0.02	0.3	0.4	B
001221	530 8.82	39° 18.48'	111° 13.42'	0.30*	0.84	7	111	0.2	0.02	0.3	0.4	B
001221	548 43.31	39° 18.26'	111° 14.12'	0.15	0.83	7	111	1.1	0.01	0.3	0.8	B
001221	558 11.87	39° 18.38'	111° 13.47'	0.15	0.57	7	108	0.2	0.03	0.3	0.5	B
001221	637 37.07	39° 18.47'	111° 13.50'	0.04	0.21	7	112	0.2	0.03	0.3	0.6	B
001221	646 26.64	39° 18.39'	111° 13.41'	0.16*	0.37	7	107	0.1	0.04	0.4	0.3	B
001221	725 54.27	39° 18.43'	111° 13.45'	0.29*	0.29	7	109	0.2	0.03	0.3	0.3	B
001221	732 17.80	39° 18.35'	111° 13.46'	0.20*	0.21	7	106	0.1	0.03	0.3	0.4	B
001221	812 33.35	39° 18.45'	111° 13.38'	0.29*	1.46	12	96	0.2	0.04	0.2	0.3	B
001221	831 5.72	39° 18.38'	111° 13.42'	0.20*	1.10	8	107	0.1	0.03	0.3	0.3	B
001221	859 8.17	39° 18.48'	111° 13.69'	0.08	0.28	7	117	0.5	0.02	0.3	2.8	B
001221	910 25.27	39° 18.51'	111° 13.53'	0.27	1.02	8	115	0.3	0.03	0.2	0.5	B
001221	936 58.76	39° 18.23'	111° 13.37'	0.18	0.86	7	87	0.2	0.01	0.2	0.5	B
001221	1109 13.48	39° 18.36'	111° 13.43'	0.26*	0.88	7	106	0.1	0.01	0.3	0.3	B
001221	1232 12.14	39° 18.35'	111° 13.53'	0.21*	0.44	7	107	0.2	0.02	0.3	0.5	B
001221	1440 26.05	39° 18.74'	111° 13.25'	0.04	0.00	7	118	0.8	0.04	0.5	3.0	C
001221	1534 32.05	39° 18.48'	111° 13.47'	0.08	0.29	7	112	0.2	0.04	0.3	0.5	B
001221	1711 46.08	39° 18.51'	111° 13.49'	0.27	1.42	10	97	0.3	0.04	0.2	0.3	B
001221	1852 23.06	39° 18.38'	111° 13.45'	0.13*	0.23	7	107	0.1	0.03	0.3	0.4	B
001221	1934 57.40	39° 18.33'	111° 13.48'	0.16	0.62	6	167	0.2	0.03	0.5	0.6	C
001221	2019 23.79	39° 18.44'	111° 13.39'	0.18	0.40	6	124	0.2	0.02	0.3	0.4	B
001221	2049 50.50	39° 18.49'	111° 13.46'	0.15	0.92	7	112	0.2	0.03	0.3	0.6	B
001221	2056 53.20	39° 18.21'	111° 13.67'	0.00	0.31	7	102	0.5	0.01	0.3	0.8	B
001221	2108 59.06	39° 18.36'	111° 13.48'	0.10	0.50	7	107	0.2	0.03	0.3	0.7	B
001221	2222 45.67	39° 18.42'	111° 13.31'	0.19	0.91	9	107	0.2	0.04	0.2	0.3	B
001222	59 8.63	39° 18.45'	111° 13.37'	0.15	0.44	6	125	0.2	0.02	0.3	0.5	B
001222	125 5.60	39° 18.42'	111° 13.89'	0.07	0.80	7	117	0.8	0.01	0.3	2.8	B
001222	148 29.61	39° 18.54'	111° 13.59'	0.12	0.38	7	117	0.5	0.03	0.3	0.9	B
001222	251 5.19	39° 18.55'	111° 13.59'	0.11	0.95	10	118	0.5	0.08	0.3	0.9	B
001222	317 2.69	39° 18.35'	111° 13.44'	0.15*	0.35	7	106	0.1	0.04	0.3	0.4	B
001222	339 59.07	39° 18.50'	111° 13.40'	0.28*	0.65	7	111	0.2	0.02	0.3	0.4	B
001222	344 6.52	39° 18.37'	111° 13.41'	0.33*	0.94	7	106	0.1	0.01	0.3	0.3	B
001222	354 23.12	39° 18.45'	111° 13.38'	0.19	0.55	7	109	0.2	0.03	0.3	0.4	B
001222	520 28.22	39° 18.34'	111° 13.45'	0.13*	0.25	7	105	0.1	0.03	0.3	0.4	B
001222	624 51.90	39° 18.62'	111° 13.30'	0.69*	1.15	12	90	0.5	0.19	0.4	0.8	B
001222	627 33.14	39° 18.47'	111° 13.44'	0.01	0.25	7	110	0.2	0.04	0.3	0.7	B
001222	726 14.04	39° 18.36'	111° 13.39'	0.25*	0.79	7	106	0.0	0.02	0.3	0.3	B
001222	837 18.28	39° 18.50'	111° 13.87'	0.02	0.13	7	121	0.8	0.08	0.5	3.5	C
001222	859 0.84	39° 18.41'	111° 13.35'	0.24*	0.99	8	106	0.1	0.03	0.3	0.4	B
001222	911 51.71	39° 18.49'	111° 13.54'	0.31*	0.78	7	114	0.3	0.01	0.3	0.5	B
001222	1001 47.64	39° 18.49'	111° 13.39'	0.22*	0.94	7	111	0.2	0.02	0.3	0.5	B
001222	1045 26.90	39° 18.47'	111° 13.49'	0.17	0.30	7	112	0.2	0.03	0.3	0.5	B
001222	1128 9.63	39° 18.35'	111° 13.51'	0.13	0.54	7	107	0.2	0.03	0.3	0.6	B
001222	1226 27.53	39° 18.38'	111° 13.59'	0.15	0.46	7	109	0.3	0.01	0.3	0.6	B
001222	1240 27.49	39° 18.35'	111° 13.36'	0.21*	0.34	7	77	0.1	0.02	0.3	0.3	B
001222	1436 40.07	39° 18.36'	111° 13.68'	0.02	0.78	7	110	0.4	0.03	0.3	0.7	B
001222	1758 0.02	39° 17.98'	111° 14.00'	0.40	0.71	9	129	1.1	0.10	0.4	5.7	B
001222	2022 15.47	39° 18.03'	111° 13.68'	0.01	1.19	9	93	0.8	0.09	0.3	0.8	B
001223	136 17.53	39° 18.42'	111° 13.87'	0.04	0.82	7	118	0.7	0.02	0.3	2.8	B
001223	137 5.92	39° 18.53'	111° 13.31'	0.31*	1.03	10	111	0.3	0.06	0.2	0.4	B

Date	Origin Time		Latitude		Longitude		Depth	Mag	No	Gap	Dmin	Rms	Erh	Erz	Q
001223	324	34.28	39°	18.50'	111°	13.60'	0.35	0.64	7	116	0.4	0.02	0.3	0.4	B
001223	410	15.78	39°	18.35'	111°	13.46'	0.12*	0.55	7	105	0.1	0.03	0.3	0.5	B
001223	529	41.34	39°	18.57'	111°	13.66'	0.20	0.98	10	120	0.6	0.05	0.2	0.6	B
001223	728	30.51	39°	18.42'	111°	13.88'	0.03	0.60	7	118	0.8	0.02	0.3	2.8	B
001223	734	24.54	39°	18.04'	111°	13.70'	0.34	1.43	17	93	0.8	0.08	0.2	0.4	B
001223	1204	4.82	39°	18.37'	111°	13.44'	0.31*	0.75	7	106	0.1	0.02	0.3	0.3	B
001224	442	43.67	39°	18.20'	111°	13.86'	0.36	0.91	10	104	0.8	0.04	0.2	0.5	B
001224	1008	6.43	39°	18.35'	111°	12.65'	0.03	0.26	7	88	1.1	0.07	0.3	3.9	B
001224	1123	8.07	39°	18.27'	111°	14.10'	0.29	0.72	7	112	1.1	0.02	0.3	0.7	B
001224	1729	49.06	39°	18.09'	111°	13.18'	0.02	0.00	6	114	0.6	0.07	0.3	0.9	B
001224	1753	9.64	39°	18.34'	111°	13.46'	0.20*	1.12	10	105	0.1	0.05	0.2	0.3	B
001224	1822	6.68	39°	18.22'	111°	13.65'	0.06	0.63	7	102	0.5	0.01	0.3	0.7	B
001224	1824	21.51	39°	17.68'	111°	14.17'	0.39	0.19	5	101	1.7	0.06	0.9	41.7	D
001225	127	25.07	39°	18.43'	111°	13.39'	0.32*	0.77	8	108	0.2	0.03	0.2	0.3	B
001225	817	26.96	39°	18.39'	111°	13.48'	0.27*	0.77	7	108	0.2	0.01	0.3	0.4	B
001225	2012	0.10	39°	17.79'	111°	11.65'	0.05	1.56	10	81	1.2	0.12	0.3	1.5	B
001226	1608	41.77	39°	18.20'	111°	13.52'	0.36*	1.02	11	100	0.3	0.04	0.2	0.3	B
001228	936	1.53	39°	18.33'	111°	13.50'	0.17	0.84	9	106	0.2	0.04	0.2	0.4	B
001228	1441	58.01	39°	18.46'	111°	13.60'	0.26	0.52	9	113	0.3	0.04	0.2	0.3	B
001229	910	57.75	39°	18.35'	111°	13.53'	0.18	0.42	7	107	0.2	0.02	0.3	0.5	B
001229	1011	40.17	39°	18.36'	111°	13.91'	0.00	0.23	7	115	0.8	0.03	0.3	0.8	B
001229	1746	2.45	39°	18.41'	111°	13.89'	0.08	0.60	7	117	0.8	0.03	0.3	2.9	B
001229	1802	44.17	39°	18.39'	111°	13.45'	0.07	0.83	8	107	0.1	0.07	0.3	0.4	B
001229	1840	3.21	39°	17.55'	111°	13.43'	0.37	0.99	7	88	1.4	0.03	0.2	999.9	B
001229	1935	43.80	39°	17.90'	111°	13.42'	0.08	0.92	6	90	0.9	0.01	0.3	3.2	B
001230	856	23.97	39°	18.45'	111°	13.65'	0.10	0.37	8	114	0.5	0.10	0.5	1.1	C
001230	1332	7.37	39°	18.37'	111°	13.50'	0.15	0.71	9	107	0.2	0.05	0.2	0.5	B
001230	1435	51.50	39°	18.37'	111°	13.75'	0.01	0.31	8	112	0.6	0.05	0.3	0.6	B
001230	1623	6.02	39°	18.44'	111°	13.70'	0.11	0.64	9	115	0.5	0.04	0.2	0.8	B
001231	107	51.78	39°	18.31'	111°	13.55'	0.01	1.12	9	105	0.2	0.04	0.2	0.5	B
001231	1658	57.39	39°	18.10'	111°	13.53'	0.03	0.93	7	95	0.6	0.05	0.3	0.8	B
010101	1052	2.61	39°	18.33'	111°	13.89'	0.01	1.28	11	112	0.8	0.11	0.3	1.3	C
010101	1053	21.11	39°	18.47'	111°	13.42'	0.20*	0.28	7	110	0.2	0.02	0.3	0.5	B
010102	641	46.26	39°	17.95'	111°	13.58'	0.04	0.65	7	89	0.8	0.09	0.3	3.9	B
010102	744	44.64	39°	17.90'	111°	12.72'	0.10	0.69	7	80	0.3	0.01	0.3	3.1	B
010102	825	46.13	39°	18.27'	111°	13.96'	0.04	0.86	7	110	0.9	0.01	0.3	2.8	B
010102	1632	8.62	39°	18.49'	111°	13.39'	0.35*	0.74	7	111	0.2	0.02	0.3	0.4	B
010102	1811	56.68	39°	18.35'	111°	13.47'	0.13	0.50	7	105	0.2	0.02	0.3	0.5	B
010102	1830	45.83	39°	18.56'	111°	13.35'	0.15	0.00	6	131	0.3	0.02	0.3	0.8	B
010102	1842	26.67	39°	18.33'	111°	13.44'	0.15*	0.32	7	104	0.1	0.03	0.3	0.4	B
010102	1911	43.03	39°	18.49'	111°	13.31'	0.18	0.28	6	130	0.2	0.02	0.3	0.5	B
010102	1912	34.69	39°	18.48'	111°	13.44'	0.11	0.36	7	112	0.2	0.04	0.3	0.9	B
010102	1921	19.71	39°	18.34'	111°	13.47'	0.16	0.83	7	105	0.2	0.03	0.3	0.4	B
010102	2008	37.07	39°	18.47'	111°	13.41'	0.30*	0.40	7	110	0.2	0.03	0.3	0.4	B
010102	2044	31.01	39°	18.48'	111°	13.47'	0.19	0.85	7	112	0.2	0.03	0.3	0.5	B
010102	2247	52.89	39°	18.37'	111°	13.50'	0.19	0.45	7	107	0.2	0.02	0.3	0.5	B
010102	2253	44.86	39°	18.37'	111°	13.38'	0.23*	1.03	7	105	0.0	0.01	0.3	0.3	B
010103	49	3.19	39°	18.51'	111°	13.33'	0.31*	1.54	12	95	0.3	0.04	0.2	0.3	B
010103	202	48.36	39°	18.49'	111°	13.57'	0.27	0.60	7	114	0.3	0.03	0.3	0.5	B
010103	207	30.78	39°	18.46'	111°	13.45'	0.29*	0.51	7	111	0.2	0.04	0.3	0.4	B
010103	218	46.59	39°	18.35'	111°	13.45'	0.15*	0.48	7	105	0.1	0.03	0.3	0.4	B
010103	244	6.89	39°	18.34'	111°	13.39'	0.07	0.62	7	104	0.1	0.06	0.3	0.3	B
010103	330	8.95	39°	18.45'	111°	13.40'	0.01	1.33	10	109	0.2	0.04	0.2	0.5	B
010103	355	59.25	39°	18.37'	111°	13.42'	0.31*	0.67	7	106	0.1	0.03	0.3	0.3	B
010103	537	11.95	39°	18.39'	111°	13.34'	0.24*	0.00	6	124	0.1	0.02	0.3	0.3	B
010103	850	13.21	39°	18.55'	111°	13.45'	0.13	1.18	7	115	0.3	0.01	0.2	0.8	B
010103	1025	52.71	39°	18.48'	111°	13.56'	0.40*	0.88	7	114	0.3	0.02	0.3	0.7	B
010103	1030	45.13	39°	18.48'	111°	13.45'	0.30*	0.56	7	112	0.2	0.03	0.3	0.4	B
010103	1400	6.68	39°	18.36'	111°	13.44'	0.19*	0.72	7	106	0.1	0.02	0.3	0.4	B
010103	1742	34.65	39°	18.37'	111°	13.34'	0.29*	1.25	7	105	0.1	0.02	0.3	0.3	B
010103	1855	35.75	39°	18.35'	111°	13.33'	0.26*	0.82	7	90	0.1	0.02	0.3	0.3	B
010103	1921	6.24	39°	18.51'	111°	13.50'	0.08	0.78	7	114	0.3	0.02	0.3	0.5	B
010103	1932	41.04	39°	18.37'	111°	13.43'	0.18*	0.27	7	106	0.1	0.03	0.3	0.3	B
010103	2015	39.88	39°	18.47'	111°	13.36'	0.32*	0.97	7	109	0.2	0.02	0.3	0.4	B
010103	2032	36.91	39°	18.59'	111°	13.82'	0.17	1.31	12	125	0.8	0.09	0.3	0.7	B
010103	2143	54.85	39°	18.35'	111°	13.39'	0.18*	0.82	7	105	0.0	0.03	0.3	0.3	B
010103	2149	11.57	39°	18.49'	111°	13.37'	0.23*	0.68	7	111	0.2	0.03	0.3	0.5	B
010103	2217	48.89	39°	18.53'	111°	13.34'	0.10	1.24	9	95	0.3	0.03	0.2	0.7	B

Date	Origin Time	Latitude	Longitude	Depth	Mag	No	Gap	Dmin	Rms	Erh	Erz	Q
010103	2236 37.07	39° 18.47'	111° 13.43'	0.19	0.42	7	110	0.2	0.04	0.3	0.5	B
010103	2301 53.73	39° 18.48'	111° 13.36'	0.29*	1.12	7	109	0.2	0.02	0.3	0.4	B
010103	2354 9.61	39° 18.35'	111° 13.42'	0.15*	0.56	7	105	0.1	0.03	0.3	0.3	B
010104	20 38.09	39° 18.48'	111° 13.46'	0.39*	0.84	7	112	0.2	0.02	0.3	0.6	B
010104	32 47.14	39° 18.40'	111° 13.36'	0.31*	0.80	7	106	0.1	0.02	0.3	0.3	B
010104	41 54.55	39° 18.51'	111° 13.31'	0.22	0.19	6	131	0.3	0.02	0.3	0.5	B
010104	104 56.60	39° 18.38'	111° 13.44'	0.18*	0.60	7	106	0.1	0.02	0.3	0.4	B
010104	238 17.21	39° 18.36'	111° 13.34'	0.22*	0.39	7	96	0.1	0.02	0.3	0.3	B
010104	330 27.30	39° 18.49'	111° 13.31'	0.19	1.41	12	109	0.2	0.05	0.2	0.4	B
010104	500 37.15	39° 18.44'	111° 13.32'	0.25*	0.38	6	127	0.2	0.02	0.3	0.4	B
010104	506 38.77	39° 18.40'	111° 13.47'	0.14	0.34	7	109	0.2	0.05	0.3	0.5	B
010104	513 44.29	39° 18.70'	111° 11.01'	1.85	1.34	6	139	2.7	0.20	1.0	3.1	D
010104	544 31.29	39° 18.37'	111° 13.34'	0.20*	0.51	7	105	0.1	0.02	0.3	0.3	B
010104	620 36.31	39° 18.35'	111° 13.35'	0.22*	1.19	7	77	0.1	0.02	0.3	0.3	B
010104	749 48.41	39° 18.21'	111° 13.44'	0.02	0.48	7	99	0.3	0.05	0.3	0.9	B
010104	834 27.70	39° 18.55'	111° 13.27'	0.04	0.94	10	94	0.4	0.06	0.2	0.6	B
010104	1203 44.57	39° 18.36'	111° 13.37'	0.16*	0.38	7	84	0.0	0.03	0.3	0.3	B
010104	1240 44.37	39° 17.64'	111° 14.15'	0.04	0.56	7	101	1.7	0.08	0.3	4.4	B
010104	1348 23.89	39° 18.45'	111° 13.89'	0.02	0.71	7	119	0.8	0.05	0.3	3.1	B
010104	1634 39.07	39° 18.38'	111° 13.31'	0.32*	1.19	7	104	0.1	0.01	0.3	0.3	B
010104	1701 27.24	39° 18.37'	111° 13.42'	0.22*	0.51	7	106	0.1	0.03	0.3	0.3	B
010104	1701 48.80	39° 18.40'	111° 13.42'	0.14*	0.53	7	107	0.1	0.05	0.3	0.4	B
010104	1731 24.10	39° 18.48'	111° 13.19'	0.26	1.18	6	136	0.3	0.03	0.3	0.5	C
010104	1808 50.04	39° 18.35'	111° 13.37'	0.15*	0.26	7	77	0.1	0.03	0.3	0.4	B
010104	1823 16.75	39° 18.38'	111° 13.43'	0.24*	1.00	7	107	0.1	0.03	0.3	0.3	B
010104	1827 7.06	39° 18.10'	111° 13.57'	0.01	0.38	6	114	0.6	0.08	0.6	1.8	C
010104	1937 10.46	39° 18.36'	111° 13.38'	0.14*	0.24	7	105	0.0	0.04	0.3	0.3	B
010104	1943 36.85	39° 18.49'	111° 13.39'	0.08	0.84	7	111	0.2	0.01	0.2	0.5	B
010104	2028 51.89	39° 18.53'	111° 13.43'	0.34*	1.31	9	113	0.3	0.05	0.3	0.4	B
010104	2136 45.85	39° 18.42'	111° 13.36'	0.37*	0.73	7	107	0.1	0.02	0.3	0.5	B
010104	2209 44.90	39° 18.41'	111° 13.38'	0.32*	0.78	6	108	0.1	0.02	0.3	0.2	B
010104	2239 46.24	39° 18.44'	111° 13.38'	0.33*	1.46	9	96	0.2	0.03	0.2	0.3	B
010104	2347 8.67	39° 18.53'	111° 13.27'	0.24	1.28	10	110	0.3	0.04	0.2	0.5	B
010105	231 19.40	39° 18.49'	111° 13.39'	0.30*	0.80	7	111	0.2	0.04	0.3	0.4	B
010105	239 49.52	39° 18.44'	111° 13.33'	0.15	0.00	6	127	0.2	0.03	0.3	0.5	B
010105	340 51.85	39° 18.39'	111° 13.45'	0.34*	0.57	7	107	0.1	0.04	0.3	0.3	B
010105	439 57.46	39° 18.34'	111° 13.42'	0.12*	1.03	7	105	0.1	0.05	0.3	0.4	B
010105	508 16.89	39° 18.34'	111° 13.37'	0.12*	0.85	7	80	0.1	0.05	0.3	0.4	B
010105	511 40.65	39° 18.33'	111° 13.43'	0.21*	1.19	7	104	0.1	0.04	0.3	0.4	B
010105	548 30.43	39° 18.56'	111° 13.45'	0.28	0.71	7	115	0.4	0.05	0.3	0.5	B
010105	612 44.88	39° 18.35'	111° 13.34'	0.24*	0.54	7	84	0.1	0.04	0.3	0.3	B
010105	846 27.07	39° 18.48'	111° 13.27'	0.26*	1.25	11	108	0.2	0.04	0.2	0.3	B
010105	856 58.81	39° 18.37'	111° 13.48'	0.18	0.33	7	107	0.2	0.02	0.3	0.4	B
010105	913 24.95	39° 18.47'	111° 13.36'	0.24*	1.35	12	109	0.2	0.04	0.2	0.3	B
010105	958 14.60	39° 18.34'	111° 13.46'	0.16*	0.52	7	105	0.1	0.02	0.3	0.4	B
010105	1025 35.43	39° 18.34'	111° 13.31'	0.24*	0.74	7	77	0.1	0.02	0.3	0.3	B
010105	1118 23.97	39° 18.48'	111° 13.52'	0.32*	0.82	7	113	0.3	0.02	0.3	0.4	B
010105	1430 7.52	39° 18.51'	111° 13.57'	0.08	0.84	7	115	0.4	0.03	0.3	0.6	B
010105	1534 50.75	39° 18.37'	111° 13.31'	0.24*	1.19	7	104	0.1	0.02	0.3	0.3	B
010105	1805 31.90	39° 18.62'	111° 13.69'	0.23	0.82	7	123	0.7	0.04	0.3	0.8	B
010105	1844 7.84	39° 18.56'	111° 13.62'	0.05	1.30	7	118	0.5	0.02	0.3	0.6	B
010105	2010 57.53	39° 18.32'	111° 13.47'	0.14	0.89	7	104	0.2	0.05	0.3	0.5	B
010105	2158 23.00	39° 18.31'	111° 13.36'	0.19*	0.36	7	77	0.1	0.03	0.3	0.4	B
010105	2258 11.69	39° 18.35'	111° 13.46'	0.08	0.62	7	105	0.1	0.04	0.3	0.4	B
010105	2359 58.58	39° 18.38'	111° 13.34'	0.29*	0.53	7	105	0.1	0.04	0.3	0.3	B
010106	41 33.49	39° 18.45'	111° 13.31'	0.34*	0.00	6	128	0.2	0.02	0.3	0.4	B
010106	114 9.11	39° 18.21'	111° 13.69'	0.04	0.50	7	102	0.5	0.03	0.3	0.9	B
010106	115 12.88	39° 18.59'	111° 13.35'	0.17	0.52	7	115	0.5	0.02	0.3	0.7	B
010106	234 43.13	39° 18.47'	111° 13.40'	0.33*	0.48	9	110	0.2	0.04	0.2	0.2	B
010106	244 52.89	39° 18.39'	111° 13.70'	0.16	0.83	7	111	0.5	0.04	0.3	0.7	B
010106	331 40.97	39° 18.87'	111° 13.13'	0.62	0.08	5	268	1.0	0.03	1.0	1.3	D
010106	331 53.98	39° 18.55'	111° 13.61'	0.11	0.77	9	118	0.5	0.04	0.2	0.8	B
010106	332 33.86	39° 18.56'	111° 13.57'	0.15	0.53	9	117	0.5	0.04	0.2	0.6	B
010106	1254 1.11	39° 18.42'	111° 13.56'	0.20*	0.80	7	111	0.2	0.01	0.3	0.5	B
010106	1557 48.67	39° 18.54'	111° 13.41'	0.18	1.21	6	113	0.3	0.03	0.3	0.7	B
010106	1634 3.77	39° 18.52'	111° 13.28'	0.48*	0.97	7	109	0.3	0.02	0.3	0.6	B
010106	1744 39.30	39° 18.46'	111° 13.43'	0.39*	0.98	6	187	0.2	0.02	0.5	0.5	D
010106	1755 42.05	39° 18.47'	111° 13.38'	0.33*	0.66	7	110	0.2	0.03	0.3	0.4	B

Date	Origin Time	Latitude	Longitude	Depth	Mag	No	Gap	Dmin	Rms	Erh	Erz	Q
010106	1932 50.22	39° 18.39'	111° 13.43'	0.13*	0.46	7	107	0.1	0.04	0.3	0.4	B
010106	1953 39.55	39° 18.14'	111° 13.94'	0.02	0.53	7	101	0.9	0.08	0.4	3.7	B
010106	2111 45.44	39° 18.36'	111° 13.35'	0.19*	0.92	7	91	0.1	0.03	0.3	0.3	B
010106	2350 15.18	39° 18.21'	111° 13.73'	0.02	0.67	7	102	0.6	0.02	0.3	0.8	B
010107	18 10.72	39° 18.34'	111° 13.18'	0.05	1.36	8	89	0.3	0.08	0.3	0.7	B
010107	34 9.84	39° 18.39'	111° 13.36'	0.16*	0.81	7	106	0.1	0.03	0.3	0.3	B
010107	50 33.70	39° 17.57'	111° 14.06'	0.41	0.88	7	100	1.8	0.03	0.3	11.5	B
010107	139 19.61	39° 18.44'	111° 13.45'	0.21*	0.28	7	109	0.2	0.03	0.3	0.4	B
010107	434 25.20	39° 18.47'	111° 13.32'	0.26*	1.09	7	109	0.2	0.02	0.3	0.4	B
010107	1623 49.43	39° 18.46'	111° 13.59'	0.32*	0.50	7	113	0.3	0.02	0.3	0.5	B
010107	1830 10.77	39° 18.26'	111° 13.90'	0.02	0.61	7	108	0.8	0.08	0.4	3.5	B
010108	234 20.23	39° 18.34'	111° 13.33'	0.25*	0.92	7	77	0.1	0.02	0.3	0.3	B
010108	1136 28.32	39° 18.39'	111° 13.32'	0.20*	0.35	7	105	0.1	0.03	0.3	0.3	B
010108	1354 28.92	39° 18.22'	111° 13.30'	0.02	0.67	7	77	0.3	0.02	0.3	0.8	B
010108	1546 13.32	39° 18.35'	111° 13.33'	0.19*	0.45	7	89	0.1	0.03	0.3	0.3	B
010108	1705 40.79	39° 18.50'	111° 13.24'	0.13	0.43	6	134	0.3	0.02	0.4	0.7	B
010108	1750 28.48	39° 18.29'	111° 13.32'	0.09	0.54	7	78	0.2	0.04	0.3	0.4	B
010108	1904 18.37	39° 18.35'	111° 13.41'	0.25*	0.60	7	105	0.1	0.02	0.3	0.3	B
010108	1905 36.88	39° 18.37'	111° 13.34'	0.13*	0.37	7	105	0.1	0.04	0.3	0.4	B
010108	1953 56.12	39° 18.35'	111° 13.37'	0.19*	0.44	7	77	0.0	0.03	0.3	0.3	B
010108	2003 22.12	39° 18.39'	111° 13.29'	0.26*	1.12	7	104	0.2	0.02	0.3	0.4	B
010108	2035 14.36	39° 18.39'	111° 13.28'	0.05	0.64	7	104	0.2	0.10	0.4	0.7	B
010108	2039 31.92	39° 18.35'	111° 13.35'	0.21*	0.49	7	77	0.1	0.04	0.3	0.3	B
010108	2214 56.07	39° 17.87'	111° 13.41'	0.27	1.51	7	80	0.9	0.24	0.6	1.9	C
010108	2224 47.85	39° 18.15'	111° 12.74'	0.01	0.09	6	145	0.8	0.03	0.5	3.4	C
010108	2316 34.87	39° 18.33'	111° 13.20'	0.08	1.14	9	85	0.2	0.10	0.3	0.6	B
010108	2322 15.42	39° 18.53'	111° 13.30'	0.01	1.05	8	111	0.3	0.05	0.3	0.7	B
010109	5 8.56	39° 18.29'	111° 13.49'	0.09	0.43	6	146	0.2	0.03	0.6	0.7	C
010109	30 18.92	39° 18.39'	111° 13.29'	0.32*	0.38	6	127	0.2	0.03	0.4	0.3	B
010109	56 37.85	39° 18.37'	111° 13.32'	0.25*	1.07	7	105	0.1	0.02	0.3	0.3	B
010109	158 5.19	39° 18.43'	111° 13.34'	0.22*	0.55	9	107	0.2	0.04	0.2	0.3	B
010109	423 26.89	39° 18.44'	111° 13.21'	0.60*	1.46	14	93	0.3	0.12	0.2	0.3	C
010109	501 30.96	39° 18.29'	111° 13.48'	0.02	0.72	9	103	0.2	0.05	0.2	0.4	B
010109	659 41.49	39° 18.33'	111° 13.36'	0.17*	0.29	9	77	0.1	0.04	0.2	0.3	A
010109	700 30.35	39° 18.53'	111° 13.39'	0.27	0.47	8	112	0.3	0.03	0.3	0.4	B
010109	714 46.73	39° 18.36'	111° 13.49'	0.11	0.34	9	107	0.2	0.06	0.2	0.6	B
010109	904 30.35	39° 18.76'	111° 13.27'	0.08	0.33	9	119	0.8	0.06	0.2	1.0	B
010109	1159 3.84	39° 18.70'	111° 13.38'	0.31	0.31	9	119	0.6	0.12	0.3	0.7	C
010109	1709 38.51	39° 18.34'	111° 13.44'	0.10*	1.57	9	105	0.1	0.04	0.2	0.2	B
010109	1716 24.45	39° 18.38'	111° 13.28'	0.13	0.94	8	104	0.2	0.04	0.3	0.5	B
010109	1726 45.75	39° 18.28'	111° 13.33'	0.08	0.31	7	77	0.2	0.03	0.3	0.5	B
010109	1727 23.44	39° 17.62'	111° 12.73'	0.13	2.17	17	86	0.5	0.19	0.3	0.8	B
010109	1900 50.45	39° 18.36'	111° 13.34'	0.25*	0.77	7	100	0.1	0.02	0.3	0.3	B
010109	1915 44.10	39° 18.47'	111° 13.28'	0.31*	1.40	7	107	0.2	0.02	0.3	0.4	B
010109	2021 9.47	39° 18.46'	111° 13.27'	0.13	0.65	6	131	0.2	0.02	0.3	0.7	B
010109	2025 58.21	39° 18.37'	111° 13.24'	0.20*	0.13	6	128	0.2	0.01	0.4	0.3	B
010109	2143 27.01	39° 18.36'	111° 13.35'	0.22*	0.51	7	105	0.1	0.03	0.3	0.3	B
010109	2150 8.15	39° 18.33'	111° 13.39'	0.18*	0.62	7	104	0.1	0.03	0.3	0.3	B
010109	2153 22.42	39° 18.46'	111° 13.36'	0.25*	0.73	7	108	0.2	0.04	0.3	0.4	B
010109	2330 19.18	39° 18.46'	111° 13.47'	0.30*	0.72	7	111	0.2	0.03	0.3	0.4	B
010110	14 33.14	39° 18.32'	111° 13.31'	0.20*	0.69	9	78	0.2	0.05	0.2	0.3	A
010110	57 17.06	39° 18.33'	111° 13.33'	0.20*	0.91	9	77	0.1	0.04	0.2	0.3	A
010110	204 0.32	39° 18.33'	111° 13.45'	0.13*	0.60	9	104	0.1	0.05	0.2	0.4	B
010110	330 28.06	39° 18.33'	111° 13.40'	0.16*	0.37	9	104	0.1	0.05	0.2	0.3	B
010110	331 59.27	39° 18.15'	111° 13.38'	0.01	0.91	9	88	0.4	0.09	0.3	0.6	B
010110	340 12.73	39° 18.41'	111° 13.34'	0.30*	0.55	9	106	0.1	0.03	0.2	0.3	B
010110	440 12.23	39° 18.34'	111° 13.33'	0.26*	0.67	9	77	0.1	0.05	0.2	0.3	A
010110	603 22.86	39° 18.35'	111° 13.32'	0.18*	0.37	7	90	0.1	0.02	0.3	0.4	B
010110	705 58.36	39° 18.36'	111° 13.31'	0.18*	0.53	7	96	0.1	0.03	0.3	0.4	B
010110	735 45.23	39° 18.50'	111° 13.46'	0.30*	0.92	8	112	0.2	0.02	0.2	0.3	B
010110	747 56.75	39° 18.70'	111° 13.15'	0.53	1.57	13	90	0.7	0.19	0.4	0.7	B
010110	811 34.46	39° 18.26'	111° 13.35'	0.08	0.14	7	78	0.2	0.03	0.3	0.6	B
010110	811 58.00	39° 18.35'	111° 13.37'	0.20*	0.43	7	77	0.0	0.02	0.3	0.3	B
010110	1124 4.11	39° 18.48'	111° 13.52'	0.42*	1.19	8	112	0.3	0.02	0.3	0.5	B
010110	1219 44.05	39° 18.47'	111° 13.35'	0.23*	0.68	7	109	0.2	0.02	0.3	0.4	B
010110	1444 37.90	39° 18.34'	111° 13.47'	0.15	0.45	7	106	0.2	0.03	0.3	0.5	B
010110	1558 48.36	39° 18.36'	111° 13.28'	0.25*	0.95	7	96	0.2	0.01	0.3	0.3	B
010110	1730 28.57	39° 18.35'	111° 13.26'	0.20*	0.87	7	94	0.2	0.02	0.3	0.4	B

Date	Origin Time	Latitude	Longitude	Depth	Mag	No	Gap	Dmin	Rms	Erh	Erz	Q
010110	2030 53.59	39° 18.49'	111° 13.31'	0.12	0.89	7	109	0.2	0.02	0.3	0.8	B
010110	2113 16.01	39° 18.34'	111° 13.24'	0.20*	0.93	7	86	0.2	0.02	0.3	0.4	B
010110	2132 24.95	39° 18.46'	111° 13.36'	0.33*	0.76	7	108	0.2	0.03	0.3	0.4	B
010110	2156 44.40	39° 18.51'	111° 13.25'	0.04	1.32	9	94	0.3	0.06	0.3	0.6	B
010110	2236 20.46	39° 18.38'	111° 13.28'	0.16	0.26	6	127	0.2	0.02	0.3	0.4	B
010111	11 23.59	39° 18.73'	111° 13.01'	0.36	0.91	5	264	0.9	0.04	1.1	20.6	D
010111	49 36.36	39° 18.42'	111° 13.38'	0.27*	0.41	9	108	0.1	0.04	0.2	0.3	B
010111	107 59.97	39° 18.50'	111° 13.27'	0.14	0.40	6	133	0.3	0.02	0.3	0.7	B
010111	123 29.71	39° 18.80'	111° 13.49'	0.37	0.47	9	126	0.9	0.10	0.3	4.4	B
010111	154 40.40	39° 18.43'	111° 13.31'	0.24*	0.94	9	107	0.2	0.03	0.2	0.3	B
010111	219 44.13	39° 18.34'	111° 13.37'	0.21*	0.78	9	80	0.1	0.05	0.2	0.3	A
010111	324 49.06	39° 18.43'	111° 13.29'	0.26*	0.56	9	106	0.2	0.04	0.2	0.3	B
010111	340 4.06	39° 18.40'	111° 13.30'	0.25*	0.79	9	106	0.2	0.03	0.2	0.3	B
010111	425 7.64	39° 19.73'	111° 12.88'	0.40	0.94	7	153	2.7	0.17	0.8	28.8	D
010111	455 35.13	39° 17.92'	111° 13.86'	0.10	1.29	13	88	1.1	0.05	0.2	0.6	A
010111	528 10.08	39° 18.49'	111° 13.48'	0.30*	0.88	9	112	0.2	0.04	0.2	0.3	B
010111	635 50.20	39° 18.34'	111° 13.40'	0.21*	1.01	9	105	0.1	0.05	0.2	0.3	B
010111	1053 12.10	39° 18.41'	111° 13.57'	0.28	0.78	9	111	0.3	0.03	0.2	0.3	B
010111	1146 30.30	39° 18.52'	111° 13.46'	0.03	0.89	9	113	0.3	0.04	0.2	0.5	B
010111	1158 54.53	39° 18.46'	111° 13.31'	0.24*	0.60	9	108	0.2	0.05	0.2	0.4	B
010111	1603 46.19	39° 18.32'	111° 13.22'	1.27*	0.46	7	80	0.2	0.09	0.4	0.9	B
010111	1639 6.00	39° 18.43'	111° 13.38'	0.09	0.83	7	108	0.2	0.04	0.3	0.4	B
010111	1643 29.33	39° 18.27'	111° 13.29'	0.06	0.52	7	78	0.2	0.03	0.3	0.7	B
010111	1645 20.50	39° 18.43'	111° 13.48'	0.36*	0.73	7	110	0.2	0.04	0.3	0.4	B
010111	1732 55.24	39° 18.12'	111° 13.04'	0.02	0.81	7	79	0.7	0.03	0.3	0.7	B
010111	1752 37.47	39° 18.46'	111° 13.43'	0.35*	0.91	7	110	0.2	0.03	0.3	0.4	B
010111	2047 3.04	39° 18.47'	111° 13.31'	0.25*	0.78	7	108	0.2	0.04	0.3	0.4	B
010111	2218 43.38	39° 18.36'	111° 13.27'	0.17	0.87	7	99	0.2	0.02	0.3	0.4	B
010111	2242 17.55	39° 18.37'	111° 13.27'	0.25*	1.14	7	104	0.2	0.02	0.3	0.4	B
010111	2248 54.74	39° 18.29'	111° 13.42'	0.09	0.48	7	103	0.2	0.04	0.2	0.4	B
010111	2304 47.51	39° 18.45'	111° 13.89'	0.01	0.92	7	119	0.8	0.05	0.3	0.8	B
010112	57 53.69	39° 18.37'	111° 13.38'	0.24*	0.67	7	105	0.0	0.02	0.3	0.3	B
010112	106 51.00	39° 17.96'	111° 13.89'	0.39	0.33	6	90	1.1	0.04	0.5	11.7	C
010112	243 9.69	39° 18.34'	111° 13.26'	0.22*	0.57	7	86	0.2	0.03	0.3	0.4	B
010112	251 24.61	39° 18.35'	111° 13.25'	0.04	0.00	7	93	0.2	0.03	0.3	0.6	B
010112	445 4.78	39° 18.55'	111° 13.63'	0.06	1.28	8	118	0.5	0.04	0.3	0.6	B
010112	445 38.65	39° 18.45'	111° 13.23'	0.22*	0.77	7	106	0.2	0.03	0.3	0.5	B
010112	446 21.43	39° 18.48'	111° 13.30'	0.08	1.14	9	109	0.2	0.04	0.2	0.5	B
010112	727 8.21	39° 18.33'	111° 13.31'	0.13*	0.42	7	77	0.1	0.04	0.3	0.5	B
010112	752 2.62	39° 18.35'	111° 13.25'	0.11	0.14	6	127	0.2	0.03	0.3	0.8	B
010112	757 30.91	39° 18.33'	111° 13.24'	0.15	0.00	7	83	0.2	0.02	0.3	0.5	B
010112	835 14.14	39° 18.11'	111° 11.65'	0.10	0.52	7	94	1.4	0.04	0.3	1.2	B
010112	845 37.84	39° 18.36'	111° 13.32'	0.15*	0.51	7	92	0.1	0.03	0.3	0.4	B
010112	1327 0.99	39° 18.43'	111° 13.44'	0.31*	0.44	7	109	0.2	0.04	0.3	0.4	B
010112	1414 20.65	39° 17.95'	111° 11.04'	0.49	0.47	5	102	3.5	0.11	0.9	32.6	D
010112	1523 33.37	39° 18.47'	111° 13.38'	0.34*	0.85	7	110	0.2	0.03	0.3	0.4	B
010112	1555 13.17	39° 18.47'	111° 13.24'	0.15	0.70	7	107	0.3	0.02	0.3	0.7	B
010112	1555 39.84	39° 17.92'	111° 14.18'	0.13	0.00	7	89	1.4	0.04	0.3	0.9	B
010112	2314 34.50	39° 18.35'	111° 13.27'	0.16	0.08	6	126	0.2	0.01	0.3	0.4	B
010113	242 15.17	39° 18.40'	111° 13.40'	0.21*	1.40	9	107	0.1	0.02	0.2	0.3	B
010113	454 40.01	39° 18.51'	111° 13.67'	0.30	0.73	7	118	0.5	0.02	0.3	0.6	B
010113	715 45.73	39° 18.42'	111° 13.84'	0.02	0.96	6	122	0.7	0.03	0.3	0.7	B
010113	1555 11.18	39° 18.36'	111° 13.55'	0.12	1.32	7	107	0.2	0.02	0.3	0.7	B
010113	1703 28.36	39° 18.44'	111° 13.29'	0.17	0.62	7	106	0.2	0.04	0.3	0.5	B
010114	358 56.45	39° 18.42'	111° 13.88'	0.01	0.49	7	117	0.8	0.06	0.3	3.3	B
010114	600 9.43	39° 18.15'	111° 13.93'	0.14	0.88	7	101	0.9	0.01	0.3	0.8	B
010114	724 39.12	39° 18.34'	111° 13.42'	0.23*	0.80	7	105	0.1	0.02	0.3	0.3	B
010114	924 50.15	39° 18.45'	111° 13.25'	0.21*	0.56	7	107	0.2	0.04	0.3	0.5	B
010114	1321 30.89	39° 18.37'	111° 13.40'	0.21*	0.51	7	106	0.1	0.04	0.3	0.3	B
010114	1348 21.93	39° 17.79'	111° 11.90'	0.16	0.57	7	87	0.9	0.05	0.3	1.1	B
010114	1506 32.66	39° 18.46'	111° 13.23'	0.08	0.59	7	107	0.3	0.05	0.3	0.6	B
010114	1656 24.17	39° 18.29'	111° 13.95'	0.02	0.13	7	110	0.8	0.03	0.3	2.8	B
010114	2244 1.63	39° 18.49'	111° 13.65'	0.29	0.82	7	116	0.5	0.02	0.3	0.5	B
010114	2302 41.03	39° 18.48'	111° 13.89'	0.04	0.43	7	121	0.8	0.01	0.3	2.8	B
010115	17 56.25	39° 18.48'	111° 13.26'	0.34*	0.85	7	108	0.3	0.02	0.3	0.4	B
010115	217 23.69	39° 18.48'	111° 13.38'	0.33*	0.56	7	110	0.2	0.03	0.3	0.4	B
010115	358 47.56	39° 18.49'	111° 13.34'	0.35*	0.60	7	110	0.2	0.03	0.3	0.4	B
010115	442 26.38	39° 18.44'	111° 13.44'	0.35*	0.53	7	109	0.2	0.03	0.3	0.3	B

Date	Origin Time	Latitude	Longitude	Depth	Mag	No	Gap	Dmin	Rms	Erh	Erz	Q
010115	1135 47.05	39° 18.35'	111° 13.30'	0.16*	0.47	7	88	0.1	0.02	0.3	0.4	B
010115	2008 34.00	39° 18.15'	111° 13.68'	0.01	1.48	8	99	0.6	0.02	0.2	0.7	B
010115	2113 9.24	39° 18.37'	111° 13.23'	0.21*	0.48	6	130	0.2	0.02	0.3	0.4	B
010115	2328 42.14	39° 18.46'	111° 13.27'	0.23*	0.39	7	107	0.2	0.03	0.3	0.5	B
010116	36 58.72	39° 18.34'	111° 13.35'	0.21*	1.39	10	77	0.1	0.04	0.2	0.3	A
010116	116 21.37	39° 19.11'	111° 12.91'	0.06	0.00	5	284	1.6	0.04	1.2	1.8	D
010116	153 3.91	39° 18.51'	111° 13.32'	0.10	0.87	9	110	0.3	0.06	0.2	0.9	B
010116	247 42.66	39° 18.38'	111° 13.19'	0.12	0.83	6	131	0.2	0.02	0.3	0.7	B
010116	249 13.88	39° 18.41'	111° 13.28'	0.22*	0.59	9	105	0.2	0.04	0.2	0.3	B
010116	303 38.91	39° 18.48'	111° 13.27'	0.25*	0.56	9	108	0.2	0.05	0.2	0.4	B
010116	320 58.11	39° 18.48'	111° 13.22'	0.09	1.32	14	94	0.3	0.05	0.1	0.3	B
010116	424 5.03	39° 18.53'	111° 13.16'	0.22	0.00	6	246	0.5	0.04	0.9	0.5	D
010116	500 12.95	39° 18.41'	111° 13.24'	0.14	0.68	7	105	0.2	0.04	0.3	0.5	B
010116	504 37.07	39° 18.45'	111° 13.27'	0.09	0.00	6	131	0.2	0.01	0.3	0.5	B
010116	613 12.23	39° 18.38'	111° 13.20'	0.12	0.00	6	131	0.2	0.03	0.3	0.7	B
010116	847 10.95	39° 18.11'	111° 13.20'	0.03	0.62	7	77	0.6	0.03	0.3	0.8	B
010116	1211 40.49	39° 18.50'	111° 13.56'	0.37*	0.56	7	114	0.3	0.02	0.3	0.7	B
010116	1631 24.35	39° 18.35'	111° 13.24'	0.14	0.94	7	93	0.2	0.02	0.3	0.5	B
010116	1649 44.45	39° 18.46'	111° 13.34'	0.36*	0.64	7	108	0.2	0.02	0.3	0.6	B
010116	1650 13.55	39° 18.49'	111° 13.28'	0.37*	1.27	6	108	0.3	0.02	0.3	0.7	B
010116	1723 17.15	39° 18.22'	111° 13.61'	0.10	0.00	7	102	0.4	0.02	0.3	0.9	B
010116	1746 31.19	39° 18.48'	111° 13.21'	0.15	0.33	6	135	0.3	0.02	0.3	0.7	B
010116	1849 58.65	39° 18.38'	111° 13.28'	0.35*	0.64	7	104	0.2	0.02	0.3	0.3	B
010116	1946 54.28	39° 18.49'	111° 13.28'	0.20	0.61	7	108	0.3	0.02	0.3	0.5	B
010116	2010 54.04	39° 18.35'	111° 13.34'	0.22*	0.00	7	89	0.1	0.03	0.3	0.3	B
010116	2122 28.40	39° 17.55'	111° 14.02'	0.43	0.58	7	99	1.8	0.04	0.3	7.3	B
010117	19 24.55	39° 18.37'	111° 13.30'	0.13*	0.56	7	104	0.1	0.03	0.3	0.5	B
010117	20 40.30	39° 18.44'	111° 13.27'	0.21*	0.82	7	106	0.2	0.03	0.3	0.4	B
010117	411 12.01	39° 18.35'	111° 13.19'	0.08	1.42	9	92	0.2	0.04	0.2	0.5	B
010117	414 5.35	39° 18.43'	111° 13.40'	0.38*	0.53	7	109	0.2	0.03	0.3	0.5	B
010117	414 23.76	39° 18.36'	111° 13.31'	0.14*	0.66	7	94	0.1	0.03	0.3	0.4	B
010117	608 12.99	39° 18.48'	111° 13.23'	0.05	0.25	7	107	0.3	0.03	0.3	0.6	B
010117	641 36.51	39° 18.37'	111° 13.27'	0.20*	0.36	7	100	0.2	0.02	0.3	0.4	B
010117	714 13.32	39° 18.35'	111° 13.25'	0.06	0.37	7	92	0.2	0.04	0.3	0.6	B
010117	827 39.40	39° 18.35'	111° 13.34'	0.23*	0.69	7	77	0.1	0.02	0.3	0.3	B
010117	835 59.11	39° 18.49'	111° 13.34'	0.36*	0.94	7	110	0.2	0.01	0.3	0.6	B
010117	904 13.30	39° 18.48'	111° 13.48'	0.27*	0.86	7	112	0.2	0.03	0.3	0.4	B
010117	918 6.49	39° 18.51'	111° 13.60'	0.28	0.52	7	116	0.4	0.02	0.3	0.5	B
010117	1310 44.09	39° 18.49'	111° 13.33'	0.32*	0.41	6	109	0.2	0.01	0.3	0.4	B
010117	1546 56.08	39° 18.26'	111° 13.97'	0.10	0.85	7	108	0.9	0.01	0.3	2.8	B
010117	2112 20.94	39° 18.24'	111° 13.42'	0.09	0.89	7	101	0.2	0.02	0.2	0.5	B
010117	2353 9.90	39° 18.50'	111° 13.25'	0.20	1.08	7	108	0.3	0.02	0.3	0.5	B
010118	12 10.41	39° 18.48'	111° 13.59'	0.30*	0.50	7	114	0.3	0.02	0.3	0.5	B
010118	424 45.24	39° 18.47'	111° 13.20'	0.02	1.49	10	93	0.3	0.06	0.3	0.6	B
010118	456 41.97	39° 18.47'	111° 13.23'	0.15	0.75	7	107	0.3	0.02	0.3	0.7	B
010118	556 31.80	39° 18.35'	111° 13.24'	0.14	0.90	7	90	0.2	0.02	0.3	0.5	B
010118	632 12.92	39° 18.50'	111° 13.22'	0.01	0.80	7	108	0.3	0.03	0.3	0.8	B
010118	645 23.34	39° 18.39'	111° 13.26'	0.10	1.03	6	128	0.2	0.03	0.3	0.5	B
010118	648 9.62	39° 18.39'	111° 13.21'	0.09	0.23	7	103	0.2	0.02	0.3	0.5	B
010118	656 30.93	39° 18.44'	111° 13.20'	0.13	0.00	6	134	0.3	0.04	0.3	0.7	B
010118	716 31.04	39° 18.43'	111° 13.28'	0.20*	0.45	7	106	0.2	0.04	0.3	0.4	B
010118	845 26.02	39° 18.47'	111° 13.22'	0.15	0.64	7	107	0.3	0.03	0.3	0.7	B
010118	1207 55.05	39° 18.48'	111° 13.44'	0.32*	0.57	7	111	0.2	0.02	0.3	0.4	B
010118	1224 32.20	39° 18.38'	111° 13.37'	0.22*	0.81	7	105	0.1	0.02	0.3	0.3	B
010118	1244 21.04	39° 18.34'	111° 13.28'	0.18	0.74	7	83	0.2	0.02	0.3	0.4	B
010118	1527 35.03	39° 18.35'	111° 13.66'	0.10	0.33	7	109	0.4	0.02	0.3	2.8	B
010118	1635 36.83	39° 17.98'	111° 13.19'	0.00	0.84	7	77	0.8	0.03	0.3	0.9	B
010118	1642 46.96	39° 18.48'	111° 13.26'	0.19	0.51	7	108	0.3	0.02	0.3	0.6	B
010118	1703 37.07	39° 18.49'	111° 13.21'	0.07	0.37	6	135	0.3	0.04	0.3	0.7	B
010118	1718 32.51	39° 18.37'	111° 13.27'	0.19	0.76	7	104	0.2	0.03	0.3	0.4	B
010118	1727 15.12	39° 18.50'	111° 13.45'	0.36*	0.78	7	113	0.2	0.02	0.3	0.6	B
010118	1806 11.24	39° 18.36'	111° 13.22'	0.13	0.28	7	95	0.2	0.03	0.3	0.6	B
010118	1833 31.65	39° 18.49'	111° 13.47'	0.36*	0.73	7	112	0.2	0.02	0.3	0.6	B
010118	2114 48.04	39° 18.39'	111° 13.31'	0.23*	0.72	7	106	0.1	0.02	0.3	0.3	B
010118	2156 26.59	39° 18.44'	111° 13.18'	0.08	1.55	12	105	0.3	0.07	0.2	0.5	B
010118	2232 21.88	39° 18.34'	111° 13.23'	0.13	0.71	7	88	0.2	0.02	0.3	0.6	B
010119	134 39.24	39° 18.44'	111° 13.23'	0.23*	0.51	7	106	0.2	0.03	0.3	0.4	B
010119	147 58.79	39° 18.50'	111° 13.18'	0.37	1.03	7	107	0.4	0.02	0.3	0.9	B

Date	Origin Time	Latitude	Longitude	Depth	Mag	No	Gap	Dmin	Rms	Erh	Erz	Q
010119	319 16.90	39° 19.12'	111° 12.26'	0.36	0.94	7	105	2.2	0.23	0.8	999.9	C
010119	322 5.86	39° 18.49'	111° 13.32'	0.36*	0.63	7	109	0.2	0.03	0.3	0.4	B
010119	901 42.94	39° 18.38'	111° 13.47'	0.15	0.50	7	108	0.2	0.02	0.3	0.5	B
010119	1157 58.29	39° 18.35'	111° 13.36'	0.21*	0.77	7	77	0.1	0.02	0.3	0.3	B
010119	1247 46.32	39° 18.37'	111° 13.62'	0.12	0.48	7	109	0.3	0.01	0.3	0.8	B
010119	1712 4.02	39° 18.50'	111° 13.16'	0.16	0.44	6	138	0.4	0.02	0.3	0.7	C
010119	1745 18.59	39° 18.48'	111° 13.17'	0.06	0.96	7	106	0.3	0.02	0.3	0.6	B
010119	1805 34.75	39° 18.36'	111° 13.19'	0.07	0.43	6	131	0.2	0.03	0.3	0.5	B
010119	1826 34.13	39° 18.47'	111° 13.31'	0.25*	0.56	7	108	0.2	0.03	0.3	0.4	B
010119	1842 51.37	39° 18.41'	111° 13.15'	0.16	0.48	6	135	0.3	0.01	0.3	0.6	B
010119	1843 37.07	39° 18.49'	111° 13.70'	0.31	0.81	7	117	0.5	0.02	0.3	0.5	B
010119	1946 32.09	39° 18.28'	111° 14.02'	0.06	0.51	7	111	0.9	0.02	0.3	2.8	B
010119	2013 14.12	39° 18.50'	111° 13.19'	0.16	0.94	7	107	0.4	0.02	0.3	0.7	B
010119	2041 24.33	39° 18.39'	111° 13.15'	0.06	0.00	6	133	0.3	0.03	0.4	0.6	B
010119	2112 31.35	39° 18.42'	111° 13.16'	0.02	0.49	6	134	0.3	0.02	0.3	0.8	B
010119	2117 30.92	39° 18.36'	111° 13.19'	0.18	0.49	6	130	0.2	0.02	0.3	0.5	B
010119	2156 44.61	39° 18.42'	111° 13.20'	0.13	0.60	6	133	0.3	0.02	0.3	0.8	B
010119	2239 6.58	39° 18.63'	111° 13.15'	0.03	0.70	7	111	0.6	0.05	0.3	0.7	B
010119	2308 8.39	39° 18.47'	111° 13.27'	0.21*	0.50	7	108	0.2	0.03	0.3	0.5	B
010119	2314 44.59	39° 18.48'	111° 13.19'	0.00	1.18	10	106	0.3	0.06	0.3	0.8	B
010119	2320 24.06	39° 18.48'	111° 13.21'	0.19	0.62	7	107	0.3	0.02	0.2	0.6	B
010120	52 31.23	39° 18.37'	111° 13.15'	0.00	0.08	6	132	0.3	0.02	0.3	0.8	B
010120	611 18.75	39° 18.39'	111° 13.43'	0.30*	0.74	7	107	0.1	0.02	0.3	0.3	B
010120	1514 8.48	39° 18.26'	111° 14.20'	0.16	0.37	7	113	1.2	0.02	0.3	0.9	B
010121	134 20.74	39° 18.37'	111° 13.47'	0.30*	0.57	7	107	0.2	0.03	0.3	0.3	B
010121	401 11.36	39° 18.38'	111° 14.21'	0.10	0.59	7	121	1.2	0.01	0.3	0.8	B
010121	433 36.25	39° 17.71'	111° 11.97'	0.03	0.44	7	85	0.8	0.10	0.4	5.2	B
010121	1025 26.90	39° 18.46'	111° 13.33'	0.30*	0.00	7	108	0.2	0.02	0.3	0.4	B
010121	1622 0.95	39° 18.49'	111° 13.43'	0.34*	0.60	7	111	0.2	0.03	0.3	0.4	B
010121	2127 30.28	39° 17.78'	111° 13.32'	0.03	1.06	7	82	1.1	0.09	0.3	4.1	B
010122	318 4.70	39° 18.22'	111° 13.24'	0.10	0.76	7	78	0.3	0.01	0.3	0.9	B
010122	409 54.70	39° 18.16'	111° 14.10'	0.23	1.05	7	103	1.1	0.02	0.3	0.8	B
010122	1954 40.99	39° 18.46'	111° 13.19'	0.32*	0.87	7	106	0.3	0.03	0.3	0.5	B
010122	2126 51.77	39° 18.37'	111° 13.18'	0.15	0.84	7	98	0.3	0.02	0.3	0.6	B
010122	2129 17.28	39° 18.42'	111° 13.25'	0.23*	0.30	7	105	0.2	0.04	0.3	0.4	B
010122	2250 38.79	39° 18.40'	111° 13.44'	0.20*	0.26	6	121	0.1	0.03	0.3	0.4	B
010122	2300 35.00	39° 18.57'	111° 13.18'	0.08	1.25	11	109	0.5	0.07	0.3	1.6	B
010122	2305 45.56	39° 18.46'	111° 13.22'	0.39*	1.02	7	107	0.3	0.03	0.3	0.7	B
010123	19 5.46	39° 18.39'	111° 13.11'	0.21	1.01	8	102	0.4	0.02	0.2	0.5	B
010123	218 11.51	39° 18.33'	111° 13.22'	0.08	0.63	7	82	0.2	0.02	0.3	0.6	B
010123	218 38.59	39° 18.37'	111° 13.13'	0.05	0.00	5	135	0.3	0.02	0.3	0.7	C
010123	236 46.84	39° 18.36'	111° 13.19'	0.16	0.79	7	97	0.2	0.02	0.3	0.5	B
010123	413 40.20	39° 18.37'	111° 13.18'	0.08	0.19	6	131	0.3	0.02	0.3	0.6	B
010123	525 34.18	39° 18.43'	111° 13.15'	0.25	0.59	7	105	0.3	0.02	0.3	0.5	B
010123	709 26.15	39° 18.43'	111° 13.18'	0.01	1.09	10	104	0.3	0.07	0.3	0.8	B
010123	1800 12.74	39° 18.34'	111° 13.18'	0.12	0.80	7	88	0.3	0.01	0.3	0.7	B
010123	1833 9.63	39° 18.48'	111° 13.18'	0.13	0.58	7	106	0.3	0.02	0.2	0.7	B
010123	1852 9.37	39° 17.70'	111° 13.22'	0.30	1.01	7	84	1.1	0.03	0.2	0.7	B
010123	1930 0.88	39° 18.20'	111° 13.26'	0.01	0.66	7	77	0.3	0.02	0.3	0.8	B
010123	2041 13.41	39° 18.47'	111° 13.27'	0.33*	0.66	7	107	0.2	0.02	0.3	0.4	B
010123	2059 15.31	39° 18.52'	111° 13.22'	0.21	0.68	7	109	0.3	0.03	0.3	0.6	B
010123	2104 57.78	39° 18.45'	111° 13.19'	0.17	0.50	7	105	0.3	0.02	0.3	0.6	B
010123	2123 49.48	39° 18.47'	111° 13.28'	0.38*	0.57	7	107	0.2	0.03	0.3	0.6	B
010123	2302 35.67	39° 18.34'	111° 13.24'	0.12	0.38	7	89	0.2	0.03	0.3	0.6	B
010123	2318 44.18	39° 18.57'	111° 13.10'	0.17	1.36	10	108	0.6	0.05	0.3	0.7	B
010124	55 9.04	39° 18.37'	111° 13.24'	0.14	0.45	7	100	0.2	0.03	0.3	0.6	B
010124	124 44.86	39° 18.40'	111° 13.12'	0.09	1.26	11	102	0.4	0.08	0.3	1.4	B
010124	231 33.17	39° 18.48'	111° 13.27'	0.37*	0.25	7	108	0.2	0.04	0.3	0.6	B
010124	309 29.49	39° 18.48'	111° 13.16'	0.08	0.47	7	106	0.4	0.03	0.3	0.6	B
010124	427 9.29	39° 18.46'	111° 13.43'	0.35*	0.78	7	110	0.2	0.03	0.3	0.4	B
010124	553 10.25	39° 19.86'	111° 12.72'	0.56	0.00	6	158	3.0	0.08	0.6	9.6	C
010124	625 0.61	39° 18.36'	111° 13.22'	0.21*	0.72	7	96	0.2	0.01	0.3	0.5	B
010124	854 35.62	39° 18.47'	111° 13.30'	0.31*	0.89	7	109	0.2	0.03	0.3	0.4	B
010124	1225 10.39	39° 18.12'	111° 13.53'	0.11	0.98	7	96	0.5	0.01	0.2	0.9	B
010124	1550 43.90	39° 18.46'	111° 13.19'	0.18	0.51	7	106	0.3	0.03	0.3	0.6	B
010124	1644 4.60	39° 18.45'	111° 13.11'	0.07	0.45	6	139	0.5	0.03	0.3	0.7	C
010124	1719 22.75	39° 18.36'	111° 13.17'	0.08	0.41	7	97	0.3	0.03	0.3	0.6	B
010124	1731 50.29	39° 18.39'	111° 13.11'	0.10	0.82	6	136	0.4	0.04	0.3	1.0	C

Date	Origin Time	Latitude	Longitude	Depth	Mag	No	Gap	Dmin	Rms	Erh	Erz	Q
010124	1818 2.83	39° 18.40'	111° 13.15'	0.08	0.25	6	134	0.3	0.02	0.3	0.6	B
010124	1843 10.96	39° 18.49'	111° 13.13'	0.09	0.28	6	139	0.5	0.02	0.3	3.5	C
010124	1845 41.27	39° 18.35'	111° 13.16'	0.20	0.79	7	91	0.3	0.02	0.3	0.5	B
010124	1919 10.65	39° 18.43'	111° 12.98'	0.10	1.19	11	101	0.6	0.09	0.3	1.8	B
010124	1944 57.52	39° 18.36'	111° 13.13'	0.05	0.34	6	134	0.3	0.01	0.3	0.7	B
010124	2211 59.81	39° 18.45'	111° 13.21'	0.33*	0.61	7	105	0.3	0.04	0.3	0.5	B
010124	2217 11.54	39° 18.48'	111° 13.23'	0.39*	0.59	7	107	0.3	0.02	0.3	0.7	B
010124	2234 4.89	39° 18.47'	111° 13.14'	0.14	0.19	6	137	0.4	0.03	0.3	0.8	C
010124	2303 57.33	39° 18.27'	111° 13.44'	0.01	0.20	5	102	0.2	0.15	0.5	1.6	D
010125	38 14.79	39° 18.37'	111° 13.18'	0.04	0.60	6	131	0.3	0.03	0.4	0.7	B
010125	43 5.84	39° 18.34'	111° 13.16'	0.07	0.68	7	91	0.3	0.02	0.3	0.6	B
010125	102 24.47	39° 18.45'	111° 13.45'	0.11	0.15	7	111	0.2	0.04	0.3	0.7	B
010125	211 12.46	39° 18.59'	111° 13.23'	0.20	1.01	10	111	0.5	0.09	0.3	0.7	B
010125	312 48.84	39° 18.36'	111° 13.20'	0.19	0.66	7	98	0.2	0.01	0.3	0.5	B
010125	315 29.75	39° 18.49'	111° 13.21'	0.22	0.14	6	136	0.3	0.02	0.3	0.5	C
010125	410 41.70	39° 18.37'	111° 13.20'	0.24*	0.98	7	98	0.2	0.01	0.3	0.4	B
010125	438 38.33	39° 18.34'	111° 13.16'	0.09	0.86	8	90	0.3	0.03	0.2	0.5	A
010125	515 57.23	39° 18.35'	111° 13.18'	0.01	0.66	7	94	0.3	0.02	0.3	0.8	B
010125	553 59.96	39° 18.46'	111° 13.07'	0.01	1.25	10	104	0.5	0.07	0.3	0.7	B
010125	843 34.74	39° 18.46'	111° 13.16'	0.17	0.62	7	106	0.3	0.03	0.3	0.6	B
010125	1110 44.33	39° 18.33'	111° 13.13'	1.30*	0.39	7	85	0.3	0.07	0.3	0.7	B
010125	1651 20.08	39° 17.84'	111° 11.83'	0.09	0.61	7	88	0.9	0.03	0.3	3.9	B
010125	1752 20.84	39° 18.33'	111° 13.15'	0.05	1.02	7	86	0.3	0.01	0.3	0.7	B
010125	1839 24.39	39° 18.37'	111° 13.18'	0.16	1.03	7	99	0.3	0.02	0.3	0.6	B
010125	2025 51.00	39° 18.45'	111° 13.23'	0.03	0.54	6	132	0.2	0.20	0.6	1.5	C
010125	2108 8.68	39° 18.38'	111° 13.41'	0.11*	0.40	7	107	0.1	0.04	0.3	0.4	B
010125	2207 0.48	39° 18.45'	111° 13.21'	0.26	0.57	7	105	0.3	0.02	0.2	0.4	B
010125	2351 13.47	39° 18.53'	111° 13.15'	0.04	0.37	8	138	0.5	0.03	0.2	0.5	B
010126	19 30.55	39° 18.40'	111° 13.16'	0.08	0.53	6	134	0.3	0.03	0.3	0.6	B
010126	36 46.92	39° 18.41'	111° 13.16'	0.08	0.43	7	103	0.3	0.03	0.3	0.6	B
010126	108 38.98	39° 18.48'	111° 13.44'	0.39*	0.63	7	111	0.2	0.03	0.3	0.6	B
010126	223 32.27	39° 18.36'	111° 13.30'	0.17*	0.49	7	97	0.1	0.03	0.3	0.4	B
010126	522 24.25	39° 18.48'	111° 13.18'	0.32*	0.53	7	106	0.3	0.03	0.3	0.4	B
010126	600 51.54	39° 18.37'	111° 13.13'	0.03	0.40	7	98	0.3	0.03	0.3	0.7	B
010126	625 48.12	39° 18.36'	111° 13.11'	0.07	0.80	7	94	0.4	0.01	0.3	0.6	B
010126	626 43.35	39° 18.34'	111° 13.17'	0.13	0.81	7	88	0.3	0.02	0.3	0.7	B
010126	905 19.14	39° 18.47'	111° 13.15'	0.08	0.29	7	106	0.4	0.03	0.3	0.6	B
010126	923 10.14	39° 18.36'	111° 13.16'	0.19	0.78	7	95	0.3	0.01	0.3	0.5	B
010126	1306 7.56	39° 18.33'	111° 13.33'	0.12*	0.55	7	77	0.1	0.04	0.3	0.5	B
010126	1823 24.13	39° 18.39'	111° 13.12'	0.07	0.46	6	136	0.3	0.02	0.3	0.6	C
010126	2329 22.67	39° 18.38'	111° 13.31'	0.22*	0.87	7	105	0.1	0.02	0.3	0.3	B
010127	257 56.28	39° 18.45'	111° 13.91'	0.00	1.04	11	119	0.8	0.11	0.4	1.8	C
010127	419 1.15	39° 17.76'	111° 11.83'	0.27	0.39	6	87	2.5	0.02	546.9	728.2	C
010127	544 11.86	39° 18.43'	111° 13.89'	0.10	0.65	7	118	0.8	0.03	0.3	0.9	B
010127	1513 16.64	39° 18.46'	111° 13.14'	0.16	0.52	7	104	0.4	0.02	0.3	0.7	B
010127	2204 55.26	39° 18.01'	111° 12.97'	0.01	0.49	7	79	0.8	0.07	0.3	3.7	B
010128	242 2.76	39° 18.12'	111° 13.39'	0.11	0.84	7	90	0.5	0.02	0.2	0.9	B
010128	250 54.81	39° 17.79'	111° 14.10'	0.14	0.80	8	93	1.5	0.03	0.2	0.8	B
010128	431 48.64	39° 18.36'	111° 13.22'	0.09	0.53	7	95	0.2	0.02	0.3	0.5	B
010128	613 5.19	39° 18.35'	111° 13.36'	0.18*	0.56	7	77	0.1	0.03	0.3	0.3	B
010128	1002 46.43	39° 18.37'	111° 13.12'	0.06	0.71	7	97	0.4	0.01	0.3	0.7	B
010128	1747 25.85	39° 18.49'	111° 13.58'	0.27	0.54	7	114	0.3	0.03	0.3	0.5	B
010129	853 34.12	39° 18.41'	111° 13.86'	0.02	0.81	7	117	0.7	0.05	0.3	0.7	B
010129	1314 0.81	39° 18.36'	111° 13.34'	0.16*	0.52	7	98	0.1	0.03	0.3	0.3	B
010129	1713 21.37	39° 18.36'	111° 13.16'	0.15	0.84	7	96	0.3	0.02	0.3	0.6	B
010129	1808 53.91	39° 18.39'	111° 13.14'	0.15	0.49	7	102	0.3	0.03	0.3	0.6	B
010129	1824 35.08	39° 18.42'	111° 13.88'	0.21	1.02	7	117	0.7	0.02	0.3	0.7	B
010129	1847 40.45	39° 18.46'	111° 13.16'	0.35*	0.63	7	105	0.3	0.03	0.3	0.4	B
010129	1929 33.20	39° 18.37'	111° 13.09'	0.07	1.08	7	97	0.4	0.02	0.3	0.6	B
010129	2053 23.76	39° 18.48'	111° 13.14'	0.11	1.48	10	106	0.4	0.04	0.2	0.7	B
010129	2158 20.07	39° 18.34'	111° 13.15'	0.10	0.82	6	123	0.3	0.02	0.3	3.6	B
010129	2158 30.46	39° 18.43'	111° 13.17'	0.39*	0.85	6	104	0.3	0.03	0.3	0.7	B
010129	2213 32.68	39° 18.35'	111° 13.15'	0.08	0.27	5	133	0.3	0.03	0.3	0.7	C
010129	2352 59.80	39° 18.37'	111° 13.09'	0.16	0.65	6	121	0.4	0.03	0.3	0.7	B
010130	246 54.26	39° 18.40'	111° 13.19'	0.16	1.13	7	103	0.3	0.04	0.3	0.6	B
010130	526 14.18	39° 18.37'	111° 13.15'	0.20	0.89	7	100	0.3	0.01	0.3	0.6	B
010130	643 55.92	39° 18.49'	111° 13.12'	0.07	0.19	6	139	0.5	0.05	0.3	0.7	C
010130	644 15.64	39° 18.36'	111° 13.12'	0.07	0.80	7	95	0.3	0.02	0.3	0.6	B

Date	Origin Time	Latitude	Longitude	Depth	Mag	No	Gap	Dmin	Rms	Erh	Erz	Q
010130	648 33.36	39° 18.47'	111° 13.93'	0.32	0.50	7	122	0.8	0.04	0.3	0.7	B
010130	752 35.25	39° 17.87'	111° 12.73'	0.03	0.90	7	80	0.3	0.01	0.3	0.7	B
010130	1035 4.35	39° 18.32'	111° 13.42'	0.31*	0.87	5	128	0.1	0.03	0.8	0.4	D
010130	1655 35.42	39° 18.35'	111° 13.12'	0.03	0.77	7	93	0.4	0.02	0.3	0.8	B
010130	1735 8.21	39° 18.36'	111° 13.14'	0.07	0.62	7	94	0.3	0.03	0.3	0.6	B
010130	1736 28.77	39° 18.35'	111° 13.10'	0.10	0.82	7	93	0.4	0.02	0.3	0.9	B
010130	1933 39.19	39° 18.47'	111° 13.21'	0.18	0.65	7	107	0.3	0.03	0.3	0.6	B
010130	2103 19.56	39° 18.37'	111° 13.06'	0.11	0.44	7	97	0.5	0.03	0.3	0.9	B
010131	36 15.70	39° 18.47'	111° 13.14'	0.32	0.75	7	105	0.4	0.02	0.3	0.5	B
010131	44 48.06	39° 18.38'	111° 13.08'	0.10	1.08	7	100	0.5	0.02	0.3	3.0	B
010131	100 5.53	39° 18.46'	111° 13.25'	0.41*	0.87	7	107	0.2	0.02	0.3	0.6	B
010131	417 56.34	39° 18.32'	111° 13.14'	0.18	0.60	7	83	0.3	0.03	0.3	0.6	B
010131	420 57.06	39° 18.37'	111° 13.08'	0.06	1.30	7	98	0.5	0.01	0.3	0.6	B
010131	619 45.95	39° 18.35'	111° 13.13'	0.10	0.96	7	92	0.3	0.01	0.3	0.9	B
010131	639 59.75	39° 18.39'	111° 13.05'	0.07	0.89	7	101	0.5	0.01	0.3	3.1	B
010131	641 56.04	39° 18.43'	111° 13.10'	0.11	0.19	6	138	0.4	0.03	0.3	0.9	C
010131	642 7.50	39° 18.35'	111° 13.09'	0.13	0.84	7	92	0.4	0.01	0.3	0.8	B
010131	702 54.96	39° 18.45'	111° 13.09'	0.01	1.18	8	104	0.5	0.06	0.3	0.8	B
010131	1021 36.64	39° 18.35'	111° 13.40'	0.24*	0.28	7	105	0.1	0.02	0.3	0.3	B
010131	1138 34.58	39° 18.35'	111° 13.41'	0.17*	0.35	7	105	0.1	0.03	0.3	0.3	B
010131	1517 59.66	39° 18.39'	111° 13.10'	0.14	0.43	6	137	0.4	0.02	0.3	0.8	C
010131	1549 22.93	39° 18.35'	111° 13.05'	0.04	0.76	7	92	0.5	0.02	0.3	0.7	B
010131	1557 27.43	39° 18.36'	111° 13.08'	0.06	0.47	6	136	0.5	0.02	0.3	0.7	C
010131	1601 54.85	39° 18.36'	111° 13.08'	0.06	0.62	7	96	0.5	0.02	0.3	0.6	B
010131	1746 8.12	39° 18.35'	111° 13.19'	0.11	0.34	7	90	0.2	0.02	0.3	0.7	B
010131	1801 58.98	39° 18.38'	111° 13.12'	0.08	0.57	7	102	0.3	0.02	0.3	0.5	B
010131	1810 3.22	39° 18.39'	111° 13.14'	0.25	0.99	7	102	0.3	0.01	0.3	0.5	B
010131	1828 13.29	39° 18.35'	111° 13.14'	0.06	0.73	7	91	0.3	0.02	0.3	0.6	B
010131	1943 33.16	39° 18.34'	111° 13.13'	0.07	0.47	7	89	0.3	0.04	0.3	0.6	B
010131	2324 28.58	39° 18.35'	111° 13.12'	0.20	1.01	7	93	0.3	0.03	0.3	0.5	B
010131	2357 58.12	39° 18.36'	111° 13.09'	0.16	0.81	7	94	0.4	0.02	0.3	0.7	B
010201	9 3.89	39° 18.46'	111° 13.12'	0.16	0.50	7	104	0.4	0.01	0.2	0.7	B
010201	14 10.45	39° 18.03'	111° 12.13'	0.09	1.08	10	73	0.7	0.05	0.2	1.2	A
010201	39 2.87	39° 18.48'	111° 13.15'	0.03	0.60	7	106	0.4	0.02	0.3	0.7	B
010201	443 56.09	39° 18.46'	111° 13.11'	0.08	0.62	7	104	0.5	0.18	0.5	6.6	C
010201	504 20.65	39° 18.39'	111° 13.07'	0.03	0.71	6	138	0.5	0.02	0.3	0.7	C
010201	521 10.95	39° 18.35'	111° 13.09'	0.18	1.06	7	93	0.4	0.02	0.3	0.6	B
010201	522 15.59	39° 18.34'	111° 13.12'	0.05	0.48	6	133	0.4	0.02	0.3	0.7	B
010201	630 55.08	39° 18.50'	111° 13.07'	0.13	0.78	7	105	0.5	0.02	0.2	0.9	B
010201	807 5.88	39° 18.25'	111° 13.33'	0.19	0.79	7	76	0.2	0.03	0.3	0.5	B
010201	955 50.52	39° 18.49'	111° 13.26'	0.21	0.34	7	108	0.3	0.02	0.3	0.5	B
010201	1012 33.54	39° 18.46'	111° 13.07'	0.01	0.19	6	139	0.5	0.02	0.3	0.8	C
010201	1037 45.64	39° 18.34'	111° 13.08'	0.06	0.78	7	90	0.5	0.02	0.3	0.7	B
010201	1551 32.75	39° 18.40'	111° 13.03'	0.00	0.37	6	140	0.5	0.02	0.3	0.8	C
010201	1649 17.55	39° 18.27'	111° 13.14'	0.03	0.23	6	129	0.4	0.03	0.6	1.1	C
010201	1649 30.62	39° 18.43'	111° 13.13'	0.36	0.73	7	103	0.4	0.03	0.3	0.5	B
010201	1649 58.83	39° 18.46'	111° 13.05'	0.01	0.00	6	141	0.5	0.03	0.4	0.7	C
010201	1654 19.89	39° 18.46'	111° 13.14'	0.16	0.70	7	104	0.4	0.03	0.3	0.7	B
010201	1701 21.87	39° 18.34'	111° 13.07'	0.06	0.29	7	89	0.5	0.04	0.3	0.6	B
010201	1701 44.02	39° 18.35'	111° 13.05'	0.03	0.00	6	138	0.5	0.03	0.3	0.7	C
010201	1708 11.66	39° 18.43'	111° 13.34'	0.35*	0.32	6	126	0.2	0.02	0.3	0.3	B
010201	1708 58.18	39° 18.31'	111° 13.39'	0.07	0.57	7	101	0.1	0.04	0.3	0.4	B
010201	1725 56.42	39° 18.42'	111° 13.03'	0.07	0.56	6	140	0.5	0.02	0.3	3.3	C
010201	1730 26.79	39° 18.37'	111° 13.09'	0.07	0.49	7	97	0.4	0.04	0.3	0.7	B
010201	1731 28.25	39° 18.33'	111° 13.12'	0.14	0.85	7	87	0.4	0.03	0.3	0.7	B
010201	1910 21.51	39° 18.33'	111° 13.09'	0.11	0.93	7	88	0.4	0.02	0.3	0.9	B
010201	1910 40.45	39° 18.40'	111° 13.06'	0.05	0.49	6	140	0.5	0.08	0.4	0.8	C
010201	1921 20.15	39° 18.39'	111° 13.08'	0.12	0.79	7	102	0.5	0.02	0.3	0.8	B
010201	2008 17.96	39° 18.46'	111° 13.07'	0.09	0.68	6	139	0.5	0.03	0.3	3.5	C
010201	2008 28.82	39° 18.53'	111° 13.77'	0.26	1.33	7	121	0.7	0.03	0.3	0.7	B
010201	2032 29.91	39° 18.36'	111° 13.08'	0.07	0.78	7	95	0.4	0.02	0.3	0.6	B
010201	2032 54.54	39° 18.25'	111° 14.01'	0.01	0.00	7	109	0.9	0.07	0.3	3.3	B
010201	2143 50.01	39° 19.67'	111° 13.26'	2.07	1.24	7	146	2.5	0.15	0.7	1.6	D
010201	2244 0.18	39° 18.36'	111° 13.10'	0.05	0.37	6	136	0.4	0.02	0.3	0.7	C
010201	2251 17.23	39° 18.47'	111° 13.05'	0.11	1.00	6	141	0.5	0.02	0.3	1.0	C
010201	2257 4.04	39° 18.38'	111° 13.07'	0.08	0.72	7	100	0.5	0.02	0.3	3.0	B
010202	124 40.35	39° 18.41'	111° 12.96'	0.13	1.11	10	100	0.6	0.10	0.3	0.8	B
010202	318 4.49	39° 18.49'	111° 13.42'	0.34*	0.97	7	111	0.2	0.01	0.3	0.4	B

Date	Origin Time		Latitude		Longitude		Depth	Mag	No	Gap	Dmin	Rms	Erh	Erz	Q
010202	441	41.36	39°	18.46'	111°	13.13'	0.20	0.37	6	139	0.4	0.03	0.3	0.6	C
010202	602	58.43	39°	18.65'	111°	13.01'	0.04	0.18	6	143	0.8	0.08	0.4	4.3	C
010202	603	12.67	39°	18.37'	111°	13.12'	0.08	0.66	7	97	0.3	0.02	0.3	0.6	B
010202	614	16.86	39°	18.38'	111°	13.05'	0.02	1.27	8	99	0.5	0.10	0.3	1.0	B
010202	623	40.47	39°	18.36'	111°	13.25'	0.13	0.97	7	99	0.2	0.02	0.3	0.6	B
010202	629	7.26	39°	18.41'	111°	12.97'	0.03	0.08	6	142	0.6	0.04	0.3	0.7	C
010202	629	23.33	39°	18.23'	111°	13.23'	0.07	0.82	7	78	0.3	0.03	0.3	0.6	B
010202	635	23.84	39°	18.43'	111°	13.03'	0.18	0.45	7	102	0.5	0.03	0.2	0.6	B
010202	713	37.11	39°	18.42'	111°	13.05'	0.05	0.42	7	102	0.5	0.04	0.3	0.7	B
010202	744	25.65	39°	18.45'	111°	13.08'	0.18	0.44	7	104	0.5	0.02	0.3	0.7	B
010202	1033	8.92	39°	18.63'	111°	13.85'	0.01	1.40	13	128	0.9	0.09	0.3	1.0	B
010202	1122	38.74	39°	18.47'	111°	13.25'	0.24	0.28	7	107	0.3	0.02	0.3	0.5	B
010202	1143	12.98	39°	18.47'	111°	13.15'	0.34	0.53	7	106	0.4	0.03	0.3	0.5	B
010202	1230	30.74	39°	18.37'	111°	13.62'	0.12	0.51	7	109	0.3	0.01	0.3	0.8	B
010202	1527	40.38	39°	18.38'	111°	13.09'	0.16	0.85	7	101	0.4	0.01	0.3	0.7	B
010202	1557	18.85	39°	18.38'	111°	13.03'	0.09	0.45	7	97	0.5	0.03	0.3	3.2	B
010202	1645	49.95	39°	18.37'	111°	13.15'	0.00	0.58	7	101	0.3	0.02	0.3	0.8	B
010202	1651	21.71	39°	18.37'	111°	13.15'	0.07	0.47	7	100	0.3	0.02	0.3	0.5	B
010202	1743	12.28	39°	18.43'	111°	13.03'	0.05	0.14	6	141	0.5	0.03	0.3	0.6	C
010202	1822	39.40	39°	18.42'	111°	13.03'	0.10	1.02	9	102	0.5	0.06	0.3	2.3	B
010202	1908	5.55	39°	18.35'	111°	13.13'	0.15	0.65	7	93	0.3	0.02	0.3	0.7	B
010202	1915	51.62	39°	18.44'	111°	13.10'	0.27	0.53	7	104	0.4	0.02	0.3	0.5	B
010202	1932	17.59	39°	18.39'	111°	13.02'	0.04	0.00	6	140	0.5	0.02	0.3	0.7	C
010202	1932	41.79	39°	19.91'	111°	11.96'	0.56	1.00	7	119	3.5	0.13	0.5	15.9	C
010202	1947	38.50	39°	18.36'	111°	13.08'	0.12	0.40	6	136	0.4	0.02	0.3	0.9	C
010202	2130	12.69	39°	18.33'	111°	13.04'	0.06	0.00	7	87	0.5	0.02	0.3	0.6	B
010202	2333	23.52	39°	18.33'	111°	13.09'	0.07	0.58	7	88	0.4	0.03	0.3	0.6	B
010203	240	37.76	39°	18.26'	111°	14.07'	0.02	0.41	7	110	1.0	0.02	0.3	2.8	B
010203	1051	33.46	39°	18.38'	111°	13.30'	0.24*	0.85	7	104	0.1	0.02	0.3	0.3	B
010203	1220	5.22	39°	17.66'	111°	14.02'	0.32	0.67	7	95	1.6	0.04	554.2	999.9	C
010204	1646	45.02	39°	18.50'	111°	13.12'	0.13	0.53	7	106	0.5	0.02	0.2	0.8	B
010205	1149	20.12	39°	18.45'	111°	13.11'	0.10	0.54	7	104	0.4	0.03	0.3	1.0	B
010205	1613	44.31	39°	18.35'	111°	13.08'	0.09	0.56	7	93	0.5	0.02	0.3	3.0	B
010206	21	50.32	39°	18.34'	111°	13.09'	0.16	0.91	6	135	0.4	0.02	0.3	0.7	B
010206	113	57.39	39°	18.35'	111°	13.07'	0.07	0.68	7	91	0.5	0.02	0.3	0.6	B
010206	127	42.50	39°	18.40'	111°	13.06'	0.06	0.78	7	101	0.5	0.01	0.3	0.6	B
010206	418	49.96	39°	18.36'	111°	13.04'	0.08	0.77	7	95	0.5	0.03	0.3	3.3	B
010206	449	8.67	39°	18.34'	111°	13.05'	0.05	0.79	7	89	0.5	0.02	0.3	0.7	B
010206	450	35.72	39°	18.36'	111°	13.06'	0.01	0.08	6	138	0.5	0.03	0.3	0.8	C
010206	456	13.13	39°	18.48'	111°	13.06'	0.19	1.01	7	105	0.5	0.01	0.3	0.7	B
010206	801	7.80	39°	18.39'	111°	13.04'	0.10	0.60	7	100	0.5	0.02	0.3	0.9	B
010206	1544	3.64	39°	18.36'	111°	12.97'	0.10	1.17	9	93	0.6	0.09	0.3	1.6	B
010206	1714	38.97	39°	18.37'	111°	13.02'	0.07	1.09	7	96	0.5	0.02	0.3	3.1	B
010206	2022	38.45	39°	18.34'	111°	13.09'	0.05	0.71	7	90	0.4	0.03	0.3	0.6	B
010206	2106	3.98	39°	18.38'	111°	13.06'	0.07	1.17	7	98	0.5	0.02	0.3	3.2	B
010206	2126	0.57	39°	18.48'	111°	13.15'	0.19	0.52	7	106	0.4	0.02	0.3	0.6	B
010206	2134	28.72	39°	18.34'	111°	13.05'	0.05	0.82	7	89	0.5	0.03	0.3	0.7	B
010207	133	43.02	39°	18.39'	111°	13.02'	0.01	1.04	8	100	0.5	0.04	0.3	0.7	B
010207	135	24.23	39°	18.37'	111°	13.02'	0.05	0.67	7	96	0.5	0.03	0.3	0.7	B
010207	416	56.44	39°	18.40'	111°	13.01'	0.12	1.11	8	101	0.6	0.06	0.3	0.8	B
010207	517	52.52	39°	18.47'	111°	13.00'	0.05	1.18	8	103	0.6	0.12	0.4	2.7	C
010207	605	55.21	39°	18.38'	111°	13.29'	0.22*	1.00	7	104	0.2	0.01	0.3	0.4	B
010207	654	32.47	39°	18.45'	111°	13.01'	0.05	1.11	9	103	0.6	0.06	0.3	0.6	B
010207	716	47.58	39°	18.35'	111°	13.42'	0.18*	0.52	7	105	0.1	0.02	0.3	0.3	B
010207	758	8.50	39°	18.22'	111°	13.33'	0.15	0.77	7	77	0.2	0.02	0.3	0.6	B
010207	822	2.57	39°	18.37'	111°	13.04'	0.08	0.52	7	95	0.5	0.03	0.3	3.1	B
010207	928	31.92	39°	18.35'	111°	13.31'	0.14*	0.21	7	84	0.1	0.03	0.3	0.4	B
010207	1012	51.53	39°	18.33'	111°	13.06'	0.14	0.66	7	87	0.5	0.02	0.3	0.7	B
010207	1043	18.50	39°	18.33'	111°	13.20'	0.20*	0.73	7	83	0.2	0.02	0.3	0.5	B
010207	1149	26.99	39°	18.36'	111°	13.15'	0.08	0.80	7	96	0.3	0.01	0.3	0.6	B
010207	1400	2.86	39°	18.38'	111°	13.22'	0.15	0.49	7	103	0.2	0.03	0.3	0.5	B
010207	1408	9.88	39°	18.38'	111°	13.33'	0.19*	0.56	7	105	0.1	0.04	0.3	0.4	B
010207	1537	48.05	39°	18.34'	111°	13.03'	0.01	0.77	7	89	0.5	0.02	0.3	0.8	B
010207	1709	33.10	39°	18.39'	111°	13.02'	0.06	0.49	6	140	0.5	0.02	0.3	0.7	C
010207	1715	21.10	39°	18.34'	111°	13.04'	0.08	0.67	7	89	0.5	0.02	0.3	3.1	B
010207	1731	13.26	39°	18.35'	111°	13.11'	0.09	0.82	7	92	0.4	0.02	0.3	3.1	B
010207	1849	12.36	39°	18.47'	111°	13.15'	0.19	0.45	6	137	0.4	0.02	0.3	0.6	C
010207	2235	32.92	39°	18.25'	111°	12.99'	0.01	0.69	7	81	0.6	0.02	0.3	0.8	B

Date	Origin Time		Latitude		Longitude		Depth	Mag	No	Gap	Dmin	Rms	Erh	Erz	Q
010208	37	53.89	39°	17.57'	111°	13.93'	0.35	0.84	7	95	1.6	0.04	999.9	999.9	C
010208	304	34.11	39°	18.33'	111°	12.99'	0.06	0.81	7	87	0.6	0.02	0.3	3.1	B
010208	307	56.97	39°	18.36'	111°	13.03'	0.04	0.73	7	94	0.5	0.02	0.3	0.7	B
010208	334	50.62	39°	18.37'	111°	13.00'	0.05	0.85	7	96	0.6	0.01	0.3	0.7	B
010208	445	31.43	39°	18.36'	111°	13.04'	0.03	0.49	6	139	0.5	0.03	0.3	0.7	C
010208	449	24.92	39°	18.36'	111°	13.02'	0.02	0.75	7	94	0.5	0.03	0.3	0.7	B
010208	649	43.64	39°	18.34'	111°	13.05'	0.05	0.75	7	90	0.5	0.06	0.3	0.8	B
010208	820	9.80	39°	18.52'	111°	13.34'	0.31*	0.60	7	111	0.3	0.03	0.3	0.4	B
010208	1011	14.38	39°	18.37'	111°	13.16'	0.09	0.72	7	98	0.3	0.02	0.3	0.6	B
010208	1328	36.64	39°	18.37'	111°	13.06'	0.07	0.84	7	97	0.5	0.01	0.3	0.6	B
010208	1716	2.22	39°	18.36'	111°	13.01'	0.03	0.42	7	94	0.6	0.03	0.3	0.7	B
010208	2035	47.19	39°	18.42'	111°	12.97'	0.03	0.58	6	142	0.6	0.04	0.3	0.8	C
010208	2220	42.46	39°	18.47'	111°	13.09'	0.20	0.86	7	104	0.5	0.02	0.3	0.6	B
010208	2242	2.07	39°	18.36'	111°	13.05'	0.05	1.03	7	94	0.5	0.06	0.3	0.8	B
010208	2322	4.35	39°	18.37'	111°	12.99'	0.04	0.32	6	141	0.6	0.02	0.3	0.7	C
010208	2333	12.20	39°	18.45'	111°	12.98'	0.05	1.33	8	101	0.6	0.10	0.3	3.8	B
010209	148	11.22	39°	18.47'	111°	13.15'	0.34	0.71	7	106	0.4	0.03	0.3	0.5	B
010209	450	15.22	39°	18.38'	111°	13.00'	0.00	0.25	6	140	0.6	0.03	0.3	0.8	C
010209	606	4.79	39°	18.44'	111°	13.20'	0.34*	0.54	7	105	0.3	0.03	0.3	0.4	B
010209	656	10.16	39°	18.47'	111°	13.51'	0.35*	0.74	7	112	0.3	0.02	0.3	0.4	B
010209	757	34.87	39°	18.37'	111°	13.00'	0.09	0.42	7	95	0.6	0.03	0.3	3.3	B
010209	849	47.64	39°	18.48'	111°	12.89'	0.11	1.10	10	101	0.8	0.09	0.3	0.7	B
010209	901	33.40	39°	18.38'	111°	13.08'	0.01	0.00	7	99	0.5	0.06	0.3	0.9	B
010209	901	36.76	39°	18.52'	111°	12.97'	0.06	0.65	8	104	0.7	0.20	0.5	4.4	C
010209	1118	15.62	39°	18.31'	111°	13.28'	0.09	0.64	7	78	0.2	0.05	0.3	0.5	B
010209	2014	56.48	39°	18.37'	111°	13.08'	0.09	0.18	6	137	0.5	0.03	0.3	3.4	C
010209	2313	51.48	39°	18.36'	111°	13.17'	0.04	0.40	7	96	0.3	0.04	0.3	0.7	B
010210	57	59.61	39°	18.37'	111°	13.62'	0.14	0.54	7	109	0.3	0.02	0.3	0.7	B
010210	106	1.24	39°	18.49'	111°	13.35'	0.29*	0.40	6	128	0.2	0.02	0.3	0.4	B
010210	223	1.98	39°	18.35'	111°	13.01'	0.03	0.39	7	92	0.6	0.04	0.3	0.7	B
010210	1604	1.35	39°	18.38'	111°	13.00'	0.01	0.55	6	140	0.6	0.02	0.3	0.8	C
010210	1650	28.84	39°	17.65'	111°	13.34'	0.04	0.71	7	85	1.2	0.08	0.3	4.9	B
010210	1748	28.16	39°	18.49'	111°	12.98'	0.04	0.29	6	143	0.6	0.07	0.3	0.9	C
010210	1839	43.40	39°	18.41'	111°	13.00'	0.05	0.47	7	101	0.6	0.05	0.3	0.7	B
010210	1931	15.29	39°	18.41'	111°	12.97'	0.03	0.47	6	142	0.6	0.04	0.3	0.8	C
010210	2029	19.09	39°	18.34'	111°	13.01'	0.04	0.53	7	90	0.6	0.04	0.3	0.8	B
010210	2029	37.91	39°	18.39'	111°	12.98'	0.06	0.08	6	142	0.6	0.08	0.4	4.1	C
010210	2135	44.91	39°	18.55'	111°	12.94'	0.14	1.07	8	104	0.8	0.09	0.3	1.0	B
010210	2206	45.86	39°	18.36'	111°	13.01'	0.13	0.45	7	93	0.6	0.05	0.3	0.9	B
010210	2251	41.63	39°	18.48'	111°	12.97'	0.14	1.05	7	102	0.7	0.02	0.3	0.9	B
010210	2305	58.13	39°	18.42'	111°	13.00'	0.06	0.52	7	101	0.6	0.03	0.3	3.2	B
010210	2311	1.78	39°	18.41'	111°	13.00'	0.09	0.59	7	101	0.6	0.03	0.3	3.2	B
010211	17	2.17	39°	18.33'	111°	13.01'	0.04	1.21	7	89	0.6	0.06	0.3	0.8	B
010211	441	27.79	39°	18.47'	111°	13.13'	0.15	0.45	7	105	0.4	0.03	0.3	0.7	B
010211	735	58.29	39°	18.45'	111°	12.77'	0.08	0.39	7	99	0.9	0.08	0.3	4.0	B
010211	952	1.45	39°	18.34'	111°	13.11'	0.01	0.78	7	90	0.4	0.02	0.3	0.8	B
010211	958	37.30	39°	18.35'	111°	13.15'	0.08	0.79	7	92	0.3	0.01	0.3	0.6	B
010211	1154	6.65	39°	17.92'	111°	13.75'	0.02	1.07	8	87	0.9	0.10	0.3	2.1	B
010211	1914	55.84	39°	18.46'	111°	13.00'	0.12	0.59	7	103	0.6	0.02	0.3	0.9	B
010211	2116	13.73	39°	18.37'	111°	13.09'	0.02	0.69	7	99	0.4	0.02	0.3	0.8	B
010212	652	56.39	39°	17.76'	111°	12.95'	0.13	1.10	8	82	0.7	0.02	0.2	0.8	A
010212	1152	36.00	39°	18.45'	111°	13.48'	0.28*	0.36	7	111	0.2	0.03	0.3	0.4	B
010212	1314	21.75	39°	18.51'	111°	13.82'	0.10	0.56	7	120	0.7	0.03	0.3	0.9	B
010212	1321	30.45	39°	18.13'	111°	13.96'	0.13	1.13	8	101	0.9	0.05	0.3	0.8	B
010212	1446	23.10	39°	18.36'	111°	13.02'	0.05	0.90	7	94	0.5	0.02	0.3	0.7	B
010212	1611	32.36	39°	18.36'	111°	12.97'	0.13	0.49	7	93	0.6	0.04	0.3	0.9	B
010212	1730	16.28	39°	18.33'	111°	13.01'	0.04	0.88	7	89	0.6	0.04	0.3	0.8	B
010212	1909	51.90	39°	18.51'	111°	12.90'	0.18	1.19	10	89	0.8	0.08	0.3	0.6	B
010212	1942	18.05	39°	18.36'	111°	13.05'	0.10	0.65	7	93	0.5	0.04	0.3	3.2	B
010212	2000	22.91	39°	18.33'	111°	13.02'	0.02	0.54	7	88	0.6	0.03	0.3	0.7	B
010212	2020	47.94	39°	18.41'	111°	12.96'	0.04	0.42	6	142	0.6	0.06	0.3	0.8	C
010212	2028	31.37	39°	18.40'	111°	13.01'	0.13	0.00	6	140	0.6	0.02	0.3	0.9	C
010212	2057	54.10	39°	18.39'	111°	12.95'	0.03	0.38	6	142	0.6	0.07	0.3	0.9	C
010212	2129	23.39	39°	18.44'	111°	12.98'	0.06	0.78	7	101	0.6	0.03	0.3	3.3	B
010212	2131	54.90	39°	18.42'	111°	12.99'	0.03	0.14	6	141	0.6	0.06	0.3	0.8	C
010212	2304	26.26	39°	18.43'	111°	13.04'	0.10	0.62	6	140	0.5	0.02	0.3	3.3	C
010212	2352	45.31	39°	18.40'	111°	12.95'	0.04	0.41	6	142	0.6	0.07	0.3	0.9	C
010213	6	58.17	39°	18.57'	111°	12.91'	0.03	0.87	8	105	0.8	0.20	0.5	3.4	C

Date	Origin Time		Latitude		Longitude		Depth	Mag	No	Gap	Dmin	Rms	Erh	Erz	Q
010213	43	10.54	39°	18.34'	111°	13.42'	0.19*	0.30	7	105	0.1	0.03	0.3	0.3	B
010213	115	5.68	39°	18.36'	111°	12.99'	0.05	0.80	7	92	0.6	0.02	0.3	0.7	B
010213	332	2.06	39°	18.33'	111°	12.97'	0.11	0.40	6	141	0.6	0.02	0.4	0.9	C
010213	411	24.49	39°	18.38'	111°	12.94'	0.05	0.13	6	142	0.7	0.08	0.4	4.1	C
010213	416	34.31	39°	18.45'	111°	12.96'	0.20	1.03	7	101	0.6	0.02	0.3	0.7	B
010213	447	47.25	39°	18.33'	111°	13.02'	0.09	0.46	7	87	0.5	0.03	0.3	3.3	B
010213	455	45.03	39°	18.39'	111°	13.01'	0.05	0.59	7	100	0.6	0.08	0.3	0.9	B
010213	456	7.92	39°	18.41'	111°	12.93'	0.09	0.00	6	142	0.7	0.03	0.3	3.3	C
010213	510	12.54	39°	18.52'	111°	13.32'	0.31*	0.41	7	111	0.3	0.02	0.3	0.4	B
010213	515	30.85	39°	18.39'	111°	12.98'	0.08	0.60	6	142	0.6	0.02	0.3	3.3	C
010213	517	51.11	39°	18.40'	111°	12.98'	0.01	0.51	7	100	0.6	0.03	0.3	0.7	B
010213	522	9.92	39°	18.36'	111°	12.99'	0.05	0.88	7	94	0.6	0.04	0.3	0.7	B
010213	527	34.30	39°	18.40'	111°	12.96'	0.02	0.00	6	142	0.6	0.02	0.3	0.8	C
010213	534	24.32	39°	18.42'	111°	13.02'	0.05	0.60	7	102	0.6	0.04	0.3	0.7	B
010213	538	46.41	39°	18.77'	111°	12.95'	0.31	0.73	7	111	1.0	0.06	0.3	0.9	B
010213	555	51.37	39°	18.44'	111°	12.96'	0.03	0.16	6	142	0.6	0.05	0.3	0.8	C
010213	602	8.66	39°	18.39'	111°	13.02'	0.07	0.43	7	100	0.5	0.03	0.3	3.3	B
010213	650	52.59	39°	18.40'	111°	12.96'	0.03	0.59	7	99	0.6	0.04	0.3	0.8	B
010213	701	18.15	39°	18.45'	111°	12.97'	0.00	0.41	7	101	0.6	0.03	0.3	0.8	B
010213	718	2.93	39°	18.39'	111°	12.93'	0.03	0.60	6	142	0.7	0.05	0.3	0.8	C
010213	727	58.52	39°	18.42'	111°	12.96'	0.04	0.73	7	100	0.6	0.02	0.3	3.2	B
010213	745	31.03	39°	18.41'	111°	12.99'	0.03	0.39	7	100	0.6	0.08	0.3	0.9	B
010213	749	16.27	39°	18.37'	111°	13.00'	0.01	0.00	6	140	0.6	0.02	0.3	0.8	C
010213	749	24.29	39°	18.39'	111°	13.03'	0.05	0.56	7	100	0.5	0.04	0.3	0.7	B
010213	821	57.34	39°	18.39'	111°	13.02'	0.06	1.12	9	99	0.5	0.03	0.2	0.5	B
010213	823	40.44	39°	18.34'	111°	13.34'	0.20*	0.59	7	77	0.1	0.03	0.3	0.3	B
010213	825	21.08	39°	18.41'	111°	12.99'	0.03	0.58	7	100	0.6	0.03	0.3	0.8	B
010213	825	34.89	39°	18.38'	111°	12.97'	0.00	0.42	6	142	0.6	0.03	0.3	0.8	C
010213	828	43.33	39°	18.40'	111°	13.01'	0.04	0.54	7	101	0.6	0.07	0.3	0.8	B
010213	906	14.92	39°	18.37'	111°	13.02'	0.00	0.96	6	140	0.5	0.02	0.3	0.8	C
010213	914	47.55	39°	18.38'	111°	12.98'	0.04	0.71	6	141	0.6	0.05	0.3	0.8	C
010213	1131	21.76	39°	18.49'	111°	13.61'	0.11	0.46	7	115	0.4	0.03	0.3	0.9	B
010213	1502	26.85	39°	18.41'	111°	12.98'	0.04	0.39	6	142	0.6	0.07	0.3	0.9	C
010213	1502	48.24	39°	18.36'	111°	12.97'	0.04	0.00	6	141	0.6	0.02	0.3	0.7	C
010213	1524	49.67	39°	18.45'	111°	12.99'	0.03	0.24	6	141	0.6	0.05	0.3	0.8	C
010213	1536	29.84	39°	18.45'	111°	13.03'	0.23	0.46	7	103	0.6	0.03	0.3	0.6	B
010213	1541	36.84	39°	18.41'	111°	12.99'	0.11	0.00	7	101	0.6	0.02	0.3	1.0	B
010213	1549	39.58	39°	18.36'	111°	12.96'	0.08	0.84	7	93	0.6	0.02	0.3	3.1	B
010213	1610	10.88	39°	18.47'	111°	12.94'	0.20	0.24	6	143	0.7	0.04	0.3	0.8	C
010213	1620	10.68	39°	18.41'	111°	12.94'	0.09	0.23	6	142	0.7	0.03	0.3	3.4	C
010213	1634	29.61	39°	18.89'	111°	12.78'	0.37	0.44	6	151	1.3	0.05	0.4	22.3	C
010213	1644	16.61	39°	18.38'	111°	12.99'	0.16	0.28	5	141	0.6	0.01	0.3	1.0	C
010213	1654	24.53	39°	18.41'	111°	12.98'	0.02	0.47	6	142	0.6	0.02	0.3	0.8	C
010213	1656	24.72	39°	18.50'	111°	12.94'	0.10	0.83	7	103	0.7	0.02	0.3	3.3	B
010213	1709	24.95	39°	18.34'	111°	13.01'	0.08	0.77	7	89	0.6	0.02	0.3	3.1	B
010213	1722	40.13	39°	18.41'	111°	12.95'	0.03	0.00	6	142	0.7	0.08	0.4	0.9	C
010213	1735	48.92	39°	18.46'	111°	12.97'	0.04	0.08	6	142	0.6	0.06	0.3	0.9	C
010213	1738	8.49	39°	18.44'	111°	12.98'	0.04	0.00	7	101	0.6	0.05	0.3	0.8	B
010213	1740	51.50	39°	18.42'	111°	12.98'	0.03	0.54	7	100	0.6	0.06	0.3	0.8	B
010213	1741	8.74	39°	18.40'	111°	12.99'	0.06	0.76	7	101	0.6	0.02	0.3	3.2	B
010213	1755	42.71	39°	18.37'	111°	12.97'	0.03	0.38	6	142	0.6	0.03	0.3	0.8	C
010213	1802	15.96	39°	18.36'	111°	12.97'	0.01	0.70	7	92	0.6	0.03	0.3	0.8	B
010213	1802	35.33	39°	18.45'	111°	12.88'	0.04	0.19	6	144	0.8	0.09	0.4	4.3	C
010213	1821	25.66	39°	18.41'	111°	12.95'	0.03	0.28	6	142	0.6	0.05	0.3	0.8	C
010213	1821	56.90	39°	18.40'	111°	12.95'	0.04	0.40	6	142	0.6	0.06	0.3	0.9	C
010213	1825	23.16	39°	18.36'	111°	13.05'	0.06	0.60	7	94	0.5	0.03	0.3	0.7	B
010213	1840	23.71	39°	18.39'	111°	12.98'	0.03	0.53	6	142	0.6	0.05	0.3	0.8	C
010213	1901	33.70	39°	18.43'	111°	13.00'	0.08	1.09	7	102	0.6	0.02	0.3	3.3	B
010213	1947	36.59	39°	18.44'	111°	12.99'	0.09	0.94	7	101	0.6	0.03	0.3	3.4	B
010213	2002	51.25	39°	18.41'	111°	12.93'	0.09	0.44	6	142	0.7	0.03	0.3	3.4	C
010213	2029	43.54	39°	18.40'	111°	13.01'	0.13	0.00	7	101	0.6	0.02	0.3	0.9	B
010213	2030	58.89	39°	18.51'	111°	12.96'	0.05	1.27	7	138	0.7	0.10	0.4	2.2	C
010213	2039	1.44	39°	18.44'	111°	12.95'	0.02	1.12	7	101	0.7	0.03	0.3	0.8	B
010213	2041	0.29	39°	18.45'	111°	12.96'	0.03	0.51	6	142	0.7	0.05	0.3	0.8	C
010213	2042	13.83	39°	18.40'	111°	12.95'	0.02	0.53	6	142	0.6	0.07	0.3	0.9	C
010213	2044	21.53	39°	18.46'	111°	13.02'	0.09	1.13	7	103	0.6	0.02	0.3	3.2	B
010213	2045	8.47	39°	18.32'	111°	13.01'	0.05	0.80	7	87	0.6	0.02	0.3	3.2	B
010213	2055	29.50	39°	18.35'	111°	12.98'	0.04	0.69	7	92	0.6	0.02	0.3	0.7	B

Date	Origin Time	Latitude	Longitude	Depth	Mag	No	Gap	Dmin	Rms	Erh	Erz	Q
010213	2115 6.00	39° 18.43'	111° 12.92'	0.09	0.24	6	143	0.7	0.03	0.3	3.4	C
010213	2115 19.54	39° 18.43'	111° 13.07'	0.09	0.13	6	139	0.5	0.02	0.3	3.2	C
010213	2150 38.50	39° 18.37'	111° 12.97'	0.04	0.52	6	141	0.6	0.05	0.3	0.8	C
010213	2207 12.89	39° 18.40'	111° 13.00'	0.04	0.00	6	140	0.6	0.05	0.3	0.8	C
010213	2207 20.15	39° 18.43'	111° 12.97'	0.08	0.69	7	101	0.6	0.02	0.3	3.3	B
010213	2210 57.10	39° 18.44'	111° 12.99'	0.03	0.65	7	102	0.6	0.07	0.3	0.8	B
010213	2220 23.66	39° 18.39'	111° 13.94'	0.12	0.69	6	116	0.8	0.01	0.3	0.9	B
010213	2238 25.85	39° 18.43'	111° 12.94'	0.07	1.08	7	101	0.7	0.03	0.3	3.2	B
010213	2248 43.73	39° 18.44'	111° 12.97'	0.00	0.45	6	142	0.6	0.02	0.3	0.8	C
010213	2249 4.96	39° 18.49'	111° 12.97'	0.08	1.04	9	103	0.7	0.11	0.3	1.5	C
010213	2252 34.30	39° 18.42'	111° 12.98'	0.03	0.45	7	100	0.6	0.07	0.3	0.8	B
010213	2254 52.83	39° 18.42'	111° 12.99'	0.04	0.00	7	100	0.6	0.08	0.3	0.9	B
010213	2303 49.84	39° 18.37'	111° 13.00'	0.04	0.59	7	96	0.6	0.04	0.3	0.7	B
010213	2328 7.28	39° 18.46'	111° 12.93'	0.09	1.04	7	102	0.7	0.02	0.3	3.1	B
010213	2338 14.96	39° 18.42'	111° 13.00'	0.00	0.59	7	101	0.6	0.02	0.3	0.8	B
010213	2358 10.67	39° 18.45'	111° 12.97'	0.04	0.76	6	142	0.6	0.07	0.3	0.9	C
010214	6 57.19	39° 19.94'	111° 12.42'	0.48	0.63	6	168	3.2	0.09	0.7	13.7	D
010214	11 56.07	39° 18.49'	111° 12.94'	0.02	0.58	6	143	0.7	0.04	0.3	0.8	C
010214	20 56.54	39° 18.44'	111° 12.96'	0.16	1.22	8	101	0.6	0.03	0.2	0.7	B
010214	21 17.02	39° 18.37'	111° 12.96'	0.01	0.67	7	95	0.6	0.02	0.3	0.7	B
010214	21 27.97	39° 18.52'	111° 13.47'	0.06	0.00	7	114	0.3	0.03	0.3	0.6	B
010214	104 5.23	39° 18.47'	111° 13.00'	0.01	1.25	8	103	0.6	0.02	0.2	0.5	B
010214	112 18.55	39° 18.41'	111° 13.02'	0.09	0.58	7	101	0.5	0.04	0.3	3.5	B
010214	118 53.97	39° 18.39'	111° 12.97'	0.03	0.00	7	98	0.6	0.04	0.3	0.8	B
010214	123 43.56	39° 18.44'	111° 12.92'	0.02	0.62	6	143	0.7	0.08	0.4	4.1	C
010214	132 56.71	39° 18.39'	111° 12.93'	0.03	0.29	6	142	0.7	0.02	0.3	0.8	C
010214	137 46.36	39° 18.44'	111° 12.93'	0.03	0.87	7	101	0.7	0.04	0.3	0.8	B
010214	141 20.17	39° 18.40'	111° 12.97'	0.03	0.67	7	100	0.6	0.02	0.3	0.7	B
010214	150 35.99	39° 18.47'	111° 12.92'	0.03	0.34	6	143	0.7	0.09	0.4	4.6	C
010214	151 31.71	39° 18.46'	111° 12.95'	0.06	0.55	6	143	0.7	0.03	0.3	3.4	C
010214	151 43.72	39° 18.43'	111° 12.97'	0.03	0.79	6	142	0.6	0.03	0.3	0.8	C
010214	154 52.84	39° 18.47'	111° 12.97'	0.04	0.47	7	102	0.6	0.03	0.3	0.7	B
010214	156 6.05	39° 18.41'	111° 12.92'	0.03	0.55	6	143	0.7	0.02	0.3	0.8	C
010214	206 58.51	39° 18.38'	111° 12.95'	0.03	0.34	6	142	0.6	0.05	0.3	0.8	C
010214	210 12.35	39° 18.45'	111° 12.96'	0.03	0.19	6	142	0.7	0.07	0.3	0.9	C
010214	220 45.12	39° 18.44'	111° 12.97'	0.03	0.82	7	101	0.6	0.06	0.3	0.8	B
010214	222 1.90	39° 18.44'	111° 12.99'	0.08	0.40	6	141	0.6	0.02	0.3	3.4	C
010214	222 55.25	39° 18.47'	111° 12.96'	0.12	0.12	6	143	0.7	0.04	0.3	1.0	C
010214	224 55.33	39° 18.45'	111° 12.99'	0.03	0.59	7	103	0.6	0.07	0.3	0.8	B
010214	226 21.32	39° 18.46'	111° 13.01'	0.08	1.15	9	103	0.6	0.03	0.2	1.0	B
010214	228 56.87	39° 18.38'	111° 12.98'	0.05	0.85	7	97	0.6	0.03	0.3	0.7	B
010214	232 42.93	39° 18.46'	111° 12.97'	0.08	0.60	7	102	0.6	0.03	0.3	3.4	B
010214	242 34.18	39° 18.35'	111° 12.98'	0.01	0.49	6	141	0.6	0.02	0.3	0.8	C
010214	243 24.00	39° 18.41'	111° 12.93'	0.03	0.64	6	142	0.7	0.07	0.3	0.9	C
010214	243 44.49	39° 18.40'	111° 12.94'	0.03	0.00	6	142	0.7	0.06	0.3	0.9	C
010214	247 17.56	39° 18.45'	111° 12.97'	0.01	0.41	6	142	0.6	0.03	0.3	0.8	C
010214	249 28.64	39° 18.40'	111° 12.98'	0.11	0.00	6	142	0.6	0.02	0.3	1.0	C
010214	308 29.02	39° 18.41'	111° 12.97'	0.04	1.04	6	142	0.6	0.02	0.3	0.7	C
010214	310 22.09	39° 18.45'	111° 12.96'	0.12	0.99	7	101	0.6	0.03	0.3	0.9	B
010214	317 34.50	39° 18.40'	111° 12.98'	0.08	0.18	6	142	0.6	0.03	0.4	3.2	C
010214	318 56.32	39° 18.41'	111° 12.96'	0.02	0.29	6	142	0.6	0.05	0.3	0.8	C
010214	455 55.10	39° 18.09'	111° 13.51'	0.03	0.72	7	94	0.6	0.04	0.2	0.8	B
010214	1017 40.49	39° 18.35'	111° 12.99'	0.03	0.46	7	92	0.6	0.04	0.3	0.8	B
010214	1252 1.69	39° 18.35'	111° 13.27'	0.14	0.30	7	89	0.2	0.02	0.3	0.5	B
010214	1252 50.69	39° 18.28'	111° 13.03'	0.05	0.23	6	136	0.6	0.01	0.4	0.7	C
010214	1618 55.56	39° 18.21'	111° 13.52'	0.03	0.78	7	100	0.3	0.04	0.2	0.8	B
010214	1721 53.08	39° 18.37'	111° 12.98'	0.01	0.52	7	96	0.6	0.02	0.3	0.8	B
010214	1911 4.03	39° 18.21'	111° 13.08'	0.00	0.65	7	80	0.5	0.02	0.3	0.8	B
010214	2140 38.92	39° 18.43'	111° 12.97'	0.11	0.19	6	142	0.6	0.02	0.3	1.0	C
010214	2159 24.36	39° 18.44'	111° 12.99'	0.04	0.52	7	102	0.6	0.06	0.3	0.8	B
010214	2201 48.78	39° 18.45'	111° 12.97'	0.04	0.60	6	142	0.6	0.07	0.3	0.9	C
010214	2227 28.60	39° 18.24'	111° 12.80'	0.02	0.43	7	83	0.9	0.06	0.3	3.5	B
010214	2237 38.80	39° 18.44'	111° 12.98'	0.04	0.82	7	101	0.6	0.04	0.3	0.7	B
010214	2243 42.76	39° 18.44'	111° 12.94'	0.09	0.26	6	143	0.7	0.03	0.3	3.4	C
010214	2301 17.00	39° 18.22'	111° 13.36'	0.14	0.81	7	85	0.2	0.02	0.2	0.6	B
010214	2307 2.46	39° 18.36'	111° 12.97'	0.00	0.27	6	141	0.6	0.02	0.3	0.8	C
010214	2325 51.40	39° 18.36'	111° 12.96'	0.04	0.53	6	142	0.6	0.02	0.3	0.7	C
010214	2331 33.01	39° 18.46'	111° 13.02'	0.09	0.00	7	103	0.6	0.02	0.3	3.2	B

Date	Origin Time		Latitude		Longitude		Depth	Mag	No	Gap	Dmin	Rms	Erh	Erz	Q
010214	2341	1.03	39°	18.37'	111°	12.99'	0.03	0.83	7	96	0.6	0.02	0.3	0.7	B
010214	2342	0.51	39°	18.38'	111°	12.95'	0.04	0.50	6	142	0.6	0.03	0.3	0.8	C
010214	2359	43.80	39°	18.44'	111°	12.96'	0.02	0.64	7	101	0.6	0.03	0.3	0.7	B
010215	2	2.67	39°	18.46'	111°	12.95'	0.03	0.83	6	143	0.7	0.06	0.3	0.9	C
010215	4	9.86	39°	18.46'	111°	12.93'	0.06	0.61	6	143	0.7	0.02	0.3	3.4	C
010215	9	37.18	39°	18.46'	111°	12.94'	0.03	0.53	6	143	0.7	0.08	0.4	1.0	C
010215	15	28.87	39°	18.41'	111°	12.98'	0.03	0.48	7	100	0.6	0.07	0.3	0.9	B
010215	20	57.87	39°	18.34'	111°	12.99'	0.03	0.79	7	89	0.6	0.04	0.3	0.7	B
010215	25	6.55	39°	18.43'	111°	12.93'	0.07	0.45	6	143	0.7	0.03	0.3	3.4	C
010215	32	14.27	39°	18.42'	111°	12.97'	0.04	0.63	7	100	0.6	0.03	0.3	0.7	B
010215	35	41.21	39°	18.46'	111°	12.95'	0.04	0.53	6	143	0.7	0.08	0.4	4.2	C
010215	43	24.35	39°	18.43'	111°	12.97'	0.01	0.00	5	142	1.4	0.12	0.5	7.8	D
010215	43	33.02	39°	18.42'	111°	12.98'	0.03	1.17	7	100	0.6	0.07	0.3	0.8	B
010215	48	48.00	39°	18.35'	111°	13.01'	0.03	0.74	7	92	0.6	0.03	0.3	0.7	B
010215	49	32.21	39°	18.41'	111°	12.94'	0.10	0.55	6	142	0.7	0.02	0.3	3.3	C
010215	51	57.01	39°	18.36'	111°	12.95'	0.01	0.00	6	142	0.6	0.03	0.3	0.8	C
010215	52	6.14	39°	18.36'	111°	12.98'	0.04	0.30	6	141	0.6	0.11	0.5	1.0	C
010215	102	34.53	39°	18.35'	111°	12.93'	0.06	0.97	7	91	0.7	0.01	0.3	3.2	B
010215	105	20.73	39°	18.40'	111°	13.00'	0.04	0.71	7	101	0.6	0.05	0.3	0.7	B
010215	107	51.63	39°	18.43'	111°	13.01'	0.04	0.92	7	102	0.6	0.05	0.3	0.8	B
010215	113	38.42	39°	18.52'	111°	12.92'	0.05	0.21	6	144	0.8	0.07	0.4	4.0	C
010215	113	58.47	39°	18.46'	111°	12.94'	0.03	0.50	6	143	0.7	0.05	0.3	0.8	C
010215	116	17.36	39°	18.48'	111°	12.96'	0.12	1.05	8	102	0.7	0.09	0.3	1.0	B
010215	117	54.09	39°	18.44'	111°	12.98'	0.06	0.00	7	101	0.6	0.02	0.3	3.3	B
010215	118	1.50	39°	18.43'	111°	12.85'	0.00	0.67	5	155	0.8	0.08	0.4	1.0	C
010215	121	39.00	39°	18.37'	111°	12.99'	0.05	0.69	7	96	0.6	0.04	0.3	0.7	B
010215	122	12.76	39°	18.46'	111°	12.97'	0.04	0.22	7	102	0.6	0.08	0.3	4.1	B
010215	122	34.75	39°	18.41'	111°	12.94'	0.09	0.84	7	100	0.7	0.03	0.3	3.3	B
010215	124	12.78	39°	18.40'	111°	12.96'	0.03	0.65	7	100	0.6	0.02	0.3	0.7	B
010215	130	52.71	39°	18.38'	111°	12.93'	0.03	0.31	6	142	0.7	0.08	0.4	0.9	C
010215	145	38.83	39°	18.42'	111°	13.03'	0.09	0.50	7	102	0.5	0.03	0.3	3.2	B
010215	210	29.54	39°	18.48'	111°	12.98'	0.08	1.05	7	102	0.6	0.04	0.3	3.4	B
010215	212	20.78	39°	18.45'	111°	12.97'	0.04	0.71	6	142	0.6	0.07	0.3	0.9	C
010215	214	33.60	39°	18.37'	111°	12.99'	0.02	0.66	6	141	0.6	0.02	0.3	0.8	C
010215	216	53.84	39°	18.42'	111°	13.00'	0.08	0.00	7	101	0.6	0.03	0.3	3.2	B
010215	217	0.37	39°	18.41'	111°	12.96'	0.04	0.76	6	142	0.6	0.11	0.5	0.9	C
010215	218	37.27	39°	18.43'	111°	12.95'	0.05	0.51	6	142	0.7	0.04	0.3	3.5	C
010215	222	34.35	39°	18.36'	111°	12.97'	0.04	0.60	6	141	0.6	0.08	0.4	4.1	C
010215	230	58.41	39°	18.37'	111°	12.97'	0.08	0.85	7	95	0.6	0.02	0.3	3.1	B
010215	241	41.27	39°	18.44'	111°	12.95'	0.03	0.90	7	101	0.7	0.02	0.3	0.8	B
010215	242	37.75	39°	18.39'	111°	12.96'	0.08	0.78	7	98	0.6	0.02	0.3	3.2	B
010215	243	45.12	39°	18.44'	111°	12.93'	0.09	1.14	8	101	0.7	0.04	0.2	2.6	B
010215	247	44.37	39°	18.41'	111°	12.95'	0.03	1.13	8	100	0.6	0.05	0.3	0.7	B
010215	251	6.46	39°	19.92'	111°	12.26'	0.63	0.36	6	229	3.3	0.10	1.1	10.2	D
010215	251	21.13	39°	18.42'	111°	12.96'	0.08	0.92	8	100	0.6	0.12	0.4	3.0	C
010215	300	5.83	39°	18.41'	111°	12.98'	0.03	0.46	6	142	0.6	0.07	0.3	0.9	C
010215	301	24.52	39°	18.37'	111°	12.97'	0.03	0.34	6	142	0.6	0.03	0.3	0.8	C
010215	303	57.23	39°	18.49'	111°	12.94'	0.04	0.49	6	143	0.7	0.07	0.4	4.1	C
010215	304	16.51	39°	18.41'	111°	12.95'	0.04	0.27	6	142	0.6	0.07	0.3	0.9	C
010215	313	49.28	39°	18.43'	111°	12.94'	0.00	0.47	6	143	0.7	0.05	0.3	0.9	C
010215	315	6.76	39°	18.39'	111°	13.02'	0.06	0.89	7	100	0.5	0.03	0.3	0.7	B
010215	316	56.02	39°	18.43'	111°	12.95'	0.05	0.67	6	142	0.7	0.04	0.3	3.5	C
010215	323	5.86	39°	18.37'	111°	12.98'	0.03	0.57	6	141	0.6	0.06	0.4	0.8	C
010215	324	35.22	39°	18.37'	111°	12.94'	0.01	0.37	6	142	0.7	0.03	0.3	0.8	C
010215	333	49.33	39°	18.38'	111°	12.97'	0.03	0.50	6	142	0.6	0.03	0.3	0.8	C
010215	339	12.45	39°	18.45'	111°	12.96'	0.04	0.79	7	101	0.6	0.03	0.3	0.7	B
010215	340	32.11	39°	18.44'	111°	12.99'	0.08	0.96	8	102	0.6	0.03	0.2	2.6	B
010215	349	33.31	39°	18.41'	111°	12.99'	0.09	0.60	7	101	0.6	0.02	0.3	3.1	B
010215	351	36.78	39°	18.41'	111°	12.93'	0.03	0.55	6	142	0.7	0.02	0.3	0.8	C
010215	352	33.11	39°	18.39'	111°	12.95'	0.03	0.41	6	142	0.6	0.05	0.3	0.8	C
010215	359	16.18	39°	18.36'	111°	12.99'	0.05	0.68	7	93	0.6	0.05	0.3	0.7	B
010215	406	18.32	39°	18.43'	111°	12.91'	0.01	0.42	6	144	0.7	0.03	0.3	0.8	C
010215	415	55.68	39°	18.45'	111°	13.01'	0.09	0.70	7	103	0.6	0.04	0.3	3.4	B
010215	416	32.01	39°	18.48'	111°	12.94'	0.00	0.43	6	143	0.7	0.02	0.3	0.8	C
010215	417	39.28	39°	18.44'	111°	12.99'	0.03	0.87	7	102	0.6	0.01	0.3	0.7	B
010215	424	6.33	39°	18.53'	111°	12.94'	0.09	1.11	7	138	0.7	0.06	0.3	1.8	C
010215	424	42.58	39°	18.43'	111°	12.90'	0.09	0.38	5	144	0.7	0.03	0.4	4.0	C
010215	425	2.29	39°	18.40'	111°	12.94'	0.03	0.47	6	142	0.7	0.07	0.3	0.9	C

Date	Origin Time		Latitude		Longitude		Depth	Mag	No	Gap	Dmin	Rms	Erh	Erz	Q
010215	425	49.52	39°	18.43'	111°	12.94'	0.09	0.19	6	143	0.7	0.03	0.3	3.4	C
010215	426	10.36	39°	18.39'	111°	12.92'	0.06	0.08	6	142	0.7	0.08	0.4	4.1	C
010215	427	31.91	39°	18.36'	111°	12.99'	0.05	0.84	7	94	0.6	0.06	0.3	0.8	B
010215	430	57.29	39°	18.35'	111°	12.98'	0.06	0.51	7	91	0.6	0.02	0.3	3.1	B
010215	435	30.93	39°	18.40'	111°	12.93'	0.13	0.69	6	142	0.7	0.04	0.3	0.9	C
010215	444	27.26	39°	18.44'	111°	12.94'	0.04	0.83	7	101	0.7	0.01	0.3	3.2	B
010215	446	57.38	39°	18.44'	111°	12.99'	0.04	0.82	7	102	0.6	0.02	0.3	0.7	B
010215	448	11.21	39°	18.34'	111°	12.98'	0.05	0.90	7	90	0.6	0.01	0.3	0.7	B
010215	450	24.02	39°	18.24'	111°	13.70'	0.00	0.97	7	104	0.5	0.02	0.3	0.8	B
010215	452	15.58	39°	18.45'	111°	12.93'	0.09	0.41	6	143	0.7	0.03	0.3	3.5	C
010215	456	50.45	39°	18.57'	111°	12.85'	0.08	1.37	11	90	0.9	0.07	0.3	1.1	B
010215	510	35.99	39°	18.43'	111°	12.90'	0.08	0.39	6	144	0.7	0.04	0.3	3.5	C
010215	513	59.01	39°	18.46'	111°	12.93'	0.10	0.60	7	101	0.7	0.04	0.3	3.4	B
010215	527	39.91	39°	18.45'	111°	12.96'	0.07	0.44	7	101	0.7	0.03	0.3	3.3	B
010215	538	20.48	39°	18.46'	111°	12.99'	0.16	0.54	7	103	0.6	0.03	0.3	0.8	B
010215	539	19.69	39°	18.40'	111°	13.05'	0.10	0.48	7	101	0.5	0.04	0.3	3.3	B
010215	613	39.30	39°	18.56'	111°	12.94'	0.04	1.24	12	105	0.8	0.05	0.2	0.8	B
010215	618	14.13	39°	18.49'	111°	12.94'	0.03	0.19	6	143	0.7	0.08	0.4	4.2	C
010215	635	47.19	39°	18.46'	111°	12.96'	0.03	0.62	7	102	0.7	0.07	0.3	0.9	B
010215	641	18.79	39°	18.43'	111°	12.90'	0.08	0.25	6	144	0.7	0.04	0.3	3.5	C
010215	641	31.73	39°	18.42'	111°	12.95'	0.04	0.44	6	142	0.6	0.07	0.3	0.9	C
010215	642	51.04	39°	18.45'	111°	12.92'	0.06	0.87	8	101	0.7	0.12	0.4	3.0	C
010215	646	54.43	39°	18.42'	111°	12.93'	0.10	0.64	8	100	0.7	0.09	0.3	2.6	B
010215	649	16.10	39°	18.54'	111°	12.95'	0.08	0.82	8	104	0.7	0.09	0.3	2.6	B
010215	701	15.81	39°	18.45'	111°	12.97'	0.03	0.60	7	101	0.6	0.04	0.3	0.8	B
010215	705	14.68	39°	18.47'	111°	12.94'	0.03	0.58	7	102	0.7	0.07	0.3	0.9	B
010215	706	33.38	39°	18.45'	111°	12.96'	0.04	0.65	7	101	0.7	0.08	0.3	4.0	B
010215	710	20.72	39°	18.39'	111°	12.98'	0.08	0.77	7	98	0.6	0.04	0.3	3.4	B
010215	712	4.44	39°	18.41'	111°	12.98'	0.05	0.94	8	100	0.6	0.10	0.3	3.3	B
010215	722	15.62	39°	18.36'	111°	12.98'	0.04	0.76	7	94	0.6	0.05	0.3	0.8	B
010215	724	34.84	39°	18.39'	111°	12.92'	0.14	0.00	6	142	0.7	0.04	0.3	0.9	C
010215	724	47.92	39°	18.40'	111°	12.91'	0.08	0.47	6	144	0.7	0.03	0.3	3.4	C
010215	732	13.20	39°	18.48'	111°	12.94'	0.13	0.65	7	102	0.7	0.02	0.3	0.8	B
010215	732	46.70	39°	18.39'	111°	12.95'	0.03	0.55	7	99	0.6	0.05	0.3	0.8	B
010215	737	31.63	39°	18.42'	111°	12.96'	0.03	0.34	7	100	0.6	0.04	0.3	0.8	B
010215	737	53.42	39°	18.45'	111°	12.97'	0.05	0.73	7	101	0.6	0.04	0.3	3.3	B
010215	741	25.81	39°	18.45'	111°	12.92'	0.02	0.58	6	143	0.7	0.07	0.4	4.1	C
010215	745	10.75	39°	18.43'	111°	12.94'	0.04	0.00	6	143	0.7	0.02	0.3	3.3	C
010215	745	19.46	39°	18.40'	111°	12.98'	0.05	0.74	6	142	0.6	0.04	0.3	0.7	C
010215	746	14.20	39°	18.51'	111°	12.94'	0.07	0.74	8	103	0.7	0.13	0.4	3.2	C
010215	749	42.09	39°	18.38'	111°	12.95'	0.04	0.56	7	96	0.6	0.08	0.3	0.9	B
010215	751	22.30	39°	18.34'	111°	12.95'	0.01	0.14	6	141	0.6	0.03	0.3	0.8	C
010215	755	24.13	39°	18.42'	111°	12.96'	0.05	0.77	7	100	0.6	0.02	0.3	3.3	B
010215	756	28.19	39°	18.41'	111°	12.92'	0.03	0.20	6	143	0.7	0.03	0.3	0.8	C
010215	756	57.92	39°	18.36'	111°	12.98'	0.02	0.32	7	93	0.6	0.04	0.3	0.8	B
010215	800	4.53	39°	18.46'	111°	12.93'	0.00	0.34	6	143	0.7	0.04	0.3	0.9	C
010215	800	19.30	39°	18.41'	111°	12.98'	0.09	0.38	7	100	0.6	0.03	0.3	3.3	B
010215	805	16.88	39°	18.49'	111°	12.94'	0.05	1.09	8	103	0.7	0.10	0.3	2.6	B
010215	811	32.93	39°	18.47'	111°	12.93'	0.03	0.33	6	143	0.7	0.08	0.4	4.1	C
010215	811	46.92	39°	18.46'	111°	12.95'	0.03	0.65	7	102	0.7	0.08	0.3	4.0	B
010215	815	3.52	39°	18.45'	111°	12.96'	0.03	0.40	7	101	0.7	0.08	0.3	0.9	B
010215	816	25.54	39°	18.42'	111°	12.94'	0.03	0.69	7	100	0.7	0.07	0.3	0.9	B
010215	832	39.25	39°	18.45'	111°	12.93'	0.00	0.53	7	101	0.7	0.03	0.3	0.8	B
010215	838	48.02	39°	18.41'	111°	12.91'	0.03	0.53	6	143	0.7	0.02	0.3	0.8	C
010215	840	58.34	39°	18.44'	111°	12.99'	0.17	0.86	7	102	0.6	0.02	0.3	0.8	B
010215	843	25.75	39°	18.46'	111°	12.94'	0.09	0.85	7	101	0.7	0.02	0.3	3.3	B
010215	846	37.03	39°	18.39'	111°	12.97'	0.02	0.38	7	98	0.6	0.03	0.3	0.7	B
010215	847	31.99	39°	18.41'	111°	12.99'	0.08	0.49	7	101	0.6	0.03	0.3	3.3	B
010215	854	28.67	39°	18.42'	111°	12.90'	0.09	1.14	8	99	0.7	0.03	0.2	2.0	B
010215	856	53.72	39°	18.42'	111°	12.91'	0.03	0.88	8	100	0.7	0.09	0.3	2.6	B
010215	857	17.05	39°	18.34'	111°	13.01'	0.02	0.08	7	90	0.6	0.03	0.3	0.8	B
010215	859	2.39	39°	18.38'	111°	12.97'	0.03	0.68	7	96	0.6	0.04	0.3	0.8	B
010215	904	37.41	39°	18.35'	111°	12.95'	0.03	0.69	7	91	0.6	0.04	0.3	0.8	B
010215	914	55.98	39°	18.44'	111°	12.99'	0.04	0.00	7	102	0.6	0.02	0.3	0.7	B
010215	934	51.69	39°	18.36'	111°	12.95'	0.00	0.58	7	93	0.6	0.03	0.3	0.8	B
010215	940	14.16	39°	18.45'	111°	12.99'	0.08	0.61	7	102	0.6	0.02	0.3	3.3	B
010215	948	46.00	39°	18.50'	111°	12.94'	0.02	1.08	8	103	0.7	0.08	0.3	0.9	B
010215	951	0.04	39°	18.45'	111°	12.95'	0.02	0.81	7	101	0.7	0.05	0.3	0.8	B

Date	Origin Time		Latitude		Longitude		Depth	Mag	No	Gap	Dmin	Rms	Erh	Erz	Q
010215	954	14.90	39°	18.44'	111°	12.96'	0.08	0.63	7	101	0.6	0.03	0.3	3.3	B
010215	957	24.25	39°	18.43'	111°	12.94'	0.10	1.31	7	101	0.7	0.04	0.3	3.3	B
010215	1000	30.21	39°	18.41'	111°	12.98'	0.01	0.79	7	100	0.6	0.03	0.3	0.8	B
010215	1006	37.68	39°	18.36'	111°	12.97'	0.03	0.00	7	92	0.6	0.09	0.3	0.9	B
010215	1012	49.55	39°	18.44'	111°	12.94'	0.11	0.82	8	101	0.7	0.09	0.3	1.0	B
010215	1013	0.16	39°	18.42'	111°	12.96'	0.08	1.81	8	100	0.6	0.04	0.3	2.6	B
010215	1025	7.55	39°	18.46'	111°	12.94'	0.08	0.51	7	102	0.7	0.02	0.3	3.2	B
010215	1028	6.43	39°	18.48'	111°	12.96'	0.03	0.85	8	102	0.7	0.05	0.3	0.7	B
010215	1032	43.41	39°	18.46'	111°	12.96'	0.04	0.13	6	143	0.7	0.08	0.4	4.2	C
010215	1037	39.12	39°	18.44'	111°	12.99'	0.04	0.52	7	102	0.6	0.06	0.3	0.8	B
010215	1053	1.33	39°	18.41'	111°	12.96'	0.07	0.19	6	142	0.6	0.03	0.3	3.4	C
010215	1103	21.96	39°	18.38'	111°	13.03'	0.01	0.28	6	140	0.5	0.04	0.3	0.8	C
010215	1249	51.02	39°	18.36'	111°	12.93'	0.05	0.32	6	142	0.7	0.08	0.4	4.1	C
010215	1356	33.75	39°	18.48'	111°	12.92'	0.02	0.43	6	143	0.7	0.08	0.3	1.0	C
010215	1450	58.64	39°	18.39'	111°	12.95'	0.01	0.22	6	142	0.6	0.02	0.5	0.7	C
010215	1451	42.16	39°	18.40'	111°	13.00'	0.04	0.78	8	101	0.6	0.03	0.2	0.6	B
010215	1455	1.31	39°	18.38'	111°	12.97'	0.04	0.33	7	97	0.6	0.06	0.3	0.8	B
010215	1456	30.63	39°	18.37'	111°	13.00'	0.05	0.52	7	96	0.6	0.03	0.3	0.7	B
010215	1457	2.01	39°	18.40'	111°	12.94'	0.00	0.54	6	142	0.7	0.03	0.3	0.8	C
010215	1523	52.96	39°	18.43'	111°	12.97'	0.06	0.56	7	101	0.6	0.02	0.3	3.2	B
010215	1524	23.47	39°	18.44'	111°	12.97'	0.08	0.00	7	101	0.6	0.04	0.3	3.4	B
010215	1552	38.91	39°	18.44'	111°	12.99'	0.03	0.70	7	102	0.6	0.06	0.3	0.8	B
010215	1555	52.77	39°	18.47'	111°	12.92'	0.02	0.68	6	143	0.7	0.04	0.3	0.8	C
010215	1557	20.02	39°	18.46'	111°	12.93'	0.02	0.90	6	143	0.7	0.06	0.3	0.9	C
010215	1558	25.09	39°	18.37'	111°	12.96'	0.03	0.49	6	142	0.6	0.03	0.4	0.7	C
010215	1607	28.49	39°	18.37'	111°	12.94'	0.03	0.61	7	95	0.7	0.05	0.3	0.8	B
010215	1610	6.40	39°	18.35'	111°	12.95'	0.04	0.60	7	91	0.6	0.07	0.3	0.8	B
010215	1612	31.14	39°	18.46'	111°	12.96'	0.08	0.79	6	143	0.7	0.02	0.3	3.4	C
010215	1624	11.47	39°	18.45'	111°	12.96'	0.03	0.73	7	101	0.7	0.05	0.3	0.8	B
010215	1625	34.09	39°	18.36'	111°	12.93'	0.03	0.51	6	142	0.7	0.07	0.4	0.9	C
010215	1626	51.87	39°	18.54'	111°	12.92'	0.02	1.03	9	104	0.8	0.06	0.3	1.3	B
010215	1635	38.04	39°	18.62'	111°	12.87'	0.01	0.17	6	146	0.9	0.08	0.5	4.0	C
010215	1635	51.13	39°	18.44'	111°	12.96'	0.03	0.00	7	101	0.6	0.06	0.3	0.8	B
010215	1648	23.66	39°	18.37'	111°	13.01'	0.05	0.76	7	96	0.6	0.09	0.3	4.2	B
010215	1657	39.63	39°	18.48'	111°	13.04'	0.10	0.55	7	104	0.6	0.04	0.3	1.1	B
010215	1700	24.81	39°	18.45'	111°	12.96'	0.03	0.57	6	142	0.7	0.07	0.3	0.9	C
010215	1701	33.70	39°	18.44'	111°	12.93'	0.03	0.69	6	143	0.7	0.04	0.3	0.8	C
010215	1703	29.79	39°	18.45'	111°	12.89'	0.07	0.35	6	144	0.8	0.02	0.3	3.4	C
010215	1703	49.68	39°	18.44'	111°	12.95'	0.03	0.00	6	142	0.7	0.07	0.3	0.9	C
010215	1706	15.65	39°	18.40'	111°	12.96'	0.11	0.91	7	100	0.6	0.01	0.3	0.9	B
010215	1710	25.64	39°	18.49'	111°	12.90'	0.12	0.00	6	145	0.8	0.03	0.3	1.0	C
010215	1712	44.04	39°	18.37'	111°	12.95'	0.02	1.10	7	94	0.6	0.05	0.3	0.8	B
010215	1720	55.52	39°	18.36'	111°	12.92'	0.05	0.28	6	142	0.7	0.08	0.4	4.1	C
010215	1731	7.55	39°	18.36'	111°	12.96'	0.14	0.00	7	93	0.6	0.03	0.3	0.8	B
010215	1731	16.54	39°	18.45'	111°	12.96'	0.03	0.51	6	142	0.7	0.07	0.3	0.9	C
010215	1732	23.49	39°	18.44'	111°	12.96'	0.08	0.60	7	101	0.7	0.03	0.3	3.3	B
010215	1734	5.88	39°	18.43'	111°	12.94'	0.05	0.54	7	101	0.7	0.02	0.3	3.2	B
010215	1739	14.46	39°	18.44'	111°	12.99'	0.10	0.92	7	101	0.6	0.02	0.3	3.2	B
010215	1744	5.79	39°	18.57'	111°	12.88'	0.01	1.23	9	104	0.8	0.06	0.2	1.2	B
010215	1805	55.48	39°	18.46'	111°	12.95'	0.04	0.59	7	102	0.7	0.08	0.3	4.1	B
010215	1832	20.37	39°	18.46'	111°	12.95'	0.11	0.90	7	102	0.7	0.01	0.3	1.0	B
010215	1847	12.16	39°	18.37'	111°	12.96'	0.07	0.48	6	142	0.6	0.02	0.3	3.3	C
010215	1903	15.58	39°	18.36'	111°	12.98'	0.00	0.54	7	92	0.6	0.03	0.3	0.8	B
010215	1907	39.54	39°	18.32'	111°	12.91'	0.01	0.23	6	143	0.7	0.06	0.4	0.8	C
010215	1913	59.54	39°	18.37'	111°	12.99'	0.09	0.93	7	96	0.6	0.02	0.3	3.2	B
010215	1922	1.07	39°	18.49'	111°	12.91'	0.02	0.12	6	143	0.7	0.08	0.4	4.3	C
010215	1922	35.27	39°	18.45'	111°	12.98'	0.04	0.40	7	101	0.6	0.03	0.3	0.7	B
010215	1922	56.48	39°	18.44'	111°	12.94'	0.09	0.00	7	101	0.7	0.02	0.3	3.2	B
010215	2111	37.20	39°	18.45'	111°	12.97'	0.04	0.57	7	101	0.6	0.04	0.3	0.7	B
010215	2230	51.00	39°	18.33'	111°	12.98'	0.05	0.63	7	88	0.6	0.04	0.3	0.7	B
010215	2246	18.47	39°	18.44'	111°	12.98'	0.13	0.79	7	101	0.6	0.02	0.3	0.9	B
010215	2251	11.09	39°	19.71'	111°	12.50'	0.54	0.20	6	165	2.8	0.09	0.6	9.8	C
010215	2253	22.69	39°	18.39'	111°	12.98'	0.04	0.68	7	98	0.6	0.02	0.3	0.7	B
010215	2321	57.95	39°	18.54'	111°	12.89'	0.00	0.84	9	103	0.8	0.06	0.3	1.3	B
010215	2331	23.44	39°	18.44'	111°	12.92'	0.11	0.86	8	101	0.7	0.08	0.3	1.0	B
010215	2331	55.59	39°	18.40'	111°	12.94'	0.03	0.84	7	100	0.7	0.05	0.3	0.8	B
010215	2333	47.32	39°	18.44'	111°	12.93'	0.08	0.00	8	101	0.7	0.09	0.3	2.5	B
010215	2336	42.33	39°	18.40'	111°	12.94'	0.05	1.02	8	99	0.7	0.12	0.4	3.0	C

Date	Origin Time		Latitude		Longitude		Depth	Mag	No	Gap	Dmin	Rms	Erh	Erz	Q
010215	2337	34.42	39°	18.37'	111°	12.98'	0.04	0.78	7	95	0.6	0.03	0.3	0.7	B
010215	2400	5.88	39°	18.44'	111°	12.95'	0.03	1.11	7	101	0.7	0.03	0.3	0.8	B
010215	2400	30.66	39°	18.44'	111°	12.92'	0.07	0.00	7	101	0.7	0.02	0.3	3.2	B
010216	0	53.25	39°	18.43'	111°	12.95'	0.09	0.71	6	142	0.6	0.03	0.3	3.4	C
010216	112	18.31	39°	18.45'	111°	12.84'	0.04	1.11	9	89	0.8	0.11	0.3	2.4	B
010216	112	46.01	39°	18.39'	111°	12.94'	0.03	0.00	6	142	0.7	0.07	0.4	0.9	C
010216	237	13.25	39°	18.42'	111°	12.98'	0.03	1.32	9	100	0.6	0.04	0.2	0.6	B
010216	435	23.19	39°	18.45'	111°	12.94'	0.05	1.20	8	101	0.7	0.09	0.3	2.5	B
010216	536	48.05	39°	18.37'	111°	12.90'	0.01	1.13	8	94	0.7	0.02	0.2	0.7	B
010216	554	38.90	39°	18.52'	111°	12.93'	0.09	1.16	10	103	0.7	0.07	0.2	1.5	B
010216	623	32.38	39°	18.44'	111°	12.95'	0.06	0.89	8	101	0.7	0.09	0.3	3.3	B
010216	634	2.23	39°	18.54'	111°	12.90'	0.00	1.21	10	103	0.8	0.05	0.2	0.7	B
010216	711	46.81	39°	18.44'	111°	12.92'	0.03	1.15	8	101	0.7	0.03	0.2	0.7	B
010216	742	6.50	39°	18.44'	111°	12.94'	0.08	1.11	9	101	0.7	0.04	0.2	1.0	B
010216	746	1.92	39°	18.43'	111°	12.95'	0.05	0.87	8	101	0.7	0.08	0.3	3.1	B
010216	816	28.38	39°	18.47'	111°	13.03'	0.17	1.38	9	103	0.6	0.03	0.2	0.6	B
010216	836	22.36	39°	18.44'	111°	12.93'	0.08	1.13	8	101	0.7	0.03	0.2	2.0	B
010216	909	34.15	39°	18.42'	111°	13.01'	0.22	1.55	9	101	0.6	0.04	0.2	0.5	B
010216	1157	49.39	39°	18.38'	111°	12.97'	0.04	0.83	6	142	0.6	0.02	0.3	3.3	C
010216	1521	34.99	39°	18.46'	111°	12.94'	0.06	0.87	7	102	0.7	0.02	0.3	3.3	B
010216	1525	3.88	39°	18.43'	111°	12.97'	0.02	0.96	7	101	0.6	0.04	0.3	0.8	B
010216	1527	15.73	39°	18.45'	111°	12.97'	0.05	0.64	7	101	0.6	0.02	0.3	3.3	B
010216	1532	1.48	39°	18.44'	111°	12.95'	0.02	1.02	7	101	0.7	0.03	0.3	0.7	B
010216	1537	54.44	39°	18.39'	111°	12.95'	0.04	0.77	7	98	0.6	0.05	0.3	0.7	B
010216	1554	57.58	39°	18.41'	111°	12.96'	0.03	0.85	7	100	0.6	0.06	0.3	0.9	B
010216	1557	45.14	39°	18.43'	111°	12.96'	0.13	1.00	7	101	0.6	0.02	0.3	0.8	B
010216	1619	56.27	39°	18.35'	111°	12.98'	0.08	0.65	7	91	0.6	0.02	0.3	3.0	B
010216	1621	41.73	39°	18.45'	111°	12.95'	0.06	0.95	7	101	0.7	0.02	0.3	3.3	B
010216	1631	26.49	39°	18.47'	111°	12.92'	0.08	0.88	8	102	0.7	0.09	0.3	2.5	B
010216	1639	49.43	39°	18.43'	111°	12.96'	0.13	1.26	8	101	0.6	0.02	0.2	0.8	B
010216	1648	6.21	39°	18.41'	111°	12.95'	0.03	0.68	7	100	0.6	0.05	0.3	0.8	B
010216	1726	25.74	39°	18.53'	111°	12.99'	0.01	1.36	13	91	0.7	0.04	0.2	0.4	B
010216	1732	36.26	39°	18.43'	111°	12.95'	0.03	0.56	7	101	0.7	0.07	0.3	0.9	B
010216	1735	4.97	39°	18.41'	111°	12.90'	0.10	0.62	7	99	0.7	0.03	0.3	3.2	B
010216	1738	40.02	39°	18.43'	111°	12.94'	0.06	0.66	7	101	0.7	0.03	0.3	3.3	B
010216	1741	0.24	39°	18.50'	111°	12.93'	0.05	1.12	8	103	0.7	0.19	0.5	3.3	C
010216	1742	18.24	39°	18.38'	111°	12.92'	0.03	0.72	7	97	0.7	0.06	0.3	0.8	B
010216	1748	19.52	39°	18.39'	111°	12.93'	0.01	0.73	7	98	0.7	0.02	0.3	0.8	B
010216	1807	43.70	39°	18.48'	111°	12.90'	0.03	1.05	7	101	0.7	0.08	0.3	4.1	B
010216	1811	20.79	39°	18.41'	111°	12.94'	0.02	1.15	7	100	0.7	0.05	0.3	0.8	B
010216	1811	42.49	39°	18.43'	111°	12.97'	0.01	1.05	8	101	0.6	0.04	0.3	0.7	B
010216	1905	12.01	39°	18.42'	111°	12.93'	0.03	1.12	8	100	0.7	0.08	0.3	0.8	B
010216	1934	38.25	39°	18.47'	111°	12.90'	0.10	1.18	8	101	0.7	0.05	0.3	2.8	B
010216	2105	2.99	39°	18.49'	111°	12.91'	0.04	1.11	7	101	0.7	0.08	0.3	4.2	B
010216	2137	29.45	39°	18.50'	111°	13.00'	0.01	1.25	10	104	0.6	0.05	0.2	0.5	B
010216	2137	45.18	39°	18.45'	111°	12.90'	0.02	1.51	7	100	0.7	0.05	0.3	0.8	B
010217	410	43.53	39°	18.24'	111°	12.75'	0.09	1.19	7	84	0.9	0.02	0.3	3.2	B
010219	535	16.18	39°	18.18'	111°	13.82'	0.05	1.31	8	102	0.7	0.10	0.4	2.0	B
010219	1515	6.92	39°	18.47'	111°	12.97'	0.02	1.33	8	102	0.6	0.03	0.2	0.5	B
010219	1619	15.56	39°	18.46'	111°	12.89'	0.00	1.42	11	89	0.8	0.05	0.2	0.5	A
010219	1644	4.35	39°	18.43'	111°	12.94'	0.06	1.25	10	90	0.7	0.12	0.3	1.6	B
010219	1720	52.14	39°	18.49'	111°	12.94'	0.01	1.30	12	90	0.7	0.10	0.3	0.6	B
010219	1727	2.49	39°	18.50'	111°	13.00'	0.00	1.38	10	104	0.6	0.08	0.3	0.6	B
010219	1741	36.02	39°	18.41'	111°	12.97'	0.05	1.24	9	100	0.6	0.10	0.3	1.8	B
010219	1800	18.34	39°	18.46'	111°	12.95'	0.01	1.29	8	138	0.7	0.08	0.3	0.6	C
010219	1850	58.51	39°	18.39'	111°	12.93'	0.02	0.85	7	98	0.7	0.07	0.3	0.8	B
010219	1911	28.12	39°	18.38'	111°	12.83'	0.05	1.31	8	88	0.8	0.11	0.4	3.0	B
010219	1912	42.25	39°	18.48'	111°	12.90'	0.06	1.22	8	101	0.7	0.03	0.2	2.5	B
010219	2057	49.46	39°	18.39'	111°	12.93'	0.03	0.96	7	98	0.7	0.02	0.3	0.7	B
010219	2117	25.70	39°	18.47'	111°	12.88'	0.08	1.27	9	89	0.8	0.05	0.2	1.7	A
010219	2219	41.71	39°	18.49'	111°	12.92'	0.03	1.46	11	90	0.7	0.03	0.2	0.8	A
010219	2307	47.96	39°	18.38'	111°	12.91'	0.03	1.12	7	96	0.7	0.07	0.3	0.9	B
010219	2323	9.55	39°	18.46'	111°	12.86'	0.01	0.34	6	145	0.8	0.08	0.4	4.1	C
010219	2324	14.64	39°	18.46'	111°	12.90'	0.02	1.20	8	100	0.7	0.05	0.2	0.7	B
010219	2334	31.28	39°	18.45'	111°	12.89'	0.08	1.15	8	100	0.7	0.08	0.3	2.4	B
010220	132	35.33	39°	18.38'	111°	12.91'	0.02	0.74	7	95	0.7	0.07	0.3	0.9	B
010220	349	33.83	39°	18.46'	111°	12.91'	0.01	1.14	8	100	0.7	0.06	0.3	0.8	B
010220	408	7.23	39°	18.35'	111°	12.98'	0.03	1.27	7	91	0.6	0.05	0.3	0.8	B

Date	Origin Time	Latitude	Longitude	Depth	Mag	No	Gap	Dmin	Rms	Erh	Erz	Q
010220	843 44.91	39° 18.51'	111° 12.93'	0.05	1.20	9	103	0.7	0.04	0.2	1.1	B
010220	1209 57.22	39° 18.44'	111° 12.96'	0.02	1.11	9	101	0.6	0.02	0.2	0.5	B
010220	1449 4.09	39° 18.35'	111° 12.97'	0.01	0.00	6	141	0.6	0.06	0.3	0.9	C
010220	1812 32.76	39° 18.49'	111° 13.00'	0.00	1.35	10	91	0.6	0.07	0.3	0.6	B
010220	1943 15.18	39° 18.47'	111° 12.90'	0.09	0.40	7	101	0.7	0.03	0.3	3.2	B
010220	1950 26.97	39° 18.47'	111° 12.93'	0.02	0.70	7	102	0.7	0.08	0.3	4.0	B
010220	2001 51.79	39° 18.48'	111° 12.96'	0.01	1.28	9	102	0.7	0.06	0.3	0.6	B
010221	1000 6.11	39° 18.27'	111° 14.11'	0.29	1.02	7	112	1.1	0.02	0.3	0.7	B
010221	1531 26.36	39° 18.47'	111° 12.91'	0.07	1.02	7	101	0.7	0.02	0.3	3.2	B
010221	1532 18.92	39° 18.39'	111° 12.89'	0.00	0.74	6	144	0.7	0.03	0.3	0.8	C
010221	1537 1.99	39° 18.41'	111° 12.95'	0.01	1.18	6	100	0.6	0.02	0.3	0.8	B
010221	1640 0.73	39° 18.40'	111° 12.98'	0.02	1.30	9	100	0.6	0.05	0.2	0.7	B
010221	1701 0.71	39° 18.45'	111° 12.91'	0.02	1.16	8	101	0.7	0.07	0.3	0.8	B
010221	1737 2.85	39° 18.38'	111° 12.89'	0.01	0.88	7	95	0.7	0.02	0.3	0.8	B
010221	1903 15.13	39° 18.36'	111° 12.92'	0.12	0.88	8	92	0.7	0.04	0.2	0.9	B
010221	1909 7.21	39° 18.44'	111° 12.85'	0.14	1.11	8	100	0.8	0.09	0.3	1.0	B
010221	1949 36.92	39° 18.46'	111° 12.95'	0.00	1.27	10	101	0.7	0.04	0.2	0.6	B
010221	1953 24.08	39° 18.38'	111° 12.91'	0.03	1.30	8	95	0.7	0.06	0.3	0.7	B
010221	2015 27.19	39° 18.45'	111° 12.89'	0.02	1.44	5	153	0.8	0.02	0.3	3.8	C
010221	2016 16.14	39° 18.43'	111° 12.92'	0.02	0.00	7	100	0.7	0.02	0.3	0.8	B
010221	2056 26.43	39° 18.37'	111° 12.89'	0.01	0.84	7	93	0.7	0.02	0.3	0.8	B
010221	2057 6.64	39° 18.36'	111° 12.89'	0.01	0.80	7	91	0.7	0.02	0.3	0.8	B
010221	2153 58.67	39° 18.41'	111° 12.86'	0.02	0.85	6	144	0.8	0.07	0.4	4.0	C
010221	2210 53.52	39° 18.45'	111° 12.90'	0.02	1.15	8	100	0.7	0.06	0.3	0.8	B
010221	2227 43.26	39° 18.36'	111° 12.91'	0.03	0.83	8	91	0.7	0.04	0.3	0.7	B
010221	2304 48.42	39° 18.46'	111° 12.89'	0.02	0.00	7	100	0.7	0.07	0.3	0.9	B
010221	2348 18.61	39° 18.45'	111° 12.88'	0.03	1.30	8	100	0.8	0.08	0.3	3.2	B
010222	233 37.94	39° 18.45'	111° 12.88'	0.14	0.97	8	100	0.8	0.09	0.3	1.0	B
010222	457 3.06	39° 18.46'	111° 12.89'	0.00	1.13	11	100	0.8	0.09	0.2	0.6	B
010222	613 34.60	39° 18.53'	111° 12.82'	0.14	1.27	10	101	0.9	0.07	0.3	0.7	B
010222	623 25.90	39° 18.61'	111° 12.86'	0.08	1.29	9	105	0.9	0.08	0.3	1.8	B
010222	641 28.25	39° 18.42'	111° 12.87'	0.02	0.96	8	99	0.8	0.07	0.3	3.0	B
010222	718 35.72	39° 18.54'	111° 12.81'	0.08	1.14	11	88	0.9	0.07	0.2	1.4	B
010222	758 52.00	39° 18.51'	111° 12.84'	0.10	1.07	8	102	0.9	0.03	0.2	2.0	B
010222	1443 42.78	39° 18.44'	111° 12.88'	0.01	0.40	6	144	0.8	0.07	0.4	3.9	C
010222	1616 53.95	39° 18.45'	111° 12.88'	0.06	1.01	8	100	0.8	0.09	0.3	3.3	B
010222	1635 19.23	39° 18.41'	111° 12.87'	0.01	1.05	7	99	0.8	0.08	0.3	4.0	B
010222	1720 38.40	39° 18.40'	111° 12.85'	0.02	0.79	6	144	0.8	0.07	0.4	4.0	C
010222	1803 0.91	39° 18.44'	111° 12.87'	0.07	1.20	7	100	0.8	0.03	0.3	3.3	B
010222	1849 12.43	39° 18.37'	111° 12.86'	0.01	0.60	6	94	0.8	0.03	0.3	0.8	B
010222	1952 26.95	39° 18.44'	111° 12.88'	0.01	0.60	7	100	0.8	0.09	0.3	4.3	B
010222	2044 21.25	39° 18.49'	111° 12.87'	0.05	1.21	9	101	0.8	0.17	0.5	2.3	C
010222	2129 8.74	39° 18.41'	111° 12.86'	0.01	1.11	8	99	0.8	0.08	0.3	3.1	B
010222	2217 1.33	39° 18.38'	111° 12.88'	0.02	1.02	8	96	0.7	0.07	0.3	3.0	B
010222	2253 45.37	39° 18.53'	111° 12.81'	0.16	1.41	11	88	0.9	0.07	0.2	0.6	B
010223	53 44.70	39° 18.40'	111° 12.88'	0.02	1.16	7	97	0.7	0.04	0.3	0.8	B
010223	127 20.48	39° 18.46'	111° 12.85'	0.03	1.26	8	100	0.8	0.09	0.3	2.6	B
010223	230 27.25	39° 18.44'	111° 12.88'	0.01	0.86	7	100	0.8	0.07	0.3	3.8	B
010223	230 50.67	39° 18.46'	111° 12.86'	0.01	0.00	6	145	0.8	0.08	0.4	4.2	C
010223	316 10.77	39° 18.40'	111° 12.87'	0.02	1.25	7	98	0.8	0.08	0.3	4.2	B
010223	425 15.67	39° 18.51'	111° 12.83'	0.18	1.16	8	101	0.9	0.15	0.4	1.1	C
010223	425 34.57	39° 18.46'	111° 12.89'	0.03	0.64	7	100	0.8	0.08	0.3	4.0	B
010223	458 23.42	39° 18.42'	111° 12.90'	0.04	0.88	7	99	0.7	0.07	0.3	4.0	B
010223	548 13.78	39° 17.96'	111° 13.92'	0.07	1.10	8	89	1.9	0.04	0.2	1.4	A
010223	617 31.04	39° 18.43'	111° 12.93'	0.02	1.31	8	184	0.7	0.09	0.5	0.8	D
010223	646 27.39	39° 18.43'	111° 12.86'	0.17	0.96	8	99	0.8	0.04	0.2	0.7	B
010223	744 20.58	39° 18.42'	111° 12.85'	0.04	1.11	7	99	0.8	0.07	0.3	4.0	B
010223	801 2.25	39° 18.42'	111° 12.85'	0.00	1.12	8	99	0.8	0.02	0.2	0.7	B
010223	809 48.85	39° 18.46'	111° 12.91'	0.09	1.07	8	100	0.7	0.04	0.3	2.1	B
010223	814 30.64	39° 18.43'	111° 12.85'	0.06	1.13	7	139	0.8	0.11	0.4	2.8	C
010223	900 57.38	39° 18.42'	111° 12.84'	0.07	1.18	8	99	0.8	0.03	0.2	2.6	B
010223	901 24.88	39° 18.46'	111° 12.87'	0.07	0.00	7	100	0.8	0.02	0.3	3.3	B
010223	921 36.38	39° 18.44'	111° 12.85'	0.08	0.98	8	100	0.8	0.03	0.2	2.7	B
010223	1003 39.48	39° 18.46'	111° 12.86'	0.03	1.07	8	100	0.8	0.08	0.3	3.2	B
010223	1027 17.12	39° 18.44'	111° 12.88'	0.10	0.55	7	100	0.8	0.03	0.3	3.3	B
010223	1512 42.40	39° 18.00'	111° 12.81'	0.02	0.99	7	85	0.6	0.02	0.3	0.7	B
010223	1616 30.25	39° 18.54'	111° 12.83'	0.16	1.05	8	103	0.9	0.13	0.4	1.1	C
010223	1627 28.82	39° 18.47'	111° 12.85'	0.08	1.08	8	101	0.8	0.14	0.4	3.3	C

Date	Origin Time		Latitude		Longitude		Depth	Mag	No	Gap	Dmin	Rms	Erh	Erz	Q
010223	1652	27.62	39°	18.47'	111°	12.84'	0.03	0.91	7	101	0.8	0.07	0.3	3.9	B
010223	1652	42.80	39°	18.46'	111°	12.86'	0.01	0.89	7	100	0.8	0.07	0.3	1.0	B
010223	1818	10.97	39°	18.40'	111°	12.88'	0.02	0.99	7	98	0.7	0.08	0.3	4.1	B
010223	1831	5.87	39°	18.50'	111°	12.89'	0.01	1.38	11	89	0.8	0.09	0.3	1.1	B
010223	2025	40.95	39°	18.48'	111°	12.84'	0.05	0.66	6	101	1.4	0.08	0.3	5.8	B
010223	2059	2.31	39°	18.48'	111°	12.86'	0.03	0.89	7	101	0.8	0.07	0.3	4.1	B
010223	2059	44.11	39°	18.41'	111°	12.91'	0.01	0.62	7	99	0.7	0.07	0.3	0.9	B
010223	2101	55.46	39°	18.42'	111°	12.88'	0.02	1.14	7	99	0.8	0.07	0.3	4.0	B
010223	2142	41.29	39°	18.38'	111°	12.87'	0.03	0.00	6	144	0.8	0.10	0.4	4.5	C
010223	2158	27.00	39°	18.36'	111°	12.86'	0.11	1.05	7	93	0.8	0.03	0.3	1.0	B
010223	2200	13.33	39°	18.44'	111°	12.88'	0.01	0.00	6	144	0.8	0.09	0.4	4.4	C
010223	2201	58.76	39°	18.40'	111°	12.80'	0.00	0.41	6	146	0.9	0.07	0.4	3.9	C
010223	2203	9.87	39°	18.47'	111°	12.83'	0.00	0.69	7	99	0.8	0.08	0.3	4.0	B
010223	2208	4.57	39°	18.38'	111°	12.92'	0.07	0.96	7	96	0.7	0.05	0.3	3.5	B
010223	2209	26.74	39°	18.36'	111°	12.87'	0.02	0.48	6	144	0.8	0.07	0.4	4.0	C
010223	2209	47.57	39°	18.53'	111°	12.89'	0.07	0.84	8	102	0.8	0.23	0.6	3.3	C
010223	2234	45.19	39°	18.54'	111°	13.11'	0.07	0.89	7	107	0.5	0.30	0.8	10.3	C
010223	2235	27.67	39°	18.43'	111°	12.85'	0.11	0.89	7	99	0.8	0.03	0.3	1.0	B
010223	2237	40.68	39°	18.45'	111°	12.86'	0.03	1.20	8	100	0.8	0.08	0.3	3.2	B
010223	2245	11.34	39°	18.40'	111°	12.82'	0.10	0.24	6	146	0.8	0.04	0.3	1.1	C
010223	2245	42.62	39°	18.40'	111°	12.85'	0.03	0.00	7	97	0.8	0.09	0.4	4.1	B
010223	2245	49.98	39°	18.41'	111°	12.84'	0.03	1.14	7	99	0.8	0.10	0.4	4.5	B
010224	10	9.28	39°	18.36'	111°	12.82'	0.18	0.43	7	91	0.8	0.04	0.3	0.8	B
010224	1305	33.45	39°	18.00'	111°	12.86'	0.45	1.36	9	80	0.7	0.04	0.3	0.6	B
010226	1556	25.13	39°	18.47'	111°	12.97'	0.31	0.43	6	102	0.6	0.01	0.3	0.6	B
010226	1559	39.12	39°	18.46'	111°	12.89'	0.16	0.94	6	100	0.7	0.01	0.3	1.0	B
010226	1600	55.04	39°	18.45'	111°	12.95'	0.21	0.45	5	143	0.7	0.01	0.3	0.9	C
010226	1607	12.92	39°	18.42'	111°	12.92'	0.14	0.67	6	100	0.7	0.01	0.3	1.0	B
010226	1609	30.71	39°	18.39'	111°	12.93'	0.03	0.74	6	98	0.7	0.02	0.3	0.7	B
010226	1610	32.40	39°	18.40'	111°	12.93'	0.18	0.70	6	99	0.7	0.00	0.3	1.0	B
010226	1612	22.42	39°	18.41'	111°	12.98'	0.17	0.35	5	142	0.6	0.01	0.3	1.0	C
010226	1614	18.04	39°	18.37'	111°	12.89'	0.07	0.66	6	94	0.7	0.00	0.3	4.5	B
010226	1615	13.71	39°	18.41'	111°	12.97'	0.05	0.52	5	127	0.6	0.04	0.4	4.7	C
010226	1619	19.47	39°	18.41'	111°	12.95'	0.06	0.00	6	100	0.7	0.08	0.3	5.5	B
010226	1624	40.55	39°	18.39'	111°	12.94'	0.21	0.91	6	98	0.7	0.01	0.3	0.9	B
010226	1627	55.53	39°	18.42'	111°	13.01'	0.19	0.38	6	102	0.6	0.01	0.3	0.8	B
010226	1630	57.30	39°	18.42'	111°	12.94'	0.19	0.84	6	100	0.7	0.00	0.3	0.9	B
010226	1635	14.28	39°	18.35'	111°	12.89'	0.01	0.39	5	143	0.7	0.02	0.3	0.9	C
010226	1639	48.43	39°	18.45'	111°	12.85'	0.01	0.70	7	100	0.8	0.07	0.3	3.8	B
010226	1645	2.81	39°	18.43'	111°	12.87'	0.04	0.63	7	99	0.8	0.05	0.3	3.3	B
010226	1651	52.05	39°	18.41'	111°	12.86'	0.07	0.55	7	99	0.8	0.03	0.3	3.1	B
010226	1657	5.82	39°	18.36'	111°	12.87'	0.00	0.00	7	93	0.8	0.02	0.3	0.7	B
010226	1657	14.37	39°	18.41'	111°	12.85'	0.02	0.57	6	144	0.8	0.11	0.4	4.7	C
010226	1658	39.85	39°	18.38'	111°	12.88'	0.01	0.45	6	144	0.7	0.05	0.3	0.9	C
010226	1659	35.86	39°	18.38'	111°	12.89'	0.02	0.63	7	95	0.7	0.07	0.3	0.9	B
010226	1703	1.80	39°	18.39'	111°	12.88'	0.03	0.96	7	97	0.7	0.08	0.3	4.1	B
010226	1704	51.84	39°	18.38'	111°	12.88'	0.00	0.86	7	95	0.7	0.03	0.3	0.8	B
010226	1705	51.77	39°	18.36'	111°	12.88'	0.02	0.55	7	92	0.7	0.07	0.3	0.9	B
010226	1712	2.14	39°	18.35'	111°	12.88'	0.01	0.69	7	91	0.7	0.04	0.3	0.8	B
010226	1714	33.27	39°	18.36'	111°	12.88'	0.02	0.83	7	93	0.7	0.07	0.3	3.9	B
010226	1720	42.76	39°	18.39'	111°	12.87'	0.02	0.61	7	96	0.8	0.08	0.3	4.1	B
010226	1721	21.59	39°	18.34'	111°	12.87'	0.02	0.34	7	89	0.8	0.10	0.4	4.1	B
010226	1721	44.88	39°	18.41'	111°	12.85'	0.00	0.43	6	144	0.8	0.08	0.4	1.0	C
010226	1900	7.81	39°	18.50'	111°	12.90'	0.02	1.32	8	102	0.8	0.09	0.3	2.7	B
010226	1915	30.31	39°	18.56'	111°	12.86'	0.01	1.14	8	103	0.9	0.19	0.5	3.2	C
010226	2124	56.44	39°	18.38'	111°	12.86'	0.04	1.13	8	95	0.8	0.03	0.2	2.6	B
010226	2157	8.06	39°	18.41'	111°	12.88'	0.03	1.13	8	99	0.8	0.09	0.3	3.3	B
010226	2212	44.40	39°	18.52'	111°	12.88'	0.12	1.26	8	102	0.8	0.05	0.3	0.9	B
010226	2229	20.65	39°	18.40'	111°	12.92'	0.01	1.28	9	100	0.7	0.04	0.2	0.7	B
010226	2252	52.73	39°	18.38'	111°	12.89'	0.46	1.14	9	83	0.7	0.04	0.2	0.7	A
010226	2330	37.94	39°	18.40'	111°	12.95'	0.00	1.26	9	99	0.7	0.04	0.2	0.7	B
010227	6	51.71	39°	18.39'	111°	12.84'	0.03	1.10	8	97	0.8	0.09	0.3	3.2	B
010227	37	17.16	39°	18.56'	111°	12.89'	0.08	1.26	8	103	0.8	0.08	0.3	1.6	B
010227	43	29.08	39°	18.42'	111°	12.86'	0.06	1.19	7	99	0.8	0.02	0.3	3.1	B
010227	46	48.92	39°	18.42'	111°	12.95'	0.05	1.14	8	138	0.6	0.10	0.4	1.9	C
010227	212	28.43	39°	18.43'	111°	12.88'	0.03	0.54	7	99	0.8	0.07	0.3	4.1	B
010227	212	50.21	39°	18.44'	111°	12.85'	0.02	0.22	6	145	0.8	0.08	0.4	4.2	C
010227	214	29.77	39°	18.56'	111°	12.89'	0.08	1.14	8	103	0.8	0.20	0.6	3.0	C

Date	Origin Time	Latitude	Longitude	Depth	Mag	No	Gap	Dmin	Rms	Erh	Erz	Q
010227	218 17.43	39° 18.44'	111° 12.84'	0.10	1.07	8	100	0.8	0.07	0.3	2.3	B
010227	220 56.20	39° 18.37'	111° 12.80'	0.02	0.08	6	146	0.9	0.11	0.4	4.6	C
010227	317 23.69	39° 18.54'	111° 12.83'	0.08	1.28	8	103	0.9	0.05	0.3	1.7	B
010227	326 34.02	39° 18.45'	111° 12.98'	0.33	0.00	7	101	0.6	0.02	0.3	0.6	B
010227	459 37.98	39° 18.48'	111° 12.80'	0.14	1.11	8	100	0.9	0.07	0.3	0.9	B
010227	521 22.22	39° 18.40'	111° 12.60'	0.03	1.22	8	87	1.1	0.16	0.5	3.1	B
010227	557 24.08	39° 18.43'	111° 12.86'	0.09	1.15	8	99	0.8	0.08	0.3	2.5	B
010227	626 21.50	39° 18.44'	111° 12.82'	0.01	1.17	7	140	0.8	0.07	0.3	3.1	C
010227	717 40.06	39° 18.50'	111° 12.92'	0.01	1.21	7	103	0.7	0.02	0.3	0.8	B
010227	745 6.60	39° 18.35'	111° 12.86'	0.01	1.26	8	91	0.8	0.05	0.3	0.8	B
010227	800 12.12	39° 18.43'	111° 12.86'	0.00	1.40	10	89	0.8	0.06	0.3	0.6	B
010227	806 32.70	39° 18.45'	111° 12.91'	0.03	0.08	6	144	0.7	0.09	0.4	4.4	C
010227	1156 26.56	39° 18.41'	111° 12.97'	0.01	1.18	10	90	0.6	0.05	0.2	0.6	A
010227	2119 32.29	39° 18.41'	111° 12.82'	0.10	1.12	8	97	0.8	0.04	0.2	0.9	B
010227	2122 28.47	39° 18.38'	111° 12.84'	0.02	1.27	8	95	0.8	0.08	0.3	3.1	B
010227	2214 52.52	39° 18.49'	111° 12.88'	0.01	1.30	8	101	0.8	0.07	0.3	3.1	B
010227	2217 59.18	39° 18.51'	111° 12.84'	0.05	1.07	8	102	0.9	0.11	0.3	2.2	C
010227	2225 37.67	39° 18.45'	111° 12.83'	0.06	1.02	8	99	0.8	0.14	0.4	3.2	C
010227	2305 5.99	39° 18.29'	111° 12.80'	0.09	0.98	7	83	0.9	0.04	0.3	3.2	B
010227	2305 28.57	39° 18.44'	111° 12.82'	0.03	0.00	6	146	0.8	0.09	0.4	4.4	C
010227	2314 26.99	39° 18.43'	111° 12.82'	0.06	1.05	8	98	0.8	0.12	0.4	3.0	C
010228	4 5.12	39° 18.42'	111° 12.89'	0.03	1.40	10	89	0.7	0.11	0.3	1.2	B
010228	37 30.89	39° 18.41'	111° 12.87'	0.04	1.24	8	99	0.8	0.08	0.3	3.1	B
010228	106 10.91	39° 18.37'	111° 12.80'	0.04	1.40	11	84	0.9	0.17	0.4	1.8	B
010228	122 29.00	39° 18.38'	111° 12.84'	0.00	1.33	15	83	0.8	0.15	0.3	0.6	B
010228	146 23.71	39° 18.43'	111° 12.85'	0.01	0.00	7	99	0.8	0.07	0.3	4.1	B
010228	150 45.37	39° 18.44'	111° 12.80'	0.03	1.17	9	88	0.9	0.09	0.3	2.3	B
010228	209 38.04	39° 18.43'	111° 12.84'	0.01	1.24	10	89	0.8	0.10	0.3	1.5	B
010228	220 51.05	39° 18.38'	111° 12.82'	0.01	1.22	10	88	0.8	0.05	0.2	1.2	A
010228	516 36.50	39° 18.40'	111° 12.93'	0.04	1.19	8	100	0.7	0.09	0.3	2.5	B
010228	555 31.80	39° 18.45'	111° 12.79'	0.00	1.20	10	88	0.9	0.11	0.3	1.7	B
010228	628 46.43	39° 18.44'	111° 12.62'	0.03	1.13	9	87	1.1	0.15	0.4	2.6	B
010228	629 30.20	39° 18.45'	111° 12.74'	0.10	1.15	9	87	0.9	0.06	0.2	0.8	B
010228	708 47.06	39° 18.45'	111° 12.60'	0.03	1.07	9	88	1.1	0.15	0.4	2.6	B
010228	711 29.76	39° 18.38'	111° 12.72'	0.14	1.41	13	85	0.9	0.27	0.5	1.3	C
010228	729 19.82	39° 18.39'	111° 12.84'	0.01	0.61	7	96	0.8	0.07	0.3	3.8	B
010228	729 36.95	39° 18.43'	111° 12.70'	0.05	1.24	9	87	1.0	0.13	0.4	2.5	B
010228	740 56.62	39° 18.47'	111° 12.81'	0.09	0.99	8	99	0.9	0.04	0.2	2.7	B
010228	743 36.99	39° 18.49'	111° 12.82'	0.06	0.98	7	100	0.9	0.02	0.3	3.4	B
010228	822 39.89	39° 18.33'	111° 12.83'	0.08	1.56	14	84	0.8	0.11	0.3	1.0	B
010228	855 34.33	39° 18.41'	111° 12.82'	0.04	0.96	8	97	0.8	0.10	0.3	2.7	B
010228	1026 50.67	39° 18.44'	111° 12.82'	0.02	1.11	8	99	0.8	0.07	0.3	3.1	B
010228	1027 44.41	39° 18.42'	111° 12.84'	0.00	1.12	8	99	0.8	0.09	0.3	2.6	B
010228	1051 51.64	39° 18.34'	111° 12.86'	0.20	0.76	7	89	0.8	0.03	0.3	0.7	B
010228	1125 21.61	39° 18.46'	111° 12.82'	0.00	1.27	10	88	0.9	0.05	0.2	1.4	A
010228	1153 35.23	39° 18.35'	111° 12.84'	0.01	1.14	8	91	0.8	0.07	0.3	3.0	B
010228	1200 42.99	39° 18.35'	111° 12.85'	0.00	1.09	8	91	0.8	0.03	0.2	0.7	B
010228	1306 43.15	39° 18.36'	111° 12.84'	0.08	0.74	7	92	0.8	0.03	0.3	3.3	B
010228	1306 53.67	39° 18.43'	111° 12.81'	0.01	1.11	7	98	0.9	0.03	0.3	3.5	B
010228	1452 53.48	39° 18.39'	111° 12.88'	0.01	1.26	9	89	0.8	0.05	0.3	1.7	B
010228	1531 19.62	39° 18.43'	111° 12.81'	0.00	0.95	7	98	0.8	0.03	0.3	3.3	B
010228	1531 37.84	39° 17.92'	111° 13.87'	0.36	1.36	7	88	1.1	0.03	0.3	999.9	B
010228	1545 40.82	39° 18.39'	111° 12.91'	0.06	1.13	7	97	0.7	0.09	0.3	4.1	B
010228	1547 39.69	39° 18.46'	111° 12.84'	0.01	1.20	8	100	0.8	0.05	0.3	2.8	B
010228	1548 45.26	39° 18.41'	111° 12.84'	0.04	1.00	8	98	0.8	0.08	0.3	2.5	B
010228	1617 14.18	39° 18.38'	111° 12.85'	0.02	0.71	7	95	0.8	0.07	0.3	4.0	B
010228	1701 57.68	39° 18.44'	111° 12.89'	0.04	1.24	8	100	0.7	0.09	0.3	3.4	B
010228	1732 45.10	39° 18.41'	111° 12.82'	0.02	1.48	9	88	0.8	0.11	0.3	2.2	B
010228	1743 22.33	39° 18.52'	111° 12.86'	0.09	1.17	8	102	0.8	0.03	0.2	2.0	B
010228	1808 0.90	39° 18.43'	111° 12.87'	0.09	1.32	8	99	0.8	0.03	0.2	2.6	B
010228	1820 1.28	39° 18.34'	111° 12.81'	0.04	1.15	7	173	0.8	0.09	0.5	2.6	C
010228	1849 19.94	39° 18.45'	111° 12.84'	0.05	1.02	8	100	0.8	0.08	0.3	3.1	B
010228	1917 42.22	39° 18.40'	111° 12.82'	0.11	1.37	8	97	0.8	0.02	0.2	0.9	B
010228	1920 18.29	39° 18.39'	111° 12.81'	0.02	1.18	8	95	0.8	0.07	0.3	3.0	B
010228	2007 10.94	39° 18.42'	111° 12.84'	0.00	1.00	8	99	0.8	0.08	0.3	3.2	B
010228	2012 32.77	39° 18.47'	111° 12.80'	0.03	0.39	7	99	0.9	0.08	0.3	4.2	B
010228	2131 36.02	39° 18.43'	111° 12.85'	0.15	0.95	7	99	0.8	0.03	0.3	0.8	B
010228	2138 36.78	39° 18.51'	111° 12.73'	0.08	1.43	10	87	1.0	0.08	0.3	1.7	B

Date	Origin Time	Latitude	Longitude	Depth	Mag	No	Gap	Dmin	Rms	Erh	Erz	Q
010228	2202 4.38	39° 18.49'	111° 12.83'	0.09	1.45	9	101	0.8	0.08	0.3	2.1	B
010228	2210 2.26	39° 18.47'	111° 12.84'	0.04	1.24	7	101	0.8	0.10	0.3	4.0	B
010228	2211 2.37	39° 18.43'	111° 12.82'	0.03	1.19	8	98	0.8	0.09	0.3	2.5	B
010228	2216 33.88	39° 18.37'	111° 12.82'	0.04	0.88	7	93	0.8	0.08	0.3	4.0	B
010228	2216 50.43	39° 18.45'	111° 12.80'	0.03	1.09	7	99	0.9	0.08	0.3	4.1	B
010228	2244 10.31	39° 18.42'	111° 12.81'	0.14	1.04	8	98	0.9	0.04	0.2	0.8	B
010228	2307 58.33	39° 18.43'	111° 12.82'	0.04	1.16	7	98	0.8	0.08	0.3	4.0	B
010228	2316 22.72	39° 18.46'	111° 12.76'	0.22	1.23	9	98	0.9	0.06	0.3	0.7	B
010228	2344 10.31	39° 18.51'	111° 12.77'	0.14	1.47	12	88	0.9	0.07	0.2	0.6	B
010228	2347 33.55	39° 18.42'	111° 12.83'	0.02	1.17	8	98	0.8	0.08	0.3	3.1	B
010228	2347 45.08	39° 18.52'	111° 12.95'	0.09	2.02	8	104	0.7	0.06	0.3	2.3	B
010301	35 16.39	39° 18.49'	111° 12.77'	0.01	1.28	11	88	0.9	0.12	0.3	1.8	B
010301	45 53.93	39° 18.46'	111° 12.85'	0.01	1.16	8	100	0.8	0.06	0.3	2.2	B
010301	156 59.36	39° 18.38'	111° 12.83'	0.01	1.16	8	94	0.8	0.07	0.3	2.9	B
010301	200 43.21	39° 18.45'	111° 12.78'	0.04	1.13	10	99	0.9	0.12	0.3	1.9	C
010301	225 49.86	39° 18.46'	111° 12.80'	0.05	1.23	8	99	0.9	0.16	0.4	3.6	C
010301	327 12.31	39° 18.48'	111° 12.82'	0.05	1.12	8	100	0.9	0.13	0.4	3.1	C
010301	348 21.24	39° 18.40'	111° 12.79'	0.11	1.29	10	88	0.9	0.03	0.2	0.6	A
010301	415 14.78	39° 18.51'	111° 12.79'	0.15	1.26	11	88	0.9	0.06	0.2	0.5	B
010301	511 27.73	39° 18.54'	111° 12.78'	0.09	1.30	8	101	0.9	0.06	0.3	2.6	B
010301	537 13.22	39° 18.39'	111° 12.84'	0.01	1.19	8	96	0.8	0.07	0.3	3.1	B
010301	537 35.35	39° 18.40'	111° 12.84'	0.02	0.00	6	145	0.8	0.07	0.4	4.0	C
010301	552 31.58	39° 18.46'	111° 12.82'	0.02	1.10	7	99	0.9	0.07	0.3	4.1	B
010301	630 1.48	39° 18.50'	111° 12.76'	0.19	1.31	10	100	0.9	0.07	0.2	0.6	B
010301	637 50.19	39° 18.46'	111° 12.75'	0.22	1.19	10	98	0.9	0.08	0.3	0.7	B
010301	653 3.07	39° 18.41'	111° 12.82'	0.00	1.19	8	98	0.8	0.04	0.2	2.7	B
010301	653 20.57	39° 18.47'	111° 12.79'	0.09	1.07	8	99	0.9	0.05	0.3	1.8	B
010301	704 46.26	39° 18.49'	111° 12.80'	0.07	1.25	8	100	0.9	0.02	0.2	2.6	B
010301	743 18.63	39° 18.48'	111° 12.76'	0.18	1.09	9	100	0.9	0.06	0.2	0.7	B
010301	829 38.22	39° 18.58'	111° 12.74'	0.22	1.31	10	101	1.0	0.07	0.3	0.6	B
010301	1525 35.20	39° 18.44'	111° 12.82'	0.09	0.00	8	98	0.8	0.04	0.2	2.7	B
010301	1626 16.42	39° 18.52'	111° 12.76'	0.06	1.39	10	87	0.9	0.13	0.3	2.6	B
010301	1702 13.83	39° 18.43'	111° 12.78'	0.12	1.08	8	98	0.9	0.04	0.2	0.9	B
010301	1732 37.39	39° 18.42'	111° 12.80'	0.04	1.17	8	98	0.9	0.10	0.3	3.6	B
010301	1803 54.81	39° 18.44'	111° 12.82'	0.16	1.21	8	99	0.8	0.03	0.2	0.7	B
010301	1838 19.14	39° 18.43'	111° 12.81'	0.01	1.19	7	98	0.9	0.07	0.3	3.9	B
010301	1902 15.63	39° 18.55'	111° 12.79'	0.13	1.05	8	102	0.9	0.09	0.3	1.0	B
010301	1922 6.64	39° 18.42'	111° 12.80'	0.03	1.08	8	98	0.9	0.08	0.3	3.1	B
010301	1952 58.14	39° 18.44'	111° 12.81'	0.03	1.00	8	98	0.8	0.08	0.3	3.1	B
010301	2029 13.55	39° 18.37'	111° 12.84'	0.00	0.75	7	93	0.8	0.07	0.3	0.9	B
010301	2058 14.79	39° 18.38'	111° 12.82'	0.03	0.48	6	145	0.8	0.07	0.4	4.0	C
010301	2058 48.73	39° 18.46'	111° 12.82'	0.01	0.52	6	146	0.9	0.08	0.4	4.2	C
010301	2059 21.79	39° 18.38'	111° 12.81'	0.04	1.66	6	146	0.8	0.08	0.4	4.2	C
010301	2110 55.58	39° 18.43'	111° 12.79'	0.02	1.00	7	98	0.9	0.07	0.3	3.8	B
010301	2304 0.47	39° 18.52'	111° 12.80'	0.07	1.27	9	101	0.9	0.11	0.3	3.2	C
010301	2321 2.31	39° 18.47'	111° 12.84'	0.21	0.36	6	145	0.8	0.03	0.3	0.8	C
010301	2322 1.21	39° 18.38'	111° 12.82'	0.07	0.67	7	94	0.8	0.03	0.3	3.1	B
010301	2350 2.62	39° 18.46'	111° 12.80'	0.00	0.19	6	146	0.9	0.08	0.4	4.1	C
010301	2351 1.24	39° 18.42'	111° 12.82'	0.02	0.89	7	98	0.8	0.07	0.3	3.9	B
010302	8 9.00	39° 18.45'	111° 12.80'	0.08	1.01	8	99	0.9	0.03	0.2	2.6	B
010302	104 48.24	39° 18.46'	111° 12.79'	0.03	1.04	8	99	0.9	0.11	0.3	3.6	C
010302	108 29.78	39° 18.46'	111° 12.69'	0.05	1.44	10	87	1.0	0.14	0.4	2.3	B
010302	111 2.04	39° 18.41'	111° 12.82'	0.02	1.08	7	97	0.8	0.07	0.3	3.8	B
010302	140 7.84	39° 18.52'	111° 12.78'	0.23	1.26	9	101	0.9	0.06	0.3	0.7	B
010302	204 29.74	39° 18.43'	111° 12.81'	0.01	1.20	7	98	0.8	0.06	0.3	3.8	B
010302	204 57.57	39° 18.33'	111° 12.84'	0.13	0.00	7	87	0.8	0.02	0.3	0.9	B
010302	231 8.80	39° 18.37'	111° 12.83'	0.09	1.07	7	92	0.8	0.02	0.3	3.3	B
010302	248 47.26	39° 18.41'	111° 12.81'	0.12	1.14	8	98	0.8	0.03	0.2	0.8	B
010302	248 59.04	39° 18.45'	111° 12.79'	0.03	0.94	7	99	0.9	0.08	0.3	4.0	B
010302	252 19.04	39° 18.44'	111° 12.79'	0.07	1.03	8	98	0.9	0.04	0.2	2.6	B
010302	328 49.56	39° 18.46'	111° 12.86'	0.01	1.08	7	100	0.8	0.07	0.3	4.0	B
010302	505 23.96	39° 18.46'	111° 12.79'	0.01	1.34	8	99	0.9	0.07	0.3	3.1	B
010302	526 8.41	39° 18.50'	111° 12.77'	0.00	1.29	9	100	0.9	0.11	0.3	3.1	C
010302	629 3.23	39° 18.41'	111° 12.85'	0.03	0.86	7	99	0.8	0.07	0.3	4.0	B
010302	630 10.79	39° 18.44'	111° 12.82'	0.02	0.92	7	98	0.8	0.07	0.3	3.8	B
010302	809 58.13	39° 18.54'	111° 12.79'	0.09	1.17	10	102	0.9	0.07	0.3	1.4	B
010302	819 49.75	39° 18.47'	111° 12.85'	0.10	1.17	8	100	0.8	0.02	0.2	2.0	B
010302	1024 34.54	39° 18.37'	111° 12.87'	0.04	0.00	6	93	0.7	0.09	0.4	4.7	B

Date	Origin Time		Latitude		Longitude		Depth	Mag	No	Gap	Dmin	Rms	Erh	Erz	Q
010302	1640	41.32	39°	18.39'	111°	12.81'	0.01	0.72	7	94	0.8	0.07	0.3	3.8	B
010302	1726	52.60	39°	18.46'	111°	12.81'	0.00	1.15	7	99	0.9	0.07	0.3	4.0	B
010302	1950	25.71	39°	18.45'	111°	12.81'	0.00	0.39	6	146	0.9	0.08	0.4	4.3	C
010302	1952	53.73	39°	18.43'	111°	12.81'	0.03	0.00	6	146	0.9	0.01	0.3	3.3	C
010302	2109	40.59	39°	18.48'	111°	12.77'	0.01	1.20	8	100	0.9	0.08	0.3	3.3	B
010302	2117	20.96	39°	18.46'	111°	12.80'	0.03	0.75	7	99	0.9	0.08	0.3	4.1	B
010302	2232	44.19	39°	18.46'	111°	12.81'	0.00	0.96	7	99	0.9	0.07	0.3	3.9	B
010302	2240	33.35	39°	18.35'	111°	12.83'	0.03	1.15	7	90	0.8	0.07	0.3	3.9	B
010302	2333	0.56	39°	18.49'	111°	12.78'	0.08	1.18	9	100	0.9	0.05	0.2	1.1	B
010303	1640	30.99	39°	18.53'	111°	12.76'	0.37	1.29	9	101	0.9	0.06	0.3	10.8	B
010303	1706	34.85	39°	18.41'	111°	12.80'	0.02	1.04	8	97	0.9	0.07	0.3	3.1	B
010303	1742	22.92	39°	18.45'	111°	12.78'	0.02	1.19	7	99	0.9	0.01	0.3	3.2	B
010303	1807	12.81	39°	18.36'	111°	12.81'	0.00	1.10	7	91	0.8	0.06	0.3	3.7	B
010303	1827	21.27	39°	18.46'	111°	12.86'	0.00	1.03	7	100	0.8	0.05	0.3	0.8	B
010303	1843	40.36	39°	18.37'	111°	12.84'	0.02	0.55	7	93	0.8	0.08	0.3	3.9	B
010303	1954	58.46	39°	18.42'	111°	12.81'	0.03	1.11	7	98	0.8	0.08	0.3	4.1	B
010303	2021	56.56	39°	18.35'	111°	12.78'	0.08	0.90	7	90	0.9	0.03	0.3	3.2	B
010304	4	34.23	39°	18.40'	111°	12.86'	0.01	1.16	9	98	0.8	0.08	0.3	0.8	B
010304	119	42.26	39°	18.38'	111°	12.83'	0.02	1.38	9	93	0.8	0.04	0.2	1.0	B
010304	320	14.40	39°	18.40'	111°	12.86'	0.00	1.27	10	98	0.8	0.05	0.2	0.5	B
010305	1604	46.23	39°	18.41'	111°	12.79'	0.03	1.00	7	97	0.9	0.08	0.3	4.0	B
010305	1609	29.93	39°	18.38'	111°	12.81'	0.04	1.06	7	93	0.8	0.08	0.3	4.0	B
010305	1726	37.50	39°	18.39'	111°	12.79'	0.07	1.26	7	95	0.9	0.02	0.3	3.2	B
010305	2027	16.82	39°	18.43'	111°	12.75'	0.00	0.64	7	97	0.9	0.07	0.3	3.7	B
010305	2211	41.36	39°	18.39'	111°	12.78'	0.12	0.36	6	146	0.9	0.02	0.3	1.0	C
010305	2211	57.29	39°	18.42'	111°	12.78'	0.05	0.37	6	146	0.9	0.07	0.4	4.1	C
010305	2212	35.33	39°	18.39'	111°	12.77'	0.12	0.70	6	146	0.9	0.02	0.3	1.0	C
010305	2216	29.33	39°	18.41'	111°	12.79'	0.07	1.15	7	140	0.9	0.11	0.4	2.8	C
010305	2253	11.12	39°	18.48'	111°	12.72'	0.02	1.23	9	87	1.0	0.13	0.3	2.2	B
010306	455	23.25	39°	18.48'	111°	12.69'	0.20	1.16	9	98	1.0	0.06	0.3	0.7	B
010306	639	1.22	39°	18.40'	111°	12.77'	0.09	1.04	8	96	0.9	0.03	0.2	2.7	B
010306	1035	17.70	39°	18.35'	111°	12.84'	0.02	0.39	7	90	0.8	0.09	0.4	4.2	B
010307	35	4.02	39°	18.39'	111°	12.77'	0.02	0.82	6	146	0.9	0.08	0.4	4.1	C
010307	47	54.15	39°	18.33'	111°	12.81'	0.14	0.23	6	145	0.8	0.04	0.4	0.9	C
010307	48	22.22	39°	18.40'	111°	12.75'	0.03	0.00	6	148	0.9	0.02	0.3	3.3	C
010307	141	54.39	39°	18.50'	111°	12.70'	0.10	1.16	8	99	1.0	0.08	0.3	2.5	B
010307	158	37.66	39°	18.49'	111°	13.10'	0.21	0.00	6	139	0.5	0.02	0.3	0.6	C
010307	158	42.36	39°	18.38'	111°	12.75'	0.06	0.75	7	92	0.9	0.09	0.3	4.2	B
010307	256	31.20	39°	18.42'	111°	12.75'	0.09	1.17	7	97	0.9	0.02	0.3	3.4	B
010307	304	13.77	39°	18.40'	111°	12.75'	0.01	1.18	6	147	0.9	0.07	0.4	4.0	C
010307	531	46.54	39°	18.39'	111°	12.77'	0.02	1.30	8	95	0.9	0.05	0.3	2.7	B
010307	637	8.22	39°	18.41'	111°	12.75'	0.00	1.22	8	95	0.9	0.07	0.3	3.1	B
010307	839	35.93	39°	18.39'	111°	12.77'	0.05	0.08	6	146	0.9	0.09	0.4	4.4	C
010307	840	5.83	39°	18.48'	111°	12.72'	0.05	0.00	8	98	0.9	0.14	0.4	3.4	C
010307	913	18.14	39°	18.38'	111°	12.77'	0.03	0.50	7	94	0.9	0.07	0.3	4.1	B
010307	1954	23.47	39°	18.43'	111°	12.75'	0.04	0.89	6	148	0.9	0.07	0.4	4.1	C
010307	1954	56.20	39°	18.44'	111°	12.77'	0.05	0.34	6	147	0.9	0.08	0.4	4.3	C
010307	2218	42.26	39°	18.44'	111°	12.73'	0.36	1.21	6	148	0.9	0.04	0.3	999.9	C
010308	749	45.36	39°	18.53'	111°	12.76'	0.01	1.15	10	101	0.9	0.12	0.3	1.5	C
010308	952	34.43	39°	18.47'	111°	12.70'	0.18	1.30	11	98	1.0	0.07	0.2	0.6	B
010308	1623	31.55	39°	18.46'	111°	12.68'	0.03	1.24	8	97	1.0	0.10	0.3	2.1	B
010308	1659	31.05	39°	18.44'	111°	12.82'	0.02	0.60	6	146	0.8	0.02	0.3	3.3	C
010308	1909	50.96	39°	18.40'	111°	12.75'	0.01	0.70	6	147	0.9	0.07	0.4	4.1	C
010310	405	2.19	39°	18.06'	111°	13.18'	0.43	1.49	10	75	0.6	0.06	0.2	0.8	B
010311	1549	29.51	39°	18.53'	111°	12.71'	0.05	1.23	9	100	1.0	0.06	0.3	1.1	B
010313	1223	6.65	39°	17.94'	111°	14.05'	0.10	1.50	13	89	1.2	0.06	0.2	0.9	B
010313	1326	38.33	39°	17.95'	111°	13.73'	0.01	0.95	6	88	0.9	0.07	0.3	3.9	B
010313	1540	30.97	39°	18.25'	111°	13.07'	0.01	0.37	6	131	0.5	0.01	0.4	0.8	B
010313	1706	21.39	39°	18.43'	111°	12.76'	0.05	0.19	6	147	0.9	0.09	0.4	4.5	C
010313	1823	27.90	39°	18.33'	111°	13.88'	0.02	0.65	6	112	0.8	0.06	0.3	3.4	B
010313	2105	52.25	39°	18.36'	111°	12.84'	0.03	0.95	6	144	0.8	0.08	0.4	4.2	C
010314	534	53.15	39°	18.47'	111°	13.75'	0.03	0.52	7	117	0.6	0.04	0.3	0.7	B
010314	1251	18.40	39°	18.40'	111°	12.76'	0.06	0.61	7	96	0.9	0.09	0.3	4.5	B
010314	2126	32.50	39°	18.41'	111°	12.79'	0.01	0.97	5	146	0.9	0.07	0.4	4.7	C
010317	1400	28.01	39°	18.29'	111°	14.24'	0.38	0.39	6	115	1.2	0.03	0.3	9.4	B
010318	2135	47.81	39°	18.05'	111°	14.06'	0.04	1.66	13	95	1.1	0.14	0.3	1.3	C
010330	2133	16.62	39°	18.62'	111°	13.82'	0.00	1.50	13	127	0.8	0.08	0.2	0.8	B
010410	149	25.60	39°	17.80'	111°	13.92'	0.38	0.83	6	86	1.3	0.04	0.3	14.1	B

DATE	ORIGIN TIME	LATITUDE	LONGITUDE	DEPTH	MAG	NO	GAP	DMIN	RMS	ERH	ERZ	Q
010426	1638 19.99	39° 17.87'	111° 11.69'	0.38	1.28	12	72	1.1	0.08	0.2	1.3	B

EXPLANATION

ID	A sequential identification number assigned to each seismic event for reference purposes.
DATE	Date in Universal Coordinated Time (UTC). Subtract seven hours to Mountain Standard Time.
ORIGIN TIME	Hour, minute, and seconds of the start time of the seismic event (UTC).
LATITUDE	Seismic event location coordinates in degrees and minutes, North.
LONGITUDE	Seismic event location coordinates in degrees and minutes, West.
DEPTH	Seismic event depth in kilometers. The asterisk indicates an "A" quality depth (DMIN ≤ DEPTH and ERZ ≤ 2.0 km).
MAG	Duration magnitude.
NO	The number of P and S arrival readings used in the event solution.
GAP	The largest azimuthal separation in degrees between the recording stations used in the solution.
DMIN	The epicentral distance in kilometers.
RMS	The root mean square of the travel time residuals in seconds.
ERH	Standard horizontal error in kilometers.
ERZ	Standard vertical error in kilometers.
Q	Assigned epicentral quality parameter based on an average of the following two schemes:

Station Distribution Scheme			Statistical Measure Scheme		
	NO	GAP		RMS (sec)	ERH (km)
A	≥ 8	≤ 90°	A	≤ 0.05	< 0.2
B	≥ 6	≤ 135°	B	≤ 0.10	< 0.4
C	≥ 6	≤ 180°	C	≤ 0.20	< 0.6
D	others	others	D	others	

APPENDIX E

CONSTRAINTS ON LOCATIONS OF MINING SEISMICITY IN THE TRAIL MOUNTAIN AREA

by

Kristine L. Pankow, Matthew E. Jensen, and James C. Pechmann
University of Utah Seismograph Stations
Department of Geology and Geophysics
University of Utah

CONSTRAINTS ON LOCATIONS OF MINING SEISMICITY IN THE TRAIL MOUNTAIN AREA

by

Kristine L. Pankow, Matthew E. Jensen, and James C. Pechmann
University of Utah Seismograph Stations
Department of Geology and Geophysics
University of Utah

As discussed in section 3.3.2 of the main text, great effort was expended to refine hypocentral locations. In this Appendix we discuss the details.

E.1 STATION DISTRIBUTION, TOPOGRAPHY, AND VELOCITY MODEL

The Problem

During routine data processing, it was observed that P-wave arrival times at stations TB1 and TB2 were consistently early (residuals of ~0.5 sec.) when compared to the theoretical arrival times calculated by our routine earthquake location program. Residuals this large can severely bias a location, so it was important to learn the cause of these early arrivals.

Hypoinverse (Klein, 1978) is an earthquake hypocenter location program used routinely at UUSS. It works by calculating travel times from a trial earthquake location to the surrounding stations, comparing these times with the observed times, repositioning the earthquake and repeating the above process. This algorithm continues until the difference between the calculated and observed travel times is minimized. To calculate accurate travel times a detailed velocity model is required. Hypoinverse can only accept one-dimensional layered velocity models. However, it does have a UUSS added option to correct for differences in station elevation, which works as follows. Given a layered velocity structure and an earthquake within that structure, hypoinverse calculates the travel time from the earthquake to the top of the velocity model, called the datum (Figure E-1). It then corrects the travel time for the difference in elevation between the datum and the station. Figure E-1(a) illustrates this technique. The time difference between the station (S) and the station projected to the datum (S') is the time from A to S'. This time is approximated using a simple trigonometric equation. Figure E-1(b) illustrates the case when the stations and the datum are in different layers. The figure shows that the difference in travel time is the difference from A to B (travelling at velocity V_s) plus the time from B to S' (travelling at velocity V_d). Since the velocity changes the angle of the ray changes and the total time difference is no longer a simple trigonometric calculation. Hypoinverse is not designed to account for this situation, and thus gives incorrect results, expressed as high residuals. Note that the diagrams in Figure E-1 are simplifications of the Trail Mountain situation because they omit the thin topmost layer in the model, which we

interpret to be a weathering layer present everywhere at the earth's surface regardless of elevation. As explained in Appendix B, we assume that the elevation changes are accommodated by changes in the thickness of the second layer in the Trail Mountain model (corresponding to layer 1 in Figure E-1), and therefore, we use the velocities of the second layer (V_p = 4.0 km/sec) to compute elevation corrections.

The Solution

Figures E-2 and E-3 show map and cross-sectional views, respectively, for the local study area. Returning to the earlier noted travel time inconsistency at TB1 and TB2 note that both of these stations as well as TU1 are in the velocity layer below the layer used to calculate elevation corrections (as in Figure E-1(b)). Figure E-3 shows an added complication of calculating all rays to the top of the datum. For station TB2 the energy probably travels as a direct ray, but hypoinverse calculates a refracted ray. Since hypoinverse is not designed to accurately calculate the travel times to stations TB1, TB2, and TU1, data from these stations were removed from the location process. Including them would have biased the resulting locations.

E.2 PICKING S-WAVE ARRIVAL TIMES

Gomberg *et al.* (1990) showed that a correctly picked S-wave recorded within about 1.4 focal depth's distance from the epicenter can be an important constraint on focal depth. However, they also found that an incorrect pick can lead to depth and depth error estimates that are significantly incorrect. Picking accurate S-wave arrival times for this data set was challenging. To ensure that the picks made were as accurate as possible, data from three-component stations were processed to enhance the visibility of the S-wave arrivals. Because this level of processing was time consuming, S-picks were added only to the USGS and UUSS data sets.

To enhance the S waves, the horizontal-component data (north-south and east-west) were rotated to a coordinate system with axes parallel to and perpendicular to the source-receiver azimuth, i.e., the predicted P and S ray path directions in a laterally homogeneous earth. This rotation relies on an accurate epicenter. Thus, depending on the distance to the station, small errors in epicentral location can result in large errors in the rotation angle. Ideally the rotation minimizes the amount of P- and P-to-S converted energy on the seismogram perpendicular to the ray direction, which is called the transverse component. The seismogram parallel to the incoming ray is called the radial component and contains both P- and S-wave energy. Since the transverse component ideally contains only S-wave motion, the P wave should not be seen on this trace, and the first recorded motion should be the S wave. Figure E-4 shows the results of rotating the horizontal components from USGS event #42 recorded at station TM2. The P-wave motion is not entirely suppressed, but in this example it is sufficiently damped making identifying the S-phase easier. Unfortunately, the rotation does not sufficiently suppress P-wave motion for all event station pairs, or else reflected P wave energy or surface waves are recorded on the transverse component masking the direct S-wave (Figure E-5). Only when there was a clear arrival on the transverse component was an S-arrival time picked.

E.3 RMS VARIABILITY WITHIN A RANGE OF FIXED DEPTHS

The forty-nine events sent to the USGS were each analyzed to determine the uniqueness and stability of the focal-depth solutions. This analysis was done by examining the variability of the weighted root mean square difference between the observed and computed arrival times (RMS) for a range of fixed focal-depth values (Williams and Arabasz, 1989; Johnston *et al.*, 1984). There were two primary objectives for this exercise: 1) to improve focal-depth resolution (i.e. provide tighter focal-depth constraint) for the USGS data set, and 2) to check focal-depth values for the deeper events in this data set (events below mine level, i.e., more than 500 to 600 meters below the datum).

We located each of the events using Hypoinverse for a range of fixed depths from 0.1 to 10.0 km. Because mining induced seismicity is generally shallow, the fixed depth spacing for the first kilometer was 0.1 km. This spacing gradually increased to 1.0-km increments for depths between 7.0 and 10.0 km. The RMS values obtained from this process were plotted as a function of the fixed focal depth. On the same plot, the focal depth obtained from routine processing (i.e., the free depth Hypoinverse solution) was plotted along with error bars corresponding to the 95% confidence interval (Figure E-6). The minimum in the plot, if one occurs, is the focal depth that best fits the data.

Focal-depth resolution was generally not significantly improved through this procedure. As evident in Figure E-6, the minima were not always sharp. In many cases, RMS was constant or nearly constant for fixed depths at and above mine level (Figure E-6). While this observation indicates that these events are near or above mine level, it does not allow us to further constrain the focal depth. Other events did exhibit a defined minimum as in Figure E-6(b), but the difference between the minimum and the adjacent points was usually a statistically insignificant 0.01 seconds RMS. Although the depth vs. RMS plots did not improve focal-depth resolution, they did confirm the focal depth results obtained in routine processing. On all forty-nine of the Depth vs. RMS plots the set of focal depths with the minimum RMS value lies within the 95% confidence interval of the original focal-depth solution.

Based on the original locations, only events #6, #24, #35, and #38 (see Appendix C-1) were below the mine. For these four events, additional depth vs. RMS plots were made which included the stations TB1 and TB2 (Stations TB1 and TB2 were left out of routine processing for reasons explained in Section E.1). If an event was below TB1 and TB2, these stations could be used in the location procedure. Figure E-7(a) is a plot of event #24. The RMS for this event is consistently lower when including TB1 and TB2 in the location (the dashed line). Similarly, events #6 and #35 also have lower RMS when TB1 and TB2 were used. In contrast, when TB1 and TB2 were used for shallower events, RMS values generally increased. This result suggests that these three events are in fact lower than TB1 and TB2, and are therefore at or below mine level. The minimum between 0.5 and 0.7-km depth in the dashed line in Figure E-7(a) is consistent with this conclusion.

Event #35 is of particular interest because it is the only event in the USGS data set with a computed focal depth greater than 1 km. This event is located north of the 1st right longwall panel at a focal depth of 2.07 km. The depth vs. RMS plot for this event is shown in Figure E-7(b). Note the lack of focal-depth control. Using TB1 and TB2 in the location, the minimum

extends from 0 to 2-km depth with a small increase at 1-km depth. The actual focal depth could be anywhere in that range. Without using TB1 and TB2 in the location, the zone of uncertainty extends to 2.5-km depth with four separate, insignificant minima in the topmost 1.4 km. In general, this event is poorly located compared to other events in the USGS data set. The RMS value is relatively large, 0.15 seconds, as is the azimuthal gap, 146°.

In summary, the focal-depth resolution was not significantly improved by this procedure. However, the procedure did confirm that the focal depth 95% confidence limits obtained in routine processing are large enough to include the entire range of best-fit focal depths. There were four events possibly deeper than mine level with one possibly deeper than 1 kilometer. Lower RMS values were obtained for three of the four events by using TB1 and TB2 in the locations. This result suggests that these events are below the level of these stations. Even so, the depth vs. RMS plots did not satisfactorily confirm that these "deep" events have focal depths below the mine level.

E.4 ANALYSIS OF PARTICLE MOTION AND THREE-COMPONENT FIRST MOTIONS

Stations TB1, TB2, and TU1 were located in a unique position relative to the active longwall (Figure E-3). Since they were at approximately the same elevation, seismic energy traveled almost horizontally from the longwall to these stations, especially at the closer TU1. This phenomenon first became apparent by analysis of the raw data. At TU1 the first arriving energy was on the east component (nearly parallel to the direction to the longwall). On most seismograms, the first arriving P-wave energy is seen on the vertical component.

This anomalous horizontal propagation was exploited to validate the locations in the USGS data. To do this, the particle motion in a time window including the first 1-1.5 cycles of energy on the east and north components was examined (Figure E-8). We measured the horizontal incident angle (HIA) from the particle motion plots and compared it to the backazimuth (the angle from the station to the previously determined earthquake location). Figure E-9 shows the results of comparing HIA's from TB2 and TU1 to their respective backazimuths. Since the particle motion matches the backazimuth to both stations (within ~15°) we conclude that the majority of these events are well located. Further, plotting the horizontal particle motion versus time reveals that with 4 exceptions the USGS data set is located within 0.5 km of the coal panel being actively mined (Figure E-10). The particle motion of the radial (see Section E.2) versus the vertical energy was also examined. However, most of the particle motions were elliptical and measuring the vertical incident angle was difficult if not impossible for most events. Thus, we were able to validate the epicentral locations, but not the depths using the particle motion analysis.

REFERENCES

Gomberg, J.S., Shedlock, K.M., and S.W. Roecker (1990). The effect of S-wave arrival times on the accuracy of hypocenter estimation, *Bull. Seism. Soc.* **80**, 1605-1628.

Johnston, A.C., Reinbold, D.J., and S.I. Brewer (1984). Seismotectonics of the southern Appalachians, *Bull. Seism. Soc. Am.* **75**, 291-312.

Klein, F.W. (1978). Hypocenter location program HYPOINVERSE, *U.S. Geol. Surv., Open-File Rept. 78-694*, 113 pp.

Williams, D.J. and W.J. Arabasz (1989). Mining-related and tectonic sesimicity in the East Mountain area, Wasatch Plateau, Utah, *PAGEOPH* **129**, 345-368.

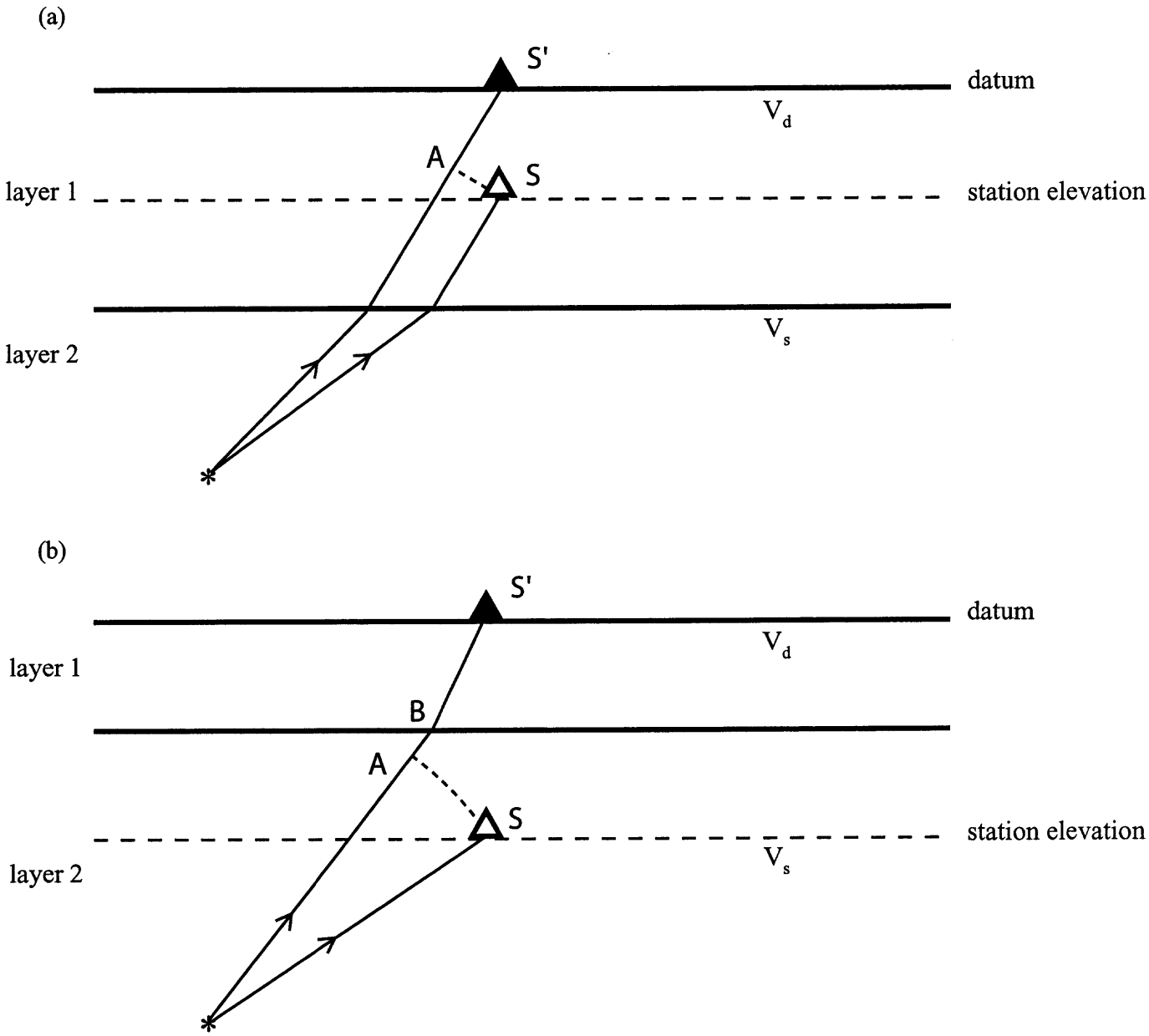

Figure E-1. Example ray paths illustrating how hypoinverse corrects for station elevation. Datum is the top of the velocity model. S is the true position of the station. S' is the station projected to the datum. V_d is the velocity in layer 1. V_s is the velocity in layer 2. The star is the position of the earthquake. The dashed curve between A and S is a wavefront. (a) The case when both S and S' are in the same velocity layer. The travel time difference is the time from A to S'. (b) The case when S and S' are in different velocity layers. The travel time difference is the time from A to B plus the time from B to S'.

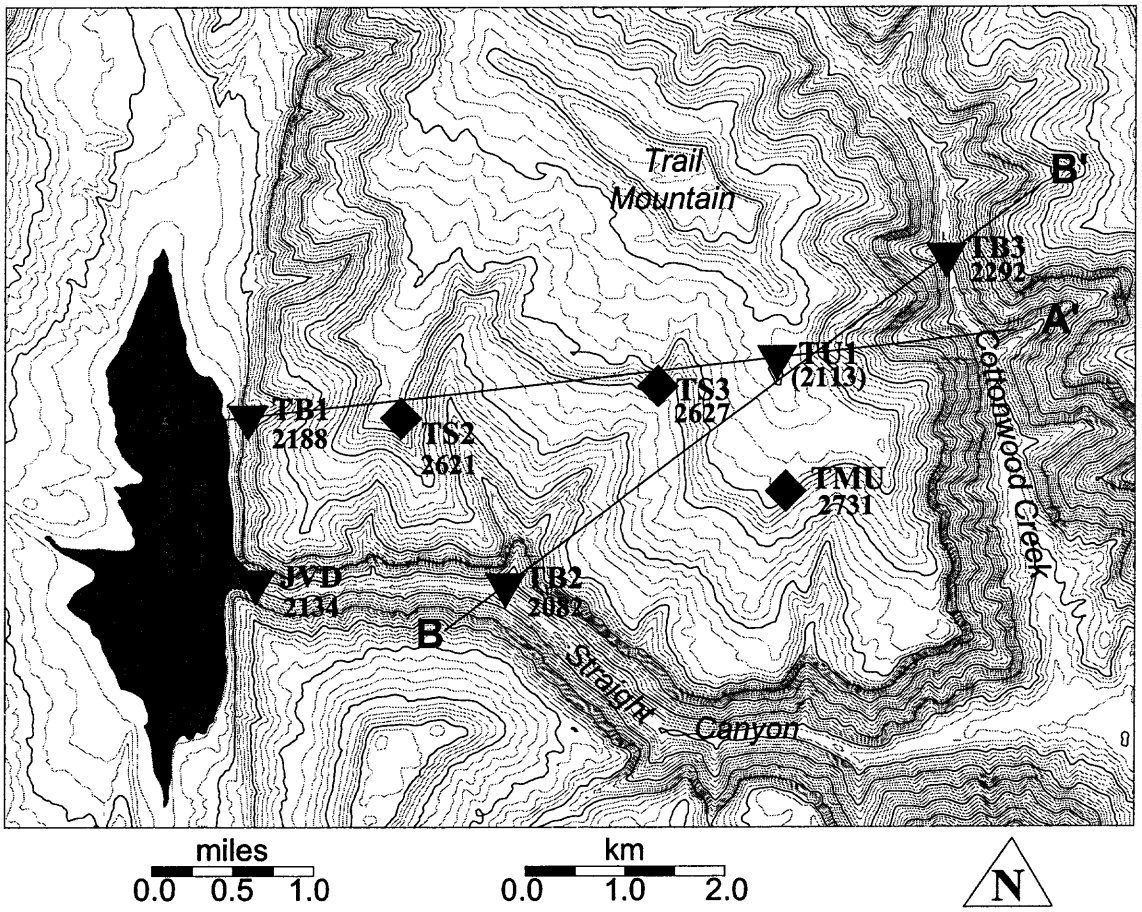

Figure E-2. Map view of the local area. AA' and BB' are the locations of cross-sections shown in Figure E-3.

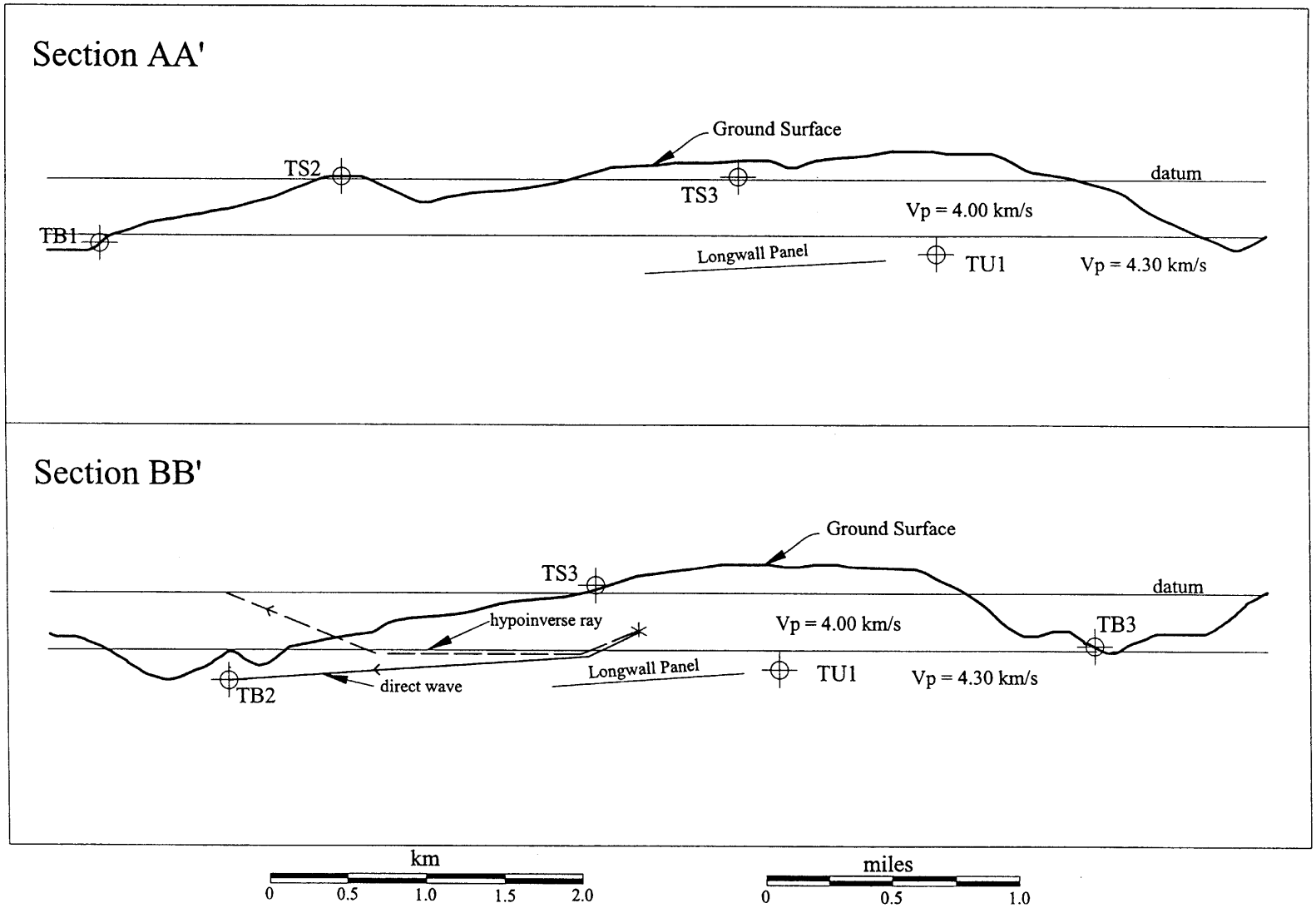

Figure E-3. Cross-sections along AA' and BB' (see Figure E-2 for locations) showing the positions of the stations relative to the longwall. The Trail Mountain velocity model is superimposed. For simplicity, the model's 100-m-thick top layer with Vp=3.5 km/sec has been omitted. Note that stations TB1, TB2, and TU1 are located at or below the position of the longwall and in the layer with Vp=4.3 km/sec. Superimposed on BB' are theoretical ray paths. The dashed ray path is the ray calculated by hypoinverse. The solid ray path is an approximation of the true ray path for the model shown.

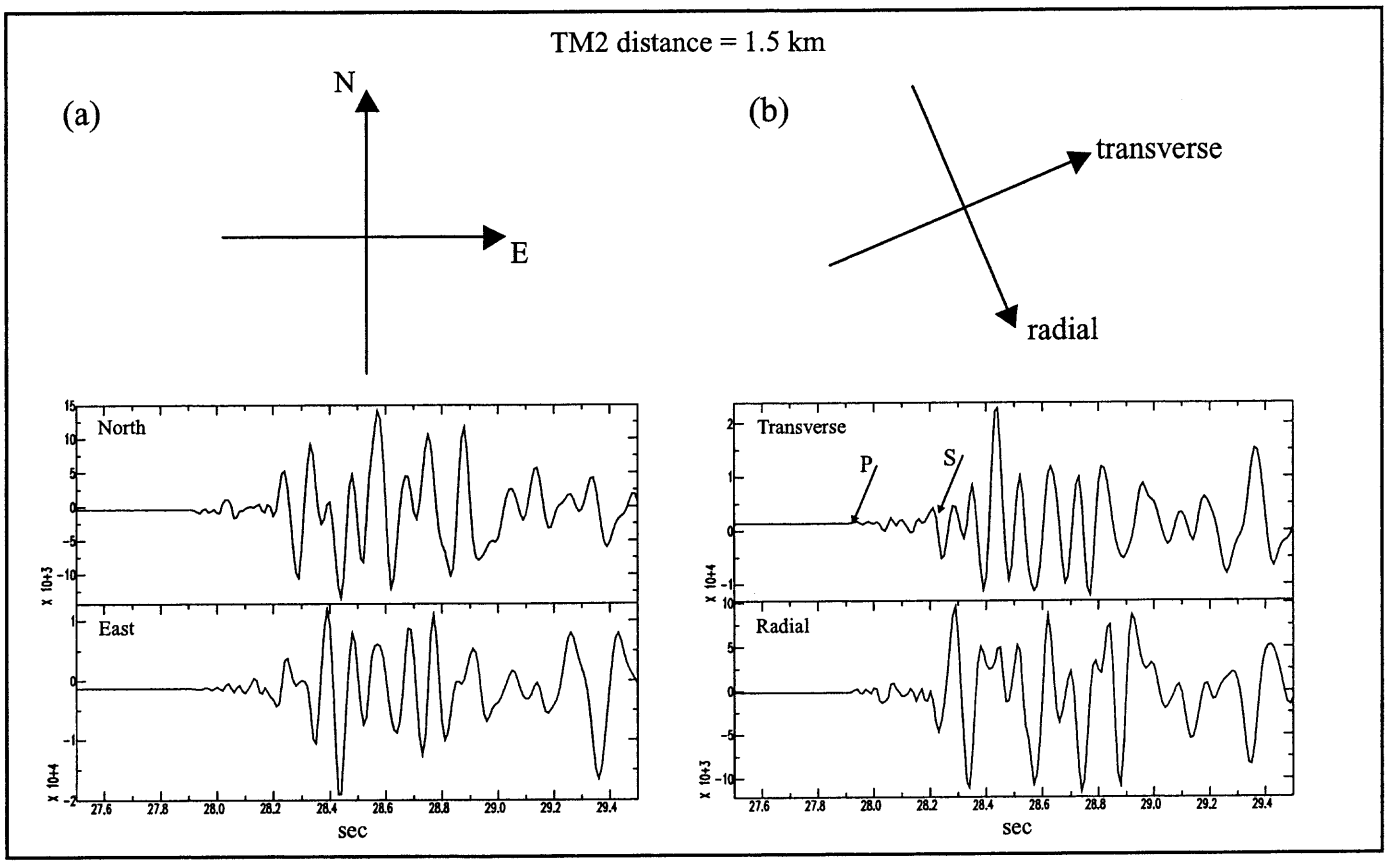

Figure E-4. (a) The standard orientation for horizontal component data. The two traces are the recordings on the north and east components of station TM2 from USGS event #42. Event #42 was located N23°W of TM2. (b) The data from (a) after rotating the component orientations to the radial and transverse directions, which are defined as the directions parallel and perpendicular to a line from the source to the receiver, respectively. This rotation minimizes the amount of P and P-to-S converted energy on the transverse component, thereby enabling more accurate S-wave arrival-time picks.

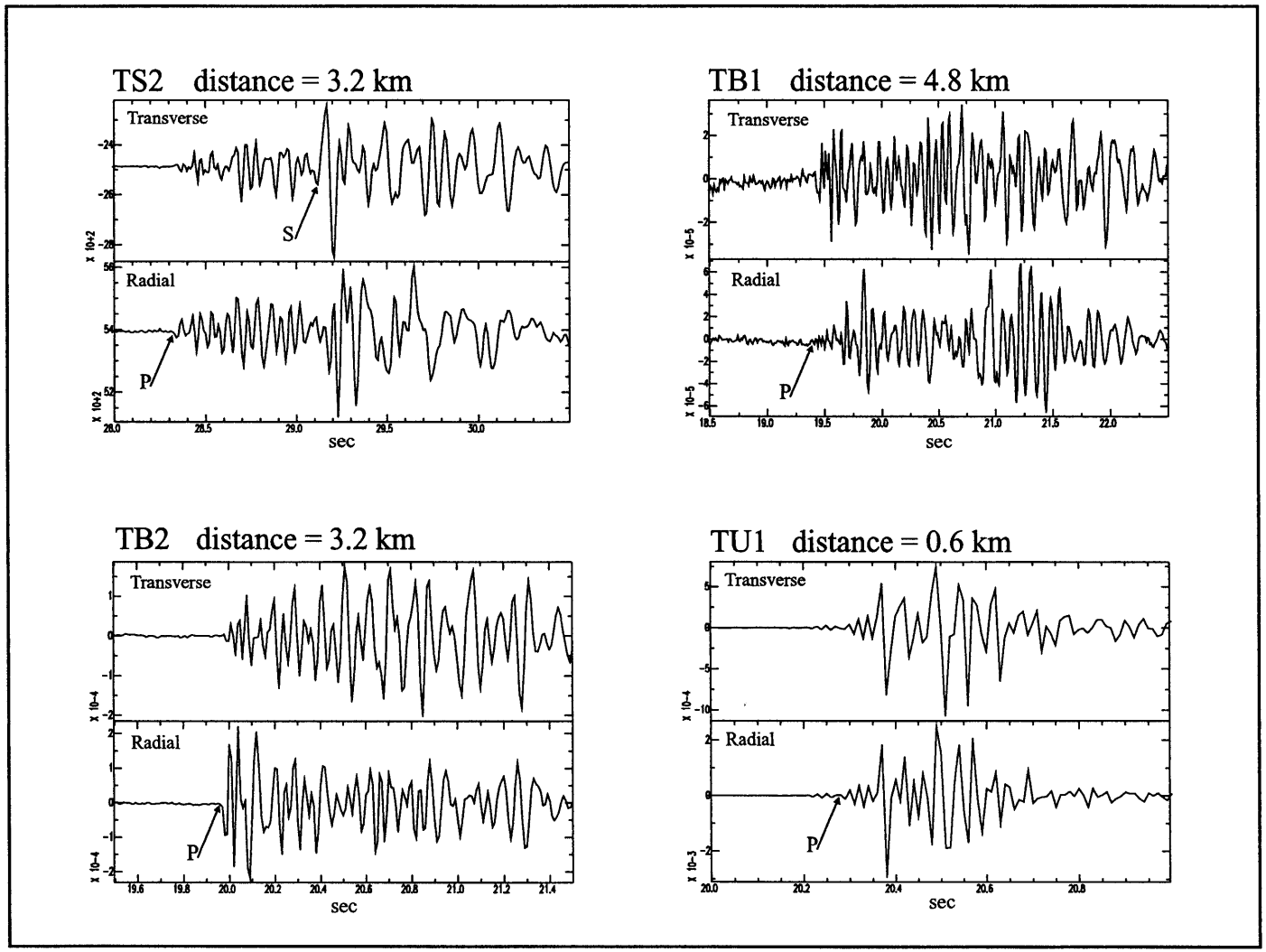

Figure E-5. Additional transverse and radial component data from USGS event #42. For the four examples shown an S-pick was only made at TS2.

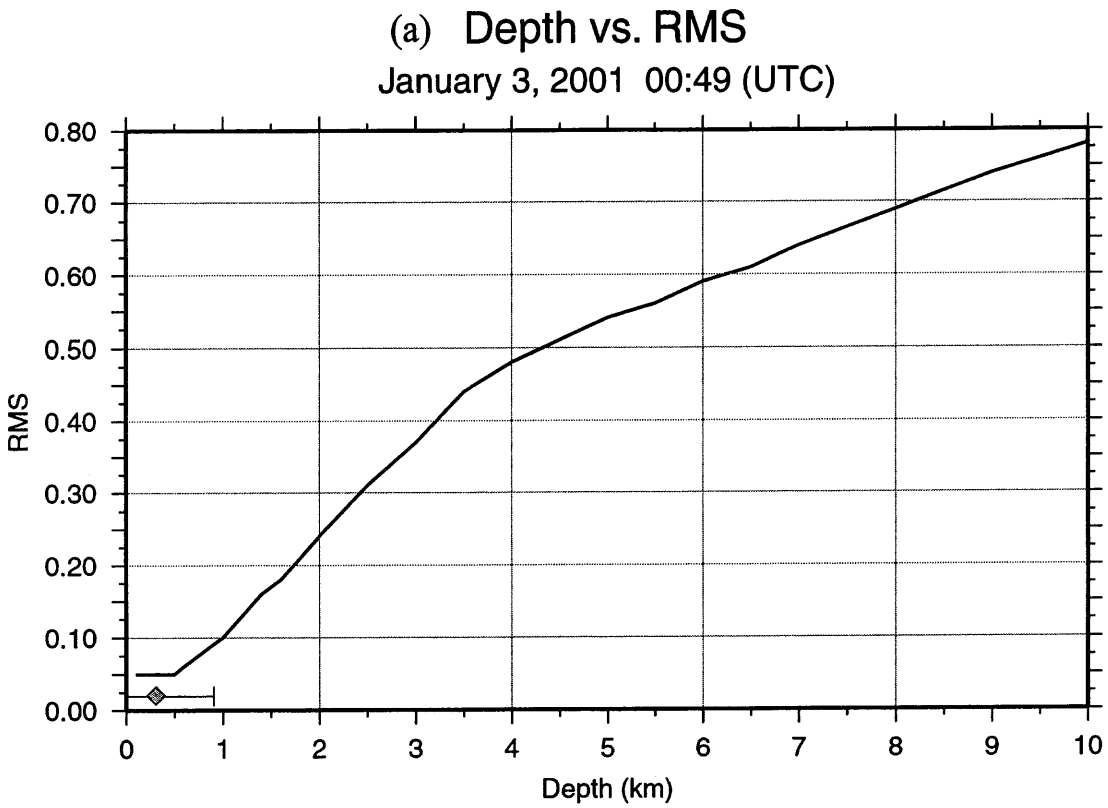

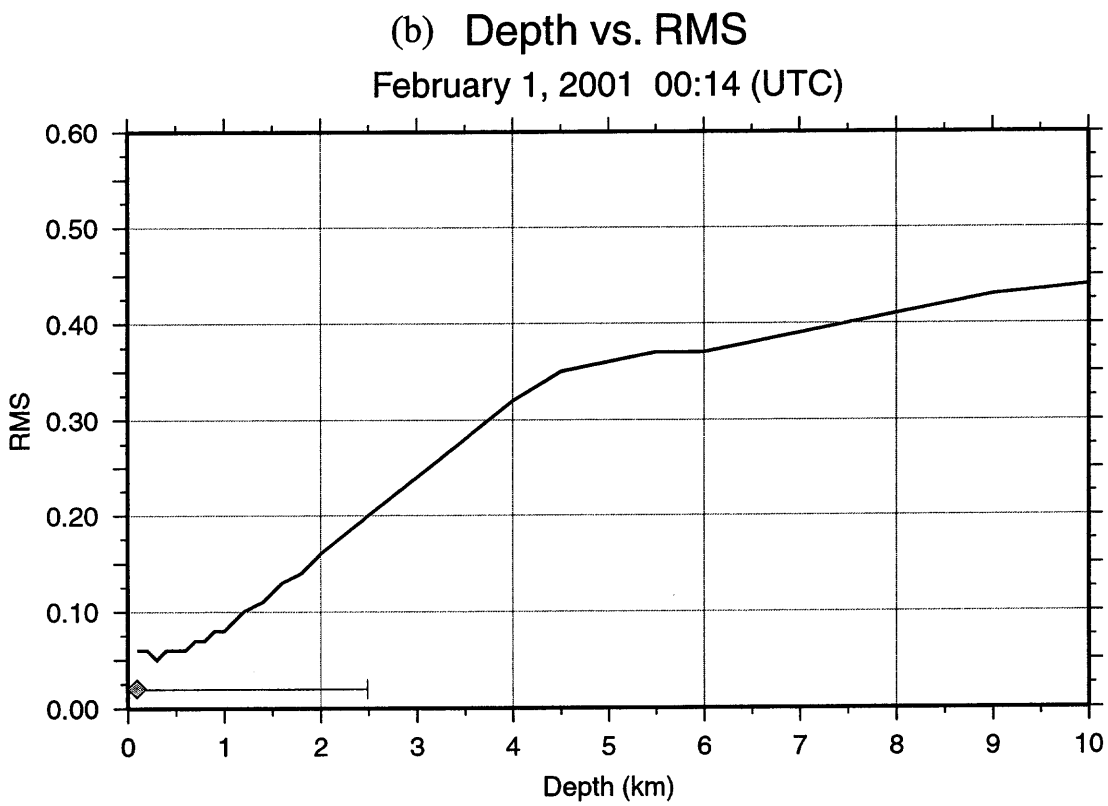

Figure E-6. Plots of RMS value as a function of fixed focal depth. The diamonds are the focal depths obtained from routine processing with 95% confidence error bars. (a) Plot for event #16. RMS is constant and minimum from 0.0 to 0.5-km depth suggesting that the event is at or above mine level. (b) Plot for event #34. A minimum at 0.3 km indicates the best-fitting focal depth. However, the RMS difference between this and the adjacent trial depths is only 0.01 seconds.

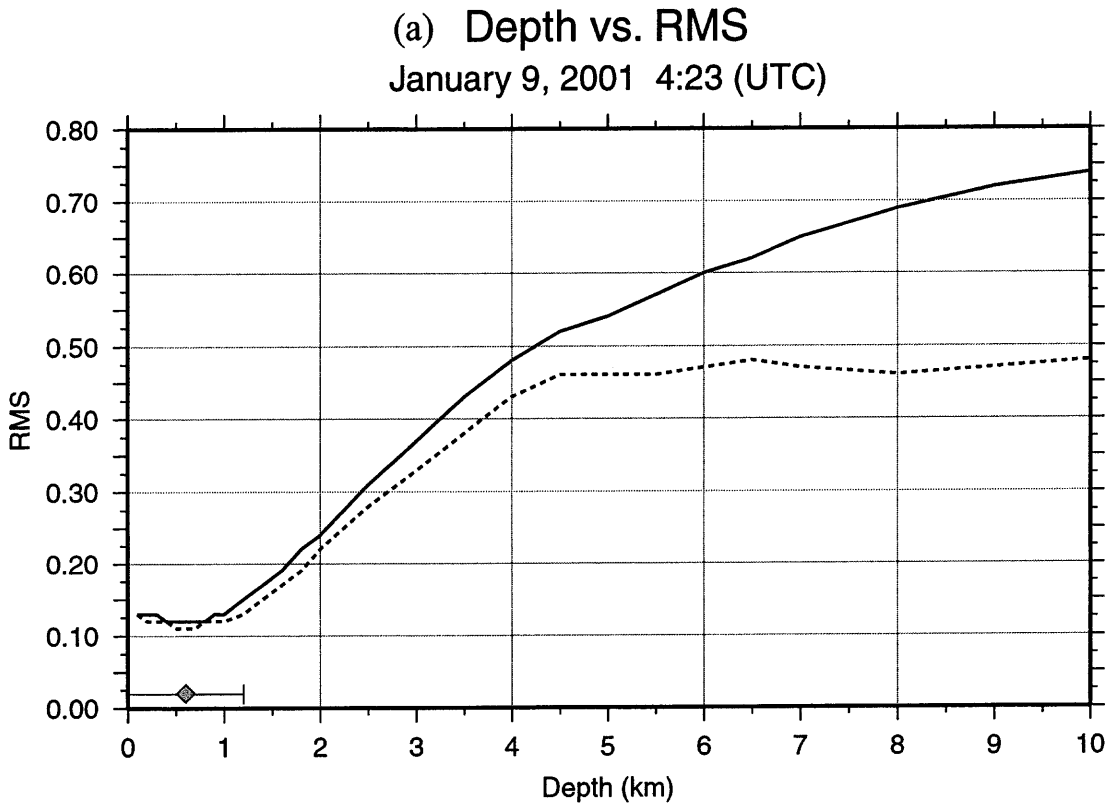

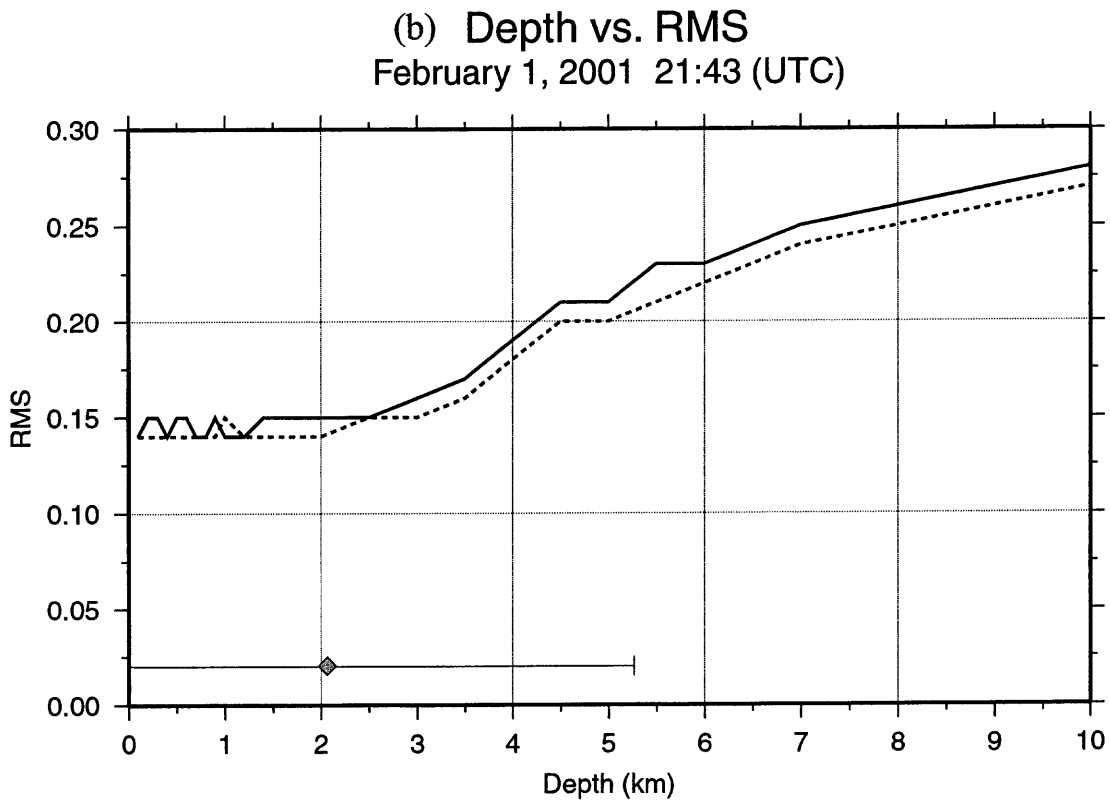

Figure E-7. The dashed and solid lines show RMS value as a function of fixed focal depth with and without using TB1 and TB2 in the location, respectively. The diamonds are the focal depths obtained from routine processing (without TB1 and TB2) with 95% confidence error bars. (a) Plot for event #24. Note the minimum in the dashed line between 0.5 and 0.7-km depth. The focal depth is likely in this range. (b) Plot for event #35. This event is the deepest one in the USGS data set. There is no single minimum, and the lack of focal-depth control is apparent.

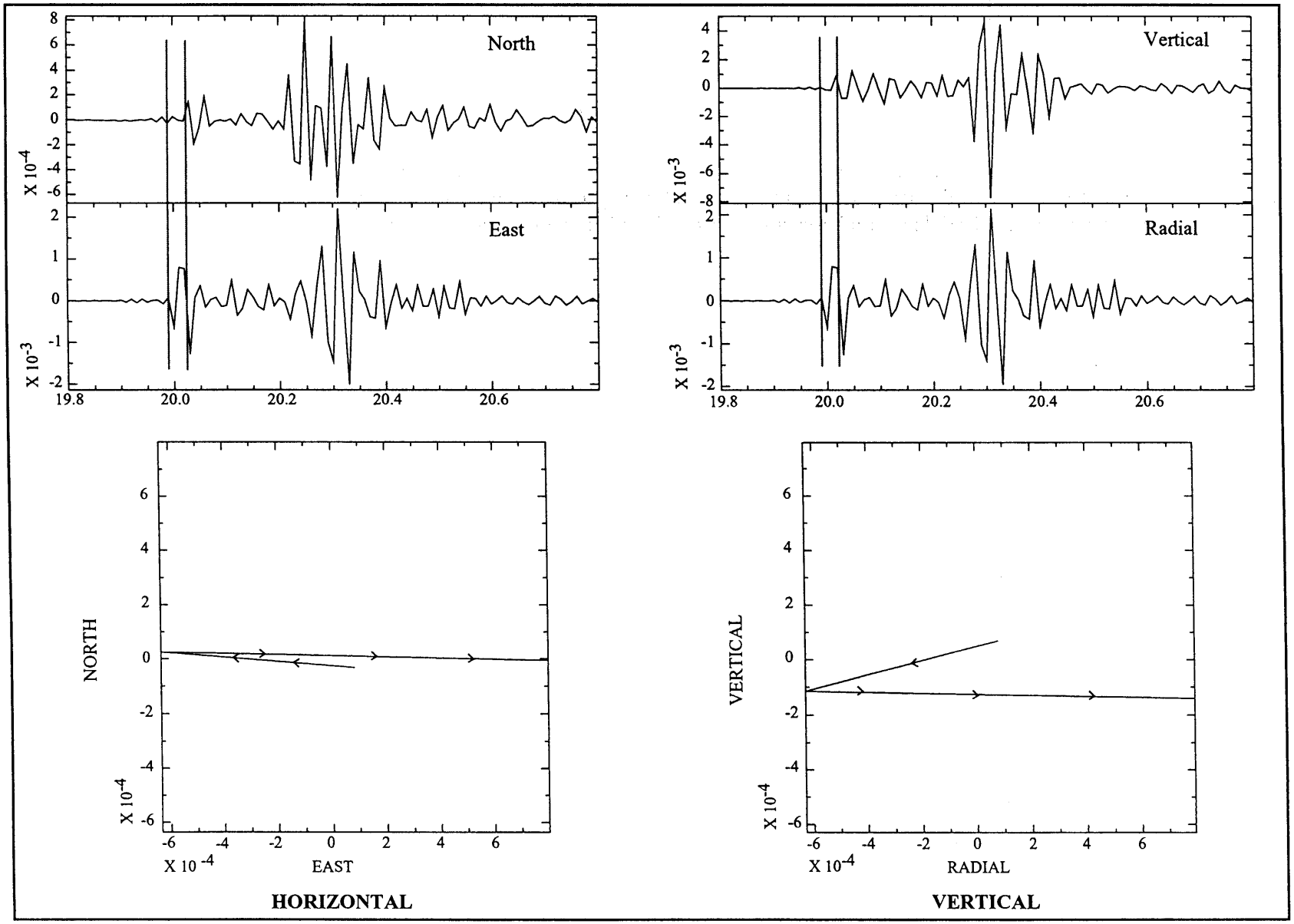

Figure E-8. Examples of TU1 particle motion plots from USGS event #7. (Left) Horizontal-component accelerograms (top) and horizontal plane particle motion plot (bottom) for the time window marked by the vertical gray lines on the accelerograms. The arrows on the particle motion plot indicate the direction of motion, which in this case is nearly due east during the time window analyzed. (Right) Vertical- and radial-component accelerograms (top) and vertical-radial plane partical motion plot (bottom) for the time window between the vertical gray lines on the accelerograms. The arrows show the particle motion direction, which is nearly horizontal for the time window analyzed.

(a)

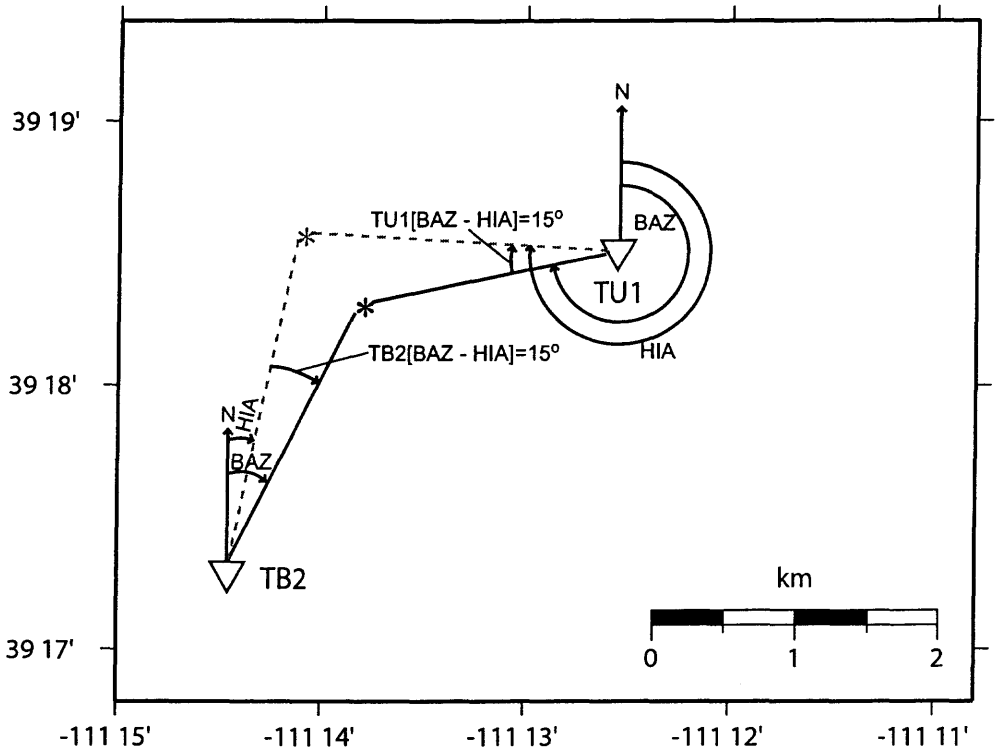

(b)

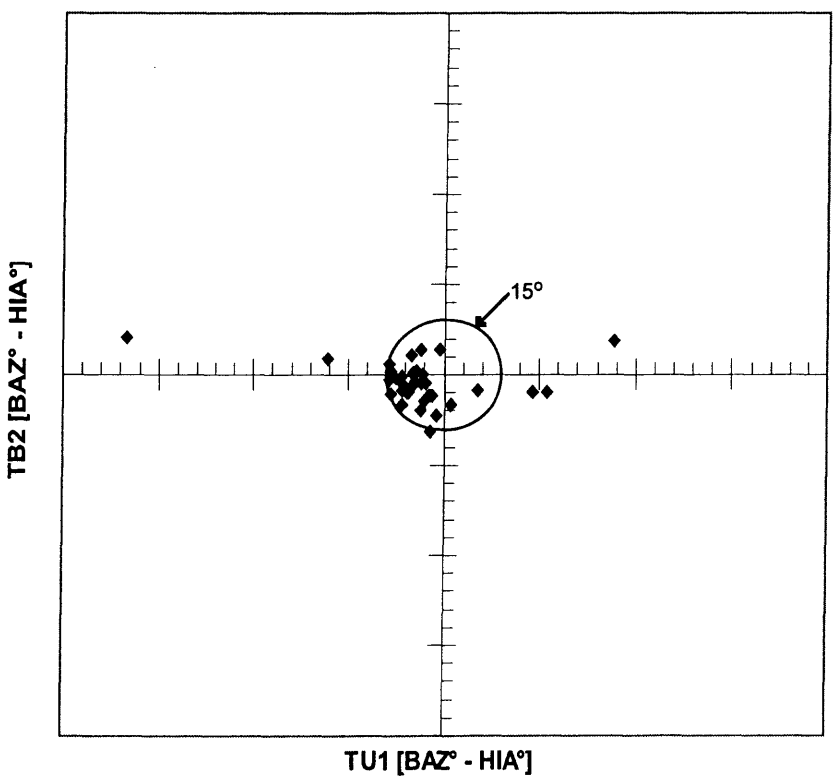

Figure E-9. (a) Map view depicting rays traveling from an event to stations TU1 and TB2. The solid line is the ray from the event position calculated in routine processing. The angle from north to this ray is the backazimuth (BAZ). The dashed line is the ray determined from the horizontal particle motion analysis. The angle from north to this ray is the horizontal incident angle (HIA). The difference between BAZ and HIA in this example is 15°. (b) A plot of the difference between the backazimuth and the horizontal incident angle for all events in theUSGS data set recorded at both TU1 and TB2. The circle denotes a difference of 15°.

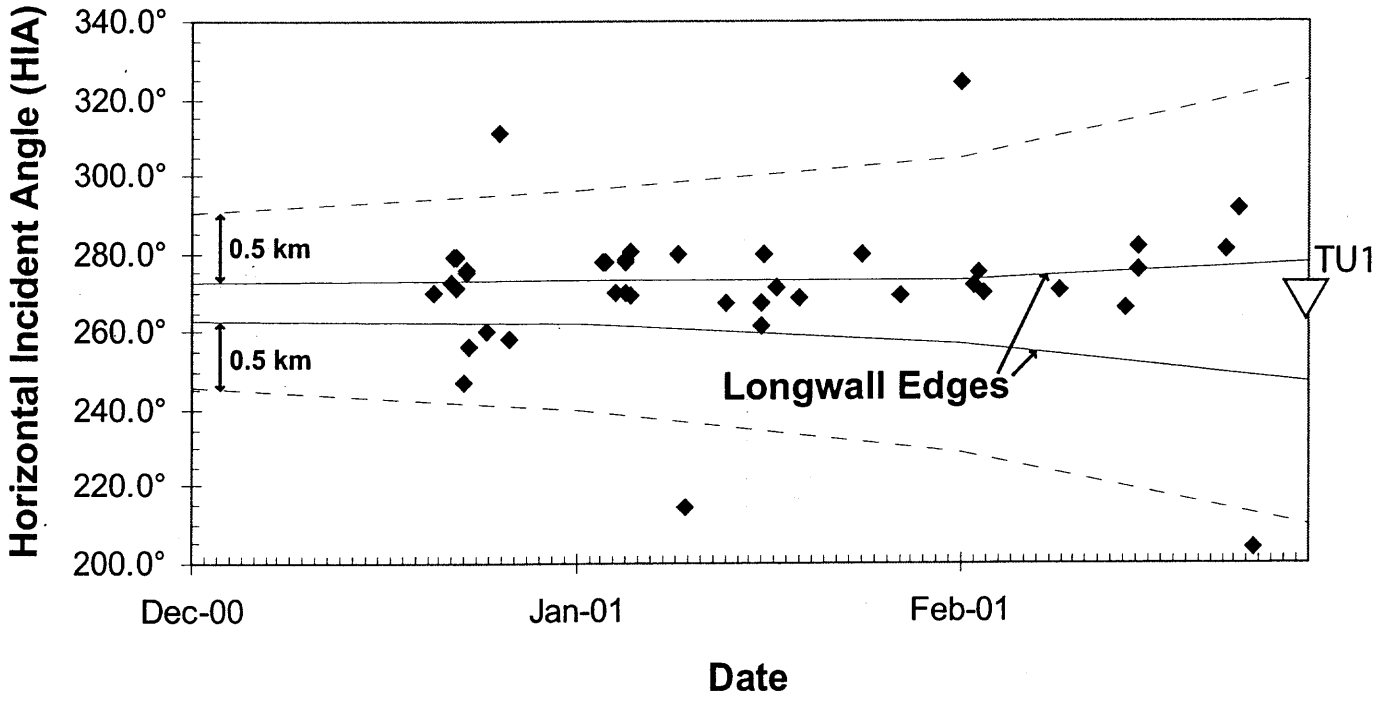

Figure E-10. A plot of the horizontal incident angles measured at station TU1 (triangle) as a function of time for all events in the USGS data set. The solid lines depict the azimuths of the longwall edges and the dashed lines depict the azimuths of points 0.5 km beyond the ends of the longwall.

APPENDIX F

TRAIL MOUNTAIN PROJECT – MINING ENGINEERING CONSIDERATIONS FOR ASSESSING MAXIMUM MAGNITUDE FOR SEISMIC EVENTS

by

Michael K. McCarter, with contributions from Jefferson D. McKenzie
Department of Mining Engineering
University of Utah

TRAIL MOUNTAIN PROJECT – MINING ENGINEERING CONSIDERATIONS FOR ASSESSING MAXIMUM MAGNITUDE FOR SEISMIC EVENTS

by

Michael K. McCarter, with contributions from Jefferson D. McKenzie
Department of Mining Engineering
University of Utah

INTRODUCTION

The purpose of this appendix is to identify geologic and mining factors which may influence the frequency and severity of mining-induced seismicity in the vicinity of Joes Valley Dam located approximately 17 miles west of Huntington, Utah. Concern exists over the effect mining in the Cottonwood Tract may have on the integrity of the Dam. The Cottonwood Tract is located immediately to the north and east of the Dam (see Figure F-1). To assess this impact, it is necessary to estimate the maximum probable seismic event resulting from conventional longwall mining. For this purpose, the Trail Mountain Project, conducted jointly by USBR, USGS and UUSS has resulted in a database of seismic events produced by mining the last two panels in the Trail Mountain Mine. This data provides a benchmark for event frequency and magnitude for possible future mining of the Cottonwood Tract. The largest Trail Mountain events recorded for the period October 3, 2000, to April 30, 2001, are on the order of M_L 2.2. Larger events have been recorded elsewhere in the Wasatch Plateau and Circle Cliffs areas with similar conditions and mining methods. The question is then, what is the maximum credible mining-induced seismic event which could be expected in mining the Cottonwood Tract? There is no quantitative means for accessing this magnitude, but a comparison of factors may shed some light on whether or not the maximum credible event would be larger or smaller than those experienced in the past. A comparison of conditions will be presented in this appendix with the purpose of subjectively assessing this potential. The comparison will be limited to those events identified in Table F-1.

BACKGROUND

Underground coal mine bumps, bursts, or bounces result from sudden releases of strain energy. If this occurs in active sections of the mine, several tons of coal may be ejected horizontally into openings putting personnel and equipment at risk. The term bump is often associated with expulsion of coal into mine workings (Ellenberger et al., 2001). The term bounce is used occasionally for a mining-related disturbance which results in perceived effects of a seismic

event such as ground motion or roof falls rather than expulsion of coal. These terms are often used interchangeably and confusion exists between the effects and the causes. The term Mining-Induced Seismicity (MIS) (Arabasz et al., 1997) is more appropriate in that it simply refers to an event which results in the release of seismic energy. The site of this event may be at the mining horizon or in the strata above or below the horizon. The interaction of strain energy with underground openings produces variable results. Large seismic events may go unnoticed underground while small seismic events may produce catastrophic problems for mining operations. The causes of MIS are not well understood and there are undoubtedly a number of mechanisms which give rise to seismic events related to mining operations. Hopefully, continued research will help identify the principle mechanisms and allow development of engineering solutions.

Rice (1935) identifies two types of bumps: Pressure bumps are caused when strong and brittle coal pillars or portions of pillars are loaded beyond their load-carrying capacity resulting in sudden and violent failure. Shock bumps are attributed to rupturing of strong strata above the coal seam. These strata form beams or arches in response to the caving action resulting from extraction of coal in longwall operations. The portion of the seismic pulse propagating downward impacts the coal pillars left to support the mine openings or the face which is being mined by the longwall. In either case, the portion of the seismic energy which propagates upward would be perceived as an earthquake by people on the surface and has the potential of adversely affecting susceptible surface structures.

MIS may also be described as floor bounces or roof bounces (McKenzie, 2002). Experienced miners in a longwall section can sense whether the disturbance originated above or below their location. It is logical to visualize a rock beam bending into an opening under the influence of gravity. But, of course, vertical stress must be in equilibrium, so the stress acting upward on the bottom of a coal pillar must equal the force acting downward resulting from the weight of the overlying strata. Perturbations in the original lithostatic stress field caused by the excavation can, therefore, result in rock/joint failure below the seam horizon as well as above.

According to Peng (1986) bumps are more likely to occur when:

(1) The overlying strata exceed 500 feet in thickness.
(2) The overlying strata are strong and form beams which project above the gob (caved area which extends behind the advancing longwall face).
(3) The stratum forming the floor of the coal seam is strong and does not heave readily.
(4) The coal being mined is strong and does not crush easily.
(5) The mining methods create localized stress concentrations.

Overburden Thickness - Rice (1935) concludes that bumps are more likely to occur when the depth of cover exceeds 1000 feet, but he reports bump incidents where cover is 500 to 1000 feet. Because of the date, this reflected conditions relative to room and pillar mining. Peng (1986) indicates that bumps resulted in the Cumberland coalfields under 1500 feet of cover and became severe when overburden was more than 2000 feet. Again, these episodes were the

B. *Valid Date/Time Range: December 15, 2000 (23:51 UTC) – December 21, (21:54 UTC)*
Digitizer: Kinemetrics Altus Series K2 (19-bit resolution); SN 1561

Component	Digitizer Channel No.	Sensor Serial No.	Sensor Model	Sensor Component Serial No.	Gain	Span (volts/g)	Cal-Coil Sensitivity (g/volts)	Instrument Sensitivity (volts/g)
Z	1	2915	L4C	2915	0.125	n/a	n/a	n/a
E	4	756	Episensor	4025	1	1.2501	0.0548	1.2501
N	5	756	Episensor	4038	1	1.2509	0.0555	1.2509
Z	6	756	Episensor	4043	1	1.2490	0.0552	1.2490

Comments:

A Kinemetrics gain board was installed in the K2s used for the Trail Mountain project. This board is used to damp the signal from an external short period sensor. The board was factory installed in channels 1-3. UUSS Technicians thought the gain board was installed in channels 4-6 since K2s with internal sensors came wired that way. As a result of this misunderstanding, channel 1 records of Episensor data have a gain of 0.125 during this time period. The problem was corrected by moving the Episensor to channels 4-6, beginning on December 15, 2000 for this station (TB3).

Polarity Convention

Episensor: positive output for positive acceleration
L4C: positive output for positive ground motion

Displacement Response Data

The Poles and Zeros listed below are those of a ratio of polynomials of the Laplace Transform variable "s".

	Z	E	N
Zeros 2 (radians/second)	0.0 ± 0.0i	0.0 ± 0.0i	0.0 ± 0.0i
	0.0 ± 0.0i	0.0 ± 0.0i	0.0 ± 0.0i
Poles 4 (radians/second)	-981.0 ± 1009.0i	-981.0 ± 1009.0i	-981.0 ± 1009.0i
	-3290.0 ± 1263.0i	-3290.0 ± 1263.0i	-3290.0 ± 1263.0i
Gain Constant (counts/micron)	0.1051×10^{14}	0.1052×10^{14}	0.1053×10^{14}

C. *Valid Date/Time Range: December 21, 2000 (22:05 UTC) – January 23, 2001 (18:51 UTC)*
Digitizer: Kinemetrics Altus Series K2 (19-bit resolution); SN 1561

Component	Digitizer Channel No.	Sensor Serial No.	Sensor Model	Sensor Component Serial No.	Gain	Natural Frequency (hertz)	Damping Factor (units of critical)
Z	1	2915	L4C	2915	0.125	n/a	n/a
L (N) Y	4	-	FBA-23	28385	1	53.7	0.65
V (Z)	5	-	FBA-23	28386	1	51.5	0.66
T (E) X	6	-	FBA-23	28387	1	51.4	0.65

Comments:

Episensor (#756) failed and was sent back to manufacturer for repairs. An FBA-23 sensor was temporarily installed.

Polarity Convention

FBA23: negative output for positive acceleration
L4C: positive output for positive ground motion

Displacement Response Data

The Poles and Zeros listed below are those of a ratio of polynomials of the Laplace Transform variable "s".

	Z	E	N
Zeros 2 (radians/second)	0.0 ± 0.0i	0.0 ± 0.0i	0.0 ± 0.0i
	0.0 ± 0.0i	0.0 ± 0.0i	0.0 ± 0.0i
Poles 3 (radians/second)	-213.6 ± 243.1i	-209.9 ± 245.4i	-219.3 ± 256.4i
	-1500.0 + 0.0i	-1500.0 + 0.0i	-1500.0 + 0.0i
Gain Constant (counts/micron)	0.6717×10^8	0.6659×10^8	0.7327×10^8

D. *Valid Date/Time Range: January 23, 2001 (19:03 UTC) – June 14, 2001*
Digitizer: Kinemetrics Altus Series K2 (19-bit resolution); SN 1561

Component	Digitizer Channel No.	Sensor Serial No.	Sensor Model	Sensor Component Serial No.	Gain	Span (volts/g)	Cal-Coil Sensitivity (g/volts)	Instrument Sensitivity (volts/g)
Z	1	2915	L4C	2915	0.125	n/a	n/a	n/a
E	4	756	Episensor	4025	1	1.2501	0.0548	1.2501
N	5	756	Episensor	4038	1	1.2509	0.0555	1.2509
Z	6	756	Episensor	4043	1	1.2490	0.0552	1.2490

Comments:

Repaired Episensor (#756) installed. It is possible that this instrument was wired improperly during this time. Using empirical relations we believe the channel mapping in the above table to be correct. However, the cable was cut when the Trail Mountain Mine personnel removed the instrument. Therefore, we CANNOT validate the above mapping with certainty.

Polarity Convention

Episensor: positive output for positive acceleration
L4C: positive output for positive ground motion

Displacement Response Data

The Poles and Zeros listed below are those of a ratio of polynomials of the Laplace Transform variable "s".

	Z	E	N
Zeros 2 (radians/second)	0.0 ± 0.0i	0.0 ± 0.0i	0.0 ± 0.0i
	0.0 ± 0.0i	0.0 ± 0.0i	0.0 ± 0.0i
Poles 4 (radians/second)	-981.0 ± 1009.0i	-981.0 ± 1009.0i	-981.0 ± 1009.0i
	-3290.0 ± 1263.0i	-3290.0 ± 1263.0i	-3290.0 ± 1263.0i
Gain Constant (counts/micron)	0.1051×10^{14}	0.1052×10^{14}	0.1053×10^{14}

Station TU1

Location Information

Latitude:	39° 18.51′ North	UTM North:	14275013.8
Longitude:	111° 12.55′ West	UTM East:	1581251.8
Elevation:	2113 meters		

Telemetry

On-site digital recording to local disk; independently triggered when local ground motion exceeds 0.001%g (acceleration).

Instrumentation

A. Valid Date/Time Range: December 5, 2000 (installation date) – March 17, 2001
Digitizer: Kinemetrics Altus Series K2 (19-bit resolution); SN 1564

Component	Digitizer Channel No.	Sensor Serial No.	Sensor Model	Sensor Component Serial No.	Gain	Span (volts/g)	Cal-Coil Sensitivity (g/volts)	Instrument Sensitivity (volts/g)
E	1	K1564	Episensor	4142	1	1.2502	0.0589	1.2502
N	2	K1564	Episensor	4083	1	1.2492	0.0570	1.2492
Z	3	K1564	Episensor	4160	1	1.2499	0.0603	1.2499
Z	4	831	L4C	831	0.125	n/a	n/a	n/a

Comments:

Internal Episensor.

Polarity Convention

Episensor: Vertical component positive output for positive acceleration. Horizontal components negative output for positive acceleration.

L4C: positive output for positive ground motion

Displacement Response Data

The Poles and Zeros listed below are those of a ratio of polynomials of the Laplace Transform variable "s".

	Z	E	N
Zeros 2 (radians/second)	0.0 ± 0.0i	0.0 ± 0.0i	0.0 ± 0.0i
	0.0 ± 0.0i	0.0 ± 0.0i	0.0 ± 0.0i
Poles 4 (radians/second)	-981.0 ± 1009.0i	-981.0 ± 1009.0i	-981.0 ± 1009.0i
	-3290.0 ± 1263.0i	-3290.0 ± 1263.0i	-3290.0 ± 1263.0i
Gain Constant (counts/micron)	0.1052×10^{14}	0.1052×10^{14}	0.1051×10^{14}

Station TMU

Location Information

Latitude:	39° 17.79′ North	UTM North:	14270655.0
Longitude:	111° 12.49′ West	UTM East:	1581516.1
Elevation:	2731 meters		

Telemetry

Continuous digital telemetry via spread spectrum radio and leased microwave circuits to the UUSS lab. Data are archived into continuous files that are 900 seconds long.

Instrumentation

A. Valid Date/Time Range: December 1, 2000 – February 28, 2002 (end of project)
Digitizer: Refraction Technology 72A/08 (24-bit digitizer); SN 1184

Component	Digitizer Channel No.	Sensor Serial No.	Sensor Model	Sensor Component Serial No.	Gain	Span (volts/g)	Cal-Coil Sensitivity (g/volts)	Instrument Sensitivity (volts/g)
Z	1	758	Episensor	4342	8	0.6260	0.0560	5.0080
E	2	758	Episensor	4165	8	0.6248	0.0599	4.9984
N	3	758	Episensor	4254	8	0.6253	0.0573	5.0024

Comments:

Three short-period signals (S13 sensors) are recorded on channels 4, 5, and 6 at this site. Due to internal UUSS downstream merging issues, these channels assigned a different station code, TM2, and are listed separately.

Polarity Convention

Episensor: positive output for positive acceleration.

Displacement Response Data

The Poles and Zeros listed below are those of a ratio of polynomials of the Laplace Transform variable "s".

	Z	E	N
Zeros 2 (radians/second)	0.0 ± 0.0i	0.0 ± 0.0i	0.0 ± 0.0i
	0.0 ± 0.0i	0.0 ± 0.0i	0.0 ± 0.0i
Poles 4 (radians/second)	-981.0 ± 1009.0i	-981.0 ± 1009.0i	-981.0 ± 1009.0i
	-3290.0 ± 1263.0i	-3290.0 ± 1263.0i	-3290.0 ± 1263.0i
Gain Constant (counts/micron)	0.6587×10^{13}	0.6574×10^{13}	0.6579×10^{13}

Station TM2

Location Information

Latitude:	39° 17.79′ North	UTM North:	14270655.0
Longitude:	111° 12.49′ West	UTM East:	1581516.1
Elevation:	2731 meters		

Telemetry

Continuous digital telemetry via spread spectrum radio and leased microwave circuits to the UUSS lab. Data are archived into continuous files that are 900 seconds long.

Instrumentation

A. Valid Date/Time Range: December 1, 2000 – February 28, 2002 (end of project)
Digitizer: Refraction Technology 72A/08 (24-bit digitizer); SN 1184

Component	Digitizer Channel No.	Sensor Model	Sensor Component Serial No.	Gain	Nomin al Coil Resistance (ohms)	Damping Resistance (ohms)
Z	1	Geotech S-13	X573	1	3600	5182
E	2	Geotech S-13	3668	1	3600	5182
N	3	Geotech S-13	1118	1	3600	5182

Polarity Convention

Z component: positive output for positive ground motion.
E component: positive output for horizontal ground motion in the east direction.
N component: positive output for horizontal ground motion in the north direction.

Displacement Response Data

The Poles and Zeros listed below are those of a ratio of polynomials of the Laplace Transform variable "s".

	Z	E	N
Zeros 3 (radians/second)	0.0 ± 0.0i	0.0 ± 0.0i	0.0 ± 0.0i
	0.0 ± 0.0i	0.0 ± 0.0i	0.0 ± 0.0i
	0.0 ± 0.0i	0.0 ± 0.0i	0.0 ± 0.0i
Poles 2 (radians/second)	-4.44284 ± 4.44284i	-4.44284 ± 4.44284i	-4.44284 ± 4.44284i
Gain Constant (counts/micron)	194.627	194.627	194.627

Station TS1

Location Information

Latitude:	39° 21.82′ North	UTM North:	142955102.9
Longitude:	111° 12.71′ West	UTM East:	1580546.5
Elevation:	2827 meters		

Telemetry

Continuous analog telemetry via FM radio and leased microwave circuit to the UUSS lab. A discrete time window is recorded when ratio of short-term to long-term average exceeds a pre-set threshold. Data form the entire UU seismograph network is recorded when a trigger occurs.

Instrumentation

A. Valid Date/Time Range: October 10, 2000 – August 20, 2001
Digitizer: Concurrent Computer Corporation (formerly Masscomp) 7200C computer (12-bit digitizer)

Component	Sensor Serial No.	Sensor Model	VCO model (serial number)	Gain	Damping Resistance (ohms)	Measured Coil Resistance (ohms)
Z	2916	L4C	UUSS Standard (14)	3200	7887	5510
E	2912	L4C	UUSS Standard (147)	3200	8665	5590
N	2911	L4C	UUSS Standard (69)	3200	9486	5535

Polarity Convention

L4C: positive output for positive ground motion

Station TS2

Location Information

Latitude:	39° 18.19′ North	UTM North:	14273104.7
Longitude:	111° 15.17′ West	UTM East:	1568896.9
Elevation:	2621 meters		

Instrumentation

A. Valid Date/Time Range: October 3, 2000 – October 17, 2001
Digitizer: Concurrent Computer Corporation (formerly Masscomp) 7200C computer (12-bit digitizer)

Telemetry

Continuous analog telemetry via FM radio and leased microwave circuit to the UUSS lab. A discrete time window is recorded when ratio of short-term to long-term average exceeds a pre-set threshold. Data form the entire UU Seismograph network is recorded when a trigger occurs.

Component	Sensor Serial No.	Sensor Model	VCO model (serial number)	Gain	Damping Resistance (ohms)	Measured Coil Resistance (ohms)
Z	1069	L4C	UUSS Standard (37)	6400	8636	5502

Polarity Convention

L4C: positive output for positive ground motion

B. Valid Date/Time Range: December 7, 2000 – October 17, 2001
Digitizer: Refraction Technology 72A/08 (24-bit digitizer); SN 1185

Telemetry

Continuous digital telemetry via spread spectrum radio and leased microwave circuit to the UUSS lab. Data are archived into continuous files that are 900 seconds long.

Component	Digitizer Channel No.	Sensor Serial No.	Sensor Model	Sensor Component Serial No.	Gain	Span (volts/g)	Cal-Coil Sensitivity (g/volts)	Instrument Sensitivity (volts/g)
Z	1	808	Episensor	3015	8	0.6257	0.0593	5.0056
E	2	808	Episensor	2855	8	0.6261	0.0592	5.0088
N	3	808	Episensor	2872	8	0.6256	0.0598	5.0048

Polarity Convention

Episensor: positive output for positive acceleration.

Displacement Response Data

The Poles and Zeros listed below are those of a ratio of polynomials of the Laplace Transform variable "s".

	Z	E	N
Zeros 2 (radians/second)	0.0 ± 0.0i	0.0 ± 0.0i	0.0 ± 0.0i
	0.0 ± 0.0i	0.0 ± 0.0i	0.0 ± 0.0i
Poles 4 (radians/second)	-981.0 ± 1009.0i	-981.0 ± 1009.0i	-981.0 ± 1009.0i
	-3290.0 ± 1263.0i	-3290.0 ± 1263.0i	-3290.0 ± 1263.0i
Gain Constant (counts/micron)	0.6583×10^{13}	0.6588×10^{13}	0.6582×10^{13}

Station TS3

Location Information

Latitude:	39° 18.36′ North	UTM North:	14274112.9
Longitude:	111° 13.38′ West	UTM East:	1577337.7
Elevation:	2627 meters		

Instrumentation

A. *Valid Date/Time Range: October 3, 2000 – October 17, 2001*
Digitizer: Concurrent Computer Corporation (formerly Masscomp) 7200C computer (12-bit digitizer)

Telemetry

Continuous analog telemetry via FM radio and leased microwave circuit to the UUSS lab. A discrete time window is recorded when ratio of short-term to long-term average exceeds a pre-set threshold. Data form the entire UU Seismograph network is recorded when a trigger occurs.

Component	Sensor Serial No.	Sensor Model	VCO model (serial number)	Gain	Damping Resistance (ohms)	Measured Coil Resistance (ohms)
Z	2033	L4C	UUSS Standard (25)	3200	7496	5459

Polarity Convention

L4C: positive output for positive ground motion

B. *Valid Date/Time Range: December 6, 2000 – October 17, 2001*
Digitizer: Refraction Technology 72A/08 (24-bit digitizer); SN 1186

Telemetry

Continuous digital telemetry via spread spectrum radio and leased microwave circuits to the University of Utah lab. Data are archived into continuous files that are 900 seconds long.

Component	Digitizer Channel No.	Sensor Serial No.	Sensor Model	Sensor Component Serial No.	Gain	Span (volts/g)	Cal-Coil Sensitivity (g/volts)	Instrument Sensitivity (volts/g)
Z	1	809	Episensor	3240	8	0.6249	0.0578	4.9992
E	2	809	Episensor	3094	8	0.6263	0.0616	5.0104
N	3	809	Episensor	3238	8	0.6263	0.0589	5.0104

Polarity Convention

Episensor: positive output for positive acceleration.

Displacement Response Data

The Poles and Zeros listed below are those of a ratio of polynomials of the Laplace Transform variable "s".

	Z	E	N
Zeros 2 (radians/second)	0.0 ± 0.0i	0.0 ± 0.0i	0.0 ± 0.0i
	0.0 ± 0.0i	0.0 ± 0.0i	0.0 ± 0.0i
Poles 4 (radians/second)	-981.0 ± 1009.0i	-981.0 ± 1009.0i	-981.0 ± 1009.0i
	-3290.0 ± 1263.0i	-3290.0 ± 1263.0i	-3290.0 ± 1263.0i
Gain Constant (counts/micron)	0.6575×10^{13}	0.6590×10^{13}	0.6590×10^{13}

Station TS4

Location Information

Latitude:	39° 15.50′ North	UTM North:	14256781.2
Longitude:	111° 15.36′ West	UTM East:	1567954.0
Elevation:	2536 meters		

Telemetry

Continuous analog telemetry via FM radio and leased microwave circuits to the University of Utah Lab. A discrete time window is recorded when ratio of short-term to long-term average exceeds a pre-set threshold. Data form the entire UU Seismograph network is recorded when a trigger occurs.

Instrumentation

A. Valid Date/Time Range: October 3, 2000 – October 23, 2001
Digitizer: Concurrent Computer Corporation (formerly Masscomp) 7200C computer (12-bit digitizer)

Component	Sensor Serial No.	Sensor Model	VCO model (serial number)	Gain	Damping Resistance (Ohms)	Measured Coil Resistance (Ohms)
Z	1081	L4C	UUSS Standard (91)	6400	9404	5346

Polarity Convention

- L4C: positive output for positive ground motion

Station TS5

Location Information

Latitude:	39° 15.83′ North	UTM North:	14258730.4
Longitude:	111° 10.64′ West	UTM East:	1590226.0
Elevation:	2598 meters		

Telemetry

Continuous analog telemetry via FM radio and leased microwave circuit to UUSS lab. A discrete time window is recorded when ratio of short-term to long-term average exceeds a pre-set threshold. Data form the entire UU Seismograph network is recorded when a trigger occurs.

Instrumentation

A. Valid Date/Time Range: October 3, 2000 – October 23, 2001
Digitizer: Concurrent Computer Corporation (formerly Masscomp) 7200C computer (12-bit digitizer)

Component	Sensor Serial No.	Sensor Model	VCO model (serial number)	Gain	Damping Resistance (ohms)	Measured Coil Resistance (ohms)
Z	1064	L4C	UUSS Standard (20)	6400	7197	5242

Polarity Convention

L4C: positive output for positive ground motion

Station TS6

Location Information

Latitude:	39° 11.00′ North	UTM North:	14229383.5
Longitude:	111° 05.17′ West	UTM East:	1615999.7
Elevation:	1811 meters		

Telemetry

Continuous analog telemetry via FM radio and leased microwave circuit to the UUSS lab. A discrete time window is recorded when ratio of short-term to long-term average exceeds a pre-set threshold. Data form the entire UU Seismograph network is recorded when a trigger occurs.

Instrumentation

A. Valid Date/Time Range: October 12, 2000 – August 17, 2001
Digitizer: Concurrent Computer Corporation (formerly Masscomp) 7200C computer (12-bit digitizer)

Component	Sensor Serial No.	Sensor Model	VCO model (serial number)	Gain	Damping Resistance (ohms)	Measured Coil Resistance (ohms)
Z	7032	L4C	UUSS Standard (63)	3200	8640	5307

Polarity Convention

L4C: positive output for positive ground motion

Station JVDA

Location Information

Latitude:	39° 17.25′ North	UTM North:	14267413.4
Longitude:	111° 16.20′ West	UTM East:	1564022.9
Elevation:	2134 meters		

Telemetry

On-site digital recording to local disk; independently triggered when local ground motion exceeds 0.001%g (acceleration).

Instrumentation

A. Valid Date/Time Range: December 20, 2000 (installation date) – February28, 2002 (end of project)
Digitizer: Kinemetrics Altus Series K2 (19-bit resolution); SN 1587

Component	Digitizer Channel No.	Sensor Model	Sensor Component Serial No.	Gain	Natural Frequency (hertz)	Damping Factor (units of critical)
L	1	FBA23	51311	1	50.8	0.67
V	2	FBA23	51312	1	49.9	0.67
T	3	FBA23	51313	1	50.4	0.66

Comments:

This station is located on the right abutment of Joe's Valley Dam. One 12-channel K2 (#1587) records data from both station JVDA and station JDVC. Unlike the all the other stations in the Trail Mountain array, these sensors are oriented along the axis of the dam following traditional engineering convention, where channel 1 (L) is pointed towards the right abutment (197 degrees), channel 2 (V) is up, and channel 3 (T) is pointed upstream (287 degrees).

Polarity Convention

FBA23: negative output for positive acceleration.

Displacement Response Data

The Poles and Zeros listed below are those of a ratio of polynomials of the Laplace Transform variable "s".

	L	T	V
Zeros 2 (radians/second)	0.0 ± 0.0i	0.0 ± 0.0i	0.0 ± 0.0i
	0.0 ± 0.0i	0.0 ± 0.0i	0.0 ± 0.0i
Poles 3 (radians/second)	-213.9 ± 237.0i	-209.0 ± 232.9i	-210.1 ± 232.8i
	1000.0 + 0.0i	1000.0 + 0.0i	1000.0 + 0.0i
Gain Constant (counts/micron)	0.8722×10^8	0.8568×10^8	0.8409×10^8

Station JVDC

Location Information

Latitude:	39° 17.31′ North	UTM North:	14267777.2
Longitude:	111° 16.18′ West	UTM East:	1564118.3
Elevation:	2134 meters		

Telemetry

On-site digital recording to local disk; independently triggered when ground local motion exceeds 0.001%g (acceleration).

Instrumentation

A. Valid Date/Time Range: December 20, 2000 (installation date) – January 31, 2001
Digitizer: Kinemetrics Altus Series K2 (19-bit resolution); SN 1587

Component	Digitizer Channel No.	Sensor Serial No.	Sensor Model	Sensor Component Serial No.	Gain	Natural Frequency (hertz)	Damping Factor (units of critical)
L	4	-	FBA23	51402	1	50.8	0.65
V	5	-	FBA23	51403	1	49.9	0.67
T	6	-	FBA23	51404	1	50.4	0.66

Comments:

This station is located on the crest of Joe's Valley Dam. One 12-channel K2 (#1587) records data from both station JVDA and station JDVC. Unlike the all the other stations in the Trail Mountain array, these sensors are oriented along the axis of the dam following traditional engineering convention, where channel 4 (L) is pointed towards the right abutment (197 degrees), channel 5 (V) is up, and channel 6 (T) is pointed upstream (287 degrees).

Channel 1 was observed to have some problems when recording noise triggers. Seismic triggers appear to be recorded ok, but this is not certain. We decided to swap out the FBA23 sensor, installed a new sensor on January 31, 2001.

Polarity Convention

FBA23: negative output for positive acceleration.

Displacement Response Data

The Poles and Zeros listed below are those of a ratio of polynomials of the Laplace Transform variable "s".

	L	T	V
Zeros 2 (radians/second)	0.0 ± 0.0i	0.0 ± 0.0i	0.0 ± 0.0i
	0.0 ± 0.0i	0.0 ± 0.0i	0.0 ± 0.0i
Poles 3 (radians/second)	-207.5 ± 242.6i	-209.0 ± 237.9i	-210.1 ± 232.8i
	1000.0 + 0.0i	1000.0 + 0.0i	1000.0 + 0.0i
Gain Constant (counts/micron)	0.8690×10^8	0.8561×10^8	0.8409×10^8

B. *Valid Date/Time Range: January 31, 2001 – February 28, 2002 (end of project)*
Digitizer: Kinemetrics Altus Series K2 (19-bit resolution); SN 1587

Component	Digitizer Channel No.	Sensor Serial No.	Sensor Model	Sensor Component Serial No.	Gain	Natural Frequency (hertz)	Damping Factor (units of critical)
L	4	-	FBA23	52030	1	50.8	0.66
V	5	-	FBA23	52031	1	51.1	0.69
T	6	-	FBA23	52032	1	53.2	0.67

Comments:

This station is located on the crest of Joe's Valley Dam. One 12-channel K2 (#1587) records data from both station JVDA and station JDVC. Unlike the all the other stations in the Trail Mountain array, these sensors are oriented along the axis of the dam following traditional engineering convention, where channel 4 (L) is pointed towards the right abutment (197 degrees), channel 5 (V) is up, and channel 6 (T) is pointed upstream (287 degrees).

Channel 1 was observed to have some problems when recording noise triggers. Seismic triggers appear to be recorded ok, but this is not certain. We decided to swap out the FBA23 sensor, installed a new sensor on January 31, 2001.

Polarity Convention

FBA23: negative output for positive acceleration.

Displacement Response Data

The Poles and Zeros listed below are those of a ratio of polynomials of the Laplace Transform variable "s".

	L	T	V
Zeros 2 (radians/second)	0.0 ± 0.0i	0.0 ± 0.0i	0.0 ± 0.0i
	0.0 ± 0.0i	0.0 ± 0.0i	0.0 ± 0.0i
Poles 3 (radians/second)	-210.7 ± 239.8i	-224.0 ± 248.1i	-221.5 ± 232.4i
	1000.0 + 0.0i	1000.0 + 0.0i	1000.0 + 0.0i
Gain Constant (counts/micron)	0.8683×10^8	0.9523×10^8	0.8857×10^8

APPENDIX B

SEISMIC VELOCITY MODEL FOR THE TRAIL MOUNTAIN AREA

by

James C. Pechmann, Walter J. Arabasz, Kristine L. Pankow, and Matthew E. Jensen
University of Utah Seismograph Stations
Department of Geology and Geophysics
University of Utah

SEISMIC VELOCITY MODEL FOR THE TRAIL MOUNTAIN AREA

by

James C. Pechmann, Walter J. Arabasz, Kristine L. Pankow, and Matthew E. Jensen
University of Utah Seismograph Stations
Department of Geology and Geophysics
University of Utah

We constructed a velocity model for the Trail Mountain Mine area for use in analyzing local seismic events recorded in the Trail Mountain study (Table B-1). We refer to this model as the Trail Mountain Composite (TM) velocity model because it consists of two separate one-dimensional models for use with two different groups of stations: (1) surface stations located within the Colorado Plateau province in Utah and (2) surface stations located along the eastern margin of the Basin and Range province in Utah. The uppermost 4.14 km of both models is the same. The models differ below this depth to account for differences in the crustal structure traversed by seismic waves propagating to the two different groups of stations. The Colorado Plateau version of the model was used for stations of the Trail Mountain array and for stations of the University of Utah regional seismic network at azimuths of approximately 0 to 210 degrees from Trail Mountain. The Basin and Range version of the model was used for regional network stations at azimuths between 210 and 360 degrees. The two separate models effectively account for significant differences in crustal structure between the eastern Basin and Range Province and the Colorado Plateau interior (see Arabasz and Pechmann, 2001).

The datum for both versions of the TM model is 2600 m above sea level—the approximate elevation above the active part of the Trail Mountain Mine in 2000-2001. We computed elevation corrections for the travel times using a P-wave velocity of 4.0 km/sec and an S-wave velocity of 2.04 km/sec. These velocities were chosen because they are the velocities of the layer immediately beneath the 0.1-km-thick low-velocity near-surface layer in the models. The assumption underlying this choice is that a similar low-velocity layer is present near the surface everywhere, regardless of elevation.

The top 0.8 km of the TM model is based on a stratigraphic column for the Trail Mountain area which we constructed from a geologic map (Larsen, 1997) and some average formation velocities computed from two sonic logs (Figure B-1). These logs are from two boreholes located 60 km NNE of Trail Mountain near the Willow Creek Mine. We used sonic logs from the Willow Creek region because the available sonic logs from the Trail Mountain region do not sample the uppermost 0.8 km of the stratigraphic section. Based on the sonic logs, we assigned a P-wave velocity of 4.0 km/sec to the Price River and Castlegate formations and 4.3 km/sec to the underlying Blackhawk formation. We extended the 4.0 km/sec velocity of the Price River formation upward into the overlying North Horn formation because we lacked

velocity measurements for this unit. We also extended the 4.3 km/sec velocity of the Blackhawk formation downward through the underlying Star Point sandstone and Mancos Shale formation, consistent with sonic log data for the latter discussed below and shown in Figure B-2. The Hiawatha coal seam, in which the Trail Mountain Mine is located, is at the base of the Blackhawk formation at 0.6 km depth in the TM model (Figure B-1).

Williams and Arabasz (1989) used mean vertical-interval velocities from high-resolution seismic reflection profiles on East Mountain, centered ~6 km ENE of the Trail Mountain Mine, to construct the uppermost kilometer of their velocity model for the East Mountain area. However, this part of their model consists of a strong velocity gradient with a P-wave velocity increase from 2.4 to 4.04 km/sec. Sonic log data from this depth range elsewhere in the region indicate a much thinner near-surface velocity gradient. Based on this sonic log data, including the data from the Willow Creek area, we decided to replace the Williams and Arabasz (1989) near-surface gradient by a 0.1-km-thick top layer with a P-wave velocity of 3.5 km/sec. In our model, the average velocity above the depth of the Hiawatha coal seam is 4.0 km/sec. This velocity is at the upper end of the range of average velocities above this coal seam interpreted from the East Mountain seismic reflection data, which is 3.1 to 4.0 km/sec.

The TM model between 0.8 and 2.4 km below the 2600 m datum was generalized from sonic logs from two boreholes in the Trail Mountain Mine area: Indian Green 02-176-1, located 8 km north of the mine and Federal 41-33 located 12 km southeast of the mine (Figure B-2). From Larsen's (1997) geologic map and other information (see Figure B-2 caption), the formation boundaries in both wells are estimated to be at comparable elevations but ~0.4 km higher than their elevations in the Trail Mountain area. Consequently, we adjusted the depths of the velocities from these logs for this ~0.4 km difference in stratigraphic level. The Federal 41-33 log provides velocity information to greater depths. Williams and Arabasz used this log in constructing their East Mountain model, which is a reasonable fit to the sonic log data. Therefore, to obtain the TM model from 2.4 to 4.14 km below the datum, we modified their East Mountain model by decreasing the layer boundary elevations by 0.4 km. Figure B-2 shows that the Trail Mountain model is a reasonable generalized fit to the elevation-adjusted sonic log data.

Below 4.14 km depth, the Basin and Range version of the TM model is modified from model B of Keller et al. (1975). This model is from an unreversed seismic refraction profile beginning at an open-pit mine near Salt Lake City and extending 245 km southward along the Basin and Range/Colorado Plateau transition zone. The Colorado Plateau version of the TM model below 4.14 km depth is modified from the model determined by Roller (1965) for the northern end of a 300-km-long reversed refraction line across the Colorado Plateau in southeastern Utah and northwestern Arizona. The modifications to both of these refraction models are based on analyses of travel-time data from local and near-regional earthquakes and blasts recorded on the University of Utah seismic network (Loeb, 1986, Loeb and Pechmann, 1986).

The top three layers (2.04 km) of the TM model are the most important for the Trail Mountain study because the great majority of the seismic events, and the first arrival ray paths from these events to the local Trail Mountain stations, appear to be confined to these three layers (see Appendix E). The ratio of P-wave velocity, V_P, to S-wave velocity, V_S , typically decreases

with increasing depth from a value of around 2.0 near the earth's surface to about 1.73 at a depth of a few kilometers (e.g., Nicholson and Simpson, 1985; Moos, 1988). Considering the potential importance of S-wave arrival times for constraining focal depths, we decided to investigate the V_P/V_S ratio in the uppermost crust in the Trail Mountain region using the station pair method. In this method it is assumed that, to a first approximation, the V_P/V_S ratio is constant and therefore the ray paths for both P and S waves are the same. Under this assumption, a plot of the difference in S-wave arrival time versus the difference in P-wave arrival time for station pairs recording the same earthquake should define a straight line passing through the origin with a slope equal to V_P/V_S.

We applied the station pair method using arrival-time picks from the UUSS data set, excluding picks from the underground station TU1. Linear regression of all 111 station pair data points having perfect pick weights (0 for P-waves and 2 for S waves), with the line intercept fixed to zero, yields an average V_P/V_S ratio of 1.98 ± .03 (95% confidence limits; Figure B-3). All of these data points have P-wave arrival-time differences less than 1.2 sec. If the weight criteria are discarded there are only six data points with significantly larger P-wave arrival-time differences, and all of these differences are between 10.75 and 11.15 sec. Constrained linear regression of these six data points suggests a lower V_P/V_S ratio of 1.71 ± .01. The latter value is similar to the empirically-determined V_P/V_S ratio of 1.74 used in the velocity models for routine earthquake locations at the University of Utah. Guided by these results, we computed S-wave velocities for the TM model using V_P/V_S ratios of 1.97 in the top layer, 1.96 in the next two layers, and 1.74 in the rest of the layers. Using this model (Table B-1) to calculate P- and S-wave travel-time differences for the same station pairs as in Figure B-3 produces a regression line with a slope of 1.97—consistent with the observed slope of 1.98 ± .03. Using this model to calculate P- and S-wave travel-time differences for the six station pairs used in the second regression produces a regression line with a slope of 1.75, which is close to the lower limit value of 1.74 expected for widely-separated station pairs based on ray path geometries.

Figure 4-4 shows that the Trail Mountain velocity model provides an acceptable fit to the travel-time data from one of the larger seismic events to occur during the Trail Mountain study.

References

Arabasz, W.J. and J.C. Pechmann, with contributions from M.K. McCarter and J.D. McKenzie (2001). Seismic characterization of coal-mining seismicity in Utah for CTBT monitoring, Final Report, Lawrence Livermore National Laboratory Research Agreement No. B344836, 125 pp.

Keller, G. R., R. B. Smith, and L. W. Braile (1975). Crustal structure along the Great Basin-Colorado Plateau transition from seismic refraction studies, *J. Geophys. Res.* **80,** 1093-1098.

Larsen, K. (1997). Cottonwood Canyon Tract lease-by-application no. 8 spring map, Energy West Mining Company, scale 1:24,000.

Loeb, D. T. (1986). The P-wave velocity structure of the crust-mantle boundary beneath Utah, *M.S. Thesis*, University of Utah, Salt Lake City, Utah, 126 pp.

Loeb, D. T. and J. C. Pechmann (1986). The P-wave velocity structure of the crust-mantle boundary beneath Utah from network travel-time measurements, *Earthquake Notes* **57** (1), 10.

Moos, D. (1988). The effects of mylonitization and fractures on elastic wave velocities in crystalline rock—examples from the Cajon Pass scientific drillhole, *Geophys. Res. Lett.* **15,** 1053-1056.

Nicholson, C. and D. W. Simpson (1985). Changes in V_p/V_s with depth: Implications for appropriate velocity models, improved earthquake locations, and material properties of the upper crust, *Bull. Seism. Soc. Am.* **75**, 1105-1123.

Roller, R. C. (1965). Crustal structure in the eastern Colorado Plateaus province from seismic refraction measurements, *Bull. Seism. Soc. Am.* **55,** 107-119.

Williams, D. J. and W. J. Arabasz (1989). Mining-related and tectonic seismicity in the East Mountain area, Wasatch Plateau, Utah, *Pure Appl. Geophys.* **129**, 345-368.

Table B-1

The Trail Mountain Composite Velocity Model

Eastern Basin and Range Province Stations (Datum =2600 m)			*Colorado Plateau Province Stations* (Datum = 2600 m)*			*Stratigraphy (from this study and Williams and Arabasz, 1989)*	
P-Wave Velocity (km/sec)	**S-Wave Velocity (km/sec)**	**Depth to Top of Layer (km)**	**P-Wave Velocity (km/sec)**	**S-Wave Velocity (km/sec)**	**Depth to Top of Layer (km)**	**Formation Bounding Base of Layer**	**Age of Formation at Base of Layer**
3.50	1.78	0.00	3.50	1.78	0.00	North Horn	Tertiary
4.00	2.04	0.10	4.00	2.04	0.10	Castlegate Ss	Cretaceous
4.30	2.19	0.36	4.30	2.19	0.36	Mancos Sh	Cretaceous
4.40	2.53	2.04	4.40	2.53	2.04	Morrison	Jurassic
4.84	2.78	2.48	4.84	2.78	2.48	Moenkopi	Triassic
5.81	3.34	3.88	5.81	3.34	3.88	Kaibab Ls	Permian
5.90	3.39	4.14	6.20	3.56	4.14		
6.40	3.68	19.90	6.80	3.91	30.70		
7.50	4.31	32.00	7.90	4.54	45.00		
7.90	4.54	45.00					

*Includes all of the stations in the local Trail Mountain network

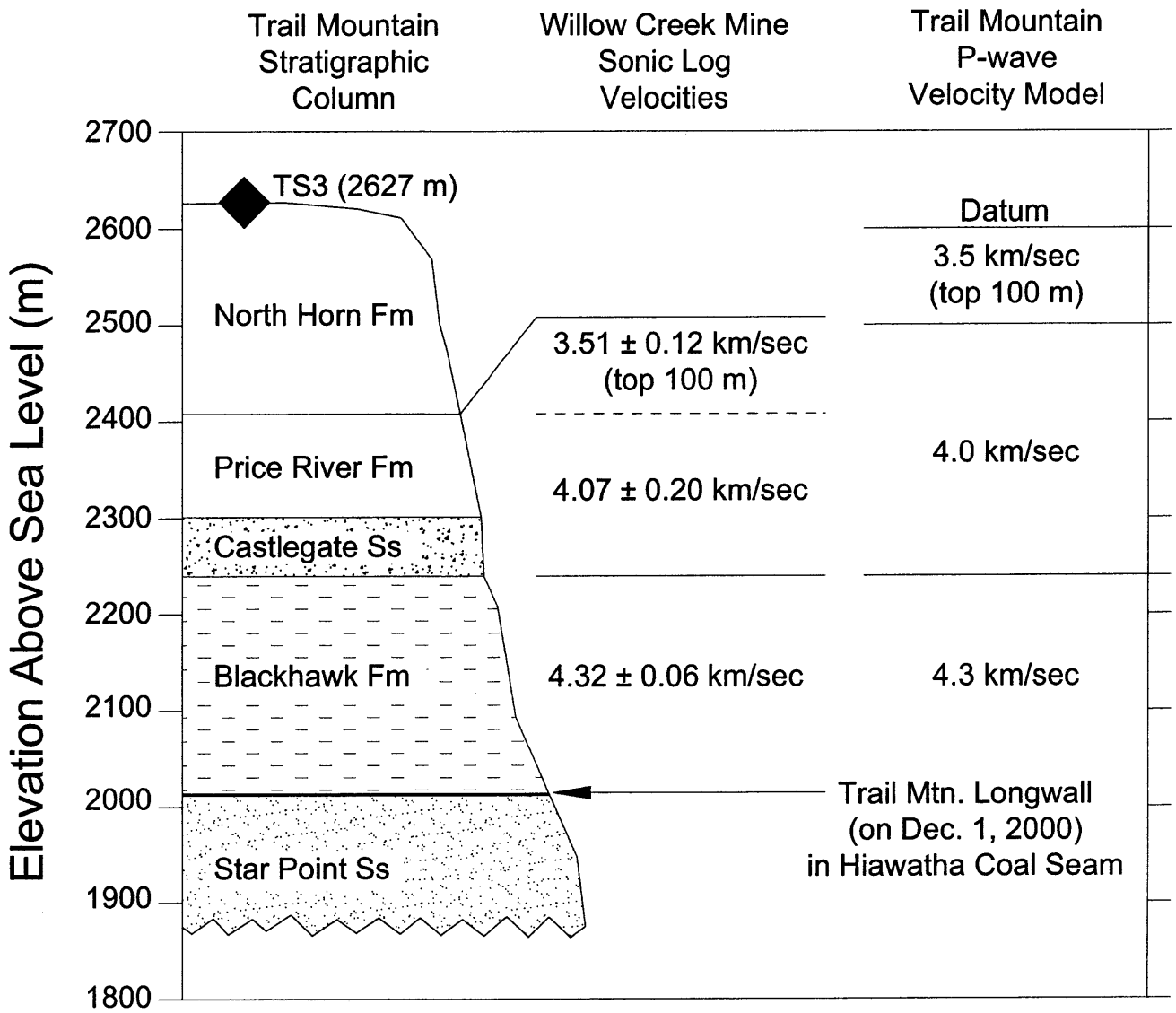

Figure B-1. Illustration of the construction of the uppermost 0.8 km of the Trail Mountain P-wave velocity model (right side) from a stratigraphic column for the Trail Mountain area based on Larsen's (1997) geologic map (left side) and average formation velocities computed from sonic logs (center). The sonic logs are from two boreholes located 60 km NNE of Trail Mountain near the Willow Creek mine: Cyprus Plateau Mining hole numbers 96-25-3 and 96-30-3. The solid diamond marks the elevation of 3-component seismic station TS3, the closest surface station to the Trail Mountain Mine.

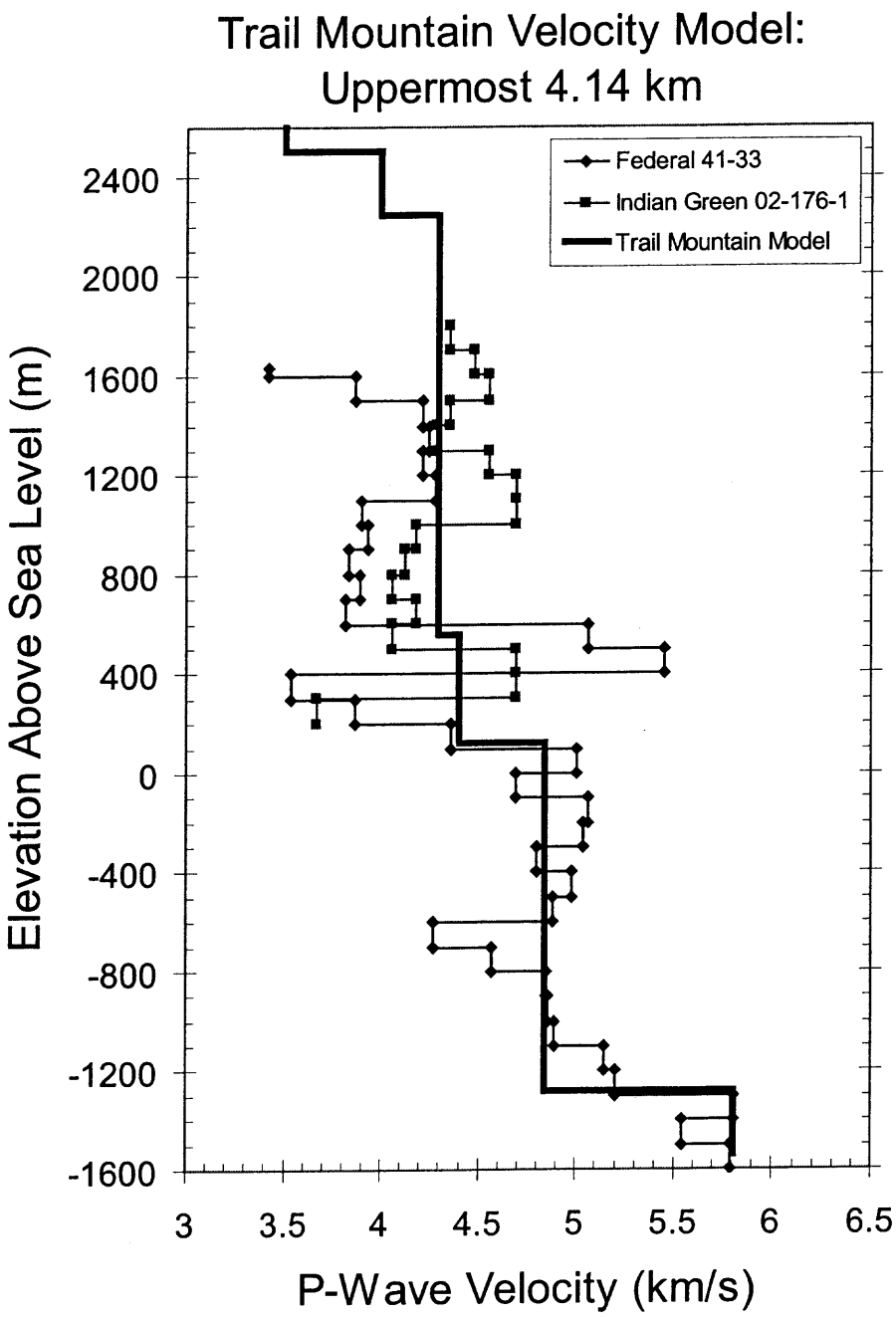

Figure B-2. Comparison between the Trail Mountain P-wave velocity model (heavy line) and sonic log velocities from the Federal 41-33 well (line with diamonds) and Indian Green 02-176-1 well (line with squares). The sonic log velocities shown are mean values for 100 m depth intervals. These velocities have been shifted downward 400 m in elevation to account for stratigraphic column elevation differences between the Trail Mountain Mine and the Indian Green 02-176-1 well, estimated from elevations of the base of the Castlegate sandstone shown on Larsen's (1997) geologic map. The formation elevations at the Federal 41-33 well (39° 13.2' N, 111° 8.0' W) are assumed to be similar to those at the Indian Green well (39° 22.47' N, 111° 13.02' W) because the former is 19 km SSE (157°) of the latter and the regional strike direction of the bedding is SSE.

result of pillar extraction in room and pillar mining. The practice in this form of mining is to recover coal by driving a series of openings in the coal seam (forming a panel) and then recovering as much of the coal in the remaining pillars as possible as operations retreat from the panel.

Agapito, Goodrich and Moon (1997) report increased burst frequency as cover depths reach 1,800 to 2,000 feet. Most of the bursts occurred in the gate pillars and to a lesser extent in the longwall face. These observations were made in the Deer Creek Mine. The geologic conditions at this location are similar to those expected in the Cottonwood Tract. These conditions include, competent immediate roof, numerous sandstone channels above the coal seam, strong coal, and similar overburden strata. The Deer Creek Mine also employs longwall mining utilizing a two-entry gate-road system. The two-entry system, as opposed to three or more entries, has proven to be an effective technique for controlling and minimizing gate pillar bursts and, in all likelihood, would be the method of choice for the Cottonwood Tract. It is expected that bounces will become more frequent and severe as the depth of cover exceeds 2000 feet.

Overlying Strata - The strata above the coal seam are divided into two distinct zones (Peng and Chiang, 1984). The immediate roof is that portion of the overburden which is directly above the coal seam and caves behind the longwall props (shields) as the face advances. The main roof is that portion of the overlying strata that fractures and sags in response to the caving of the immediate roof. It breaks in blocks along lines parallel to the longwall face and moves downward in large units. Vertical movements of these units are maximum above the immediate roof and become progressively less toward the surface. It is this portion of the overlying strata that forms beams that project over the gob area. These beams are subjected to shearing forces parallel to the bedding planes within the beam. The stress on the coal seam produced by the cantilever is at a minimum just after a vertical crack forms at the longwall face. The stress increases as the coal is removed and the beam deflects in response to the pressure imposed by the overlying strata. This stress reaches a maximum just before the beam fails. This cycle is repeated continuously as the longwall advances down the panel and is referred to as "periodic weighting."

Underlying Strata - Coal seams are frequently underlain by shale or clay. If material of this nature is present, coal pillars in the panel entries or the longwall face itself can be forced (punched) into the floor. Such action can allow the vertical stress to dissipate gradually rather than suddenly. If the floor is strong and competent, the coal pillar is more likely to fail resulting in a pillar burst.

Strength of Coal - The more competent the coal, the more likely failure will be sudden and violent. The bump conditions improve when the coal is friable enough to crush readily as the superimposed load increases. This reduces the opportunity of accumulating elastic strain energy. It is this phenomenon which governs the success of the two-entry system in reducing bursting. Instead of designing rows of robust chain pillars, the two-entry system relies on pillars that will crush, accumulate permanent strain rather than store elastic energy, and transfer the load to adjacent areas.

Mining Method - Most of the coal mined in Central Utah is produced from longwall operations or from development of entries to establish longwall panels. In the past, continuous miner sections employed room and pillar methods. The sequencing and geometry of the openings employed in the room and pillar technique strongly influenced the potential for bounces.

In longwall mining, removal of coal and the resulting void causes redistribution of lithostatic stress forming abutment pressure along the lateral margins of the panel and front abutment pressure at the longwall face (Peng, 1986). This results in vertical stress near the margins of the panel in excess of the average overburden pressure. This is illustrated in Figure F-2. The interaction and summation of side abutment pressure, front abutment pressure and redistribution of vertical stress over panel entries frequently result in higher face and pillar bursting activity near the head and tail gates. Redistribution of stress is complicated as successive panels are mined. Mining of the first panel usually proceeds with a minimum of difficulty in so far as roof control and bounces are concerned. Bounce activity can be expected to increase in successive panels because the abutment pressure of a mined-out prior panel adds to the abutment pressure of the next panel in succession. Abutment pressure on mined out panels, however, decreases with time as subsidence reaches the surface.

Panel Width - Critical width is defined as that width that results in maximum possible subsidence at one point on the surface (Agapito et al., 1997). For longwall panels that are less than critical width, abutment pressures are high and pressure bumps can be expected. As the width increases, abutment pressures also increase to a maximum. For supercritical widths, arching in the main roof is destroyed and abutment pressures begin to decrease. Theoretically, abutment pressure will remain constant regardless of panel width provided panels are wider than the critical width. This, of course, assumes a constant depth of overburden. Once subsidence has progressed to the surface, the load imposed by the broken material is supported by the floor of the gob area rather than the abutments. The practical reality is that the depth of overburden is not constant especially in the mountainous terrain of the Wasatch Plateau and Circle Cliffs. Also, the greater the width, the greater the likelihood of encountering adverse geologic conditions such as sand channels in the roof, faults and other geologic features. Other than topography, these features are difficult to predict and, therefore, present random hazards which may increase the likelihood of unexpected MIS.

Rate of Mining - The rate of advance of the longwall face horizontally through the panel is a direct function of the amount of coal produced per unit of time. The rate of advance, therefore, governs the periodic weighting described above. For a given rate of production, the periodic weighting cycle is longer for wide panels compared to narrower panels. Consequently, the frequency of MIS varies inversely with the panel width and directly with the production rate. This relation between event frequency and production is documented by Arabasz and Pechmann (2001). It is, however, unclear whether or not the production rate affects the magnitude of the resulting events. Assuming event magnitude follows some statistical distribution, the greater the number of events in the sample, the greater the likelihood of including extreme events. Therefore, occurrence of large events in a high production period may be a statistical artifact rather than the large event being caused by the higher advance rate. One may also argue that higher advance rates result in a greater likelihood of stress build up

with less time for relaxation. Earth materials do possess rheologic characteristics and the time-dependent behavior may actually exacerbate the magnitude of MIS.

Regional Stress - Regional stress as well as stress redistribution caused by mine geometry plays an important role in ground control. Regional stress directions and magnitudes can be evaluated by borehole measurements, and geometrical effects of mine openings on stress fields can be estimated by numerical modeling. These methods are expensive and complicated and little has been done to correlate MIS potential with these perturbations in the stress field, particularly in deep western U.S. settings..

STRATIGRAPHIC UNITS

The lithologic environments for the three areas identified in Table 1 are similar and are present in the Cottonwood Tract as well. The coal horizons all occur in the Blackhawk formation and the overlying units are the same but have varying thicknesses. The following description applies to all areas that will be compared in this appendix (see Figure F-3).

Star Point Sandstone - This is the lowest of the four formations comprising the Mesaverde Group of upper Cretaceous age (Doeling, 1972). It consists of yellow-grey massive cliff-forming sandstone units ranging from 90 to 1000 feet thick. In places it is separated by shale or partings of thin-bedded sandstone. This unit is below the shale and mudstone floor of the Haiwatha coal seams in the Deer Creek, Cottonwood, and Trail Mountain mines as well as the Cottonwood lease area. Where competent, the Star Point appears to store and release significant elastic energy. The Star Point Sandstone is absent in the Castle Gate area. The Aberdeen Sandstone (a component of the Blackhawk Formation) occurs below the D and K seams that are mined in the Castle Gate area

Blackhawk Formation - This unit consists of layers of siltstones, mudstones, shales, sandstones and coal (Ellenberger et al., 2001). It contains alternating slope- and cliff-forming layers and is less resistant than the sandstone layers that occur above and below it. The cliff-forming sandstones are generally yellow-gray or white-gray. The proportion of shale to sandstone increases to the north. The ratio of sandstone to shale is 2:1 (Doelling, 1972). The material above the coal beds consists of braided stream deposits with numerous lenticular channel sandstones which make up the immediate and main roof of the mineable coal seams.

Castlegate Sandstone - The Castlegate Sandstone is a massive cliff-forming unit that ranges from about 200 to 600 feet in thickness. It consists of medium- to coarse-grained sandstone with some conglomerate and sandy hard shale. The lower portions of the unit are more compact and dense compared to the upper portions. This unit often caves with difficulty and is suspected of generating large seismic events when failure ultimately occurs.

Price River Formation - The rock above the Castlegate is less resistant to erosion and consists mainly of coarse-grained sandstone with occasional interbeds of gray to brown shale forming step-like outcrops. The unit ranges from 600 to 1000 feet in thickness (Doeling, 1972).

North Horn Formation - Identification of the contact between the North Horn and Price River formations is not obvious. This formation is, however, less resistant to erosion and forms slopes and rolling topography instead of steps. The lower portions are of Cretaceous age and the upper portions are Tertiary in age. Thickness ranges from 500 to 2500 feet. Thickness increases northward.

Flagstaff Limestone - The Flagstaff is more resistant than the North Horn and consists of beds of lacustrine limestone. It is dark yellow-gray or cream in color. Thickness ranges from 200 to 1500 feet. Small amounts of interbedded sandstone, shale and volcanic ash are present. In the Cottonwood Tract only a small portion of the Flagstaff remains at the upper extreme of the topography. Most has been eroded away.

MINING ENGINEERING AND GEOLOGICAL FACTORS IN PAST EVENTS

Willow Creek Event M_L 4.2

Topography - The topography is characterized by deeply incised canyons with prominent ridges formed by eroding narrow canyons cutting into the adjacent highlands. This topography results in rapidly changing depths of overlying strata producing highly variable lithostatic stress. As shown on Figure F-4, the elevations in the vicinity of the mine vary from 6400 to over 8000 feet with significant portions of the exposure being nearly vertical. Experience has shown the highly variable overburden thickness compared to areas of more moderate relief contributes to a higher probability for MIS.

Seam Characteristics - Recent mining is confined mainly to the Castelgate D seam. The mining horizon ranges from 8 to 20 feet in thickness with a mining height of 8 to 10 feet (Ellenberger, 2001). Testing of twenty samples indicates a compressive strength for the coal ranging from 1498 to 7652 psi (Hurst, 2000). The coal is described as strong and brittle, more so than coal from the Hiawatha seam on the Wasatch Plateau (McKenzie, 2002). Seam geometry reflects discrete pods several miles in extent that developed on a low-lying deltaic plain. Thickening and thinning of the seam is a result of merging or splitting of consecutive lenticular horizons. Floor strata consist primarily of siltstone or fine-grained sandstones. Immediate roof is composed of carbonaceous mudstones overlain with thin to thick laminated sandstones (Schissler and Mercier, 1999). Higher strength and brittle failure characteristics of the coal make this deposit more bump-prone compared to coal from the Hiawatha seam. The seam and adjacent strata also contain more hydrocarbons in gas and liquid form than the Hiawatha. This can affect face bursts but is not considered a major factor in production of MIS for this area.

Main Roof Characteristics - The Castlelgate D seam occurs near the center of the Blackhawk Formation. Braided stream deposits with numerous lenticular channel sandstones occur between the immediate roof and the bottom of the Castlegate Sandstone. Directly above the mine, the Castlegate Sandstone is approximately 600 feet thick (see Figure F-3). The floor of the mining horizon is 5600 feet in elevation and the overlying strata continue vertically upward

to more than 8000 feet (McCarter, 2001). The depth of cover is, therefore, approximately 2400 feet. This is well above the depth identified by Agapito, Goodrich and Moon (1997) as contributing to MIS. The presence of sand channels in the immediate roof also contributes to bump prone conditions. Figure F-4 illustrates that the M_L 4.2 event occurred when the longwall face reached the maximum depth of cover.

Width of Panel - The first panel mined was approximately 800 feet wide and 2000 feet in length before mining ceased. The second panel was started with a width of approximately 550 feet and advanced to a position roughly equivalent to the length of the first panel at which time the
M_L 4.2 event occurred. It is not clear whether or not subsidence had reached the surface before the event. Presumably, it had not in that the cause of the event is attributed to the Castlegate Formation falling into the gob (Ellenberger et al., 2001). If this is the case, abutment pressure would have been high but no coal bumps were reported. It appears that the MIS source was ahead of the face and above the coal bed. It was also located on the southwest side of the panel closest to the previously mined panel (Ellenberger et al.l, 2001). The rate of advance of the longwall face varied up to 3 feet per hour during the period of February 14 - 21 (Westman et al., 2001). The average appears to be about 1 foot per hour for this same period of time.

Tectonic Features - The dip of beds in this area is to the north at about 11° (McCarter, 2001). Principal fracture trends are N 60° W with a weak secondary set trending N 75° E (Schissler and Mercier, 1999). The dips of these structures are nearly vertical. Major faults are not evident. Face cleats in the coal trend about N 60° W and butt cleats trend about N 35° E. These features are not anomalous and may have had little impact on MIS. It is interesting to note however, that one of the possible failure mechanisms is oblique reverse faulting on a plane dipping shallowly to the north-northwest (Ellenberger et al., 2001). This direction does parallel the plunge of the bedding at the base of the Castlegate Sandstone.

Local and Regional Stress - The mine is located in Price Canyon at the Eastern margin of the Wasatch Plateau. At this location, horizontal compressional stress is anomalously high (Arabasz and Wyss, 1999). In addition, an earlier event of M_L 3.8 occurred on February 5, 1998. This event is associated with sloughing of pillars in gate road development for the first longwall panel. The location of the affected pillars is very near the position of the face of the second longwall panel at the time of the March 7, 2000 event. Coal bumps of this magnitude resulting from development entries are highly unusual. The two entries were approximately 20 feet wide and up to 9 feet high, separated by a pillar 25 to 30 feet wide and 125 to 200 feet long (McCarter, 2001). The two-entry pattern normally reduces the severity of bumps on a producing longwall panel. The fact that a bump occurred under these conditions suggests a highly stressed zone existed in this location. High regional or local stresses, of course, could exacerbate MIS.

Cottonwood Mine Event M_L 3.5

Topography - The surface immediately above the longwall panel involved in this event is in transition between a steep canyon and the more gently rolling highlands into which the canyon

is eroding (see Figure F-5). As in the case of Willow Creek, the surface topography consists of an east-west trending ridge between two canyons. The one on the north is not as steep as the one on the south. The elevation of the surface above the panel ranges from 9200 to 9440 feet. The depth of cover at this location ranges from 1800 to 2000 feet (Fry, 2000). This cover depth is in the range identified earlier as bump prone (Agapito, Goodrich and Moon, 1997)

Seam Characteristics - The Hiawatha seam in this location is 10 to 12 feet thick. Mining height is approximately 9 feet. Reportedly, the coal it is more friable than the Castlegate seam (McKinzie, 2002). Coal that is prone to crushing reduces the severity of coal bumps in that permanent strain decreases the amount of energy that can be stored before bursting occurs.

Main Roof Characteristics - The Hiawatha seam occurs near the bottom of the Blackhawk Formation (see Figure F-3). Sand channels occur in the immediate roof. One located approximately 1000 feet to the north of the panel trends east and west. This channel displays slickensides along the margins. The Blackhawk Formation is approximately 700 feet thick in this area and is overlain by the Castlegate Sandstone which is up to 300 feet thick. The Blackhawk contains a significant amount of shale which promotes caving. So the added thickness relative to the Willow Creek area would tend to reduce MIS potential. The presence of sand channels, however, is an exacerbating feature.

Width of Panel - The panel shown on Figure F-5 is one of several that were mined starting in the south and working to the north. This panel is approximately 600 feet wide and was more than 1800 feet long at the time the event occurred. Since a number of panels had been mined to the south, caving was probably well developed on the south side of the panel. Given this scenario, overhanging beam elements and higher abutment pressure would occur on the north side of the panel. Panel development consisted of three entries on 100 foot centers separated by 80 x 80 foot pillars. Development using three entries has been replaced in recent years by the two-entry system because two-entry development has been found more effective in ameliorating bump potential and decreases the time and expense of panel development. The M_L 3.5 event coincided with pillar bursts involving nine pillars on the head gate (north) side of the panel directly below the ridge line. The mechanism, therefore, could be either a pressure bump or possibly a shock bump caused by failure of beam elements on the north abutment. It is interesting to note that approximately one month earlier (June 3, 1992) a bump occurred on the north side of this same panel. The depth of cover was approximately 200 feet higher than the event on July 5, 1992. It involved fewer pillars and produced a M_L 3.2 event. The depth of cover, use of a three entry system, depth of overburden, and topography transition may have contributed to the M_L 3.5 event.

Tectonic Features - The dip of beds in this area is to the north at 1 to 2° (Fry, 2000). No information is presently available on faults or cleating in the seam. The dip of the bed is not anomalous and probably had little impact on MIS.

Local and Regional Stress - No information is currently available on anomalous stress conditions.

Trail Mountain (Pre Energy West Operations) Event M_L 3.3

Mining Method - The source of this event was located in the Pre Energy West workings identified on Figure F-6. These workings employed room and pillar mining. The exact location of the event is unknown and there are no records to relate observations in the mine at the time of the event.

Topography - The surface immediately above these workings coincides with the canyon wall on the west side of Cottonwood Creek. The depth of cover ranges from 1200 feet on the east to 1900 feet on the west (McCarter, 2001). The topography, therefore, gives rise to a rapidly changing vertical stress field which has been identified as a factor contributing to MIS. The cover depth, however, is generally lower than the bump prone threshold identified by Agapito, Goodrich and Moon (1997).

Seam Characteristics - The Hiawatha seam is the economic horizon in this area. Typically it is thicker than 7.5 feet which was the mining height in this area. The strength of coal used for design purposes is 3000 psi (Beaver Creek Coal Co., 1988) which is lower than the average for coal from the Castlegate seam and is probably similar to that encountered in the Cottonwood mine.

Main Roof Characteristics - The Hiawatha seam occurs near the bottom of the Blackhawk Formation (see Figure F-3). Sand channels occur in the immediate roof. The Blackhawk Formation is approximately 700 feet thick in this area and is overlain by the Castlegate Sandstone which is up to 300 feet thick but probably averages about 200 feet thick. The sand channels and Castlegate Sandstone are strong units that can affect caveability of the overlying strata. The Blackhawk contains a significant amount of shale which promotes caving and can serve to lessen the force transmitted to pillars by seismic events in the main roof. So the added thickness relative to the Willow Creek area would tend to ameliorate MIS potential. The presence of both the Castlegate Sandstone and sand channels, both of which are strong, have the opposite effect.

Width of Panel - Panel dimensions were reported to be 400 feet wide by 3000 feet long. The extraction ratio for pillar recovery is not known, but the panels were designed to support the overburden with less than maximum subsidence. Consequently, the abutment pressure on the chain pillars between panels was high, possibly contributing to MIS.

Tectonic Features - The dip of beds in this area is to the west at 3 - 4° . No information is presently available on faults or cleating in the seam. The dip of the bed is not anomalous and probably had little impact on MIS.

Local and Regional Stress - No information is currently available on anomalous stress conditions.

Cottonwood Tract

For a comparison of features in the Cottonwood Tract (see Figure F-1 for general location) with the three selected maximum events, it is necessary to determine the structure of the coal seam and the probable depth of cover. To do this, logs of publically available drill holes were obtained and used to plot structural contours and cover isopachs. Figure F-7 identifies the drill holes used for this purpose.

Topography - As shown on Figure F-8, the northern regions of the tract are dominated by canyons and steep slopes. To the south, the topography is typically highlands with more gradual slopes truncated at the margins by cliffs formed by stream erosion on the south and the Joes Valley fault escarpment on the west. Elevations range from 7600 feet in Joes Valley to 9600 feet at the north end of the tract.

Seam Characteristics - The Hiawatha seam intercept in hole GS-TM-7 is approximately 14.5 feet (Foster and Sommer, 1986), and the seams decrease in thickness to the north and to the south. Hole C-302 encountered about 8.5 feet of Hiawatha coal on the north side of the tract and the bed is less than 5 feet in hole GS-TM-13 on the south side. The coal also increases in ash content as the bed approaches the south boundary of the Tract. The trend of the seam shows the effects of the Straight Canyon syncline. To the south of the syncline the bed strikes north-northwest and dips to the west at about 4°. To the northwest of the syncline, the bed strikes east-west and dips to the south at about 4°. The immediate roof is composed of sandstone, shale, siltstone and lenses of Blind Canyon coal. The immediate floor consists of carbonaceous shales and the stronger units of Star Point Sandstone at depth.

Main Roof Characteristics - As in other locations, the Hiawatha seam occurs near the bottom of the Blackhawk Formation (see Figure F-3) and above the Star Point Sandstone. Sand channels occur within the Blackhawk and their distribution and orientation will likely be similar to those encountered in the Trail Mountain Mine. The total depth of hole GS-TM-7 is approximately 2500 feet. The hole is collared in the North Horn Formation. Consequently, the thickness of the stratigraphic units must be greater than those shown for the Cottonwood/Trail Mountain column shown on Figure F-3. The column labeled local stratigraphic column was generated on the basis of surface geology (Larsen, 1997) and the hole log provided by Foster and Sommer (1986). In this column, the Castlegate Sandstone is shown as 300 feet thick. It may be thinner, perhaps 200 feet in places as portrayed on the geologic map (Larsen, 1997) . The Blackhawk formation is shown as 1000 feet thick, it may vary from 700 to more than 1200 feet thick in places. The thicker sections will be located in the central portion of the Tract. Again, as the distance between the mining horizon and the Castlegate Sandstone increases, the likelihood of MIS will decrease. The presence of sand channels, however, increases the likelihood of bumps and resulting MIS. The occurrence of sand channels is more or less random, and their influence on frequency and magnitude of events will be difficult to predict. The depth in the central region of the Tract is likely to be 2400 feet or greater see Figure F-9. Consequently, the magnitude and frequency of events are expected to be higher than in the Trail Mountain study area (cover depth up to 2200 feet), the older Trail Mountain workings (cover

depth up to 1900 feet, and the Cottonwood Mine (cover depth of 1800 to 2000 feet). The depth of cover is comparable to the Willow Creek Mine.

Width of Panel - The operating experience gained in the Trail Mountain Mine in recent years will ultimately guide the selection and orientation of panels. Panels will likely be 700 feet or more wide and in excess of 6000 feet long and oriented in an east-west direction similar to those shown in Figure F-6.

Tectonic Features - The major structures in the area include the Straight Canyon syncline and Joes Valley fault shown on Figure F-10. The axis of the syncline trends approximately 50° east of north. The Joes Valley fault is a major feature which can be followed in excess of 100 miles. The displacement of this fault is in excess of 2000 feet in places (Doelling, 1972). Several other structures are projected into the area (Larsen, 1997). These include the Mill Fork graben and Roan's Canyon graben with associated faults. If these structures do exist as projected, the stress field may be complicated, especially near the central and south portions of the Tract. Similar fault structures have been known to increase vertical stresses at the margins of a graben by as much as twice those predicted by the depth of overburden (Goodrich et al., 1998). It can also be argued that the presence of faults and other discontinuities can serve to inhibit stress buildup thus reducing the risk of large magnitude MIS. Until proven otherwise, it will be assumed that such structures will contribute to increased frequency and severity of MIS.

Local and Regional Stress - No information is currently available on anomalous stress conditions.

MINING SCENARIOS

A competent detailed plan for the mining of the Cottonwood Tract would require greater knowledge than that derived from public logs of drill holes. Orientation of the Hiawatha coal seam and approximate depth of cover need to be refined before serious planning can be done. Some information has been obtained by professionals working in the area but it is of a proprietary nature. Additional drill holes and geologic study may be necessary before raising large sums of capital needed to develop the area for mining.

Two scenarios can be considered in a preliminary way:

Scenario 1 - The first and most likely approach to mining would be to develop panels parallel to the last panel mined in the Trail Mountain Mine. This could be done by driving entries to the north and developing panels to the east and west from these entries. In this way mining would proceed from the south toward the north. The most advantageous place to begin longwall mining would be at location 1A on Figure F-1. This is the thickest section of the Cottonwood Tract coal seam. It could be reached with a minimum of development work. Unfortunately, it is also where the depth of cover is greatest and roof control and the potential for bumps will be proportionally greater. The distance to Joes Valley Dam would begin at approximately 14,000 feet and would increase as mining operations moved northward. Mining consecutive panels

uphill would be preferred especially if water is encountered. It could also result in more favorable overburden load transfer. Alternatively, mining could begin under Scenario 1 at the location marked 1B on Figure F-1. Here the cover is less but the amount of development work would be much greater. Also, stress and water conditions which may be influenced by the proximity of the Joes Valley fault are unknown, and the distance to the Dam would be less, approximately 10,000 feet. Starting at either 1A or 1B would leave the rectangular area between the current Trail Mountain Mine and Joes Valley Fault to be mined at a later date although access could become difficult. Beginning mining operations at a distance of 14,000 feet (position 1A) would allow accumulation of operating experience in this area while at a safer distance from the Dam. Adjustments could then be made to limit the extension of mining toward the Dam to further safeguard this structure.

Scenario 2 - Mining could begin parallel to the south boundary near Straight Canyon in the southern rectangular extension of the Tract (position 2 on Figure F-1). It is doubtful that the first panel would encroach on the southern boundary itself, because doing so could risk the integrity of the cliffs and result in loose rocks. Rolling rocks could compromise safety of the public road at the base of the cliffs. In addition, development work would be costly, production would be delayed until the necessary development work could be completed, and the quality and thickness of the coal in this area are questionable. The possibility of significant amounts of water near the fault is also an important consideration for mining. It would be better to mine consecutive panels uphill rather than downhill under wet conditions. If water is a problem, mining uphill would allow using the previously mined openings as a sump from which water could be pumped. Water would be a continual problem for downhill mining. The advantage of this location for the initial panel is the low cover depth 1400 to 1800 feet. This would reduce but not eliminate the possibility of events as large as the M_L 3.3 event which occurred in the Old Trail Mountain Mine. The main disadvantage is that mining would begin at a distance of about 4200 feet from the Dam. If difficulty is experienced, there is little that could be done but abandon the panel and move uphill at considerable expense and loss of coal resources.

The following tables are assessments of conditions present in the Cottonwood lease relative to the areas discussed above. Four descriptors are used in the ranking: Higher is used to indicate that the conditions in the Tract area have a higher risk of producing MIS than those present in the comparison area. For example, the depth of cover for Scenario 1 compared to the Cottonwood Mine will be ranked "higher" since the depth of cover in Scenario 1 is greater than that in the Cottonwood Mine. Equal will indicate that the conditions are essentially the same, and Lower indicates that conditions in the Tract area have a lower risk of producing MIS than the comparison area. A question mark indicates unknown or unassessed conditions. This ranking will be performed for both scenarios.

CONCLUSIONS

On a purely subjective basis, but guided by the above rankings, the maximum credible earthquake due to mining in the Cottonwood Tract is likely to be in the range of M_L 3.2 to 3.5 or slightly higher for Scenario 1. Events of greater magnitude could be expected at 1A relative

to 1B. At either location, events probably will not be as high as M_L 4.2 as experienced at Willow Creek. For Scenario 2, the maximum credible earthquake due to mining in the Cottonwood Tract is likely to be less than M_L 3.2 to 3.5 provided that there exists no abnormal regional or local stress in the extreme southern portion of the Tract. It is, however, likely to be higher than the M_L 2.2 maximum magnitude recorded during the Trail Baseline Study. In all cases, more emphasis was placed on the depth of cover than the other factors.

ACKNOWLEDGMENTS

Jeff McKenzie's assistance in locating public documents dealing with mine plans and drill hole logs is gratefully acknowledged. He participated in this project while serving as an adjunct faculty member in the Department of Mining Engineering at the University of Utah. He also provided a valuable resource in defining practical aspects of mining in the Wasatch Plateau and Castle Gate areas. Matt Jensen provided terrain data above mine workings for some of the illustrations used in this appendix. Their help is greatly appreciated.

REFERENCES

Agapito, J.F.T., R. R. Goodrich and M. Moon, 1997, "Dealing with Coal Bursts at Deer Creek," Mining Engineering, Society for Mining, Metallurgy and Exploration, Inc.(SME), July 1997, p. 31-37.

Arabasz, W. J., S. J. Nava and W. T. Phelps, 1997, "Mining seismicity in the Wasatch Plateau and Book Cliffs coal mining districts, Utah, USA," *Rockbursts and Seismicity in Mines*, Proceedings of the 4th Internatinal Symposium on Rockbursts and Seismicity in Mines, Krakow, Poland, S. J. Gibowicz and S. Lasocki eds, A. A. Balkema Publisher, August 11-14, 1997.

Arabasz, W. J. and J. C. Pechmann, 2001, *Seismic Characterization of Coal-Mining Seismicity in Utah for CTBT Monitoring,* Final, Report, LLNL Research Agreement No. B344836, March 1, 2001.

Arabasz, W. J. and M. Wyss, 1999, "Spatially-varying b-values in coal-mining seismicity in Utah: Inferred influence of heterogeneity and stress differences on local mean magnitude" [abs.]: EOS, Trans. Am. Geophys. Union 80 (46).

Beaver Creek Coal Company, 1988, Trail Mountain No. 9 Mine, Mining Permit, Division of Oil Gas and Mining, Jan. 2, 1988.

Doelling, H. H. (1972), *Central Utah Coal Fields: Sevier-Sanpete, Wasatch Plateau, Book Cliffs, and Emery, Utah*, Utah Geological and Mineralogical Survey, Monograph. Series, No. 3.

Goodrich, R. R. , J.F.T Agapito, C. Pollastro and L. J. LaFrentz, 1998, "Longwall Mining Through a Graben With Anomalous Stresses At the Deer Creek Mine," Third North American Rock Mechanics Symposium, 3-5 June 1998, Cancun, Mexico Paper Number USA-801.

Foster, D. A. and S. N. Sommer, 1986, *Description, Correlation, and Summary of Coal Drill Core TM-7,* Utah Geological and Mineral Survey, Report of Investigation No. 205, March 1986, pp 1 - 30.

Fry, R. C., 2000, Exploration Administrator, Interwest Mining Co., personal communication, July 31, 2000.

Ellenberger, J. L. K. A. Heasley, P. L. Swanson, and J Mercier, (2001), "Three dimensional microseismic monitoring of a Utah longwall," *Rock Mechanics in the National Interest*, Proceedings of the 38th U.S. Rock Mechanics Symposium, DC Rocks 2001, Washington D.C., July 10, 2001, Elsworth, Tinucci and Heasley eds., A.A. Balkema Publishers, p. 1321- 1326.

Hurst, D. T., 2000, Personal Communication, Plateau Mining Corporation, Willow Creek Mine, July 19 2000.

Larsen, K, 1997, Cottonwood Canyon Tract Lease - by - Application No. 8, Spring Map, Energy West Mining Company, Huntington, Utah, March 12, 1997.

McCarter, M. K., 2001, Documentation of Ground Truth for Significant Seismic Events Related to Underground Mining in Utah and Wyoming, Appendix C, *Seismic Characterization of Coal-Mining Seismicity in Utah for CTBT Monitoring,* Prepared by W. J. Arabasz and J. C. Pechmann, March 1, 2001.

McKenzie, J. D., 2002, Personal Communication.

Peng, S. S., and Chiang, H. S., 1984, *Longwall Mining,* John Wiley and Sons, Inc., USA, p 17-71.

Peng, S. S., 1986, *Coal Mine Ground Control*, Second Edition, John Wiley and Sons, Inc., USA, p. 314 - 335.

Rice, G.S., 1935, "Bumps in coal mines of the Cumberland Field, Kentucky and Virginia - causes and remedy." U.S. Bureau of Mines, RI 3267.

Schissler, A. P. and J. M. Mercier, 1999, "Geotechnical tools to analyze, predict and mitigate high stress in longwall mining systems," Proceedings, Thirtieth Annual Institute on Mining Health, Safety and Research, Salt Lake City, August 8 - 11, 1999, p. 96 - 99.

Westmann, E. C., K. A. Heasley, P. L. Swanson, and S. Peterson, 2001, "A correlation between seismic tomography, seismic events and support pressure," *Rock Mechanics in the National Interest*, Proceedings of the 38th U.S. Rock Mechanics Symposium, DC Rocks 2001, Washington D.C., July 10, 2001, Elsworth, Tinucci and Heasley eds., A.A. Balkema Publishers, p. 319 - 326.

Table F-1

Events recorded at other locations with similar conditions.

Nearest Mine	Date	Local Magnitude
Willow Creek	7 March 2000	4.2
Cottonwood Mine	5 July 1992	3.5
Trail Mountain (prior to Energy West operations)	16 December 1987	3.3

Table F-2

Risk of Scenario 1 conditions producing greater MIS magnitude relative to the comparison area

Category	Willow Creek	Cottonwood Mine	Old Trail Workings	Trail Mountain Study Area
Depth of Cover	Equal	Higher	Higher	Higher
Topography	Lower	Lower	Lower	Equal
Strength of Coal	Lower	Equal	Equal	Equal
Presence of Sand Channels	Equal	Equal	Equal	Equal
Distance to Castlegate SS	Lower	Lower	Lower	Lower
Thickness of Castlegate SS	Lower	Equal	Equal	Equal
Regional/Local Stress	Lower	?	?	?
Tectonic Features	Higher	Higher	Higher	Higher
Panel Width	?	Equal	Equal	Equal
Design of Panel Entries	Equal	Lower	?	Equal
Floor Conditions	Equal	Equal	Equal	Equal
Extraction Rate	?	?	?	?

Table F-3

Risk of Scenario 2 conditions producing greater MIS magnitude relative to the comparison area

Category	Willow Creek	Cottonwood Mine	Old Trail Workings	Trail Mountain Study Area
Depth of Cover	Equal	Higher	Equal	Lower
Topography	Equal	Equal	Equal	Higher
Strength of Coal	Lower	Equal	Equal	Equal
Presence of Sand Channels	Equal	Equal	Equal	Equal
Distance to Castlegate SS	Lower	Equal	Equal	Equal
Thickness of Castlegate SS	Lower	Equal	Equal	Equal
Regional/Local Stress	Lower	?	?	?
Tectonic Features	Higher	Higher	Higher	Higher
Panel Width	?	Equal	Equal	Equal
Design of Panel Entries	Equal	Lower	?	Equal
Floor Conditions	Equal	Equal	Equal	Equal
Extraction Rate	?	?	?	?

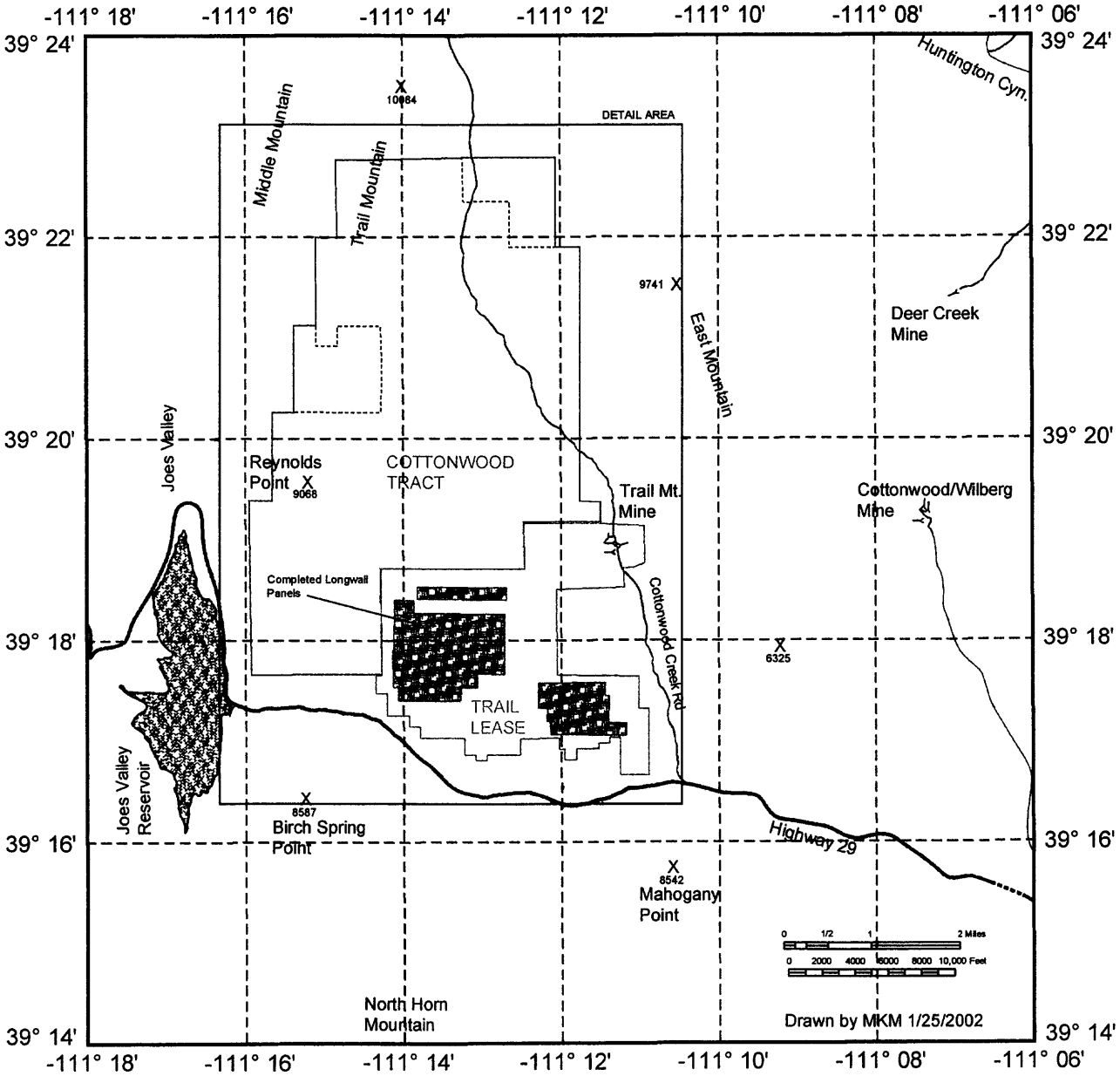

Figure F-1. Cottonwood Tract Regional Setting and Possible Sites for Initial Longwall Panels

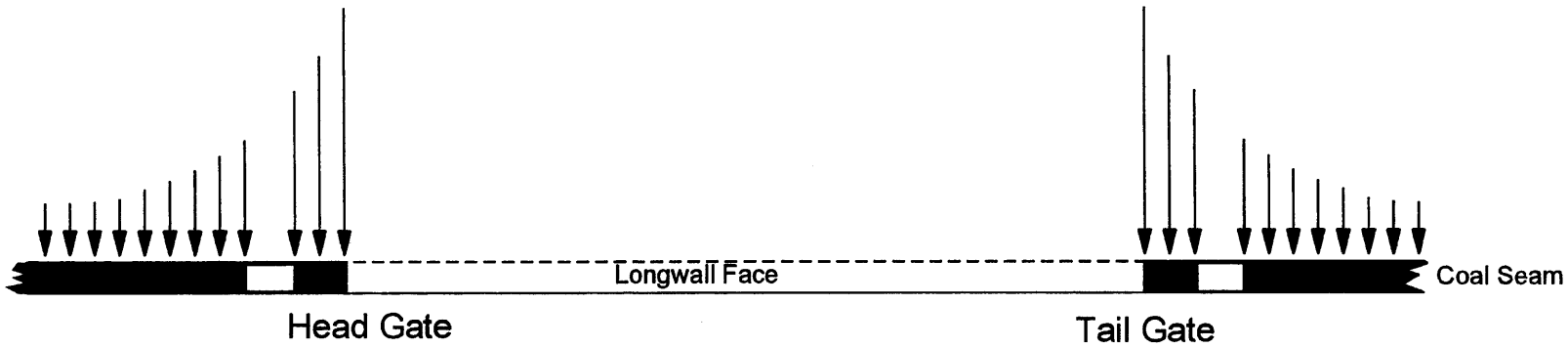

Figure F-2. Development of Abutment Pressure in a Longwall Panel

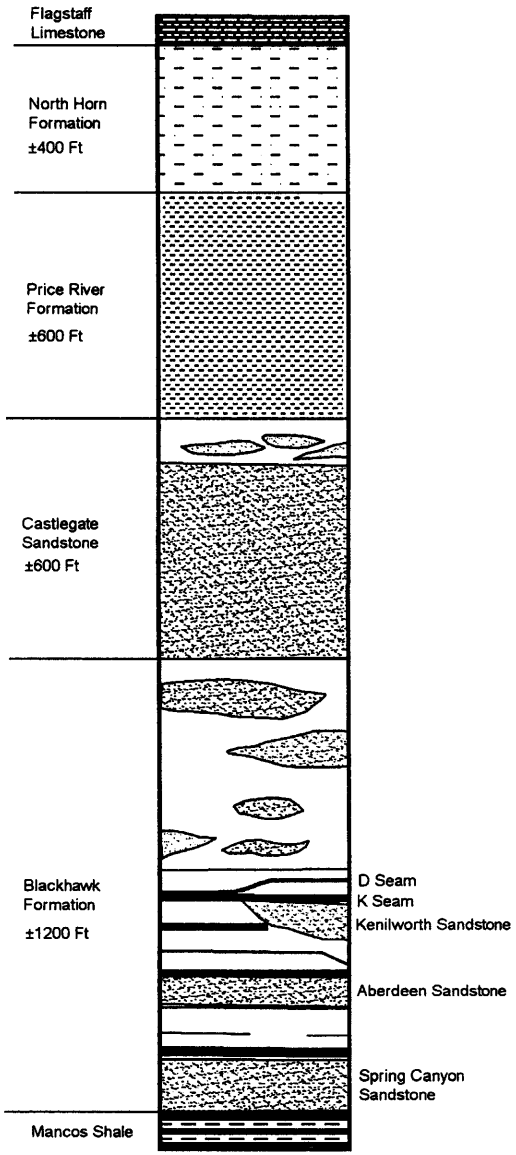

GENERALIZED STRATIGRAPHIC COLUMN
WILLOW CREEK
(Hurst, 2000)

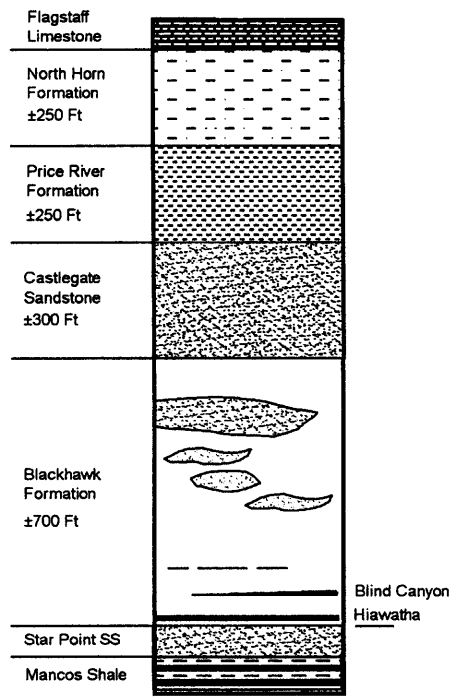

GENERALIZED STRATIGRAPHIC COLUMN
COTTONWOOD / TRAIL MOUNTAIN
(Agapito, Goodrich and Moon, 1997)

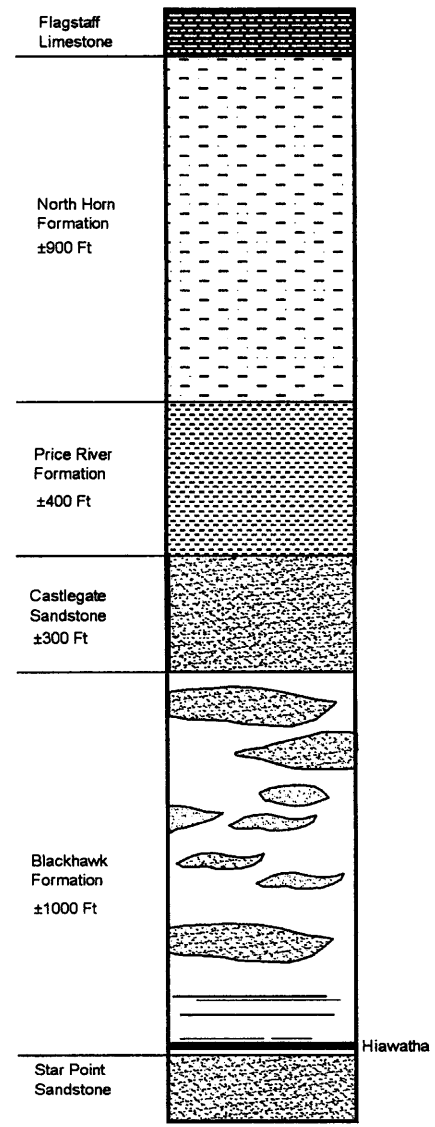

LOCAL STRATIGRAPHIC COLUMN
COTTONWOOD TRACT
(Larsen, 1997; Foster and Sommer, 1986)

Figure F-3. Wasatch Plateau and Castle Gate Stratigraphy

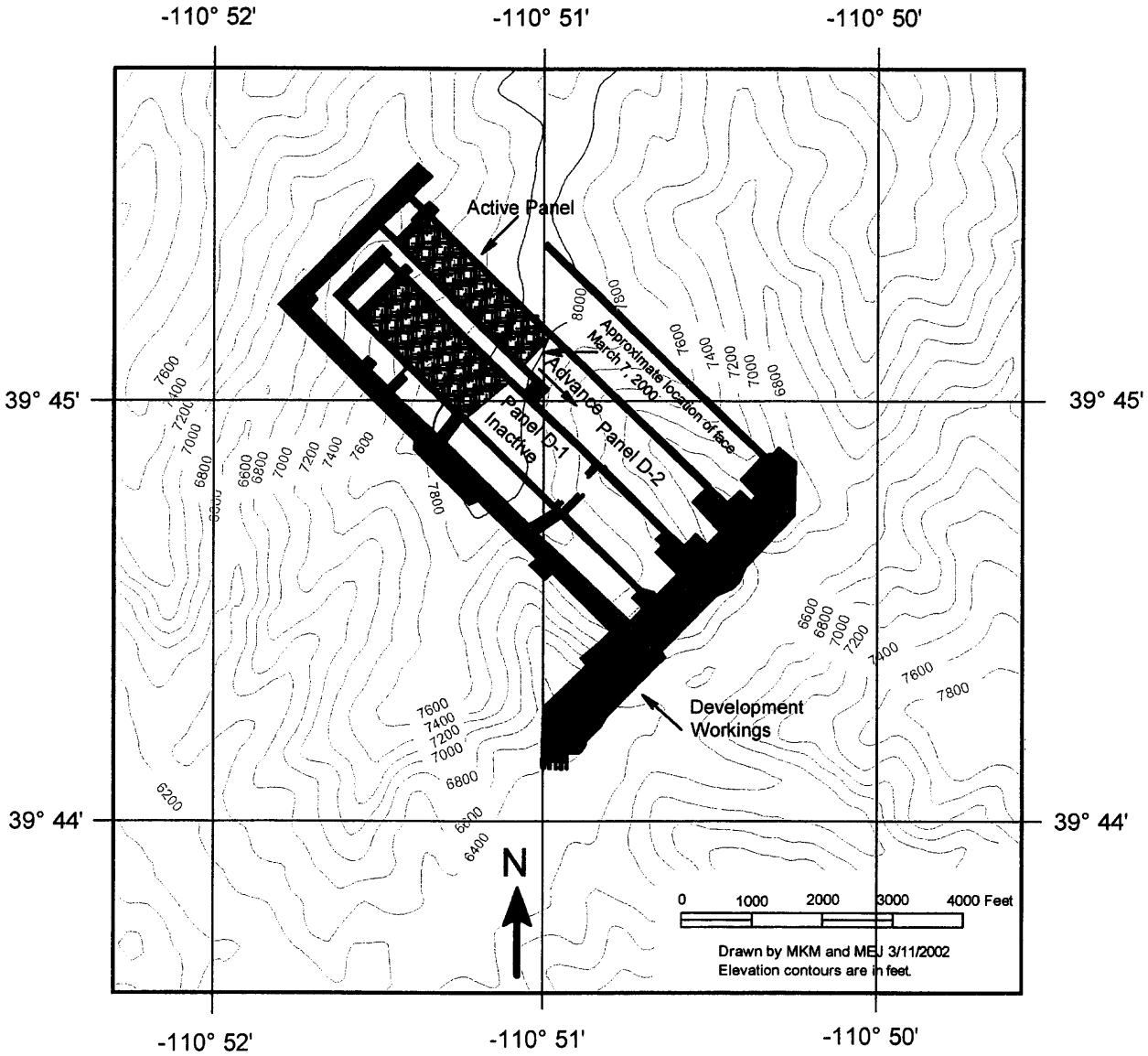

Figure F-4. Willow Creek Mine Workings - March 7, 2000

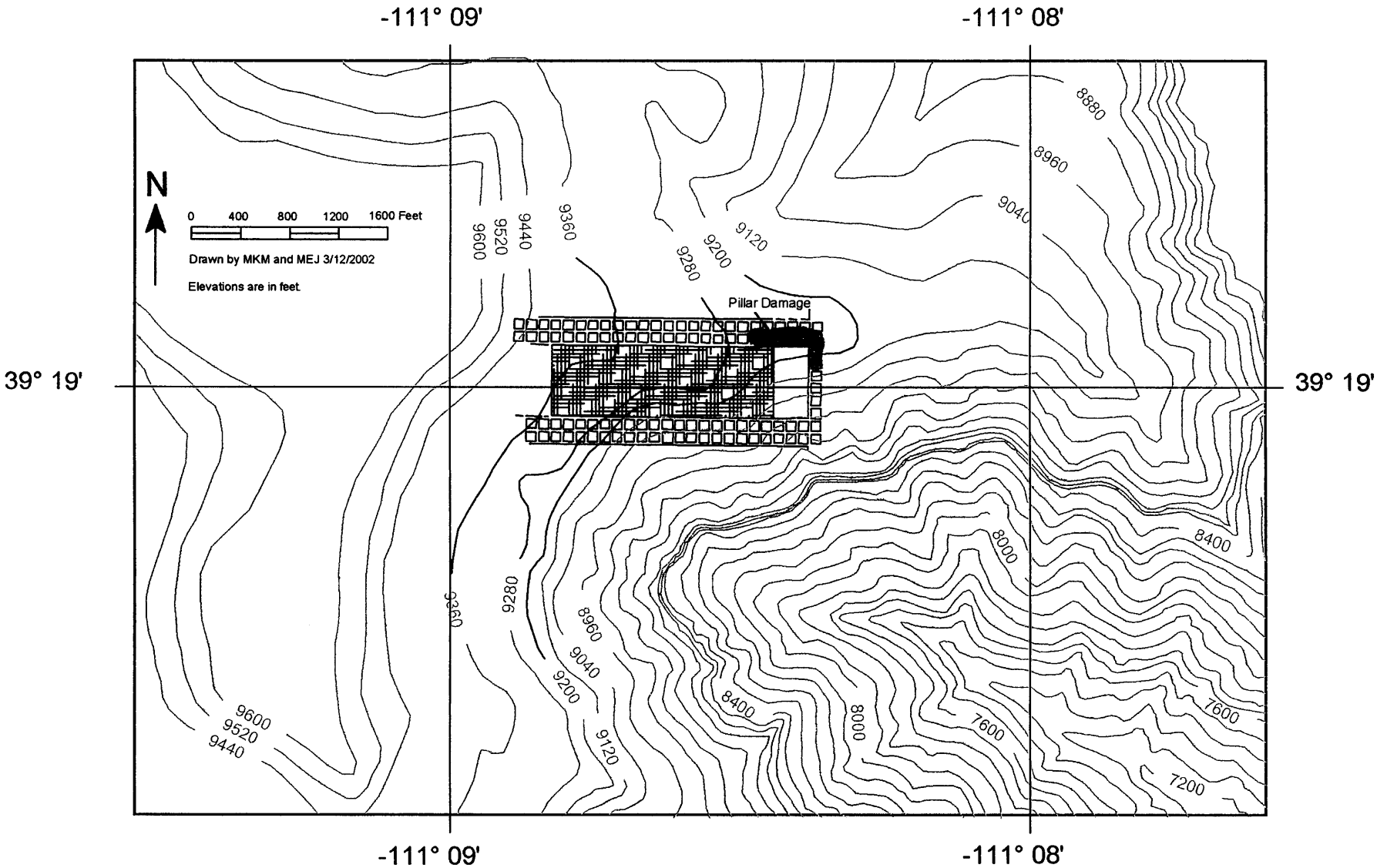

Figure F-5. Cottonwood Mine - July 5, 1992

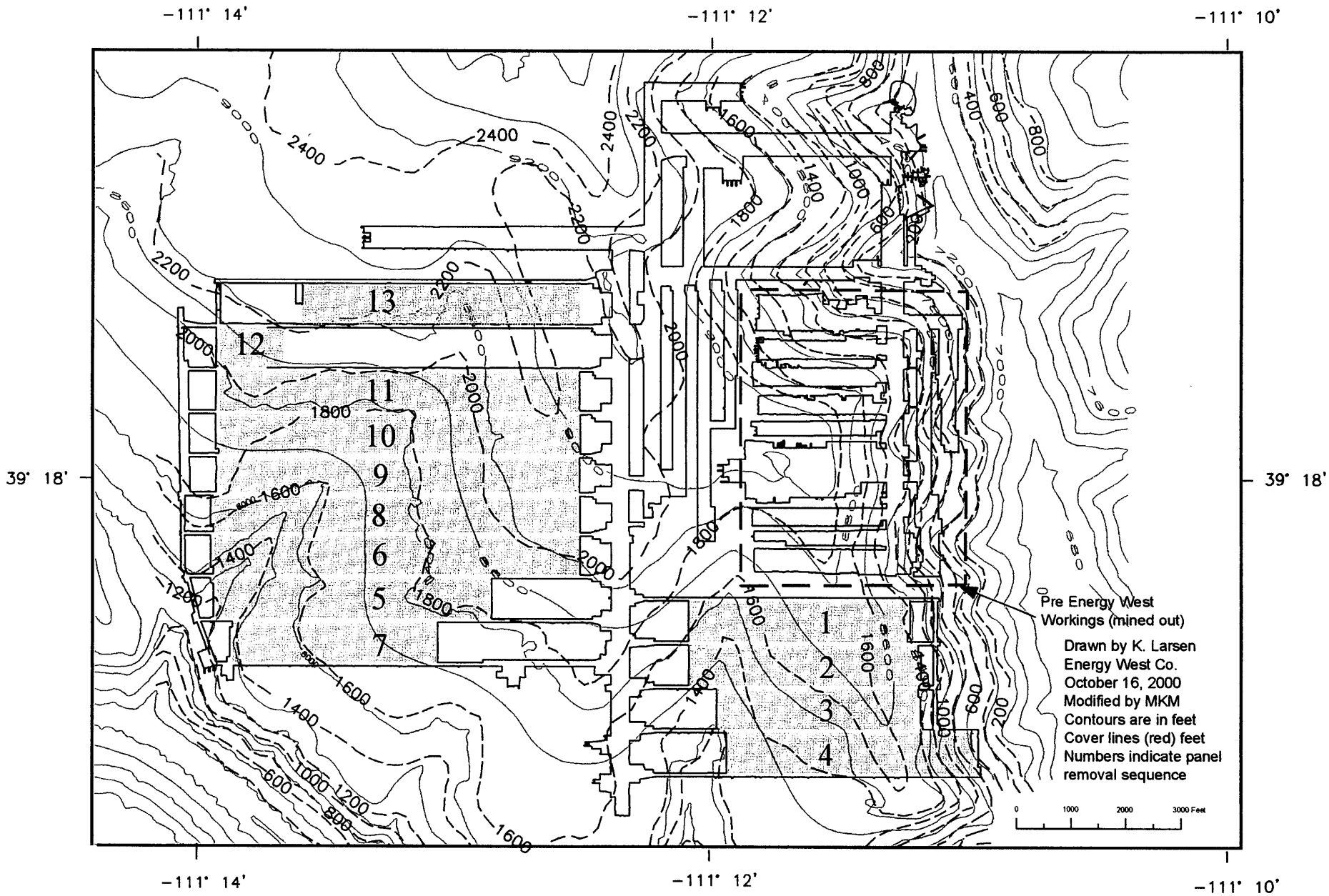

Figure F-6. Trail Mountain Mine

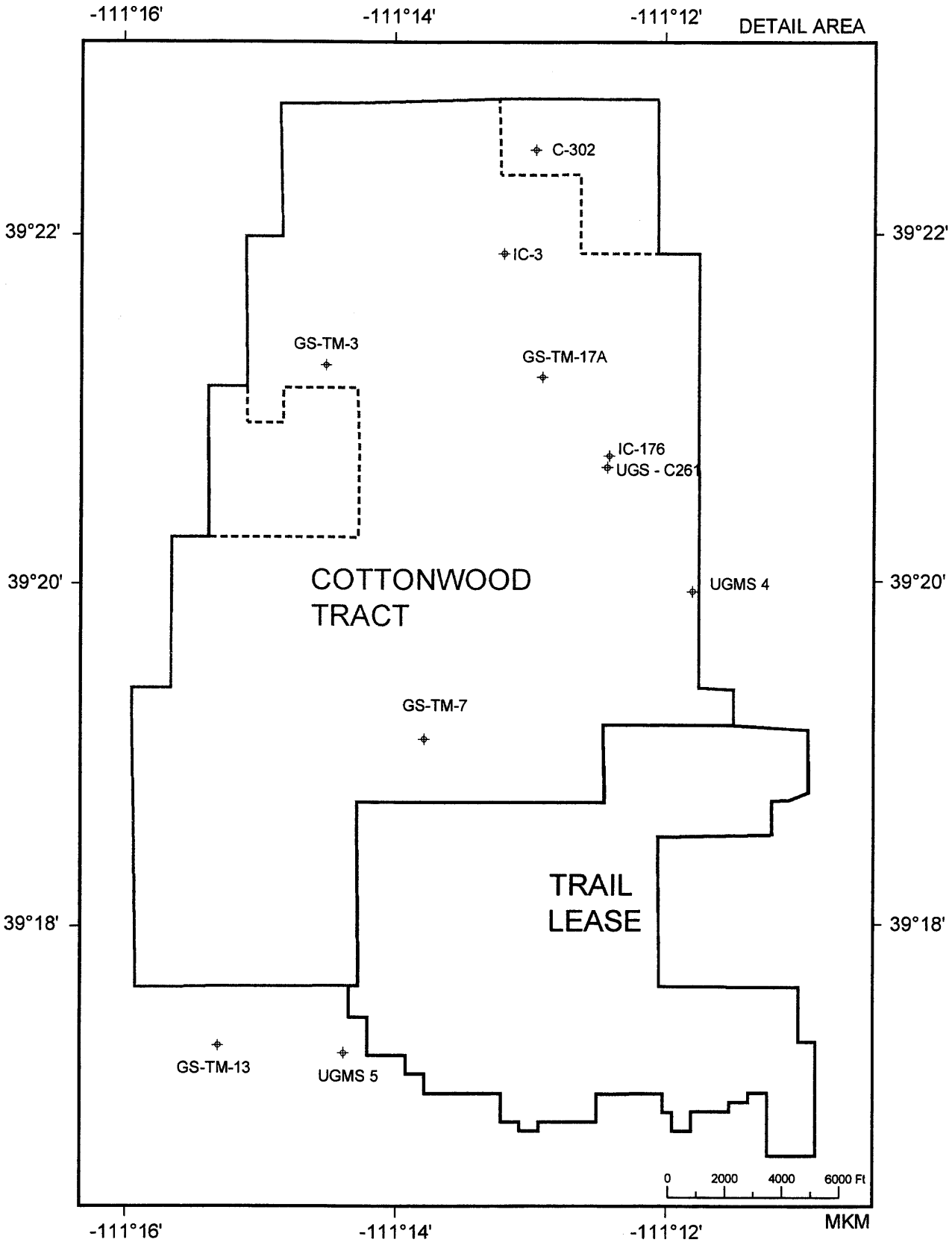

Figure F-7. Location of Drillholes

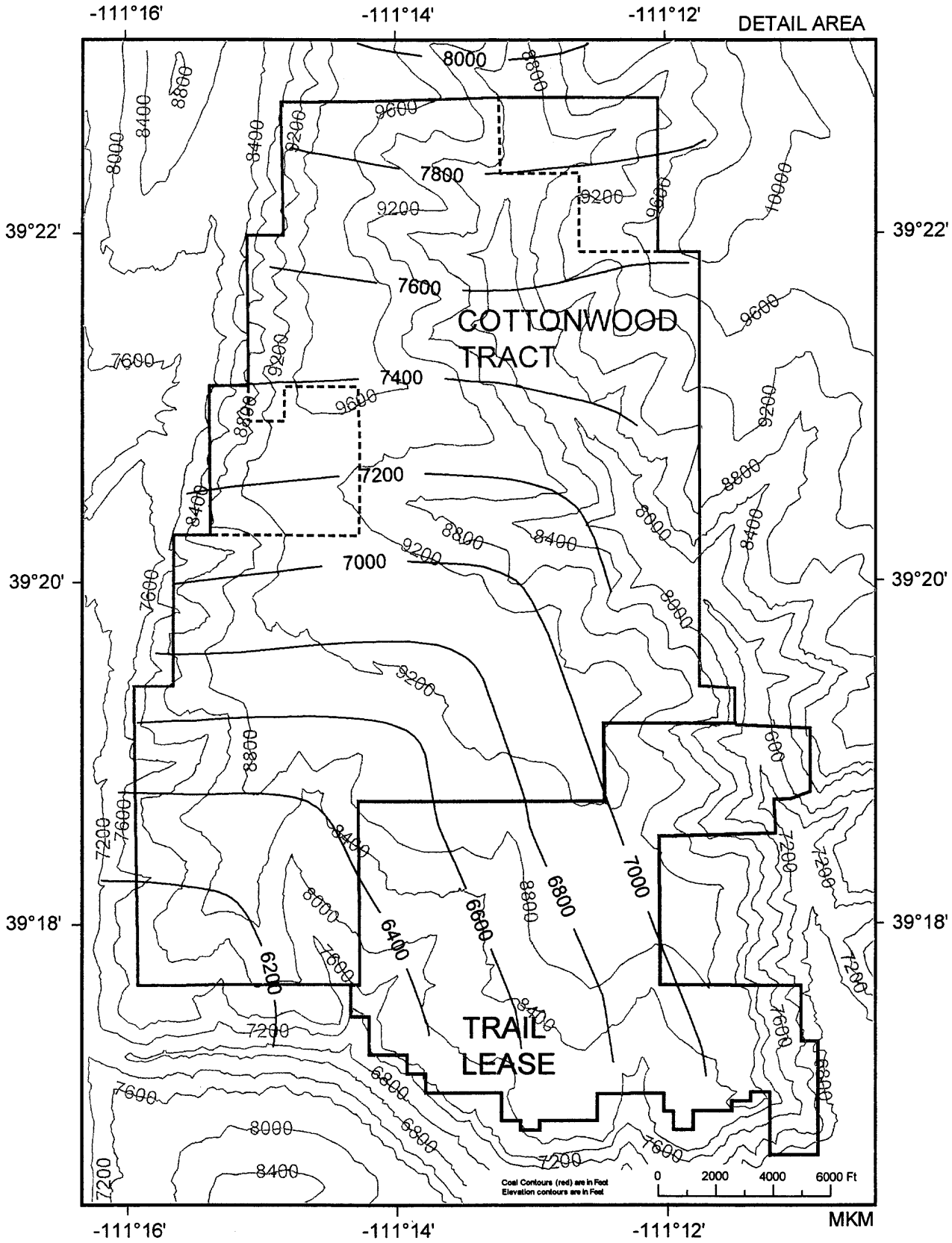

Figure F-8. Topography and Inferred Coal Horizon

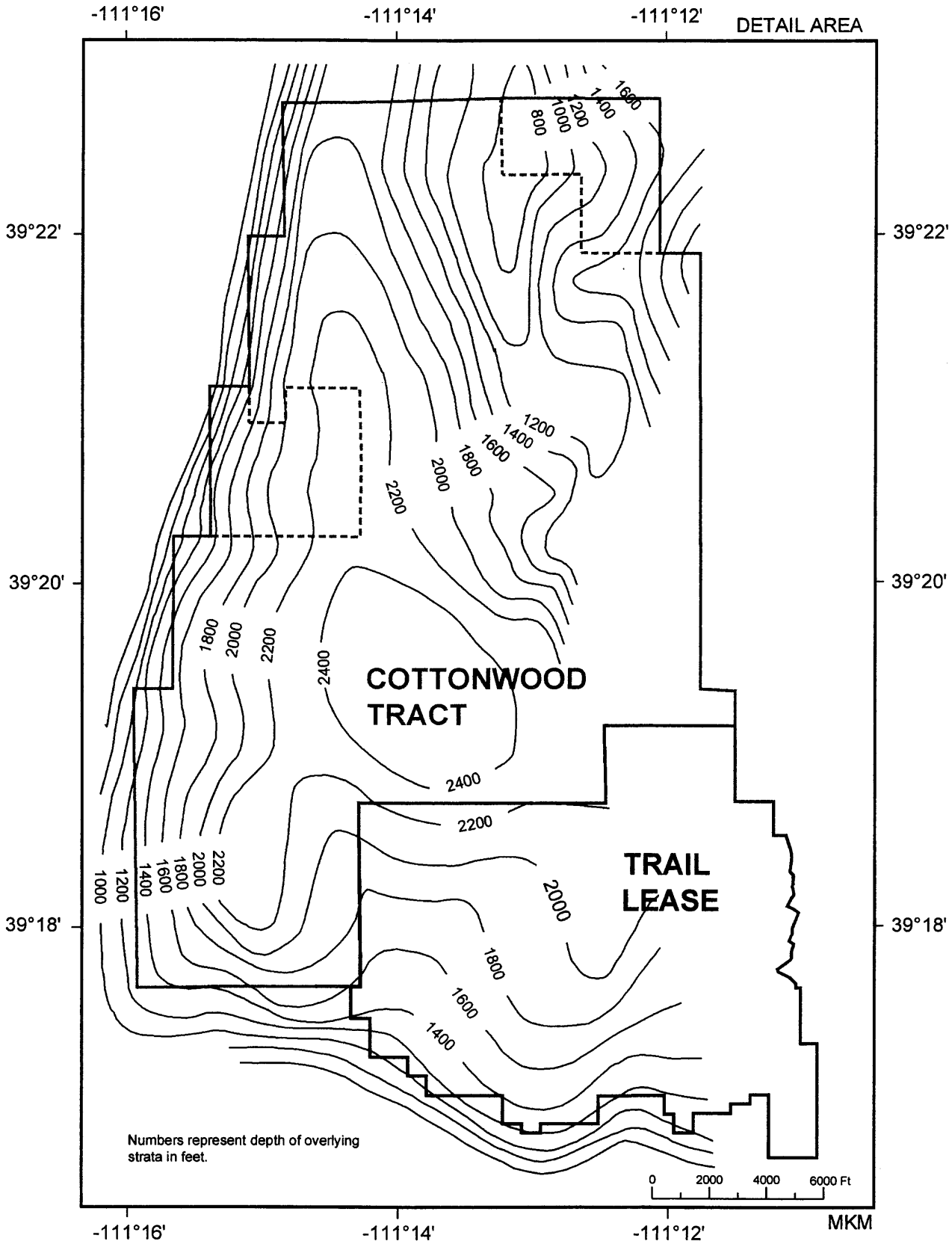

Figure F-9. Approximate Generalized Cover Lines

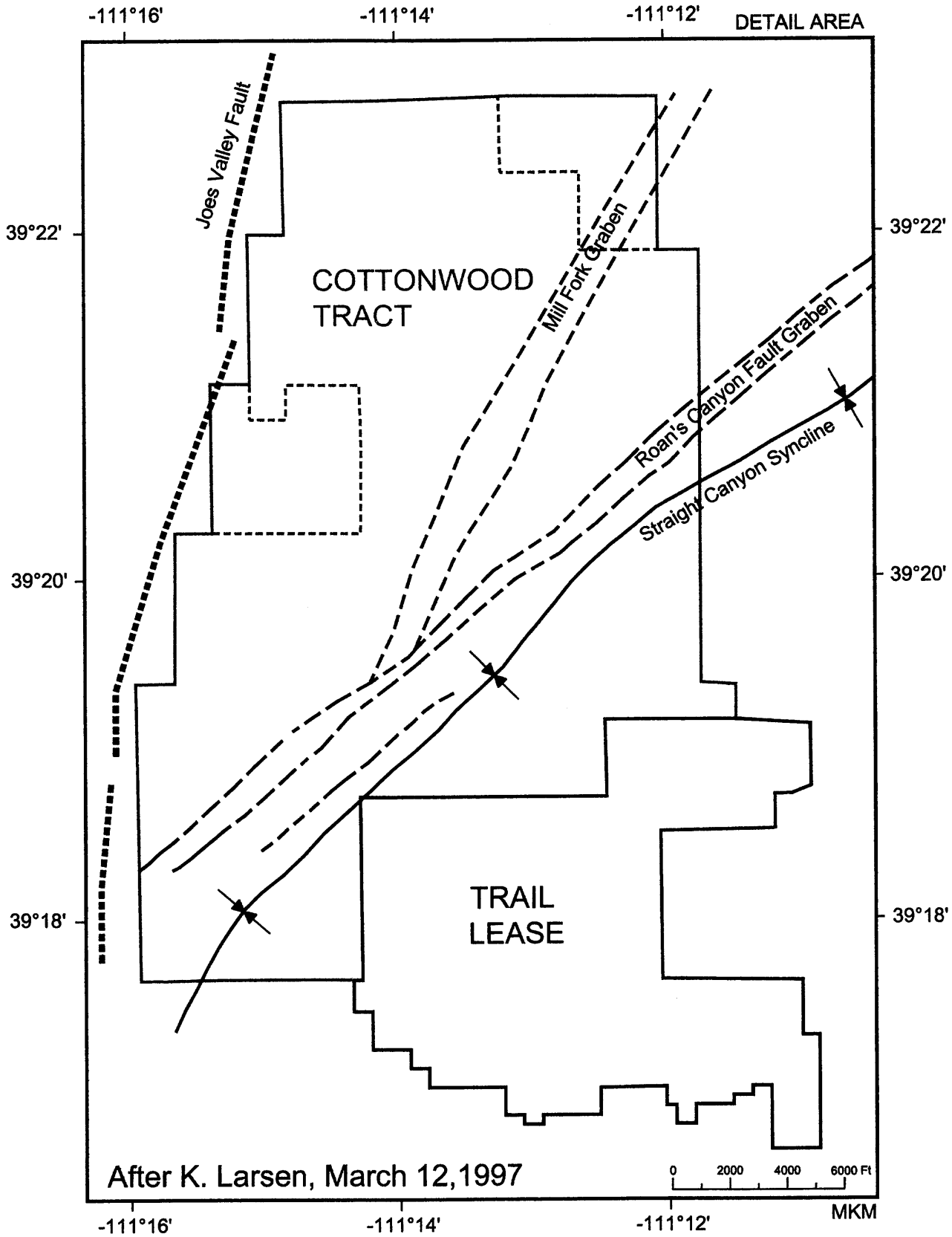

Figure F-10. Major Geological Features